Fusion of airborne LiDAR, multispectral imagery and spatial modelling for understanding saltmarsh response to sea-level rise

---

PhD

Miriam Fernández Núñez

Coastal and Estuarine Research Unit
Department of Geography, University College London

A thesis submitted for the degree of

Doctor of Philosophy

May 2016

To S.L. & E.L.

Declaration

I, Miriam Fernández Núñez, confirm that the work presented in this thesis is my own. Where information has been derived from other sources, I confirm that this has been indicated in the thesis.

25 May 2016

Acknowledgement

My first thoughts go to my supervisors Dr. Helene Burningham and Dr. Jon French for their guidance, support, patience and kindness throughout this PhD. In particular, I wish to thank Helene who has invested a lot of her time guiding me from the very beginning and has paid very detailed attention to every aspect of my work. Her experience, knowledge and enthusiasm have been a source of inspiration, and I really valued and enjoyed the time that we spent discussing different matters integrated in this PhD. My second thoughts go to my Spanish tutor Dr. Jose Ojeda Zujar (University of Sevilla) for his guidance and support, and providing important data for this PhD. Thanks also to my colleagues in the Department of Geography at University College London, especially Darryl, Katerina, Jose, Sam, Charlotte, Mandy, TV, Pooya and other PhD students for our discussions and their encouragement during lunch time and coffee breaks. Thanks also to my colleagues in the Department of Geography at University of Seville, Natalia, Arsenio, Inma, Pablo, Noela, Antonio, Jose and other colleagues for their help and support during my time in Spain. Particularly, I would like to thank to Antonio (el topografo), J. Antonio (el teniente), Jesus Pedrero, and the manager and workers of the 'Paraje Natural Marismas del Odiel' for their help during my field work, and Paco and Cesar Borja for their advices about bibliography and support. Thanks to my family for their unconditional support, especially to my mum. Thanks also to Uncle John Barker for his help and advices throughout this PhD. Warm thanks to Naoko Lam and Pilar Diaz for their support and for helping me to look after my wonderful daughter Sophie, without them I could not have finished this PhD on time. A special thanks to my wonderful husband for his support and encouragement during all these years. He has been a key person at the beginning and the end of my thesis, and his criticism helped me to improve my academic writing.

Finally, I acknowledge the two research projects that this work has benefited from: one funded by the Spanish National Research Plan and European Regional Development Fund (ERDF) ("Detail mapping and web dissemination of demographic, tourist and environmental data for vulnerability assessments linked to beach erosion in the Andalusia Coast (sea-level rise associated to climate change)"; CSO2010-15807) and the other one by Andalusia regional government ("Espacialización y Difusión Web de Datos de Urbanización, y Fitodiversidad para el Análisis de Vulnerabilidad ante los Procesos de Inundación Asociados a la Subida del Nivel del Mar en la Costa Andaluz"; RNM-6207).

Abstract

Coastal ecosystems are considered to be sensitive to changes in environmental forcing, particularly sea-level rise. Saltmarshes occupy a discrete lateral and vertical position that is fundamentally controlled by the position of sea level, but the nature of other factors such as broader scale shoreline dynamics and anthropogenic ensure that the nature and extent of sea-level rise impacts on saltmarshes are globally variable, and locally complex. Thus, there is a need to understand these controls and to predict the potential response of saltmarsh systems to sea-level change at the local scale. The present research presents a multifaceted methodology for investigating the response of saltmarshes due to sea-level rise at local scales with application to the Odiel saltmarshes (SW-Spain), using elevation data derived from Light detection and ranging (LiDAR), high spatial resolution multispectral imagery and spatial modelling, that in combination with historical estuary evolution and field observation can be applied for effective management and conservation of saltmarshes in the context of sea-level change. SLAMM (Sea Level Affecting Marshes Model) has been used to evaluate coastal wetland habitat response to sea-level rise Accurate model spatial model inputs such as digital elevation models (DEMs) and saltmarsh habitat map are essential to reduce uncertainties in the model outputs, and part of this thesis has been focused on improving accuracy in saltmarsh elevation and habitat maps. Additionally, a sensitivity and uncertainty analysis was undertaken to explore first the relative importance of data quality and resolution (spatial and vertical) in the elevation data and saltmarsh habitat classification layers, and then the global uncertainty of the model outputs using a Monte Carlo approach. Our findings suggested that model is sensitive to DEM and habitat map resolution, and that historical sea-level trend and saltmarsh accretion rates are the predominant factors that influence uncertainty in predictions of change in saltmarsh habitats.

Table of contents

List of Figures **15**

List of Tables **23**

1. Introduction and literature review **27**

1.1. Overall study aim 27

1.2. Nature and importance of saltmarshes 28

1.3. Saltmarsh formation, development and zonation 30

1.4. SW Iberian Peninsula saltmarshes in a global and European context 35

1.5. Contemporary sea-level rise and saltmarshes 41

1.6. Predictive models of saltmarsh in a context of sea-level rise 45

1.7. Remote sensed data for surveying saltmarshes 51

1.7.1. Multispectral data for saltmarsh mapping 51

1.7.2. Altimetry data: Light Detection And Ranging (LiDAR) 54

1.8. Summary 58

1.9. Aims and objectives 59

2. Research Design **61**

2.1. Study site 61

2.1.1. Northern coasts of the Gulf of Cadiz: site selection 61

2.1.2. The evolution of the Tinto-Odiel Estuary 64

2.1.3. The Odiel saltmarshes and the Tinto-Odiel estuary: site description 70

2.2. General methodology: work packages and work flow 76

2.3. Data description 79

2.3.1. Andalusian Vegetation map 79

2.3.2. Airborne LiDAR 80

2.3.3. Aerial photography 80

2.4. Field campaigns 81

3. Historical evolution of the Odiel saltmarshes (Tinto-Odiel estuary) **83**

3.1. Methods 83

3.1.1. Data 83

3.1.2. Decadal estuarine changes 86

3.1.3. Saltmarsh patch analysis 87

3.1.4. Shoreline changes: horizontal erosion and sedimentation rates 89

3.2. Decadal geomorphological and anthropologic changes 92

3.3. Saltmarsh patch analysis at landscape scale 102
3.4. Decadal shoreline change: horizontal erosion and sedimentation rates 104
3.5. Forcing of coastal change 110
3.5.1. Wind speed and wave climate 110
3.5.2 Rainfall and river discharge 114
3.5.3. Local mean sea-level change 118
3.6. Summary and discussion 121
4. Contemporary baseline assessment of the saltmarsh bio-geomorphology 129
4.1. Introduction: environmental factors controlling saltmarshes 129
4.2. Methods 132
4.2.1. Vegetation survey design and analysis 132
4.2.2. Soil survey and analysis 134
4.2.3. Sediment traps design and analysis 135
4.3. Characterization of Odiel saltmarsh vegetation 138
4.4. Habitat environmental characterisation 145
4.5. Short accretion rates 149
4.6. Summary and discussion 151
5. Remotely sensed data for saltmarsh habitat classification 157
5.1. Introduction 157
5.2. Class definition and preliminary data processing 162
5.3. Training and validation areas sampling design for image classification 164
5.4. Method 166
5.4.1. Pixel Based Image Analysis (PBIA) 167
5.4.2. Object Based Image Analysis (OBIA) 168
5.4.2.1. Image segmentation 168
5.4.2.2. Image classification 169
5.4.3. Accuracy assessment 169
5.5. Exploring the best approach for mapping saltmarsh habitats 169
5.6. Odiel saltmarsh mapping 175
5.7. Discussion and summary 177
6. Correction and assessment of LiDAR-derived DEM 181
6.1. Introduction 181
6.2. Method 182
6.2.1. Study sites 183
6.2.2. Field data 185
6.2.3. Remote sensed data 185

6.2.4. DEM corrections based on HSCF 186
6.2.5. Saltmarsh habitat map 187
6.3. Results 188
6.3.1. Ground survey 188
6.3.2. DEM production and accuracy assessment 190
6.4. Discussion and summary 194
7. Future response of Odiel saltmarsh due to SLR using SLAMM: sensitivity analysis and uncertainty assessment 197
7.1. Introduction 197
7.2. SLAMM model inputs 198
7.2.1. Elevation data 198
7.2.3. Processes involved in the spatial model 199
7.2.4. Wetland conversion 199
7.3. Data and methods 201
7.3.1. SLAMM sensitivity analysis on spatial data 201
7.3.2. The Odiel saltmarshes SLAMM simulation 206
7.3.3. SLAMM uncertainty analysis 207
7.3.4. Classification of saltmarsh vulnerability due to sea-level rise 212
7.3.5. Comparison of SLAMM and UCL-modified SLAMM 214
7.4. Results 216
7.4.1. Sensitivity analysis based on spatial inputs 216
7.4.2. Potential impacts due to sea-level rise in the Odiel saltmarshes 224
7.4.3. SLAMM uncertainty analysis 229
7.4.4. Odiel saltmarsh vulnerability due to sea-level rise 237
7.4.5. Comparison of original and modified SLAMM 240
7.5. Summary and discussion 242
8. Final discussion and conclusions 249
8.1 The SLAMM model for saltmarsh management in the context of sea-level rise: uncertainties and limitations 249
8.2. Conclusions 251
9. References 255

List of Figures

Chapter 1

Figure 1.1 Aerial view of saltmarsh environments in Southwest Spain [Photo taken by Jose Antonio Fernandez in 2011] 28

Figure 1.2 Forcing factors and linkages of saltmarsh system (Allen, 2000) 31

Figure 1.3 (A) High level tidal flat. (B) Low level marsh in which vascular plants have colonized the higher points of the tidal flat. (C) High marsh with a fully vegetated surface, except for the creeks and pans which are sharply defined by their steep banks [Source: modified from (Long & Mason 1983)]. 32

Figure 1.4 Biogeographic regions of European saltmarshes. The main regions are (1) Artic, (2) euro-Siberian, (3) Mediterranean, (4) the Pontic region and (5) the Irano-Turanian region. The euro-Siberian zone is divided into four sub-zones: (2a) Boreo-Atlantic, (2b) North Atlantic-Baltic, (2c) Sub-Atlantic and (2d) Cantabro-Atlantic. The Mediterranean region is divided into five sub-zones: (3a) Mediterranean-Atlantic, (3b) Mediterranean-Tyrrhenian, (3c) Inland Iberian, (3d) eastern Mediterranean zone and (3e) the special zone of northern Adriatic. [Source: Géhu and Rivas-Martinez (1984)] 38

Figure 1.5 Geomorphological types of saltmarsh [Source: Pye and French, 1993]. 40

Figure 1.6 Sea level changes in Europe from 1992-2007 (map based on satellite altimeter data). [Source: Guinehut & Larnicol, 2008]. 42

Figure 1.7 Conceptual model of principal factors governing adjustment of saltmarsh elevation within the tidal frame [Source: French, 2006] 44

Figure 1.8 Processes that affect saltmarsh net elevation due to sea-level rise. Processes shown below the time line reduce elevation and those shown above the time line increase elevation. [Source: Rybczyk and Callaway, 2009] 44

Figure 1.9 Spatial and temporal scales of predictive models used to estimate saltmarsh and estuarine processes in a context of sea-level change. 46

Figure 1.10 Typical two (a) and three (b) element schematisations of ASMITA model [source: Rossington *et al*. (2011)] 49

Figure 1.11 Illustrative sample of 30m spatial resolution LandSat-5 image (on the left) and 1m spatial resolution aerial photograph (right) for a saltmarsh. 54

Figure 1.12 Example of echo (or returns) of an airborne LiDAR laser beam in two different environments: (a) is representing forest environments, where several returns are usually collected; and (b) represents saltmarsh environments, where only one return is usually collected due the short vegetation that characterises these environments 55

Chapter 2

Figure 2.1 Location of the Gulf of Cadiz. In red is shown the Odiel-Tinto estuary (Huelva). 62

Figure 2.2 The main neotectonic macrostructure of Gulf of Cadiz. From east to west, the picture shows the main faults and flexion of the province of Cadiz, Huelva and the Algarve. The red square states the study site location (Huelva) and the numbers indicate the

following location: (1) Tarifa, (2) Roche Cape, (3) Sanlucar, (4) Sta. Maria Cape, and (5) San Vincent Cape. [Source: Ojeda, 1988]. 63

Figure 2.3 Holocene evolution (based on cores) of the Tinto-Odiel Estuary and saltmarsh formation from 10,000-12,000 years ago to present. (a) Reconstruction of lower position of sea level, where areas in green simululates the emerged land at that time. (b) Reconstruction of higher sea level position during the 'Flandrien transgression'. Figures from (c) to (i) show the saltmarsh evolution in this estuary, where the areas in clear blue is water; dark blue represents tidal wetlands; yellow shows sand deposition areas such as beaches, spits and barrier islands; white represents sandy tidal flats; green represents fresh water environments. Areas in red (i) show dikes and seawalls [Source: Modified from Morales and Ojeda (2010)] 66

Figure 2.4 Holocene sea level trend for the SW Iberian coast [Source: Delgado *et al*., 2012]. 67

Figure 2.5 (a) Holocene sedimentation rates and trends in the Odiel saltmarshes, where MRSLR means mean rate of sea-level rise and SR sedimentation rate; (b) Location of the cores within the Odiel saltmarshes [Source: Lario *et al*., 2002] 67

Figure 2.6 (a) Palaeo-geographical evolution, and (b) Flandrian transgression at the central estuarine basin of the Odiel and Tinto River mouth, where 'Faun Ass.' refers to three faunal assemblages (Open bay (OB), Central estuary (CE), and Wave domination (WD)) including remains of macrofauna, foraminifers and ostracods plus depositional features (they were identified in a sedimentological log constructed from a borehole with a continuous core) [Source: Borrego *et al.* 1999] 69

Figure 2.7 Location of the Odiel saltmarshes and the Tinto-Odiel Estuary. The red line states surface area of the study site. 70

Figure 2.8 (a) Geological substratum of the Odiel and Tinto River drainage network (the Iberian Pyrite Belt) [source: López-González et al. 2006b]; and (b) sediment traps for a sediment texture analysis in the Tinto-Odiel estuary [source: Lopez-Gonzalez *et al*., 2006a] 73

Figure 2.9 Location of the sediment core sites in the Odiel-Tinto estuary. [Source: Morales *et al.*, 2003] 74

Figure 2.10Thesis work flow and work packages. 77

Chapter 3

Figure 3.1 Configuration of the Tinto-Odiel estuary mouth in 1862 [Source: map surveyed by Fernandez y Coria; and published by Spanish Royal Navy (1862)] 84

Figure 3.2 Configuration of the Tinto-Odiel estuary in 1946 [Source: map published by Cartography Institute of Andalucía, 1946] 85

Figure 3.3 Four classes of spatial pattern exhibited within land cover data [Source: Vogt *et al.,* 2006] 88

Figure 3.4 Shoreline digitalisation for calculating rate-of change in the Odiel saltmarshes. The shorelines are displayed over the 1956 aerial photography 89

Figure 3.5 Orthogonal transects generated by DSAS (ArgGIS 10.2) from a digitised onshore baseline for shoreline change analysis in the Odiel saltmarshes. 91

Figure 3.6 Percentage of surface area computed per class and year of the Odiel saltmarshes 93

Figure 3.7 Decadal changes of the Odiel Saltmarshes between 1956 and 2013 94

Figure 3.8 Geomorphological changes at the Tinto-Odiel estuary mouth between 1956 and 1979. It should be noted that some sandy bars approaching the Punta Umbria Ria mouth in 1956 are out of the study area 97

Figure 3.9 Geomorphological changes at the Tinto-Odiel estuary mouth between 1979 and 1984. The Juan Carlos I dike construction created a barrier between both Ria mouth (Punta Umbria and Huelva) favoured sandy sediment retention and sheltered environments 98

Figure 3.10 Geomorphological changes at the Tinto-Odiel estuary mouth between 1984 and 2001 99

Figure 3.11 Habitat and tidal channel fragmentation of the Saltes Island caused by the Juan Carlos I dike construction (shown as red). The black dash line represents the watershed boundary in this area. As it shown in the 1979 map, two tidal channel sections have been isolated, and the dike is preventing drainage through the natural watershed drainage 101

Figure 3.12 Patch type present in the Odiel saltmarshes in 1956, 1979 and 2013 103

Figure 3.13 Erosion and sedimentation rates (in my^{-1}) in the Odiel saltmarshes between 1956 and 2013 (displayed over 1987 spot image). The variable the end point rate (EPR) is represented in map A, and linear regression (LRR) in map B; where red dots mean erosion rates (retreatment), blue dots sedimentation rates (horizontal growth) and yellow dots no shoreline changes 105

Figure 3.14 Shoreline position relative to the 1956 location (in metres) from 1956 and 2013 at transect 348 106

Figure 3.15 Relative shoreline distance (in metres) relative to 1956 for each transect in the Odiel saltmarshes. Transects were grouped based on cluster analysis (Average Hierarchical Clustering), and each group represents some similarities in shoreline behaviour over time (1956-2013), where N indicates the number of transects in each group 108

Figure 3.16 Characterisation of the shoreline changes in the Odiel saltmarshes based on cluster analysis. The legend indicates the group of each shoreline sector; where red/orange colours state a retreatment tendency and blue/green colours progradation. 109

Figure 3.17 Wind (A) and wave (B) roses (1958-2015) for the Huelva coast (6.92° W, 37.08° N; SIMAR model point 5031022 in red). [source: http://www.puertos.es/en-us/oceanografia/Pages /portus.aspx] 110

Figure 3.18 Review of time series (1958 – 2015) wind and wave climate for the Huelva coast (6.92° W, 37.08° N; SIMAR model point 5031022). From top showing monthly mean and max wind speeds, significant wave height and mean period. [source: http://www.puertos.es/en-us/oceanografia/Pages/portus.aspx] 111

Figure 3.19 Review of time series (1996 – 2015) wind and wave data for the Gulf of Cadiz wave buoy (6.96° W, 36.48° N). From top showing monthly mean and max wind speeds

(ms^{-1}), significant wave height (m) and mean period (s). [source: http://www.puertos.es/en-us/oceanografia/Pages/portus.aspx] 112

Figure 3.20 Review of time series (1984 – 2015) wind data recorded at the Huelva weather station (6.92° W, 37.28° N; WMO station code 08383). From top showing monthly median and extreme wind speeds, annual wind direction frequency and annual median and extreme wind speed from each wind direction quadrant. [data source: http://www.badc.ac.uk] 113

Figure 3.21 Monthly and annual rainfall (mm) from 1956 to 2013 in Huelva, where SD is the standard deviation [data source: http://catalogue.ceda.ac.uk/uuid/3f8944800cc48e1cbc29a5ee12d8542d] 115

Figure 3.22 Discharge data for the Odiel River at the Gibraleon gauge station between 1969 and 1994 showing: (A) annual discharge; (B) location of the gauge stations and Odiel sub-basins; (C) monthly discharge; and (D) frequency [Source: Lopez *et al.*, 2006] 116

Figure 3.23 Annual discharge of the Odiel River in blue (at Gibraleón gauge station) and Odiel River in red between 1980 and 2006, stating the construction of three water reservoir (black lines) [Source: Olias Alvarez *et al*., 2010] 116

Figure 3.24 Monthly discharges (measured and simulated) of the Odiel River at the Gibraleon gauge station between 1982 and 2010 117

Figure 3.25 Monthly mean sea level (mmRLR) from 1997 to 2013 at the Huelva tide gauge (location shown as red dot) [source: PSMSL] 119

Figure 3.26 Monthly mean sea level (mmRLR) at different stations in the Gulf of Cadiz (Bonanza, Huelva, Cadiz (I and II) and Lagos (Portugal) tide gauges) [Source: PSMSL] 120

Figure 3.27 Tidal gauge location at different stations in the South of the Iberian Peninsula, specifying those found in the Gulf of Cadiz (Bonanza, Huelva, Cadiz (I and II) and Lagos (Portugal) tide gauges) [Source: Fraile (2011)] 121

Figure 3.28 Changes experienced the Odiel saltmarshes per time interval. Grey represents areas that did not change within the time interval; red identifies areas that changed cover class. 123

Figure 3.29 Variation and tendency followed by each cover class in the Odiel saltmarshes over the time. The Y axis represents the surface area (ha) occupied by each class and the X axis the year. 124

Figure 3.30. Horizontal Erosion and sedimentation rates (End Point Rate in my^{-1}) at different time periods in the Odiel saltmarshes 125

Chapter 4

Figure 4.1 Interrelation of environmental factors affecting saltmarshes [modified from Nibbakeb and Bertness, 2001] 130

Figure 4.2 Quadrat location of the vegetation survey undertaken in the Odiel saltmarshes. 133

Figure 4.3 Example of the 1x1m quadrat used for the random vegetation survey. 134

Figure 4.4 Location of the sediment traps. 136

Figure 4.5 Ceramic tile located at mid-low saltmarsh habitat. 136

Figure 4.6 Spatial distribution of plant species in the Odiel saltmarshes based on vegetation survey (quadrats). 139

Figure 4.7 Summary of the cluster analysis obtained in TWINSPAN. The numbers refer to number of quadrats that contain the species mentioned. 140

Figure 4.8 Canopy height for different saltmarsh habitats at the Odiel saltmarshes. 141

Figure 4.9 Examples of low (A) and mid (B) marsh habitats in the Odiel saltmarshes. 143

Figure 4.10 Salt pan habitat in the Odiel saltmarshes. *Salicornia ramosissima* appears in the front over the salt pan (pink colour) and *Salicornia macrostachyum* in the back (green colour). 144

Figure 4.11 (A) Spartina marsh and (B) high marsh habitat in the Odiel saltmarshes. 145

Figure 4.12 Environmental parameters box plots for each habitat type. 147

Figure 4.13 Ground elevation above mean sea level (m) of each habitat type in the Odiel saltmarshes. Elevation is referred to the Spanish vertical datum (zero in Alicante). Pioneers elevation (*Spartina maritima*) has been included 149

Figure 4.14 Accretion rates in the Odiel saltmarshes per habitat type and two main sampling (spring/summer and autumn/winter) seasons between 2012 and 1014. 151

Chapter 5

Figure 5.1 View of the 5 classes defined from the 2013 aerial photography (0.16 cm resolution), where each letter refers to the following class: (a) Mud, (b) Low marsh, (c) Salicornia marsh, (d) Spartina marsh, (e) Water 163

Figure 5.2 Sites of the ground-based photography integrated in the photo catalogue. 165

Figure 5.3 Location of the sub-site for performing different image analysis approaches: the Saltes Island (The Odiel saltmarshes, SW Spain) 166

Figure 5.4 Workflow diagram of the method used 167

Figure 5.5 Image classification of Saltes Island using different data and image analysis techniques: (A) Pixel-based image analysis with only spectral data; (B) Pixel-based image analysis adding elevation data (DEM); (C) Object-based image analysis with only spectral data; and (D) Object-based image analysis adding elevation data. [B, C and D results overleaf]. Note: only intertidal and saltmarsh environments are considered here, and all other habitats have been masked 171

Figure 5.6 Odiel saltmarsh habitat mapping using object-based image analysis (multispectral data and elevation data derivate from a combined photogrammetric and LiDAR flight) 176

Chapter 6

Figure 6.1 Workflow diagram of the method used 183

Figure 6.2 Study area and site locations at the Tinto-Odiel estuary (Huelva, Southwest Spain). Ground control points (GCPs) collected for both sites are represented by black dots 184

Figure 6.3 Hierarchical structure of cover classes used in eCognition. 187

Figure 6.4 Marsh habitat map of the Odiel saltmarshes (SW Spain) for applying the habitat-specific correction factor 189

Figure 6.5 Vegetation height per habitat type at different sites, where "Lmarsh" means low marsh, "SSalicor" *short Salicornia*, "TSalicor" *tall Salicornia* and "Spmarsh" spartina marsh. The numbers state different sites within the Odiel saltmarshes. 190

Figure 6.6 Habitat-specific correction factor (HSCF) map, where the correction factor for each habitat class has been spatially-distributed using the Odiel saltmarsh habitat map 192

Figure 6.7 Map of the two areas used as test sites for unmodified DEM corrections showing the unmodified and user-modifier DEM for Site 1 and Site 2, where: (a) and (b) are the unmodified and the user-modified DEM respectively in Site 1; and (c) and (d) are the unmodified and the user-modified DEM respectively in Site 2. Two transects (Transect 1 and Transect 2) were selected for comparing the height profiles of both DEMs at Site 1 and 2. In the profile graphs, note the differences in canopy heights in the unmodified DEM and the user-modified DEM, and the overlapping at creeks (where a mask was used). 193

Figure 6.8 Mean error (ME) and root mean square error (RMSE) per habitat cover class. The ME and RMSE is compared between the unmodified DEM and the User-modified DEM. 194

Chapter 7

Figure 7.1 Location of the study site (red line) for testing model sensitivity 202

Figure 7.2 Flow chart of the input data used in the sensitivity analysis based on spatial data 203

Figure 7.3 Marsh habitat maps (MHM) from Table 7.2 used as different inputs for testing SLAMM 204

Figure 7.4 Digital elevation models (DEM) Table 7.2 used as inputs for testing SLAMM 204

Figure 7.5 Sub-sites used for running SLAMM (in the simulation for the entire study area) 206

Figure 7.6 Uncertainty model integrated in SLAMM (v 6.2) 207

Figure 7.7 Example of the linear interpolation for *irregularly flooded marsh* accretion (for 1 m eustatic sea-level rise) using a set of inputs values that covered the full range of the uncertainty distribution. The values for the point dataset were calculated in SLAMM changing the SLR values while the other inputs were held constant. 211

Figure 7.8 Flow diagram of the procedure for classifying saltmarsh according to its vulnerability to sea-level rise; where RegFM is regularly flooded marsh, TF tidal flat and IrregFM irregularly flooded marsh. 213

Figure 7.9 SLAMM decision tree modification including tidal ranges (where grey arrows state inundation, and red arrows erosion) [Source: Pylarinou (2015)] 215

Figure 7.10 Surface area (%) of the outputs for 0.5 m sea level rise projected for 2100 and its variation per category when different inputs are used 216

Figure 7.11 Model outputs per test for 0.5 m sea level rise projected for 2100 (see Table 7.2 and Table 7.5) 217

Figure 7.12 Comparison of the result obtained per test performed. T_i indicates the test carried (e.g. test 1, test 2, etc.) followed by the specific input that was modified within each test, where MHM refers to Map Habitat Map, DEM to Digital Elevation Model, EIN to elevation inputs and '5/10 m' to the cell size. The pre-processor tool was (by default) off in all the tests, and only in test 4 (T4) was on (stated by 'T') and off (stated by 'F') to compare the utility of high resolution habitat maps when high resolution DEM are not available (see Table 7.2 and Table 7.5). 219

Figure 7.13 Habitat surface variation by test performed; x axis shows the surface area in hectares and y axis the different test applied. The optimum test across all categories is Test 1_5m (which uses the highest resolution input data). *This test out is the same than Test2_MHM1, Test3_EIN and Test5_DEM2 223

Figure 7.14 Potential habitat conversion due to sea-level rise in the Odiel saltmarshes using, using the IPCC A1B scenario 225

Figure 7.15 Potential Odiel saltmarshes habitat conversion (in ha) due to sea-level rise (A1B, A1T, A1F1, A2, B1 and B2 IPCC scenarios) projected for 2050, 2075 and 2100. 228

Figure 7.16 Results from Morris method showing the important input factors that influence uncertainty in the output based on 1 m sea-level rise scenario by 2100, where SLR_{2100} is the projected sea-level rise by 2100, *HisTrend* site historical trend of sea-level rise, *GT* (great diurnal tidal range), *Reg-accre* regularly flooded marsh accretion and *Irre-accr* irregularly flooded marsh accretion 231

Figure 7.17 Input-output relationship for saltmarsh categories in SLAMM (v. 6.2), where one input factor was change at a time while the rest were held constant and equal to base case. The vertical axis states the changes in hectares of each saltmarsh category in comparison with the base case, and the horizontal axis the changes in the input factor values respect the base the case. 234

Figure 7.18 Uncertainty analysis for the total saltmarsh considering 1 m sea-level rise scenario and the full variability of the input factors (*Htrend*, *reg-accre* and *irreg-accre*), where (a) shows the relative frequency of the range of outputs variability (%), and (b) the cumulative frequency (%). 236

Figure 7.19 Uncertainty analysis for the total saltmarsh considering the full variability of the sea-rise scenarios defined in the uncertainty distributions, where (A) shows relative frequency of the range of outputs variability (%), and (B) the cumulative frequency (%). 236

Figure 7.20 Odiel saltmarsh predicted change for 2050 under the IPCC scenario AB1, barriers presence in 2013, and shoreline tendency over the last 50 years. 238

Figure 7.21 Classification of the Odiel saltmarsh vulnerability due to sea-level rise based on 2050 predicted change 239

List of Tables

Chapter 1

Table 1.1 Summary of the most relevant European saltmarsh typology studies 37

Table 1.2 Saltmarsh biotopes on a geomorphological base. The proportional distribution of sites per region is shown based on Dijkema inventory [source: Dijkema, 1984; page 9]. 39

Table 1.3 Estimates of GSLR from tide-gauge records [source: updated from Gornitz, 1995]. 42

Table 1.4 Summary of properties of relevant sensor for saltmarsh mapping. 53

Table 1.5 Studies focused on calculating LiDAR vertical accuracy in saltmarshes 57

Chapter 2

Table 2.1 Published accretion rates in different environment of Odiel saltmarsh 75

Table 2.2 High tide data of the Mazagon tide gauge (Huelva) corrected by reference vertical Datum (Spanish hydrographic zero; zero in Alicante). The tide gauge's original data were referred to its own datum and the shown height in the table has been calculated. [Fraile, 2005] 78

Table 2.3 Details of the LiDAR flight carried out in February 2013 80

Table 2.4 Aerial photographs available for the study area [Source: www.idendalucia.es] 81

Table 2.5 Campaigns overtaken for field data acquisition 81

Chapter 3

Table 3.1. Indicators used for the digitalisation process 87

Table 3.2 Surface area in hectares computed per class and year of the Odiel saltmarshes 93

Table 3.3 Percentage of change (PoC) per period analysed. This percentage represents the relative surface loss or gain experienced per class during each period. Negative values state percentage of surface loss and positive values percentage of surface gain in the final year respect the initial year 95

Table 3.4 Variation of saltmarsh patch, edge and core surface area (ha) per year (1956, 1979 and 2013) 102

Chapter 5

Table 5.1 Types of image classification approaches based on different criteria. It should be noted that the inclusion in one category does not exclude a classification to be grouped into other categories. [Source: modified from Lu and Weng, 2007] 159

Table 5.2 Summary of the main classification approaches used in saltmarsh mapping 160

Table 5.3 Confusion matrices and kappa indices of different classification approaches and data at the Saltes Island (2013). The values in the confusion matrices are in percentage and represent the producer accuracy (which highlights how well the map objects have been classified) 175

Table 5.4 K-nearest neighbour confusion matrix for the 5 saltmarsh habitat cover classes. The columns represent the reference data derived from validation areas and the rows the user data derived from the classification results 177

Chapter 6

Table 6.1 Habitat-specific correction factors (HSCF), the associated standard deviation (SD) and the root mean square error (RMSE). 191

Table 6.2 Error statistic of the unmodified and user-modified DEM for each habitat cover class regard to GCP survey; where 'ME' is the mean error or vertical bias, 'SD' is the standard deviation and 'RMSE' the root mean square error. 193

Chapter 7

Table 7.1 Summary of the wetland category conversions relevant for this study due to inundation and erosion [modified from Clough *et al.* (2010)]. 200

Table 7.2 Summary of data used as inputs in SLAMM 203

Table 7.3 Site specific input parameters required for SLAMM 204

Table 7.4 Elevation inputs (EIN) specific for each habitat type 205

Table 7.5 Summary of the test specifications used for running sensitivity analysis in SLAMM 205

Table 7.6 Model parameters with sub-site specifications 207

Table 7.7 Input factors for SLAMM and assumed statistical distributions for the uncertainty analysis, where 'T' means triangular distribution (minimum, most likely, maximum) 209

Table 7.8 Vulnerability ranking for classifying irregularly flooded marsh (in 2013) converted into regularly flooded marsh 214

Table 7.9 UK default elevation ranges according to tidal ranges used in the modified SLAMM [Source: Pylarinou (2015)] 214

Table 7.10 Site parameters for original and modified SLAMM [Source: Pylarinou (2015)] 215

Table 7.11 Percentage of change of the model outputs per category respect the base case (Test1_5m), changing one input layer at a time and keeping the model parameter constant. 221

Table 7.12 Changes in the surface area (model outputs in hectares) of the each habitat type in comparison to the base case (parameters of the study site), varying ± 5, 10 and 15 % of inputs parameters directly related to saltmarsh habitats for a 1 m sea-level rise scenario in 2100; where SLR_{2100} is the projected sea-level rise by 2100, *HisTrend* site historical trend of sea-level rise, *GT* (great diurnal tidal range), *Reg-Accr* regularly flooded marsh accretion and *Irreg-accr* irregularly flooded marsh accretion. Numbers in bold indicate the maximum magnitudes of change for each input parameter, and highlighted cells state 'non-linear' behaviours for each input parameter in each category. 230

Table 7.13 Model results in hectares for Tidal flat and Low marsh habitats using the original SLAMM (v6.01), the modified SLAMM with zero erosion rates (Modified_E_0) and the modified SLAMM with erosion rates estimated for the Odiel saltmarshes (Modified_E_1). 241

Table 7.14 Sensitivity of each habitat map category to spatial layer input data. Those cells that were ticked showed sensitivity to the input data described in each column. 243

Table 7.15 Disadvantages and advantages of sea level affecting marsh model (SLAMM) 247

1. Introduction and literature review

1.1. Overall study aim

Coastal ecosystems are considered to be sensitive to changes in environmental forcing, particularly sea-level rise. Saltmarshes occupy a discrete lateral and vertical position that is fundamentally controlled by the position of sea level, but the nature of other mesoscale factors such as shoreline dynamic (which affects erosion and sedimentation processes) and anthropogenic modifications to the coastal zone ensure that the nature and extent of impacts and response are globally variable, and locally complex. In this context, there is a need to understand these controls and to predict the potential response of saltmarsh systems to sea level change at the local scale. This is challenging though because of the limited detailed and accurate information about these environments at local scales, and the issues related to model systems at landscape scales. Although saltmarshes present a challenging environment, the high ecosystem value and their vulnerability to sea-level rise mean that monitoring of change, and modelling of future responses are important research and conservation aims. The main aim of this thesis is focused on the use of LiDAR data and imagery for mapping saltmarsh habitats and as a basis for spatial models of their response to sea-level rise under- Mediterranean-Atlantic saltmarshes. This is demonstrated through application to the saltmarshes found in the Tinto-Odiel estuary (Huelva, NW Spain).

1.2. Nature and importance of saltmarshes

Saltmarshes are coastal wetlands found extensively along low wave energy coastlines (Chapman, 1974; Allen & Pye, 1992; Adam, 2002) and are the product of fine sediment accumulation and vegetation establishment (Davidson-Arnott *et al.,* 2002). They comprise low-lying areas covered by halophytic vegetation that is adapted to regular flooding by the tide, and are typically dissected by networks of tidal channels (Figure 1.1) (Broome *et al.,* 1988; Pethick, 1992; Allen, 1997; Allen, 2000). The scale of their extent (which range from tens to thousands of hectares) can vary depending on local conditions, tidal range and geographical constraints (Allen, 2000). Globally they are located throughout the mid- to high latitudes, but are replaced in the tropics and sub-tropics by mangrove systems (Allen & Pye, 1992). The latitudinal and geographic range contributes significant spatial variability in saltmarsh geomorphology, lateral and vertical extent, and plant species communities (Long & Mason, 1983).

Figure 1.1 Aerial view of saltmarsh environments in Southwest Spain [Photo taken by Jose Antonio Fernandez in 2011]

Prior to the mid-20th century, saltmarshes were often viewed as 'swampy waste lands', and have historically suffered from human activities that have intensively modified them (Doody, 2008; Adam, 2002; Silliman *et al.,* 2009; Gedan *et al.,* 2009). However, in the 1960s, attitudes began to change when international organisations drew attention to the rapid degradation and loss of wetlands (Lefeuvre *et al.,* 2003) and in order to protect worldwide wetlands, international initiatives such as the MAR conference (1962) and the

Ramsar Convention (1971) were set up. These milestone initiatives set in motion an acknowledgement and understanding of how highly valuable these habitats are.

Saltmarshes provide a myriad of important ecosystem services that range from their role in coastal ecosystem functioning such as nutrient cycling, primary and secondary productivity, and decomposition (Nixon, 1980; Costanza *et al.,* 1997; UNEP, 2006), to contributing to human well-being by providing food, fibres, water purification, climate regulation, flood regulation, coastal protection, recreational opportunities and tourism (Millennium Ecosystem Assessment, 2005; Turner *et al.,* 2008). They are among the most productive of coastal ecosystems (saltmarsh plants can produce between 100 and 1000 $gCm^{-2}y^{-1}$ (McLusky & Elliot, 2004)), providing more ecological services to coastal populations than any other coastal environment (Costanza *et al.,* 1997). For example, with regard to coastal vulnerability, saltmarshes offer protection against storm surges and tsunamis (Gedan *et al*. 2009), and act as natural sea barriers minimising waves and flooding effects in coastal settlements (King & Lester, 1995).

Saltmarshes also play a major role in coastal (Gordon *et al.*, 1985; Kaswadji *et al.*, 1990) and estuarine food chains (Gordon *et al.,* 1985; Lefeuvre & Dame, 1994; Zedler & Callaway, 2001; Nixon, 1980), sustaining fishery species (Heck *et al.*, 1989; Boesch & Turner, 1984). These intertidal environments are areas of high primary production (Gordon *et al.,* 1985; Kaswadji *et al.,* 1990), contributing to roughly 20% of the total net biosphere primary production (Duarte & Cebrian, 1996) and their varied halophytes communities provide diverse habitats for wildlife such as birds, fishes, crustaceans, macroinvertebrates, amphibians and mammals. Furthermore, these environments account for 90% of the world's fish catch (UNEP, 2006). They act as nurseries for many species of fish and do so for two main reasons: the food chain is based on the high production of vascular plant detritus, and the existence of refuges for escaping from predators (Boesch & Turner, 1984). Their shallow and spatially complex habitats generate diverse refuges for many fish species that develop partially or completely within their life cycle in these environments.

In the context of climate change, saltmarshes have acquired a newfound significance as carbon sinks (Chmura *et al.,* 2003). Plants such as *Spartina spp*. have been shown to function as a net sink of CO_2 from the atmosphere (e.g. Gribsholt and Kristensen, 2003; Wang *et al.*, 2007), thereby having an important role in carbon cycling (Cai *et al.,* 2003; Sousa *et al.,* 2010). In estuaries, the gross primary production enables CO_2 capture from the atmosphere and production of organic carbon (Sousa *et al.,* 2010).

The high value of ecological services that saltmarshes provide and the importance they play in coastal ecosystems and populations is no longer in doubt, but saltmarshes remain vulnerable to continued pressures from climate change and anthropogenic

activities (e.g. Hartig *et al.*, 2002). Saltmarshes face the threat of permanent inundation from accelerated sea-level rise combined with decreasing opportunities for upslope migration due to extensive human development of coastal areas (Smith, 2009). Thus, in the context of global change and sea-level rise, the study and conservation of these important intertidal ecosystems should be prioritised.

1.3. Saltmarsh formation, development and zonation

Contemporary saltmarshes have evolved under varying directions and rates of sea level change. In particular, the sea level changes that have characterised the Quaternary (comprising the Pleistocene and Holocene epochs) (Tooley, 1992) have driven significant shifts in shoreline position and as a consequence facilitated the development of coastal sedimentary environments such as saltmarshes. During the last glaciation maximum (in the late-Pleistocene around 20,000 years BP) global sea level was roughly 120 m below present (Fairbanks, 1989; Siddall *et al.,* 2003; Lambeck & Chappel, 2001). There is limited information about the geomorphology of the coastline at this time (Kennish, 1986), but the likelihood of areas supporting saltmarshes would have been low due to climate conditions and the limited accommodation space (Adam, 1990; Wolanski *et al.,* 2009).

As global temperatures warmed in the early-Holocene, global sea level rose quickly as a consequence of eustatic processes. Between 15,000 years BP to 7,000 years BP sea level rise was roughly 10 mm yr^{-1} (Fairbanks, 1989; Lambeck *et al.,* 2002), leading to great changes to coastlines. Adam (1990) posits that during this time, the rate of change of the coastline position would possibly have been too much to allow for widespread and comprehensive marsh development.

However, from 7,000 years BP onwards, the global sea level stabilised to within metres of the present level with relatively small fluctuations (Lambeck *et al.,* 2002; Lambeck & Chappel, 2001) which enabled, in conjunction with the right natural conditions, the creation of the present saltmarshes known as the *Holocene saltmarshes*. From a holistic point of view, *Holocene saltmarshes* are complex morphosedimetary systems that are a product of various interrelated components and factors (Allen, 2000). The main forcing factors and the linkages have been well-described by several authors (Reed, 1990; French, 1991, 1993; Allen, 2000) who have considered the relative importance, and eco-morphodynamic feedbacks associated with changes in relative sea level and tidal range, mineral sediment supply, productivity and autocompaction at the marsh surface (Figure 1.2).

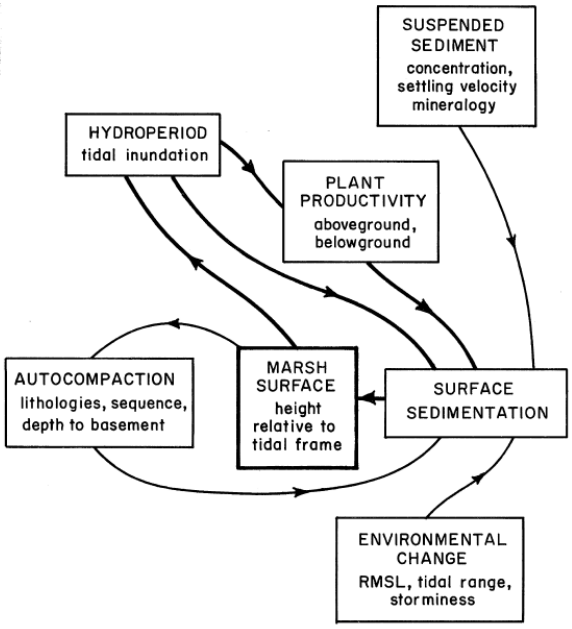

Figure 1.2 Forcing factors and linkages of saltmarsh system (Allen, 2000)

The *Holocene saltmarshes* can be traced back to c. 6,000-7,000 years ago (Redfield, 1972; Thomas & Varekamp, 1991) but many are much younger (Adam, 2002). Generally, youthful allochthonous (minerogenic) marshes grow rapidly and can mature in a few hundred years; most saltmarshes within Europe are minerogenic (Adam, 2002), which reflects both climate controls on vegetation development and productivity, but also sediment supply. Allochthonous (organogenic) marshes are usually dated from earlier due to the physical and sediment supply conditions on the coastal marsh by that time, when peats were free to form (Allen, 2000). For example, in Massachusetts and Louisiana (USA), minerogenic saltmarshes date back to roughly 3,000-4,000 years ago (Pendland *et al.,* 1987) and a relic saltmarsh peat found on the continental shelf from 5,000-11,000 years ago (Fairbridge 1960; Bricker-Urso, *et al*. 1989).

Saltmarshes formed in the late-Holocene have generally evolved in the context of other coastal sedimentary environments that have developed during this period, such as barrier islands, spits, embayments, and lagoons (Allen, 2000; Adam, 2002). These systems have largely provided more accommodation space than those developed in open coasts of previous colder climates, and secondary structures such as spits and barrier islands have facilitated low-energy conditions that have favoured the deposition of fine sediments for saltmarshes to form. Formation and evolution of *Holocene saltmarshes* is linked to climate, relative sea level position, physical shoreline structure and coastal dynamics (e.g. tidal range, sediment supply) resulting in large diversity of geomorphologic forms.

The early stages of saltmarsh development require low sloping intertidal accommodation space where low wave energy dominates and there is a ready supply of

fine sediment (Pethick, 1992; Allen, 2009). Saltmarsh formation is mainly controlled by the capability of an intertidal system to retain fine sediment and to accrete its elevation (Boorman, 2003), which it is possible when tidal streams are slack during the low and high water (Allen, 2009; Allen, 2000). However, the settle sediments can be eroded and re-suspended, depending of ebb/flood currents dynamics (Allen, 2009) and the nature of the sediments (Long & Mason, 1983).

Once the optimum elevation for vegetation establishment (MHWN) is reached (B in Figure 1.3), halophyte seeds distributed by tidal water (Chang *et al.*, 2007; Huiskes *et al.*, 1995) may germinate when they find the optimal salinity conditions (Ungar, 1978; Chapman, 1974; Naidoo & Naicker, 1992). Initial plant colonisation of tidal flats reduces the speed of tidal flows and facilitates sediment trapping, stabilization and sedimentation (Erfanzadeh, 2010; Lopez & Garcia, 1998; Neumeier & Ciavola, 2004), which alters the hydrodynamics of the intertidal system and facilitates vertical accretion of the marsh platform (Nepf, 1999; Nepf *et al.,* 1997; Leonard & Reed, 2002). As the marsh surfaces builds up, depth of inundation (over the marsh surface) decreases, which reduces tidal sedimentation and increases bio-productivity, leading saltmarshes toward an equilibrium elevation relative to mean sea level (Morris, 2007; Morris *et al.,* 2002).

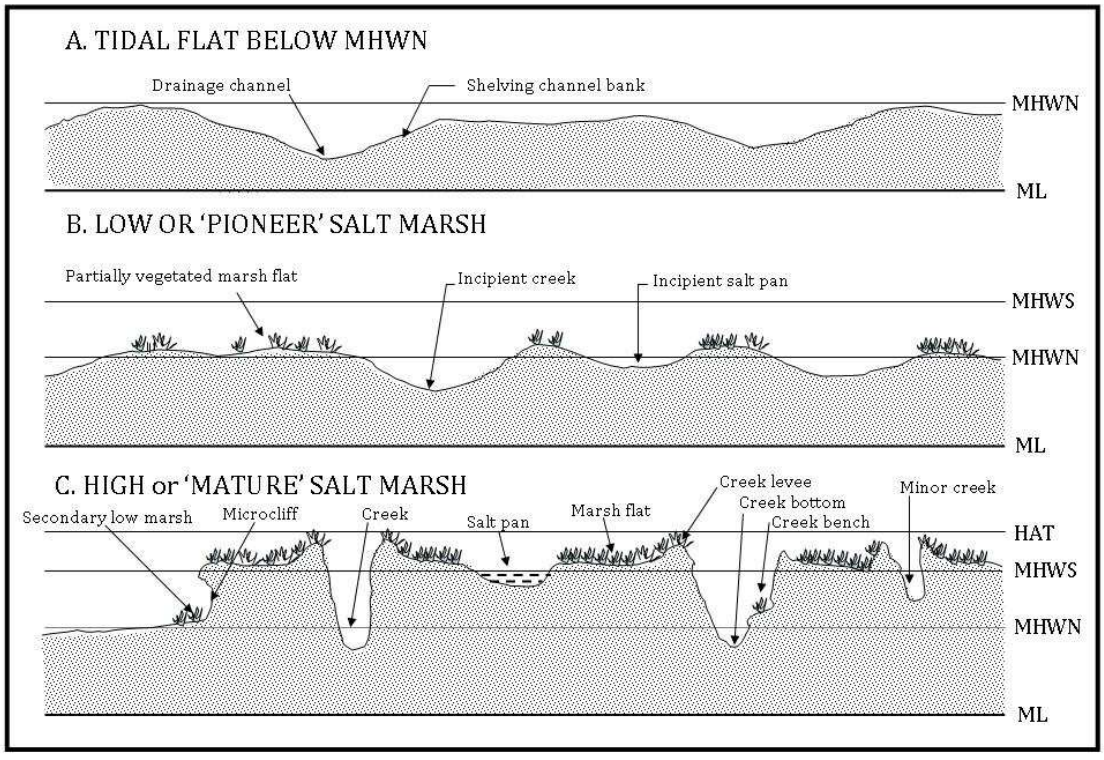

Figure 1.3 (A) High level tidal flat. (B) Low level marsh in which vascular plants have colonized the higher points of the tidal flat. (C) High marsh with a fully vegetated surface, except for the creeks and pans which are sharply defined by their steep banks [Source: modified from (Long & Mason 1983)].

Pioneer plant colonisation drives topographic changes due to both surface accretion and influence on tidal flow, leading to the development of creek networks (C in Figure 1.3). Increased deposition leads to further accretion and the saltmarsh surface builds up through the tidal frame; this shift in vertical position drives a change in species assemblages as a result of changes in environmental stress and competition (Erfanzadeh, 2010; Castellanos *et al.,* 1994; Bertness & Callaway, 1994; Hacker & Bertness, 1995; Bertness & Yeh, 1994). Saltmarshes that have accreted to the highest elevations of the tidal frame can be described as a mature and stable climax ecosystems (Odum, 1971). This vegetation change may respond primarily to an elevation gradient resulting in plant zonation that might be related to succession processes, which are also influenced by abiotic and biotic factors. However, zonation in saltmarshes does not always show clear boundaries and is created by different and commonly overlapping vertical ranges of individual plant species (Gray, 1992).

Early ecological studies of saltmarshes (e.g. Chapman, 1939, 1941) have provided the basis for the understanding of saltmarsh development, zonation and vegetation succession, which were focused on understanding the presence and controls on species distribution and zonation patterns. However, since those early investigations, spatial and temporal patterns of halophytes, and their interactions with local physical and biotic factors, remain largely uncertain due to the complexity of vegetation dynamics in saltmarshes (Silvestri & Marani, 2004). Vegetation response to interactions between environmental controls may change geographically, and this complicates the general understanding of spatial organisation of species and habitats.

Broadly, ecological conditions in saltmarshes can range from marine-dominated to terrestrial-dominated influences (Pielou & Routledge, 1976; Doody, 2008), forcing patterns of habitats and organisms, and often zonation (Frey & Basan, 1978; Saintilan *et al.,* 2009). In general, saltmarsh plant zonation can be considered at two levels: ecosystem level and sub-environment or habitat level (Frey & Basan, 1978). The first level mainly relates to changes from strictly marine halophytes (e.g. Zostera), through to those species tolerant of high salinities (e.g. Salicornia), and those limited between brackish and terrestrial conditions (e.g. Juncus). The second level refers to differences in plant species features or growth forms caused by variations in the micro-habitat (e.g. Salicornia and Spartina ecotypes) (Frey & Basan, 1978).

As the saltmarsh develops, some parts of the marsh evolve into older and more mature ecosystems occupying higher elevations and comprising increased species diversity (Adam, 1990; Long & Mason, 1983; Frey & Basan, 1978) associated with terrestrial influences caused by the reduction of tidal submersion. Those areas located in higher topographic position are commonly referred to as 'high marsh' and those found in

low elevations, which are younger, as 'low marsh'. However, boundaries on these zones are not always clear with distance from the sea (Chapman, 1974; Frey & Basan, 1978) due to the effect of micro-topography (e.g. depressions, hummocks, creeks) (Boon *et al.,* 2011) and the broad tolerance of some species which can be found across a large range of marsh/coastal margin elevations (Adam, 1990).

Additionally, saltmarsh vegetation does not always follow a clear succession pattern, and other factors (e.g. climate variation or disturbances) may play an important role (De Leeuw *et al.,* 1993; Erfanzadeh, 2010). Hence, the idea of zonation as belts parallel to the shore with a well-defined successional (chronosequence-based) gradient is controversial and some authors have argued for an appreciation of greater complexity of these processes in the saltmarsh environment (e.g. Frey & Basan, 1978; Adam, 1990; Gray, 1992; Saintilan *et al.,*2009; Erfanzadeh, 2010). For example, Gray (1992) states that "essentially, it must not be assumed that zonation along an elevational gradient (a spatial feature) has been wholly, or partly, generated by succession (a temporal phenomenon)".

Some studies show that ecological zonation is not consistent between sites, even when considering vertical (tidal frame) position (Frey & Basan, 1978; Adam, 1990; Boorman *et al.,* 1998; Nixon, 1982), and the identification of biological criteria to define universally comparable zones is not possible (Adam, 1990). This is because ecological boundaries are relative rather than absolute (Long & Mason, 1983), and environmental forcing (e.g. tidal regime, wave climate, microclimate) is not geographically consistent. For example, on large tidal amplitude coasts exposed to some wave action, the low marsh may start near to mean high water (MHW), whereas on sheltered coasts with low tidal amplitude, vegetation can begin closer to mean low water neaps (MLWN) (Beeftink, 1977). Therefore it is very difficult to generalise, and the criteria for defining zones may vary from coast to coast. However, there is a general consensus that the lower boundary of vascular plants is controlled by tolerance of saltwater submersion, whereas the upper limit is governed by interspecific competition (Pielou & Routledge, 1976; Gray, 1992; Gray, 1980; Gray, 1985; Emery *et al*., 2001).

1.4. SW Iberian Peninsula saltmarshes in a global and European context

At global scales, typologies of saltmarshes are dominated by studies from the 1970-1980s, such as Chapman (1974) and Adam (1990), which were based on vegetation distribution. Chapman's (1974) seminal work grouped saltmarshes according to community and species distribution, and has provided the basis of most general discussions of global distribution of saltmarshes (Adam, 1990, 2009). His observations implied that plant species richness could vary significantly among different regions, suggesting after further investigations that globally, saltmarshes fell into different groups characterised by distinct vegetation types. In his work, 15 saltmarsh types (based mainly on vegetation types) were defined; a further step of this work sub-divided some of the most common types into smaller groups based on sediment and local coast characteristics.

Adam (1990) used Chapman's (1974) work as a basis of his proposed typology but hypothesised that certain classes created in Chapman's typology, due to geographical differences in species, were not warranted given that there are many genera which are common across geographic regions. Listed below are Adam's revised global saltmarsh types:

1. Arctic
2. Boreal
3. Temperate
    a. European
    b. Western North American
    c. Japanese
    d. Australasian
    e. South African
4. West Atlantic
5. Dry Coast
6. Tropical (seasonal or permanent dryness)

According to Adam (1990), saltmarshes in southwest Spain and Portugal (the Iberian Peninsula) would come under the *Dry Coast* type rather than, intuitively, the *Temperate – European* type as this geographical area is influenced by proximity to the Mediterranean and is subjected to a seasonally dry climate and high soil salinities regimens. He notes that in this type of saltmarsh the vegetation is '*characteristically fairly open and dominated by low shrubs, most frequently succulently stemmed shrubby chenopods*' which is a fair description of saltmarsh vegetation in South-Atlantic Iberian Peninsula. However, Adam left the *Dry Coast* type partially unrefined by stopping short of defining subclasses as he felt that to do so would have resulted in a bias towards the

Mediterranean[1] coastline which would not have been a true reflection of the considerable vegetation diversity that exists globally. Finally, he specifically suggests that saltmarshes found on the South-Atlantic Iberian Peninsula could be considered an extreme of the *Temperate* class. Adam considered the creation of a new class *semi-Mediterranean* to emphasise the intercontinental affinities.

It has been roughly 20 years since Adam published his typology and it seems that there has been no significant progress in the development of global saltmarsh typology. However, there have been studies that have attempted to compare the saltmarshes found in the *Dry Coast* type environments. For example, Peinado *et al.* (1995) studied the vegetation patterns between saltmarshes found in California, Baja-California and on the Iberian Peninsula, and found distinct phytosociological similarities. Considering saltmarsh plant community studies in South Africa (Day, 1981), California (Macdonald, 1977b; Macdonald, 1977a) and southwest Iberia (Gehu & Rivas-Martinez, 1984), similarities can be also found, where a *Spartina* marsh (*S. maritima* or *S. Foliosa*) dominates the low marsh and a range of low shrubs (principally chenopods) occupy the mid and upper marsh. Comparison of these studies supports the saltmarsh patterns discussed in Peinado *et al.* (1995), showing that southwest Iberian saltmarshes have more similarities with California saltmarshes than with European ones.

Another work that is worthy of mention here is Britton & Crivelli (1992), which includes reference to saltmarshes within a global inventory of wetlands. A continental scale grouping is divided into similar bio-climatic sub-regions, describing the physical and biotical setting of the major wetland types in each sub-region. In contrast to the Chapman/Adam typologies, this scheme places south Europe and North Africa into the same group -*Mediterranean wetlands*- recognising the similarities of these zones. Within the Atlantic division of *Mediterranean wetlands*, tidal wetlands are defined and characterised by five classes:

i. permanently flooded estuaries;
ii. unvegetated sand and mud flats;
iii. vegetated flats colonised by *Zostera noltii, Z. nana or Ruppia maritima*;
iv. saltmarshes that flood at most high tides and are dominated by *Spartina maritima* and *Salicornia* sp.; and
v. saltmarshes that flood only at spring tides (characterised by *Arthrocnemum* spp.)

The classes defined here reflect habitats that occur within the tidal wetland in this region rather than specifically relating to saltmarsh. But this provides a fair description of the different habitats that occur in southwest Iberia and the Atlantic coast of North Africa.

[1] which interestingly strengthens the relevance of this type for the Iberian peninsula, but then weakens it for global comparison purposes.

More generally, it would seem that there is not a vast amount of literature devoted to this topic at a global scale and the small number of studies referring to global saltmarsh typologies may be a reflection of the regional and local variability of worldwide saltmarshes and the complexity of classifying them.

Out of the currently available studies of saltmarsh classification, saltmarshes in Europe are broadly classified based on vegetation (bio-geographical regions) and geomorphology. Table 1.1 summarises the current state of studies relevant for the present study. Classes based on vegetation are restricted to biogeographical zones whereas geomorphic types in many cases have little association with vegetation. Ecological typologies depend on climate conditions whereas geomorphic typologies express tidal range and physiographical constraints.

Table 1.1 Summary of the most relevant European saltmarsh typology studies

Scope	Vegetation-based	Geomorphology-based
Europe	Beeftink (1966); Géhu (1972); Westhoff & Schouten (1979); Géhu & Rivas-Martinez (1984)	Dijkema (1984, 1987)
NW Europe		Pye & French (1993)
Southwest-Iberia	Peinado *et al,* (1995); Sanchez *et al.* (1998), Costa *et al.* (2009);	

Biogeographic controls impact species composition and growing season, and this imposes a clear north-south pattern. For example, northern marshes have a simpler structure influenced by a limited growing season, and southern marshes are characterised by year-round continuous growth controlled by temporary summer droughts (Boorman, 2003). These vegetation differences have enabled the division of Europe saltmarshes into different regions such as those presented by Beeftink (1966), Géhu (1972), Westhoff & Schouten (1979) and Géhu & Rivas-Martinez (1984) on the level of vegetation units based on Western Europe surveys.

For example, Géhu & Rivas-Martinez (1984) proposed a saltmarsh typology based on the distribution of saltmarsh flora. They defined five main biogeographical regions and 7 sub-zones (Figure 1.4). Within this typology, the Mediterranean region (3) is divided into five zones: Mediterranean-Atlantic, Mediterranean-Tyrrhenian, Inland Iberian, eastern Mediterranean zone and the special zone of northern Adriatic. Here, the Mediterranean-Atlantic zone (3a) covers the southwest of the Iberian Peninsula and northwest of Morocco as a separate zone from the rest of the Mediterranean saltmarshes due to the persistence of Atlantic species such as *Puccinellia maritima* and *Spartina maritima* (Gehu, 1984). Thus, the vegetation found in southwest Iberian saltmarshes tends

to be different from that found in the Mediterranean basin or in euro-Siberian saltmarshes, and shows similarities to those found in north-Atlantic Africa.

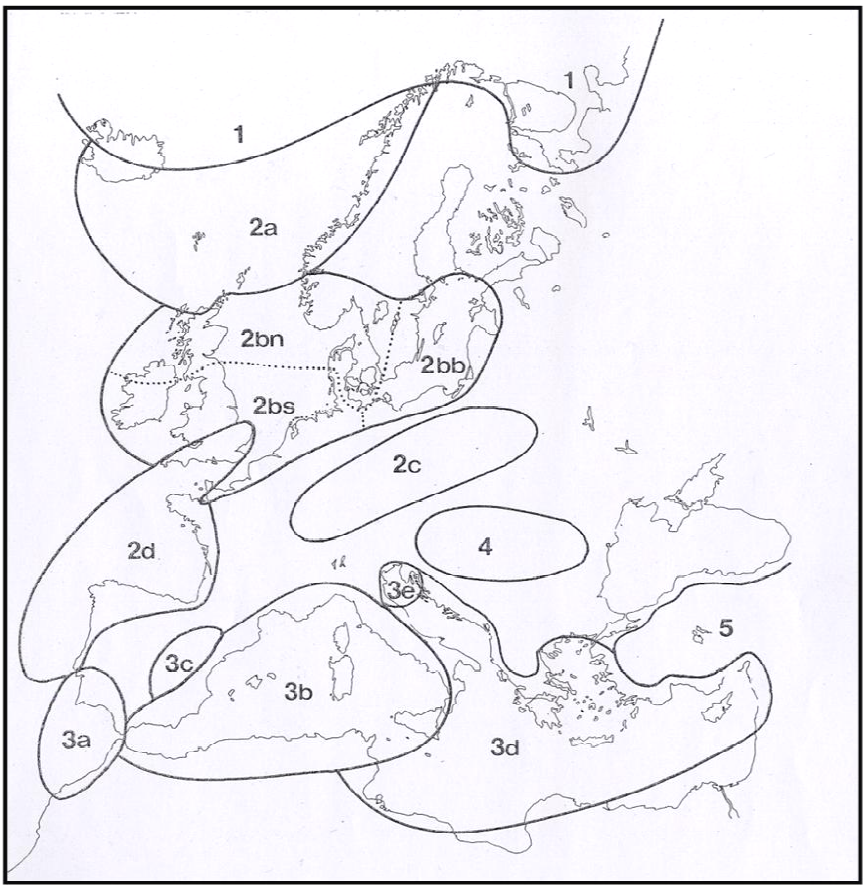

Figure 1.4 Biogeographic regions of European saltmarshes. The main regions are (1) Artic, (2) euro-Siberian, (3) Mediterranean, (4) the Pontic region and (5) the Irano-Turanian region. The euro-Siberian zone is divided into four sub-zones: (2a) Boreo-Atlantic, (2b) North Atlantic-Baltic, (2c) Sub-Atlantic and (2d) Cantabro-Atlantic. The Mediterranean region is divided into five sub-zones: (3a) Mediterranean-Atlantic, (3b) Mediterranean-Tyrrhenian, (3c) Inland Iberian, (3d) eastern Mediterranean zone and (3e) the special zone of northern Adriatic. [Source: Géhu and Rivas-Martinez (1984)]

Costa *et al.* (2009) compare Eurosiberian vs. Mediterranean (sub-zone: Mediterranean-Atlantic) saltmarshes, confirming the results of Gehu and Rivas-Martinez (1984). They explain that colder air from the Atlantic and the larger tidal regime compared to those saltmarshes in the Mediterranean basin are essential factors that distinguish halophytic plants and communities in these two sub-regions (Costa *et al.*, 2009). Vegetation distribution in Eurosiberian saltmarshes is controlled by tidal inundation and soil saturation (Sanchez *et al.,* 1998), but in the microtidal Mediterranean basin, distribution may be related to other processes such as the salt water hydrology movements and, in the summer, the presence of a saline phreatic sheet (Corre, 1978). In southwest Iberia, halophytes are influenced by both the seawater inundation period and the salt content of the phreatic sheet (Costa *et al.,* 2009), explaining the unique

characteristics of the plant communities of these areas in a European context. These features have further implications for the ecology and geomorphology that probably make their functioning different to other European saltmarshes. Due to the Atlantic influence on the tidal regime in these saltmarshes, from here to onward these saltmarshes will be referred to as south-Atlantic Iberian saltmarshes.

Based on geomorphological features, the studies focusing on Europe have tended not to cover the Mediterranean and far southwest in detail in comparison to northern regions. Saltmarsh biotopes of Europe were identified by Dijkema's (1983) saltmarsh inventory of Europe (Table 1.2). Based on this broad inventory, he proposed a geomorphological classification distinguishing autochthonous vs allochthonous saltmarshes, and grouped European saltmarshes into five main classes and 12 sub-classes. Pye & French (1993) proposed a classification that has many similarities with Dijkema's, but with classes more representative of northwest Europe that link with neighbouring sedimentary environments such as mudflats and/or sandflats (Figure 1.5). In Pye and French's (1993) classification, saltmarsh types such as *lagoonal saltmarshes* or *salines,* which are very common in the Mediterranean, are not described. Drawing from these classifications and the geomorphological description of this coast by Ojeda (1988), the saltmarshes of the south-Atlantic Iberian saltmarshes can be classified as follows:

Table 1.2 Saltmarsh biotopes on a geomorphological base. The proportional distribution of sites per region is shown based on Dijkema inventory [source: Dijkema, 1984; page 9].

Development		Saltmarsh Type	Code	Fenno-Scandinavia	North Sea + Wadden S.	Great B. Ireland	South Atlan (Fran., Sp., Port.)	Mediterranean West (+Fran.)	Mediterranean East (+Italy)
Marine Transport	Rocky shore	Ria bay	A 1 a						
		Loch/fjour	A 1 b						
		Beach head	A 1 c						
	Sedimentary shore	Barrier connect.	A 2 a						
		Lagoonal	A 2 b						
		Foreland (+coastal plain con.)	A 2 c						
		Estuarine	A 2 d						
		Saline	A 2 e						
Autochthonous material	Shore types	Land upheaval, flat	B 1 a						
		Land upheaval , skerry	B 1 b						
		Peat type	B 1 c						
River deposition	Deltaic shore	River plain	c						

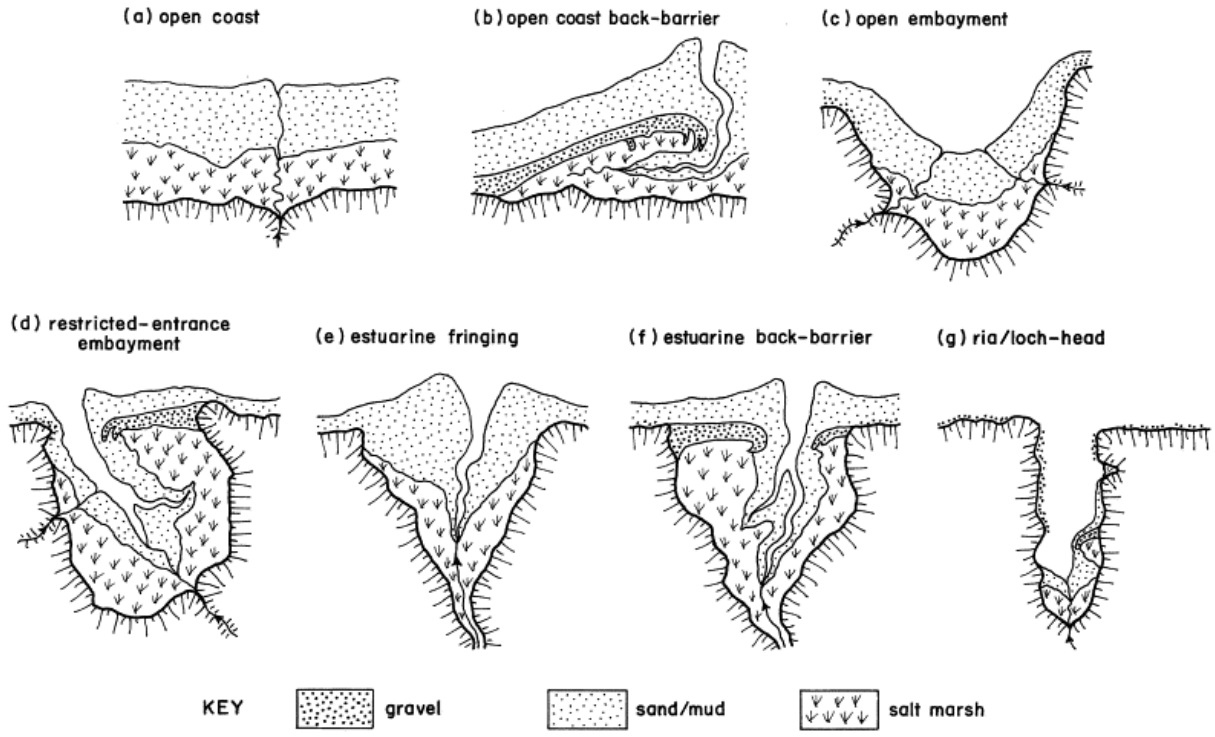

Figure 1.5 Geomorphological types of saltmarsh [Source: Pye and French, 1993].

Barrier connected saltmarsh (Dijkema (*A2a*); Pye and French (*b*))

- saltmarshes that are developed on the lee side of various types of barrier/spits or barrier islands or on beach plains
- they are found in the province of Huelva, SW Spain (e.g. Ayamonte, rio Piedras, rio Odiel and Tinto) and in Faro, S-Portugal

Foreland saltmarshes (Dijkema (*A2c*); Pye and French (*d*))

- saltmarshes developed on the seaward margin of alluvial coastal plains sheltered by a barrier-protected sea, a shallow bay or some tidal flats
- they can be found in the province of Huelva (e.g. Ayamonte, rio Piedras, rio Odiel and Tinto) and Cadiz (e.g. rio Guadalete)

Estuarine saltmarsh (Dijkema (*A2d*); Pye and French (*e*))

- the brackish zone located in estuaries (defined as semi-enclosed systems in free connection with the open sea)
- they can be found in the Huelva coast (e.g. Ayamonte, rio Piedras, rio Odiel and Tinto) and in the Algarve coast (e.g. Lagos and Portimao).

Salines (Dijkema (A2e); not defined in Pye and French)

- saltmarshes that have been turned into salt factories or fish-farms
- usually have halophytes on dikes and when they are abandoned, low marsh vegetation conquers the basins

- they are found in Castro Marin (Portugal), in the province of Huelva (e.g. rio Odiel), and in the province of Cadiz (e.g. rio Barbate and rio Guadalete).

1.5. Contemporary sea-level rise and saltmarshes

Saltmarsh environments are considered to be sensitive to changes in environmental forcing, particularly to sea-level rise (Luque *et al.,* 1998; Adam, 2002; Smith, 2009; Nicholls, 2004; Nicholls *et al.,* 1999; EEA, 2008; IPCC, 2007). Therefore the understanding of historical trends and future projections of this phenomenon and their geographic variations are extremely important. In this context, in order to study local development and responses of saltmarshes, it is essential to understand both global and local sea-level change, fluctuations and how these affect and physical processes (e.g. inundation, sedimentation and salinity regime) and therefore ecosystem dynamics, in the past, present and future.

Published studies (Table 1.3) corroborate increasing trends in observed *global sea-level rise* (GSLR) during the last century, indicating rates ranging between 1 and 2 $mmyr^{-1}$. Based on corrected gauge records[2] from the Permanent Service for Mean Sea Level (PSMSL[3],) data, several investigations (Miller & Douglas, 2006; Church & White, 2006; Holgate & Woodworth, 2004; Douglas, 2001; Peltier, 2001) point out that global rates of rise are closer to 2 $mmyr^{-1}$ than 1 $mmyr^{-1}$ during the 20^{th} century. Steric[4] changes and glacial eustasy seem to be crucial factors that have contributed to this observed GSLR (Meehl *et al.,* 2007; Domingues *et al.,* 2008; Church *et al.,* 2011).

[2]Gauge records are corrected by models for the glacial isostatic adjustment (GIA), but not for other vertical movements. The error in tide-gauge based global average sea level change resulting from GIA is assessed as 0.15 mm/year (IPCC, 2007).

[3] PSMSL--Bidston Observatory, Birkenhead, England (www.pol.ac.uk/pmsl). It compiles world-wide records from over 1400 tide-gauge stations in different countries in order to estimate sea level trends. However, because of the poor quality of the records or short time series, only around 400 are useful stations (Gornitz, 1995).

[4] Changes in sea level due to density variation are referred to as *steric changes*.

Table 1.3 Estimates of GSLR from tide-gauge records [source: updated from Gornitz, 1995].

Rates (mmy^{-1})	Comments	References
1.1 ± 0.8	Many stations, 1807-1939	(Gutenberg, 1941)
1.5	Many stations, 1900-1975	(Klige, 1982)
1.2 ± 0.3*	130 stations, 1880-1982	(Gornitz & Lebedeff, 1987)α
1.75 ± 0.13 ^	84 stations, 1900-1986	(Trupin & Wahr, 1990)#
1.8 ± 0.1	21 stations, 1880-1980	(Douglas, 1991)#
1.8	25 stations, 1930-2000	(Douglas, 2001)#
1.7 ± 0.4	177 stations, 1948-2002	(Holgate & Woodworth, 2004) #
1.5 – 2.0	9 stations, 20th century	(Miller & Douglas, 2006) #
1.8 ± 0.3	1950-2000	(Church *et al.,* 2004)#
1.7 ± 0.3	Combined methods, 1870-2001	(Church & White, 2006) #
1.8 ± 0.3	1971-2008	(Church *et al.*, 2011)

*Value plus 95% confidence interval; ^Mean and standard deviation; α Long term crustal motion removed; # Glacio- and hydro-isostatic removed

On the other hand, rates in GSLR, based on satellite altimetry, are around 3.1±0.7 mmy^{-1} for the period 1993 to 2003 (Miller & Douglas, 2006; Cazenave & Nerem, 2004; Leuliette *et al.,* 2004), and around 2.5±0.4 mmy^{-1} (Cazenave *et al.,* 2009) for the period 2003-2008. Although these rates are appreciably higher than the average rate for the 20th century, short term sea-level rise is difficult to judge due to tidal periodicities which are up to 19 years in length. Unlike gauge records, data provided by satellites show the spatial variability of sea-level change at the regional scale (Figure 1.6). For example over the period 1992 to 2007, the rate of sea level rise range from 0-1 mmy^{-1} around southwest England, to 1.5-2 mmy^{-1} in southwest Spain and more than 4 mmy^{-1} in the Black Sea.

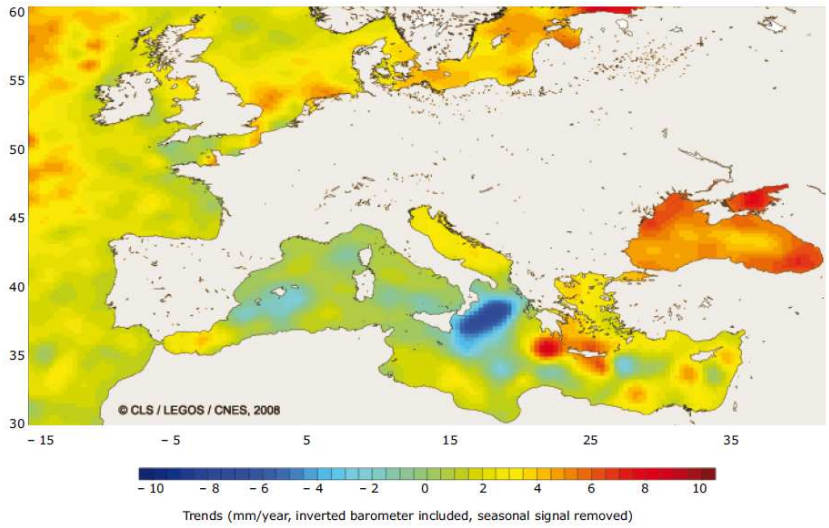

Figure 1.6 Sea level changes in Europe from 1992-2007 (map based on satellite altimeter data). [Source: Guinehut & Larnicol, 2008].

However, complex mechanisms over different time scales play a crucial role in sea-level change, which complicates the understanding of this phenomenon as well as the contribution of different processes (Rahmstorf, 2007; Meehl *et al.,* 2007; EEA, 2008). This has resulted in significant dissimilarities in future projections varying from 0.18 - 0.59 m over the period 1999 and 2100 based on physical models (Meehl *et al.,* 2007) to 0.5-1.4 by 2100 respect the 1990 level (Rahmstorf, 2007) based on semi-empirical models. In addition, Katsman *et al.* (2008), for the same period and method as Rahmstorf, predicts that GSLR possibly be ≥0.8 m in the northeast Atlantic Ocean. These results show that there are still significant uncertainties in future predictions, obscuring the magnitude of this phenomenon and therefore the severity of possible impacts in coastal areas.

Although there are still uncertainties about future GSLR projections, there are two things that are clear - we are certain that global sea level is rising and we are certain that it varies regionally - both of which are indicated in the trends from tide-gauges and satellite-altimeter data. With relation to saltmarshes, it is very important to consider local sea-level changes, regardless of cause, for local studies. In this sense, *Relative Sea-Level Rise*[5] (RSLR), which is affected by GSLR and vertical land movements (Pugh, 1987), is a crucial variable for foreseeing potential impacts in coastal areas and saltmarsh responses.

On the marsh surface, RSLR should be estimated as a function of GSLR, deep subsidence (deep primary compaction, secondary compaction and other processes such as tectonic activity), and shallow subsidence (primary compaction and decomposition in upper few metres sediments) (Rybczyk & Callaway, 2009). These variables have been identified in marsh conceptual models (Figure 1.7) as some of the main factors that govern adjustments of saltmarsh elevation in a context of sea-level rise (French, 2006). In this context, net elevation (considering deep subsidence autocompaction) in saltmarshes is subject to RSLR and sediment accretion. The saltmarsh net elevation will determine whether or not a saltmarsh will response positively (vertical accretion > sea-level rise) or negatively (vertical accretion < sea-level rise) due to sea-level rise. For example, saltmarsh systems have responded positively under moderate rates of sea-level rise (1-10 mmy^{-1}) as it has been shown in studies of sedimentary sequences (Redfield, 1972; McCaffrey & Thompson, 1980) corresponding to mid/late Holocene.

However, future net elevation is difficult to predict accurately due to multiple processes for estimating this variable operate at different scales (Figure 1.8) (Rybczyk & Callaway, 2009) and they are subject to numerous uncertainties such as future projections of GSLR and future shallow subsidence rates (for example, below-ground biomass is a

[5] 'Long-term, absolute vertical relationship between the land and the water surface' (Rybczyk & Callaway, 2009)

variable difficult to understand and model). Furthermore, the key linkages are non-linear, therefore historical data are only of limited value and process models are required for future predictions (French, 2006).

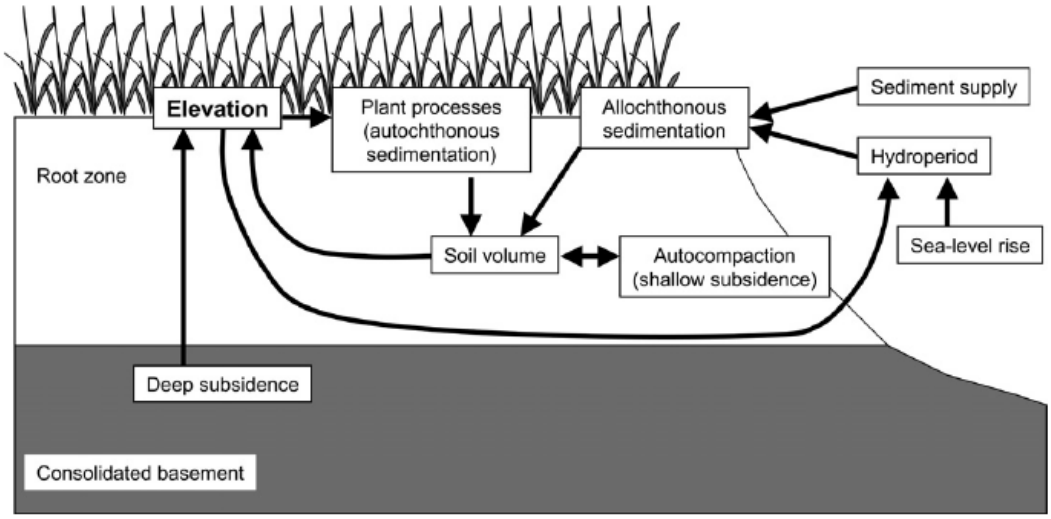

Figure 1.7 Conceptual model of principal factors governing adjustment of saltmarsh elevation within the tidal frame [Source: French, 2006]

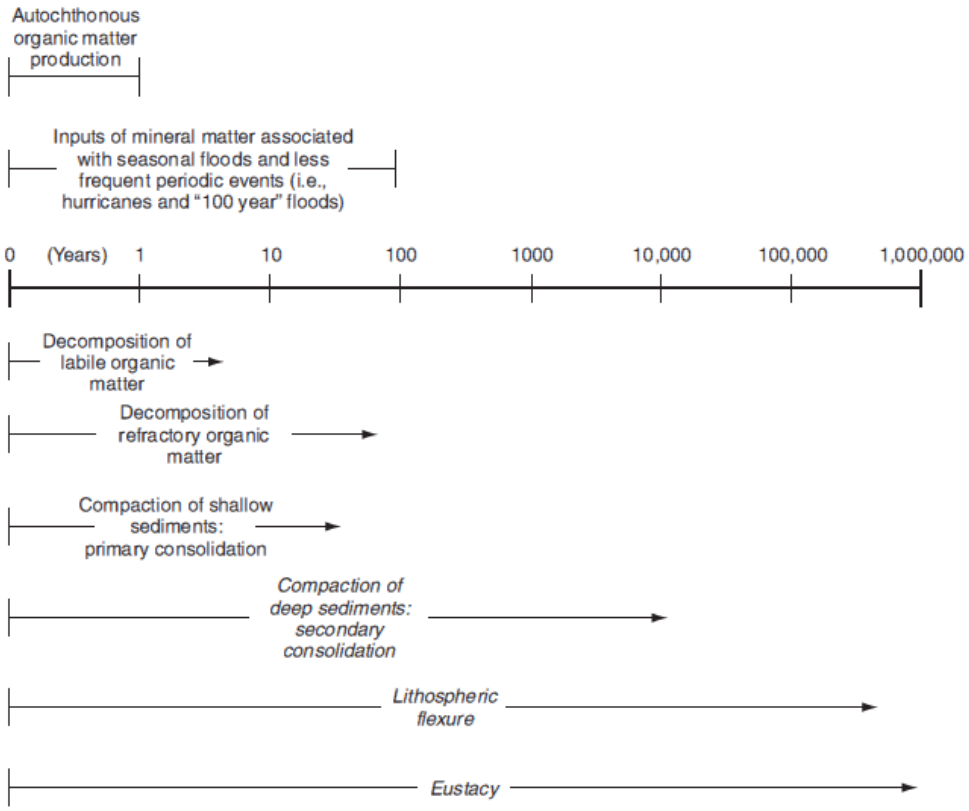

Figure 1.8 Processes that affect saltmarsh net elevation due to sea-level rise. Processes shown below the time line reduce elevation and those shown above the time line increase elevation. [Source: Rybczyk and Callaway, 2009]

Currently, those saltmarshes that respond positively to GSLR will accrete as sea-level rises and may remain stable during long time periods (Gornitz, 1995; Morris *et al.,* 2002; Rybczyk & Callaway, 2009), and those that respond negatively may face more frequent and longer inundation periods, which may induce habitat conversion or higher erosion rates. Tidal wetland loss through erosion, submergence, and related processes have been well-documented (Dean *et al.,* 1987; Titus, 1988; Allen & Pye, 1992; Wray *et al.,* 1995; Van der Wal & Pye, 2004), showing the importance of these issues.

Sea-level rise is not the only future threat for saltmarsh survival. For example, Nicholls (2004) reviews the potential sensitivity of inundation over certain coastal wetlands at local scales under all SRES scenarios proposed by IPCC[6] and concludes that there will be losses in all scenarios. However, he also stated that anthropogenic marsh destruction (e.g. land reclamation) is predicted to be larger in comparison with losses due to sea-level rise. Furthermore, the existence of land claim and hard infrastructures can be critical for the survival of saltmarshes in a context of sea-level rise. For example, Doody (2004, 2012) describe 'coastal squeeze' and report current and potential impacts over some saltmarshes in England. This term refers to the process where coastal habitats (such as saltmarshes) are retreat landward due to sea-level rise or other factors such as storminess (Doody, 2012), and they become squeezed into a narrowing zone due to artificial margins that have been created (e.g. coastal defences). This process potentially occurs in those areas where the saltmarsh accretion rates are lower than the sea-level rise rates and the only hope for surviving is to migrate inland. In this sense, the resilience[7] to sea-level rise of saltmarshes at local scales is strongly related to natural factors such as the RSLR and accretion, and also to anthropogenic factors such as habitat fragmentation, modification and destruction.

1.6. Predictive models of saltmarsh in a context of sea-level rise

During the last few decades, different models have been developed at different scales to understand saltmarsh evolution in the context of sea-level rise. The majority of these models are surface elevation models that investigate the relationship between sea-level rise and saltmarsh elevation (Reyes, 2009). Among those models, different types are found depending on the scale (Figure 1.9): zero-dimensional models, geomorphic/ecological models and landscape models. These models involve different processes operating at different scales and they can be very useful to simulate either or both the complex physical processes and the sedimentary response in saltmarshes. Although the modelling of

[6] Intergovernmental Panel of Climatic Change

[7] Here, resilience is understood as the capacity of ecological systems to absorb recurrent disturbances such as storms or floods and to retain essential structures, processes, and feedbacks (Adger et al. 2005).

saltmarshes has experienced considerable improvements (Allen, 1990; Allen, 1997; French, 1993; French, 2006; French *et al.,* 1995; Woolnough *et al.,* 1995; Temmerman *et al.,* 2004), the relative speed and frequency of geomorphological and sedimentological variability still need to be assessed at different time scales (Davidson-Arnott *et al*., 2002). For example, some of the medium- to long-term processes previously shown in Figure 1.7 (e.g. deep subsidence) are difficult to simulate due to the difficulties in extrapolating imperfectly understood sedimentation parameters beyond the time scale of observations (French, 1993).

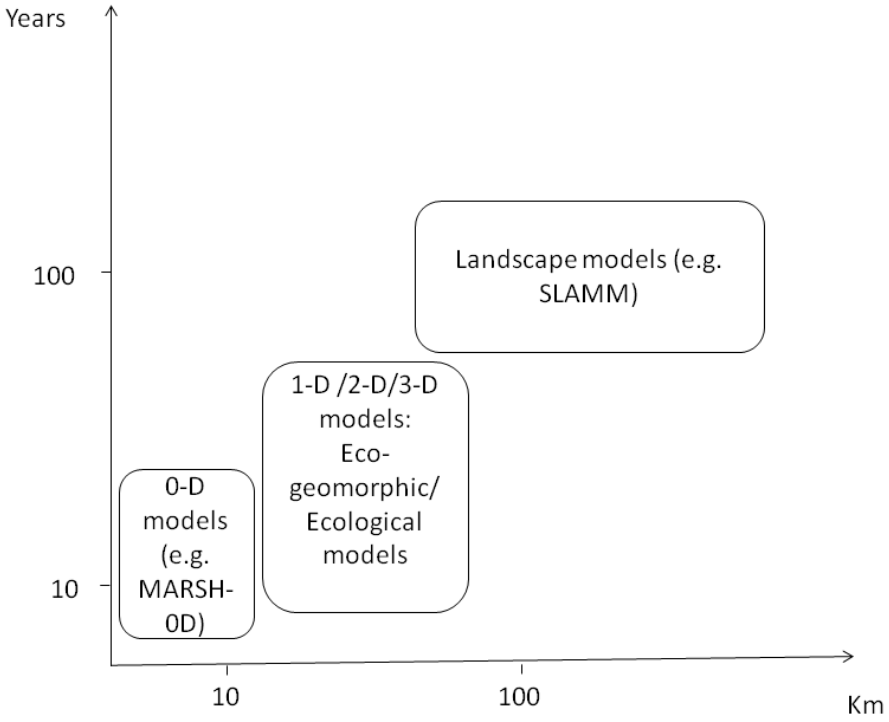

Figure 1.9 Spatial and temporal scales of predictive models used to estimate saltmarsh and estuarine processes in a context of sea-level change.

At the smallest spatial scale, zero-dimensional models are mainly focussed on simulating processes (e.g. elevation change) at one specific point of the saltmarsh. Tidal frame sedimentary infilling and factors controlling the equilibrium marsh elevation have been modelled by several authors (Krone, 1987; Allen, 1990; French, 1993; Allen, 1991), and as Allen (2000) posits, they involve numerical simulation of the basic mass balance equation

$$\Delta E = \Delta S_{min} - \Delta S_{org} - \Delta M - \Delta P \qquad (1.2)$$

where ΔE is the change in marsh surface elevation relative to a tidal frame of reference, ΔS_{min} is the inorganic sediment input added to the marsh surface, ΔS_{org} is the additional

thickness of organic sediment, ΔM is the change in relative sea-level and ΔP is the elevation change due to autocompaction of the marsh deposit.

The first zero-dimensional mass model to calculate sediment inputs in saltmarshes was developed by Krone (1987). He proposed an approach to simulate saltmarsh response to historical sea-level change (tested in the San Francisco Bay), based on suspended sediment concentration, elevations of water and marsh surface, and median settling velocity. The approach calculates the time-dependent sedimentation on a saltmarsh unit area, integrating tidal periods. Allen (1990) used a similar approach in order to understand long-term saltmarsh growth and response to changing external conditions. He tested a simple quantitative simulation model for the accretion of a saltmarsh within tidal limits in the Severn estuary (U.K.). Following a similar numerical scheme, French (1991) simulated regional subsidence and long-term marsh adjustments to tidal levels in the North Norfolk saltmarshes (U.K.). This sedimentary infilling approach was refined for application to allochthonous marshes through more complex models. For example, Morris *et al*. (2002) developed a model driven by changes in bioproductivity instead inorganic sedimentation.

More recent work, has incorporated the relationship between suspended sediment concentration (SSC) and inundation height (Temmerman, Govers, Meire, *et al.,* 2003; Temmerman *et al.,* 2004). Temmerman *et al.* (2003) showed that the SSC increases linearly with maximum inundation height, and noted that previous works assume a constant SSC, which underestimate the observed historical growth. Thus, it is important to include this relationship to successfully simulate the long-term vertical growth in tidal marshes.

Operating at a larger spatial scale, geomorphic and ecological models simulate physical and ecological processes across the marsh (Rybczyk and Callaway, 2009). If the model simulates processes across a marsh transect is referred to as 'one-dimensional model', and if it simulates processes across a marsh platform as 'two-dimensional model' (Fagherazzi *et al.*, 2012). Additionally, if geomorphic models include feedback between physical processes and vegetation, they are referred to as 'eco-geomorphic models' (Fagherazzi *et al.,* 2012). These models can simulate physical exchanges (Allen, 1994), biogeochemical processes within the system (Simas *et al.,* 2001), population dynamics (Nunes *et al.,* 2003) and marsh platform and creek network evolution (Reyes, 2009) for instance. Some of these models introduce spatial variation in order to simulate spatial patterns of different variables within the marsh. For example, sedimentation rates vary depending on marsh platform elevation and distance from tidal channels and the seaward marsh edge (Temmerman *et al.,* 2003; Bartholody, 2012). This recognises the importance

of the spatial variability in sedimentation rates which has also been implied in previous works (e.g. French and Stoddart, 1992; French *et al.*, 1995).

An example of a one-dimensional model is the continuity-based sedimentological model for the dominant types of tidal saltmarshes in the temperate zone developed by Allen (1994). This model provides an understanding from general principles into the origin of most of the essential hydraulic and sedimentary patterns observed from saltmarshes. The results presented by Allen (1994) explain processes such as flow retardation over marsh platform with increasing distance from creeks and the overall marsh platforms vertical growth regime.

Two- and three-dimensional models have been developed by several authors including empirical and physical models of marsh sedimentation (e.g. Rinaldo *et al.*, 1999; Temmerman *et al.*, 2003b; D'Alpaos *et al.*, 2007). For example, Temmerman *et al.* (2003b) proposed a empirical sedimentation model that describes spatial patterns in marsh platform sedimentation rates following equation (1.3):

$$SR = Ke^{lH}e^{mDc}e^{nDe} \tag{1.3}$$

where *SR* is the sedimentation rate (g m^{-2} per spring-neap cycle), *H* is the marsh platform surface elevation (m relative to tidal datum), *Dc* is the distance to the nearest creek or marsh edge (m) and *De* is the distance to the marsh edge (m) measured along the nearest creek. The model parameters *k*, *l*, *m*, and *n* are estimated by multiple nonlinear regressions procedure (for which $k > 0$ and $l, m, n < 0$). Temmerman *et al.* (2005) present an example of the spatial implementation of this model for a specific tidal marsh, showing that observed sedimentation patterns are well reproduced.

Finally, at the largest scales are the *landscape* models, that operate over larger regions simulating mesoscale processes and general trends (Rybczyk & Callaway, 2009) over entire estuaries. Within this group of models different approaches can be found: long-term model concepts such as behaviour-oriented modelling (e.g. *Aggregated Scale Morphological Interaction between Tidal basin and the Adjacent coast* (ASMITA) model (Stive *et al.,* 1998)) and spatial landscape modelling such as ecosystem-based landscape models (e.g. *Coastal Ecological Landscape Spatial Simulation* (CELSS) model (Costanza *et al.* 1990) and *Sea Level Affecting Marshes Model* (SLAMM) (Clough *et al.*, 2010)).

In long-term model concepts, variations on small scales are considered as noise, and one of the key elements is the reduction of information (Stive *et al.,* 1995). Data reduction techniques are essential and allow separation of relevant information from noise and into a manageable number of parameters (De Vriend *et al.*, 1993). Information reduction involves four levels -the input, physical system or its model, output and interpretation or

generalisation (De Vriend *et al.,* 1993)-. For example, behaviour-oriented modelling is one approach to long-term modelling and it has been used in several models (e.g. Di Silvio, 1989; Van Dongeren and De Vriend, 1994; Stive *et al.*, 1998).

The ASMITA model (Stive *et al.,* 1998) is an example of the behaviour-oriented approach and represents estuarine systems schematically (Rossington *et al.,* 2011). This model schematises a tidal inlet as aggregated morphological elements (intertidal area, channels and ebb-tidal delta) and characterises each model element by a single variable: volume (Kragtwijk *et al.,* 2004). It assumes that each element tends towards a morphological equilibrium (when hydrodynamic forcing is constant) definable using empirical equations (van Goor *et al.,* 2003; Rossington *et al.,* 2011). Further details about this model can be found in van Goor *et al.* (2003) that describe single, two and three element versions of the ASMITA model, and Rossington *et al.* (2011) that present novel schematisations (Figure 1.10).

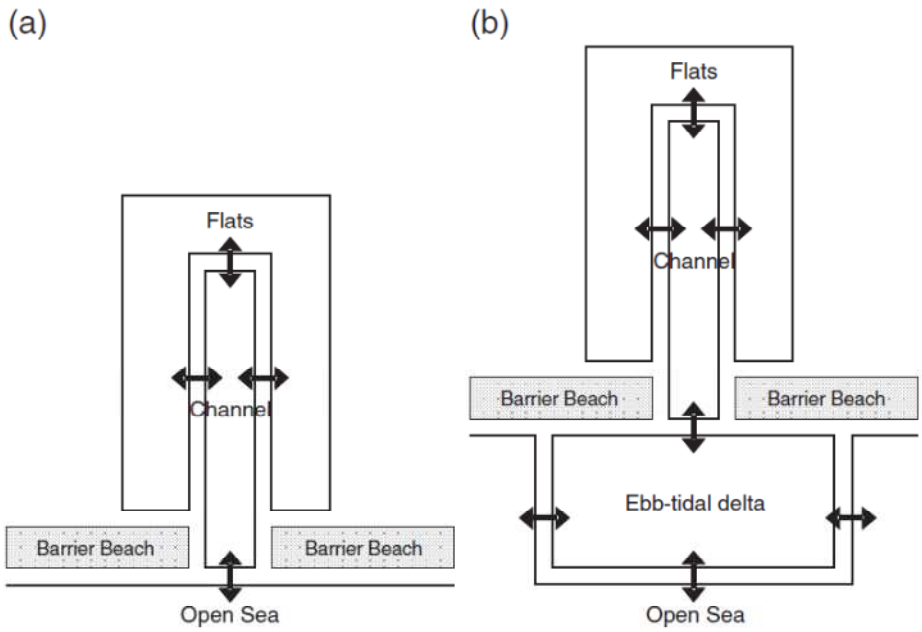

Figure 1.10 Typical two (a) and three (b) element schematisations of ASMITA model [source: Rossington *et al.* (2011)]

The ASMITA model is considered to be aspatial due to its lack of spatial details within the estuary. It considers the estuary as one unit, which limits its resolution and ability to project sea-level rise impacts over different sub-environments. Unlike ASMITA, the spatial landscape modelling approach incorporates a spatial component. These approaches usually divide the studied environment into cells (raster format), and apply dynamic ecosystem simulations over each cell, meaning that physical and ecological dynamics are performed over every cell. The dynamic simulation of this approach is

usually based on a logical decision tree (Sklar *et al.,* 1985) that determines the potential change of a cell.

Particularly, in ecosystem-based landscape models, the computation of physical processes is minimised thus they can be applied at high resolution to large surfaces and investigate the spatial interactions among different ecosystem/habitat units (Fagherazzi *et al.,* 2012). These models can be divided into models based on direct and indirect calculations. Models based on direct-calculations compute simultaneously flow, water quality and biological processes in the same time step, allowing feedback mechanisms and interactions with results (Fagherazzi *et al.,* 2012). However, they require long simulation times. Examples of this type are CELSS (Costanza *et al.,* 1990) and the Barataria-Terrebonne Ecological Landscape Spatial Simulation model (BTELSS) (Reyes *et al.,* 2000). On the other hand, models based on indirect-calculations are easier to compute and require less simulation time. They compute physical processes (e.g. hydrodynamics) first, and then use the results to simulate biological processes (Fagherazzi *et al.,* 2012). SLAMM is one example of this type of models and it has been extensively used (Akumu *et al.,* 2010; Chu-Agor *et al.,* 2010; Ehman, 2008; Craft *et al.,* 2009; Sherwood & Greening, 2014; Murdukhayeva *et al.,* 2013).

At the same time that the development of predictive models, Geographical Information Systems (GIS) has greatly improved in the last decades, and it has also been used as a tool for assessing coastal vulnerability (Mcleod et al. 2010). This tool has also been used coupled with models (e.g. mechanistic models), providing crucial analysis in support of modelling (Lyon & McCarthy, 1995; Green & King, 2003) and a powerful visualisation tool to evaluate sea-level rise scenarios. An example of combination of GIS and modelling is the global coastal geo-database created for vulnerability and impact analysis due to sea-level rise at regional/global scales in the DINAST-COAST project (Dynamic and Interactive Assessment of National, Regional and Global Vulnerability of Coastal Zones to Climate Change and Sea-Level Rise) (DINAS-COAST Consortium, 2006) and the linked DIVA model (Hinkel 2005; Hinkel & Klein 2007; Hinkel & Klein 2009). However, the DIVA tool does not include many of the processes involved in sea level changes (e.g. changes in storms frequency; and accretion) (Mcleod *et al*., 2010), and only integrates two coastal wetlands relevant to Europe (saltmarsh and unvegetated wetland such as tidal flats) (Pylarinou, 2015). Another example are inundation GIS tools (Ojeda *et al.*, 2011), which are based on flooding a specific site or region using a DEM and different sea-level rise scenarios.

The main issue with these approaches for modelling sea-level rise is that they do not take account of dynamic feedbacks between processes and coastal morphology (e.g. accretion increase and/or landward migration in saltmarshes). Despite this limitation, the

DIVA tool has been used in different projects such as the BRANCH project in the UK (BRANCH Partnership, 2007) to assess climate change impacts (particularly sea-level rise) on coastal habitats at the European Union, although it has been criticised as a basis for informing governments and coastal managers (Green & King, 2003; Mcleod *et al*,. 2010). One of the spatial models that partially addresses this limitation is SLAMM, offering a more dynamic basis for evaluations of sea-level rise impacts at local to regional scales (Mcleod *et al*., 2010; Pylarinou, 2015).

SLAMM was developed in the USA by Park (1986) with EPA (Environmental Protection Agency) funding. The model is GIS-based, and it simulates some of the main processes involved in coastal wetland changes and shoreline modifications under different scenarios of sea-level rise (Clough *et al.,* 2010) such as inundation, erosion and accretion (Akumu *et al.,* 2010). SLAMM has been run in more than 93 sites to assess changes in coastal land cover classes in USA due to sea-level rise. The advantages of this model are that it is open source, simple, quick, contains most of the major saltmarsh processes and large datasets are not required. However, although this model does not consider future changes in hydrodynamics (it assumes that the tidal regime will be constant) and it is a spatially simplified erosion model. It includes dynamic feedbacks between processes and coastal morphology (such as the ability of the saltmarsh to respond to sea-level rise by increasing accretion and/or the landward migration), which is crucial for modelling saltmarshes in a context of sea-level rise.

Despite their limitations, models such as SLAMM in combination with high resolution spatial data and GIS tools currently provide a basis for more mechanistic understanding of sea-level rise impacts in saltmarsh environments at landscape scales. However, governments and managers should be aware of the limitations of the model used to evaluate the effect of sea-level rise in coastal wetlands. In addition, more understanding about the uncertainties surrounding these models is crucial to assess the model outputs when they are used for informing governments and managers about adaptation, migration or policy development.

1.7. Remote sensed data for surveying saltmarshes

1.7.1. Multispectral data for saltmarsh mapping

Traditionally, saltmarsh mapping has been performed by a combination of laborious field surveys and photo-interpretation from conventional aerial photography. These data offer the possibility of manually mapping different marsh habitats with a spatial resolution of a few metres, using the texture and grey/colour scale of the photographs as indicators of changing vegetation communities (Smith, 2009; Provoost *et al.*, 2005; Dale *et al.*, 1996).

One of the advantages of this approach is that aerial photography is often available from present day back to the 1940s. This is very beneficial to studies of historical habitat change for instance. On the other hand, the major disadvantages are the need for large field surveys, which are labour intensive, time consuming and expensive (Gilvear *et al.*, 2004; Moffett & Gorelick, 2013) and the usually poor spectral resolution of aerial photography (black and white, or RGB: limiting automatic vegetation classifications).

Significant progress has been made in Earth Observation over the last few decades, where improved synoptic coverage and repeatability of remotely sensed digital imagery has enabled advancements in saltmarsh characterisation and the monitoring of change (e.g. Thomson, 1998; Silvestri *et al.*, 2003; Brown, 2004; Thomson *et al.*, 2004). This progress has been chiefly driven by the improvement of remote sensing from spaceborne and airborne platforms and associated technology over the time (Table 1.4), which has increased their spectral and spatial resolution and the increment of data availability for the scientific community (e.g. satellite images, high resolution satellite images and multispectral aerial photographs). Overall, remotely sensed data have offered a more efficient way of acquiring saltmarsh information compared with the conventional aerial photography.

The first Landsat was launched in 1972 and with it began the space/satellite remote sensing era. Since then, posterior Landsat were launched providing a wide range of spatial and temporal coverage of multispectral information[8]. Unlike old aerial photographs, the satellite images obtained by these sensors offered a huge improvement in spectral resolution (seven spectral bands), but their spatial resolution (30 m) has been a limitation for saltmarsh studies at fine scales (Artigas & Yang, 2006; Zhao *et al.,* 2009). Due to the spatial complexity of saltmarsh vegetation, Landsat images are not suitable for detailed saltmarsh mapping, although they can be used for other purposes at coarser scales such as land-cover mapping or for determining water, mud and vegetation boundaries using un-mixing techniques (e.g. Zhao *et al.*, 2009).

[8] http://landsat.gsfc.nasa.gov/data/where.html

Table 1.4 Summary of properties of relevant sensor for saltmarsh mapping.

	1940	1970	1986	1999	2001
	Aerial photography	**LandSat**	**SPOT**	**IKONOS**	**QuickBird**
Pixel resolution (m)	Few	15-30	2.5-10	1-4	2.44-0.61
Number of bands	1 or 3	7	1	4	4
Revolution interval (days)	N/A	16	5	3	3
Country	specific sites	US	French/ Belgian/ Swedish	US	US

Since the late nineties, high resolution satellites such as IKONOS and QuickBird combined the very high spatial resolution of aerial photographs with the increased spectral range and resolution of satellite images. These modern remote sensing technologies allow wetland information to be collected more efficiently (Moffett & Gorelick, 2013), and with higher spatial resolution (from centimetres to few metres) (Gilvear *et al.,* 2004). The high resolution images have been crucial for classifying vegetation cover across coastal wetlands (Harvey & Hill, 2001; Belluco *et al.,* 2006; Cao *et al.,* 2007; Gilmore *et al.,* 2008; Arroyo *et al.,* 2010) because they provide spatial and structural features at the fine scale (Cao *et al.*, 2007), which is essential for distinguishing vegetation patterns and creeks.

Apart from spaceborne sensors, airborne sensors can also provide very useful information for mapping saltmarshes. Unlike spaceborne, data from airborne sensors such as digital photogrammetric cameras can be collected on a specific day and at a specific time, and generally have greater spatial resolution than satellite images (Thomson *et al.*, 2004). Modern aerial sensors allow digital photographs to be acquired at greater spatial resolution (≤ 1 m) and higher spectral resolution (combining standard RGB colour photography with an additional infrared band) than old, standard aerial photography. These improvements mean that classification techniques can be applied more successfully for saltmarsh mapping, and their results are comparable to those obtained from very high resolution satellite-derived imagery (up to 5m).

One of the most significant differences between the main sensors relevant to saltmarsh mapping is their spatial resolution (Figure 1.11). Belluco *et al.* (2006) investigated how spatial resolution influences classification results in estuarine habitats. Improvement in classification is found with an increase in spatial resolution and studies show that very high spatial resolution images (e.g. IKONOS-2, QuickBird or multispectral

photography) are more suitable for mapping saltmarshes than images from 10 to 30m spatial resolution sensors such as Landsat (e.g. Artigas and Yang, 2006; Cao, 2007; Gilmore *et al.*, 2008; Arroyo *et al.*, 2010). Very high resolution satellites images (<10 m resolution) and digital aerial photographs are the most suitable data for mapping saltmarshes because they provide good spatial resolution without losing spectral information, which facilitates the characterisation of water bodies and vegetation patterns. However, the classification technique applied can also be determinant in the success of saltmarsh mapping.

Figure 1.11 Illustrative sample of 30m spatial resolution LandSat-5 image (on the left) and 1m spatial resolution aerial photograph (right) for a saltmarsh.

1.7.2. Altimetry data: Light Detection And Ranging (LiDAR)

Given the importance of elevation as a control on both the physical inundation and sedimentation regime (via hydroperiod) and plant and animal communities, accurate topographic data are crucial for assessments of saltmarsh response to sea-level rise. Existing globally-available digital elevation products such NASA Shuttle Radar Topography Mission (SRTM) fail to characterise tidal saltmarshes topography due to their limited spatial and vertical resolution (Yang, 2005). In this sense, airborne LiDAR technology may have a great potential for monitoring and assessing large areas of coastal wetlands, and thus its application to these environments is expected to increase (Cary, 2009). For example, the USA and some European countries have already started to use this technology to create regional and national *Digital Elevation Models* (DEMs) (Meng *et al.,* 2010) for various coastal and flooding applications.

Airborne LiDAR is a laser scanner that determines the distance between ground-objects and the sensor by measuring the time a pulse of transmitted energy takes to return to the LiDAR sensor receiver (Meng *et al.,* 2010). These sensors are usually coupled with ground referencing systems, which have enabled the acquisition of high-density geo-referenced elevation data (Meng *et al.,* 2010; Populus *et al.,* 2001) in a 3D coordinate (X, Y and Z) form, enabling geo-referenced altimetry calculations of the terrain and above-ground objects (e.g. building, and trees). Generally, the point measurements taken by a airborne LiDAR sensor are influenced by the following three variables shown in the equation 1.4 (all the units are in metres) (Meng *et al.,* 2010):

$$M_{sensor} = E_{ground} + E_{above-ground} + E_{noise} \quad (1.4)$$

Where M_{sensor} is the LiDAR sensor measurement, E_{ground} is the bare ground elevation, $E_{above-ground}$ is the height of above ground objects and E_{noise} is any undesired measurements (e.g. birds). The raw data collected by the sensor are 'point clouds' usually in '*LAS*' format. From these point measurements, two main products can be derived from LiDAR: the DEM comprising ground elevation data (interpolated from the last echo or return; see Figure 1.12) and the *Digital Surface Model* (DSM) comprising ground elevation plus ground-object elevation data (interpolated from the first echo or returns). Filtering is required to ensure the appropriate, high accuracy DEM is generated.

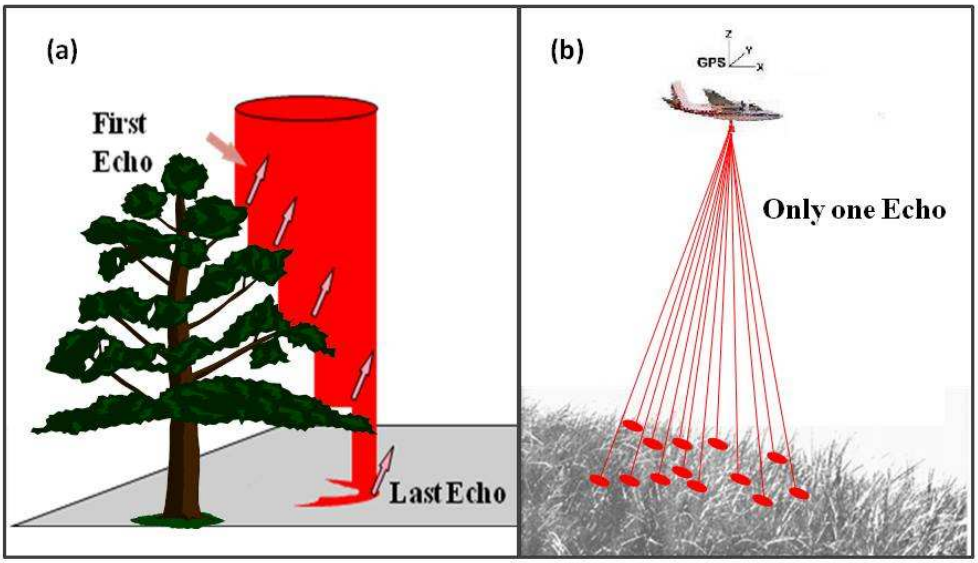

Figure 1.12 Example of echo (or returns) of an airborne LiDAR laser beam in two different environments: (a) is representing forest environments, where several returns are usually collected; and (b) represents saltmarsh environments, where only one return is usually collected due the short vegetation that characterises these environments

LiDAR technology is very useful for the characterisation, quantification and monitoring of coastal and estuarine environments (Chust *et al.,* 2008; French, 2003) particularly for saltmarshes, where subtle variations in the micro-topography can be crucial for determining vegetation spatial patterns and other important factors (e.g. oxygen and moisture). However, in saltmarsh environments, despite the resolution improvements offered by LiDAR technology in comparison with other techniques, the vertical accuracy can be different from adjacent upland (Schmid *et al*., 2011; Hladik & Alber, 2012) due to the low penetration of the laser beam through marsh vegetation layer (Schmid *et al*., 2011). Therefore erroneous assumptions and conclusions can result from vertical accuracy differences in both uplands and saltmarshes if this limitation is not considered.

LiDAR data have been applied within saltmarshes for wetland characterisation purposes (Rosso *et al*., 2006; Morris *et al*., 2005), habitat and vegetation mapping (e.g. Brown, 2004; Collin *et al.*, 2010), determination of wetland vegetation height (Genc *et al.*, 2004), evaluation of SLR impacts (Webster *et al.,* 2006), for the detection of estuarine and tidal river hydromorphology (Gilvear *et al.,* 2004) and as a basis for modelling (French, 2003). Among the applications reviewed in the literature, there are not many studies that have extensively investigated the potential of altimetry data combined with intensity data (from beam returns) for mapping coastal habitats (Brennan & Webster, 2006), which for example could be an important information for mapping low-contrast vegetation in saltmarshes.

In the context of SLR, common applications of LiDAR data in tidal saltmarshes include sea level inundation and spatial models, which require centimetre level accuracy due to the importance of the micro-topography in these environments and the scale of sea-level rise change. However, within saltmarshes, LiDAR systems can fail to distinguish centimetre variations between the vegetation canopy (DSM) and bare-ground (DEM) (Hopkinson *et al.,* 2004; K. a. Schmid *et al.,* 2011; Hladik & Alber, 2012). Ground filtering is the primary step required for DEM production (Meng *et al.,* 2010), which is particularly challenging in saltmarsh environments due to the physical structure of vegetation. Many halophytes comprise a dense and homogeneous structure. This means the halophytic vegetation often simulates a flat surface consistent with bare-ground elevation and morphology (Brovelli *et al.,* 2004; Göpfert & Heipke, 2006). This physical characteristic complicates the filtering process because is very difficult to discern if the return is vegetation or bare-ground.

Systematic instrument errors related to the sensor pulse length (laser cavity length) can also affect high resolution data in environments with low-lying vegetation such as

saltmarshes. Populus *et al.* (2001) argues that pulses less than 3 nanoseconds (ns) apart or one metre on the ground cannot be separated, which can negatively affect the identification process between low-lying vegetation and ground targets. The problem here is that in these cases is not possible to get both front and rear returns. Schmid *et al.* (2011a) refer to this problem as a technical limitation of the LiDAR, stating that the elevation of the marsh returns can be at or near the resolving threshold of LiDAR. This means that the height difference between some saltmarsh species and the ground is too small as the intensity of the first return drops (vegetation) and rises again as a second return (ground). Therefore two individual reflected impulses separated by less than the pulse length are considered as one return, instead of two returns, and thus the two targets are very difficult to separate (K. A. Schmid *et al.,* 2011; Populus *et al.,* 2001). Thus, sensors that are capable to collect multiple returns only collect one return in environments characterised by short vegetation such as saltmarshes.

On the basis that there are physical and technical limitations for the use of LiDAR in saltmarshes, and the need for high accuracy data in the research applications in these environments, some authors (e.g. Populus *et al.*, 2001; Schmid *et al.*, 2011a; Hladik and Alber, 2012) have investigated the vertical accuracy of the elevation data from LiDAR, and the possibilities of calibration on these environments (Table 1.5). For example, French (2003) found an over-estimation of ground elevation by about 10 cm in reclaimed wetlands with a grass cover. Furthermore, several studies that focus on taller vegetation such as *Spartina alterniflora* note that DEMs are overestimated with a mean error of 7-17 cm, where the error seems to increase with vegetation density and height (Morris *et al.,* 2005; Montané & Torres, 2006; Rosso *et al.,* 2006; K. A. Schmid *et al.,* 2011). Thus, saltmarshes characterised by dense tall vegetation, such those found in southern Europe, would need to take in account these limitations of LiDAR.

Table 1.5 Studies focused on calculating LiDAR vertical accuracy in saltmarshes

Purpose	Mash type	Error (cm)	References
Accuracy assessment	Tidal flats/marsh	10/20	Populus *et al.* (2001) Morris *et al.* (2005)
	Spartina alterniflora	7-17	Montane & Torres(2006) Rosso *et al.* (2006) Schmid *et al.* (2011)
	Upland/Marsh	18.2/45.7	Hladik and Meffyl (2012)
Separation of Ground and low vegetation signature	Tidal marsh		Wang *et al.* (2009)

1.8. Summary

Chapter 1 has described both the need for modelling the future response of saltmarshes due to sea-level rise and the data issues found on these environments related to saltmarsh vegetation and elevation mapping. In order to predict futures changes in saltmarsh habitats, which are tightly linked to tidal ranges, it is crucial to have a clear understanding of the accuracy and precision of vertical elevation data. Saltmarshes present a challenging environment, but the high ecosystem value and their vulnerability to sea-level rise mean that monitoring of change, and modelling of future responses are important research and conservation objectives.

Due to the importance of elevation and its relationship with ecological and geomorphological processes; morphometry, geomorphology and vegetation have been identified as features worthy of analysing and monitoring. In order to investigate these components in saltmarshes, remote sensing techniques will be applied to the current data available (e.g. LiDAR data and multispectral imagery). As such, the method developed for the interpretation of the remote sensing data should be applicable not only for recent data, but also for future gathered data in saltmarshes.

Spatial landscape models such as SLAMM have been used to evaluate coastal wetland habitat response to sea-level rise based on the simulation of key processes, and this model seems to be the most suitable for this research. One of the main strengths of SLAMM is the ability to explore system responses to different sea-level rise scenarios, but uncertainties in predicted response will also reflect uncertainties regarding the primary inputs and hence the quality of the original elevation data and habitat classification. Thus, it is crucial to undertake sensitivity analysis to explore the relative importance of data quality and resolution (spatial and vertical) in the elevation data and saltmarsh habitat classification layers. Monitoring and measurement of saltmarsh habitats is time consuming and costly, and the acquisition of the SLAMM input layers can require significant resources so some understanding of where surveying efforts should be focused is necessary.

1.9. Aims and objectives

The aim of this thesis is focused on **the use of LiDAR data and imagery for mapping saltmarsh habitats and as a basis for spatial models of their response to sea-level rise under-studied Mediterranean-Atlantic saltmarshes**. This is demonstrated through application to the saltmarshes found in the Tinto-Odiel estuary. Specific objectives for achieving this aim are:

- To investigate the historical changes (human and physical drivers) at the study area and their implications for potential impacts due to sea-level rise
- To investigate the contemporary plant communities and vegetation structure across the study area and to explore relationships with ground elevation for understanding the potential saltmarsh respond due to sea-level rise
- To examine different remote sensing techniques for mapping saltmarsh habitats at fine scales (1:2,000) and the suitability of these techniques for monitoring saltmarsh habitats
- To explore the suitability of digital elevation models (DEMs) derived from Light Detection and Ranging (LiDAR) sensor for modelling sea-level rise future projections in Mediterranean-Atlantic saltmarshes (where vegetation is both tall and high density)
- To explore the sensitivity of spatial landscape models such as SLAMM to the input data and habitat elevation accuracy and the suitability of SLAMM for predicting wetland conversion due to sea-level rise
- To investigate the potential impacts due to sea-level rise in the study site using SLAMM through a uncertainty analysis

2. Research Design

2.1. Study site

The present study is focussed on South-Atlantic Iberian saltmarshes, identified in chapter 1 as European saltmarshes with special features, comprising characteristics of both Atlantic and Mediterranean saltmarshes. These saltmarshes are found in the Gulf of Cadiz: southern Portugal and southwest Spain. In a context of sea-level rise, most of the research carried out in Europe has been focussed on northern Europe or Mediterranean saltmarshes, leaving a gap for those found in the Gulf of Cadiz. The response of these particular saltmarshes to sea level change has not been fully investigated, and this thesis is focussed on covering this gap. Pristine ecosystems are rare in Europe, and this study assumes that saltmarshes are already subject to human pressures, and it is important to investigate these pressures as a whole.

2.1.1. Northern coasts of the Gulf of Cadiz: site selection

The northern coast of the Gulf of Cadiz extends from the Cape Saint Vincent, Portugal (36.9N and 9.0W) to the Gibraltar Strait, Spain (35.95N and 5.6W) (Figure 2.1). It is located at the southern edge of the Iberian Peninsula, occupying a transition zone between the mid-latitudes and inter-tropical zones (Ojeda, 2003). Although these coasts face the Atlantic Ocean, proximity to the African continent and to the Mediterranean Sea have strongly influenced physical factors such as climate, wind, tide, swell, and marine currents (Ojeda, 1988). These coasts are subject to a complex coastal dynamic that together with other phenomena, such as its neotectonic macrostructure and past sea level changes, have enabled the formation and development of diverse coastal environments such as beaches, barriers island, saltmarshes, embayments, and rocky and sandy cliffs during the Holocene (Ojeda, 1988; Zazo, 1980; Ojeda, 2003).

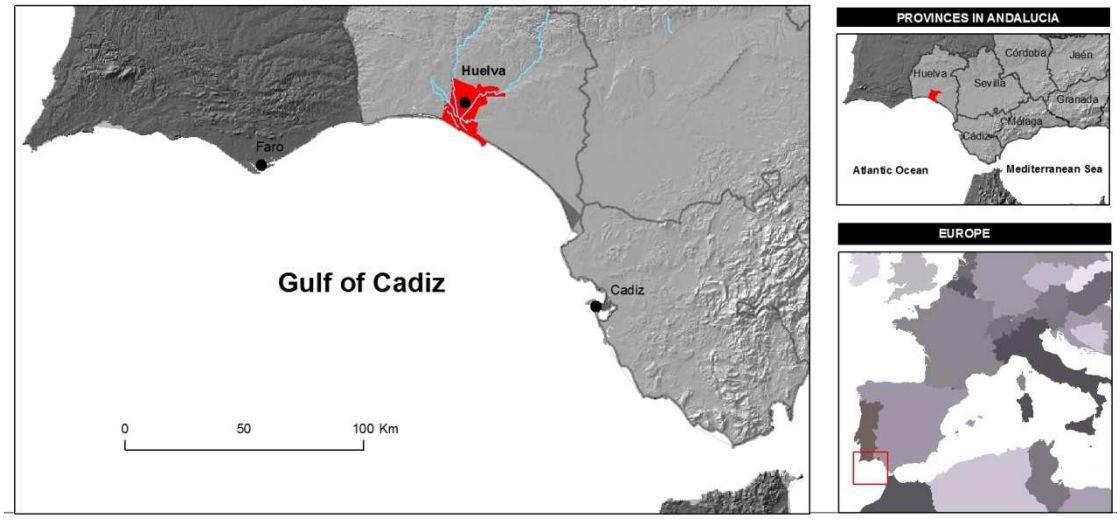

Figure 2.1 Location of the Gulf of Cadiz. In red is shown the Odiel-Tinto estuary (Huelva).

The structural framework imposed by neotectonic activity and geological processes significantly controls the coastal landscape in the Gulf of Cadiz (Figure 2.2). Intense tectonic activity associated with the location between the European and the African plates (Pedrera *et al.,* 2011) has fractured the bedrock, and active faults, subsidence and uplift are ongoing, meaning that this coastal zone is one of the most tectonically active of the Iberian Peninsula (Ojeda, 1988; Ojeda, 2003). From a morphological point of view, tectonic adjustments and variations in lithology have strongly influenced the evolution and contemporary morphodynamics of these coasts because they have imposed significant structural constraints. The faults and fractures present on the coastline of the Gulf Cadiz have led to the division of the coast into four independent sectors (Figure 2.2) with different morphologic structures (Ojeda, 1988):

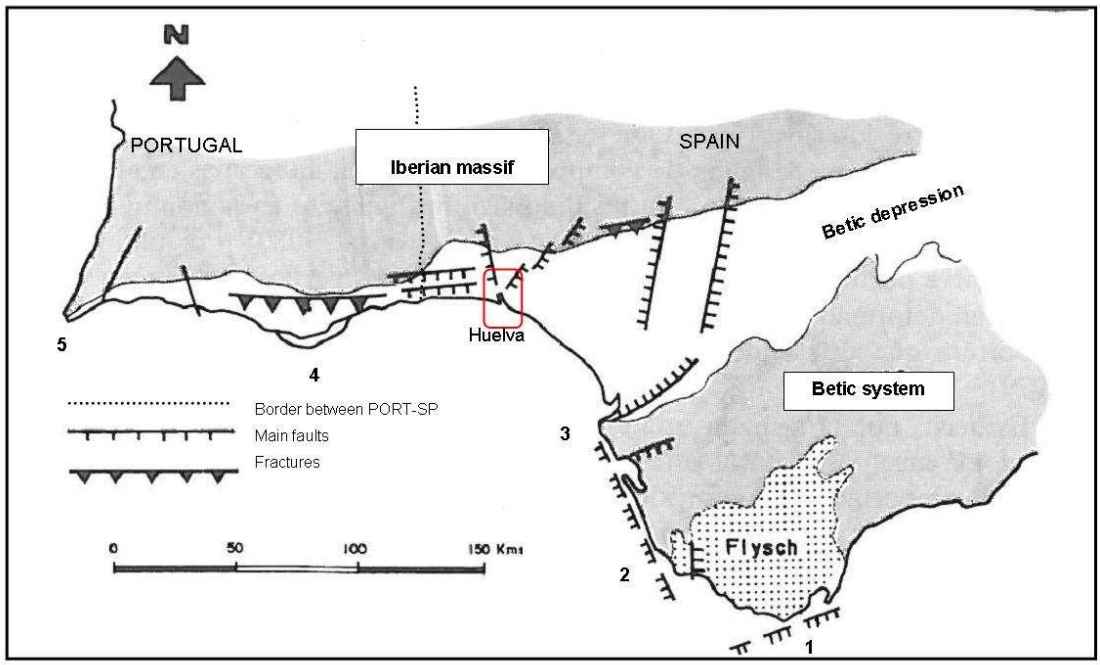

Figure 2.2 The main neotectonic macrostructure of Gulf of Cadiz. From east to west, the picture shows the main faults and flexion of the province of Cadiz, Huelva and the Algarve. The red square states the study site location (Huelva) and the numbers indicate the following location: (1) Tarifa, (2) Roche Cape, (3) Sanlucar, (4) Sta. Maria Cape, and (5) San Vincent Cape. [Source: Ojeda, 1988].

- Sector 1-2 (SP) is characterised by capes and coastal promontories that alternate with wide inlets closed by barrier beaches (Ojeda, 1988).
- Sector 2-3 (SP) is characterised by uneven tectonic levels of Pliocene series that have favoured the development of Cadiz Bay (Zazo *et al.,* 1994; Gracia *et al.,* 1990), which comprises of saltmarshes, beaches and cliffs.
- Sector 3-4 (SP) is chiefly characterised by a low-lying sedimentary coast. From east to west the following coastal environments occur: on the Spanish side, the existence of sand spits, large dune systems and wide marsh land occur associated with the Betic depression; between Huelva and the Portuguese border, evolved barrier islands and river estuaries can be found (Ojeda, 2003; Zazo *et al.,* 1994); and lastly, on the Portuguese side, large barrier systems, lagoons and tidal inlets occur (Arnaud-Fassetta *et al.,* 2006).
- Sector 4-5 (POR) is characterised by carbonate rock cliff (with intense karst processes), coves and small beaches associated with medium fluvial estuaries (Ojeda, 1988).

The current position of the Gulf of Cadiz coastline is a result of sea level stabilization that was reached in the mid-/late-Holocene, roughly 5,500 - 6,500 years ago (Pendon *et*

al., 1998; Zazo *et al.,* 1994). Conditions during this period were suitable for saltmarsh formation in southwest Andalusia within the flooded coastal valleys, such as the Tinto-Odiel estuary, and other sheltered parts of the coast (e.g. barrier islands and embayments). The Holocene evolution of the Gulf of Cadiz coast is well documented, covering the sedimentary infill of the Flandrian estuaries (Dabrio *et al.,* 2000; Borrego *et al.,* 1999; Goy *et al.,* 1996; Pendon *et al.*, 1998; Morales *et al.,* 2003; Lario, *et al.,* 2002), and the evolution of the spit barrier systems (Zazo *et al.,* 1994; Lario *et al.,* 2002; Goy *et al.,* 1996; Rodriguez-ramirez *et al.,* 1996).

In addition to the long term evolutionary framework and Holocene-modern sea level changes experienced in the Gulf of Cadiz, anthropogenic coastal structures built during the last few decades have also played an important role in recent coastal evolution (Ojeda, 2003). Sediment dynamics along the Huelva and Cadiz shoreline have been impacted by the construction of dikes, jetties, piers and sea walls, causing changes in sediment transport directions, and most notably, present an important control on the broad morphodynamics of the coastal system (Zazo *et al.,* 2005).

According to Dijkema (1984), 'barrier connected saltmarsh', 'foreland saltmarshes', 'estuarine saltmarsh' and 'salines' are found in the northern coasts of the Gulf of Cadiz. The Tinto-Odiel estuary has been identified as one of the largest estuaries in the Gulf of Cadiz and encompasses extensive tidal marsh (roughly 12,000 ha) alongside different land uses (urban, industrial, conservation, tourism and recreational). Within this estuary, the Odiel saltmarshes are considered the largest and most diverse saltmarsh system in the Iberian Peninsula (Castellanos *et al.,* 1998), and gaining protected area status in recognition of the national and international importance of these wetlands. This protected area includes saltmarshes, vegetated barrier islands, dunes and beaches, which have been assigned several conservation designations such as the 'Biosphere Reserve' (1983), 'Paraje Natural' (1984), 'Natural Place of National Interest' (1984), 'Special Protection Area' (1987) and 'Ramsar site' (1989).

2.1.2. The evolution of the Tinto-Odiel Estuary

The evolutionary context covering both Holocene and century time scales is illustrated in Figure 2.3, which shows the infilling process of the Tinto-Odiel Estuary and the transition from wave to tide dominates environments. This evolution and the associated transitions in sedimentary environments was facilitated by sea-level rise throughout the Holocene - the 'Flandrian transgression' (Zazo *et al.,* 1994). Sea level was between 125 and 120 m lower than the present level (Hernandez Molina *et al*., 1994) at the end of the last glacial, and this was followed by a rapid rise until roughly 7000 years BP (Delgado *et al*., 2012; Lario, 1996), when the rate of sea-level rise decreased (Figure 2.4). Evidence for this has

been found in analyses of organic and peat deposits and gravels and shells lags found in various cores from the Guadalete and Tinto-Odiel estuaries (Dabrio *et al*., 1995; Goy *et al*., 1996; Lario, 1996; Zazo *et al*., 1996; Dabrio *et al*., 1999). This early rapidly rising sea level (at a rate of around 1 m every 100 years) resulted in a progressive inundation of the lower zones of the Odiel and Tinto rivers, transforming this area into a huge bay with a 'Y' shape representing the confluence of the two river valleys (Morales & Ojeda, 2010). The filling rates (i.e. estuarine sedimentation) at that time were greater than 3 mm y^{-1} (Lario *et al.,* 2002b) (Figure 2.5).

A renewed acceleration in the rate of sea-level rise took place until the maximum landward advance of the marine influence was reached at 7000–6000 years BP (Lario, 1996; Dabrio *et al*., 1999). Estuarine infilling, high energy tidal currents and wave action were the dominant processes during this stage. The next stage (5,390 ±155 to present) was characterised by a stabilised sea level, when low energy processes such as tidal currents favoured deposition in shallow creeks and tidal flats (Borrego *et al.,* 1999). Complex fluvio-marine sedimentation processes created intertidal flats and early marshes.

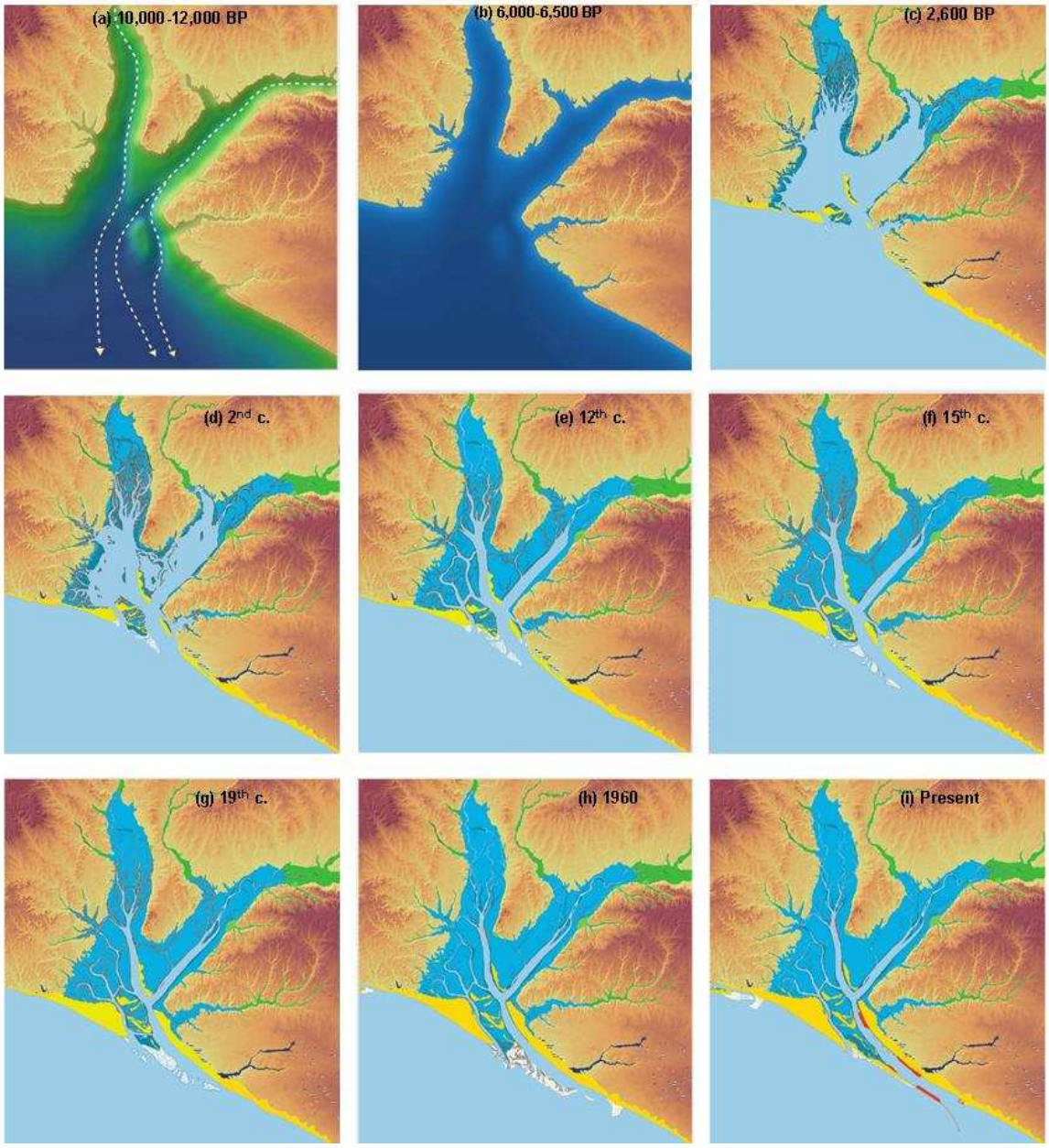

Figure 2.3 Holocene evolution (based on cores) of the Tinto-Odiel Estuary and saltmarsh formation from 10,000-12,000 years ago to present. (a) Reconstruction of lower position of sea level, where areas in green simululates the emerged land at that time. (b) Reconstruction of higher sea level position during the 'Flandrien transgression'. Figures from (c) to (i) show the saltmarsh evolution in this estuary, where the areas in clear blue is water; dark blue represents tidal wetlands; yellow shows sand deposition areas such as beaches, spits and barrier islands; white represents sandy tidal flats; green represents fresh water environments. Areas in red (i) show dikes and seawalls [Source: Modified from Morales and Ojeda (2010)]

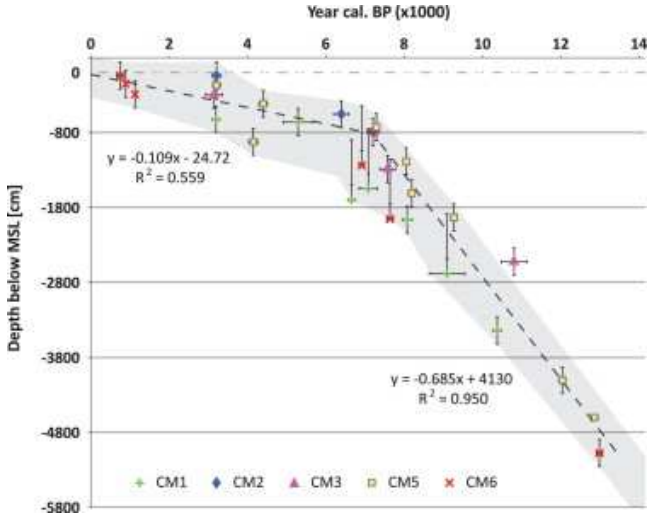

Figure 2.4 Holocene sea level trend for the SW Iberian coast [Source: Delgado *et al*., 2012].

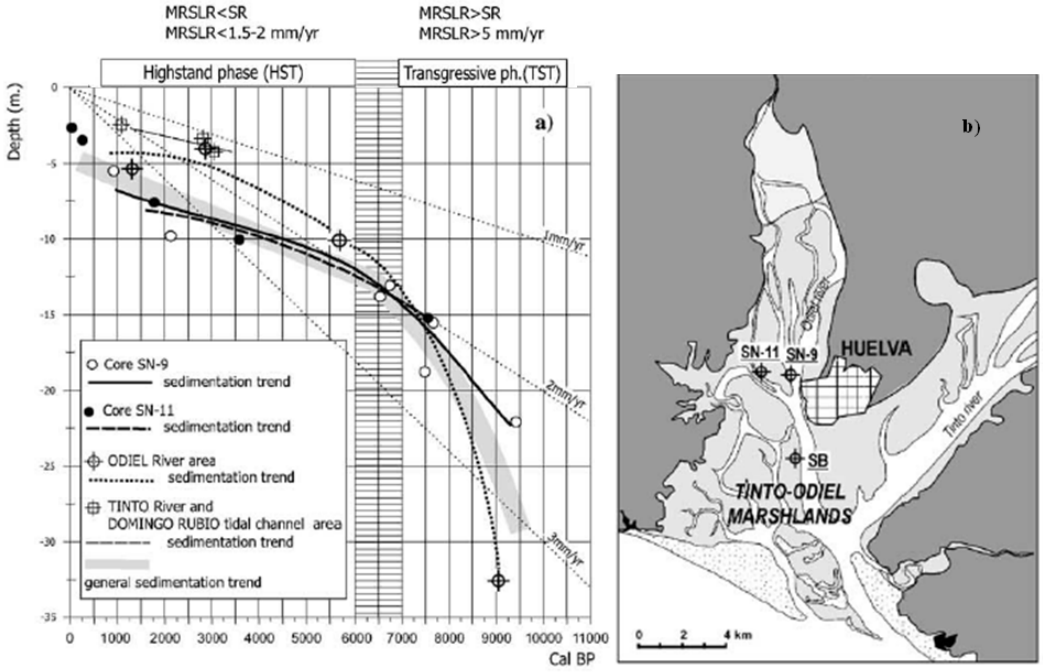

Figure 2.5 (a) Holocene sedimentation rates and trends in the Odiel saltmarshes, where MRSLR means mean rate of sea-level rise and SR sedimentation rate; (b) Location of the cores within the Odiel saltmarshes [Source: Lario *et al*., 2002]

Based on lithology and biological content (macro- and micro-fauna) in sediment samples collected from a sounding with a continuous core on Bacuta Island (in the central basin of Odiel River estuary) (Borrego *et al*., 1999), 6 estuarine facies were related to the Holocene history of sea-level rise recording the start and development of the Flandrian transgression at the Odiel estuary (Figure 2.6). The start of this transgression was recorded at 8720±260 (radiocarbon) years BP (Borrego *et al*., 1999), when sand-bar deposition also started in the central part of the Odiel estuary (Pendon *et al*. 1998). From

this time until 5,390 ±155 years BP, estuary accretion, high energy tidal currents and wave action took place successively (Borrego *et al*., 1999). The first sandy and muddy deposits were generated by sedimentation due to gravity and flocculation of suspended particles (when fresh water from the rivers mixes with sea water) (Rubio & Figueroa ,1983). Deposition occurred as marginal tidal flats toward the high water shorelines of the two valleys, and as inlet-associated island banks within the estuary mouth (Borrego *et al.,* 1999; Borrego, 1992; Dabrio *et al.,* 2000; Lario *et al,.* 2002) (Figure 2.6, a).

During the stabilised sea level phase (5,390 ±155(radiocarbon) years BP to present), the vertical energy was greatly reduced and allowed more deposition in tidal channels (Borrego *et al*., 1999). Subsequently, a barrier island formed and a sandy barrier developed at Saltes Island (Suarez Bores, 1971)(after ~3200 BP), creating a sheltered zone from the open ocean. The growth of sand barrier islands during this time started the dominance of wave activity, although the tidal current was the main agent of sediment distribution within the sheltered zone (Pendon *et al*., 1998). Barrier islands and sand spits evolved within the wide entrance (Figure 3.1c-f) which increasingly blocked the inner estuaries and caused a shift from high- to low-energy processes and sediment dynamics (Zazo *et al*., 1994; Lario *et al.*, 1995; Lario, 1996). An established fact in the evolution of the Tinto-Odiel estuary is the growth and stabilisation of the Saltes Island and Punta Umbria spit (the two outermost sand bars) (Pendon *et al*., 1998) that favoured the saltmarsh formation in the sheltered zone.

From this time onward, the Odiel estuary mouth became more channelized and the tidal channels at the upper and mid- estuary have remained relatively stable for the last few centuries (Morales and Ojeda, 2010). The estuary mouth, however, has experienced more physical changes during the last centuries and increasingly anthropogenic changes during the last decades. The recent sedimentary evolution (1829 – 1994) at the estuary mouth has been reported by Borrego *et al*. (2000), highlighting the impact of dike construction in the geomorphology of this part of the estuary.

A recent study (Morales, 2016) has shown some geological evidence (based on cores and seismic profiles) that the sediments deposited in the Tinto-Odiel estuary are affected by recent neotectonic activity. Cores and seismic profiles have showed that sediment sequences (regressive Pleistocene and transgressive Holocene sequence) at this estuary are cut by normal faults (shown in Figure 2.2). The shape of the upper sediments have adapted to the 'land displacement' caused by these faults, suggesting a slow and progressive vertical movement that cause subsidence (up to 1 mm y^{-1}) (Morales, 2016). These vertical movements within the estuary are vital in a context of sea-level rise when absolute measurements are considered. However, when relative sea-level rise is used, vertical movements are included in the final measurement. For example, sea level

measurements from local tidal gauges are relative because they include vertical movements plus sea level change.

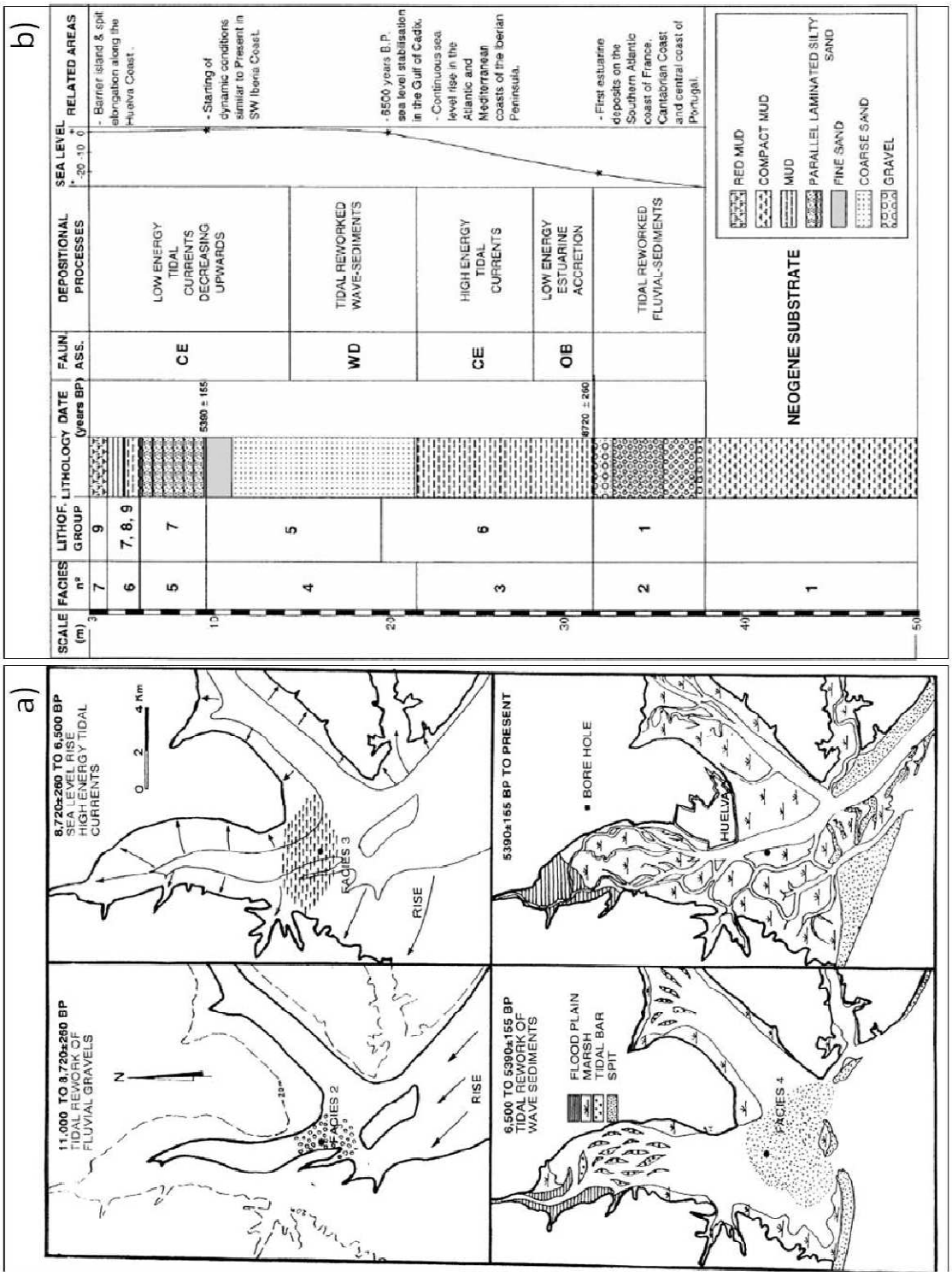

Figure 2.6 (a) Palaeo-geographical evolution, and (b) Flandrian transgression at the central estuarine basin of the Odiel and Tinto River mouth, where 'Faun Ass.' refers to three faunal assemblages (Open bay (OB), Central estuary (CE), and Wave domination (WD)) including remains of macrofauna, foraminifers and ostracods plus depositional features (they were identified in a sedimentological log constructed from a borehole with a continuous core) [Source: Borrego *et al.* 1999]

2.1.3. The Odiel saltmarshes and the Tinto-Odiel estuary: site description

At the beginning of this project the aim was to cover the whole estuary, including both Tinto and Odiel saltmarshes. However, the large surface area of these saltmarshes in addition with others issues (such as the difficulties associated to field work in saltmarshes, the fixed time of this research project and LiDAR data availability) led to the reduction of the study area to the Odiel saltmarshes. The Odiel saltmarshes of the Odiel-Tinto estuary are situated on the southwest coast of the Iberian Peninsula (Figure 2.7). The Odiel-Tinto estuary is positioned in southwest Andalucía and occupies the central part of the Huelva coast, where the Odiel and Tinto rivers meet each other in the marine influence sector, before entering the Atlantic Ocean. This estuarine system is locally known as the *Huelva Ria*. The Odiel saltmarshes comprise extensive marsh land and unvegetated sand spits, coastal sand dunes, beaches and saline lagoons.

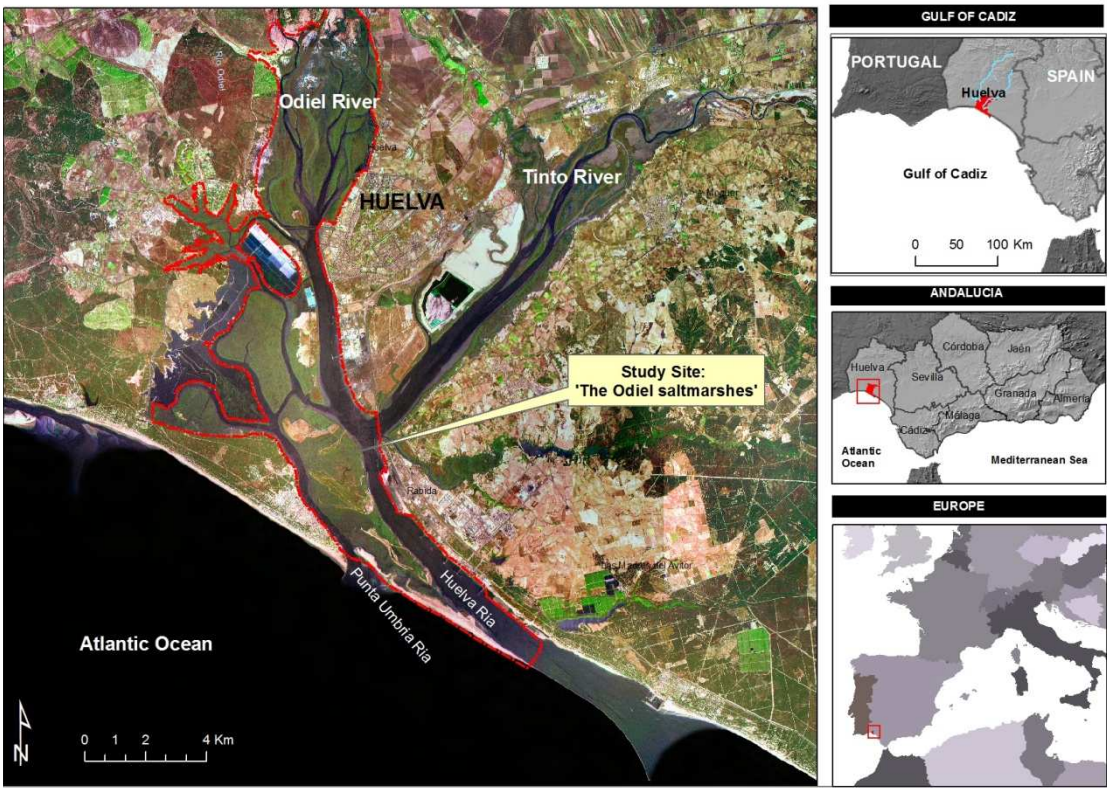

Figure 2.7 Location of the Odiel saltmarshes and the Tinto-Odiel Estuary. The red line states surface area of the study site.

The Tinto-Odiel estuary is a bar-built system (López-González *et al*., 2006) with a semidiurnal tidal range (Carro *et al.,* 2011). The valleys run through Neogene sediments (marly deposits) of the Guadalquivir depression (Cánovas *et al.,* 2007). Within the Gulf of Cadiz, the flood tide progresses from the Gibraltar strait to the Portuguese Algarve and the

ebb is in the opposite direction (Morales & Borrego, 2000); long-shore drift is from west to east. The mean tidal range is 2.1 m and the mean spring range is 2.97 m (Borrego, 1992), which is meso-tidal according to Hayes' (1979) classification. The tidal wave travels into the estuary at between 25 and 45 kmh^{-1}, which is attenuated by two dikes (Borrego, 1992) located at the mouth of the *Huelva Ria* and the *Punta Umbria Ria.* At the open coast, wave energy is considered 'medium' because wave height exceeds 0.5 m 25% of the time (Dabrio *et al.,* 2000). The dominant swell is from the southwest, but swell from the southeast also contributes an important characteristic to the local wave climate (Borrego, 1992).

The area has a Mediterranean climate (Csb or Csa according to Koppen classification) modified by Atlantic influences, experiencing hot-dry summers (August mean temperature of 25°C) and warm-wet winters (January mean temperature of 11°C). Wet years can reach an average of 1,200 mmy^{-1} and dry years an average of 400 mmy^{-1} (Sainz *et al.,* 2004). The Mediterranean climate controls the hydrology in this area, resulting in rivers with high discharge variability between summer and winter, and between years. The Tinto and Odiel rivers have an average flux of 49.8 Hm^3 per month, which may vary between 100 Hm^3 in wet years and 5 Hm^3 per month in dry years (Borrego, 1992). This great variability in the Odiel hydrologic regime is due to the torrential rainfall characteristic of this area. For example, the winter flooding are 500 greater than in summer, and the 80 % of annual discharge occurs in only few weeks. Maximum discharge values during flash flooding can be between 12 and 16 times greater than average discharge values (Lopez *et al.*, 2006).

Variability in river discharge controls the salinity levels within the estuary, affecting sedimentation processes (flocculation and decantation). Additionally, processes of acid neutralisation also occur within this estuarine system, where the pH values greatly vary (from 2.5-3.5 to more than 7) in a short distance (Carro *et al*., 2011), which is also affected by the intra- and inter-annual discharge variability. The low pH values of these rivers are due to the high content of suspended and dissolved trace elements released from the acid drainage of the Iberian Pyrite Belt (the largest sulphide open mining area in Europe). The neutralisation process also affects the sedimentation within the estuary, favouring the sedimentation of fine grains in those areas where the pH contrast is high.

The main land use in the Odiel river basin is forestry and there is a low development of agriculture and industrial activities (Galván *et al.*, 2016). The substrate of the hydrographic network is mainly rocky, and the alluvial deposits are scarce at the upper and mid River basin (Lopez *et al*., 2006). Unlike other small river basins along this coast (e.g. Partido river basin (Borja *et al*., 2009)) strong erosion problems have not been

reported in the Odiel River and its water flow has not been regulated (Cendrero *et al*., 2005).

The main geological substratum of the Odiel River drainage network is the Iberian Pyrite Belt (Figure 2.8, a) (very rich in polymetallic massive sulphide deposits), where mining activities have had a long history starting around 3000 BP (Nocete *et al*., 2005). However, large scale exploitation of polymetallic massive sulphide is more recent, operating from the second half of the nineteenth century until the end of the twentieth century (Olías & Nieto, 2015). This intensive exploitation during decades has left large amounts of mining wastes deposited in the Odiel and Tinto watersheds. These wastes (rich in sulphide) exposed to the atmosphere leads to the oxidation of sulphides that release acidity, sulphate and toxic metals (a process often known as acid mine drainage) (Galván *et al*., 2016). However, these deposits have not contributed to add new amount of sediments to the rivers, but soluble pollutants that deteriorate the water quality in this basin and in the estuary (decreasing pH levels). The geological substratum at the Odiel estuary are Holocene sediments overlying Miocene Pliocene siliciclastic sediments formed in marine and continental environments (Civis *et al.,* 1987). These sediments are basal gray-blue clays and silt (upper estuary), and upper fine sands and grey-yellow silt (mid-estuary), and constitute a large system of cliffs along the inner perimeter of this estuary (López-González *et al*. 2006b).

In the Odiel estuary the sediment composition is mainly silt (45%), sand (42%), and clay (12%), according to the results presented by Lopez-Gonzalez *et al.* (2006a). They reported a longitudinal gradient (Figure 2.8, b) of sediment texture that showed a strong seasonal pattern. For example, in winter and autumn the highest sand content is located at both fluvial (12s) and marine (1s) extremes (Figure 2.8, b), and decreases toward the mid-estuary (9s and 10s). Here, the content of silt presented an opposite tendency, reaching their maximum values at sites 9s and 10s, where the process of saline mixture and acid neutralisation occur in winter and autumn (Lopez-Gonzalez *et al,.* 2006a). In contrast, in spring, the finest sediments (silt and/or clay) are found at the fluvial and marine extremes. At the site 10s, fine sediments are also found at site 10s, where the saline mixture and acid neutralisation occur in spring (Carro *et al*., 2011). In summer, the fluvial discharge is very low, and thus the fluvial processes are restricted to the upper part of the estuary. Tidal processes dominate the estuary at this time of the year and the pH is more homogeneous through the estuary. The longitudinal gradient observed in the sediment texture is similar in summer and winter, where the sand content decrease from the upper estuary to site 10s (Figure 2.8, b), and silt content increase.

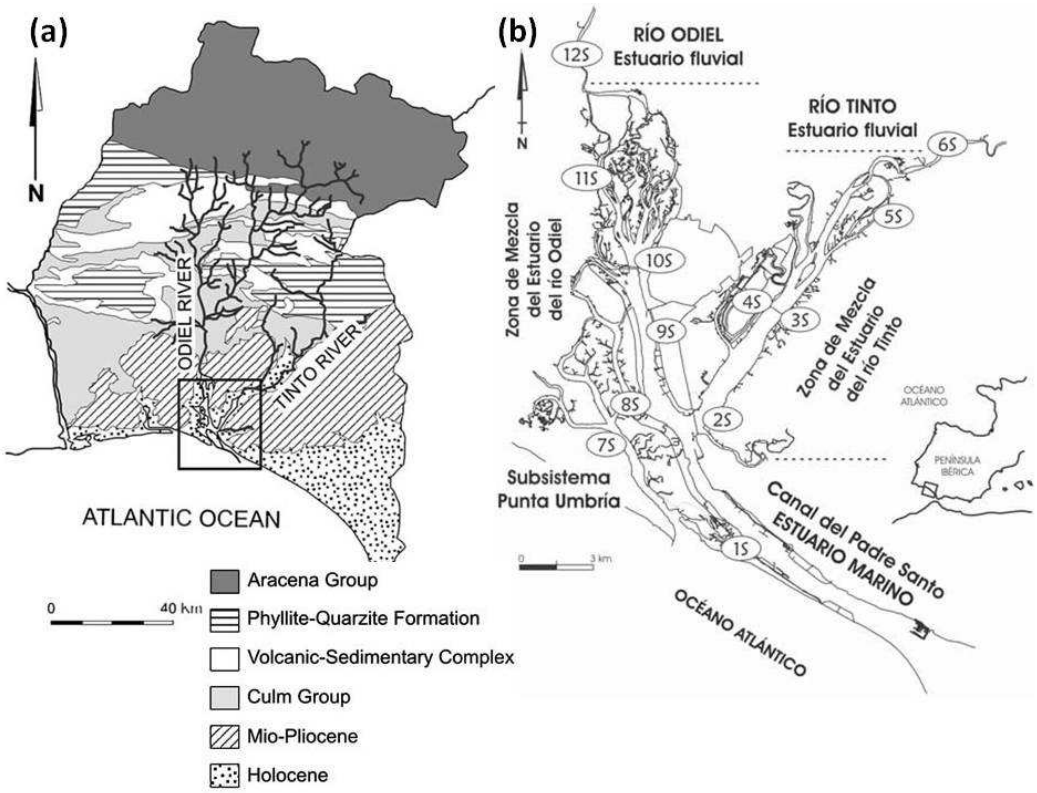

Figure 2.8 (a) Geological substratum of the Odiel and Tinto River drainage network (the Iberian Pyrite Belt) [source: López-González et al. 2006b]; and (b) sediment traps for a sediment texture analysis in the Tinto-Odiel estuary [source: Lopez-Gonzalez *et al*., 2006a]

The main source of sediments in the Odiel saltmarshes comes from the sediment transported by the fluvial currents from the North (mainly from the lower river basin) and tidal currents from the South (Atlantic Ocean). Fluvial sediments come mainly from the Odiel River (with a river basin of 2,333 km^2), although the Tinto River (with a river basin of 739 km^2) also provide some sediments at the lower estuary confluence. The fluvial currents introduce an average of 5,600 tonnes per year in the estuary that in combination with marine sediments enable the vertical growth of the saltmarsh (Ruiz *et al*., 1994). The short term accretion rates estimated for the Odiel estuary ranged between 1 and 1.7cm y^{-1} (Ruiz *et al*. 1994).

Intra and inter-annual variability in suspended sediment concentrations is a common occurrence in tidal marshes and other coastal ecosystems (Schile *et al*., 2014). At the study site, the influence of the Mediterranean climate and storm-based sediment pulses on marsh accretion increases the uncertainty on sediment supply when short time series are used, because they do not cover the natural variability in suspended sediment concentration. In the Odiel saltmarshes, the historical suspended sediment concentration is unknown. However, historical accretion rate data are available and provide some information about sediment availability and the ability of this particular saltmarsh to growth vertically. Long-term accretion rates are crucial for investigating the response of

the Odiel saltmarshes due to sea-level rise because they take in account soil compaction over the time. Previous research on the Odiel saltmarshes includes the acquisition of several cores (Figure 2.9; Table 2.1), where radiocarbon analysis has enabled the calculation of accretion rates (Davis *et al.*, 2000; San Miguel *et al.*, 2001; Morales *et al.*, 2003). These rates have shown that most of the sites investigated at the Odiel saltmarshes have been growing vertically a few millimetres per year. However, these rates vary depending on the location within the estuary and environment. Figure 2.5 and Table 2.1 show that different saltmarsh environments have different sedimentation rates.

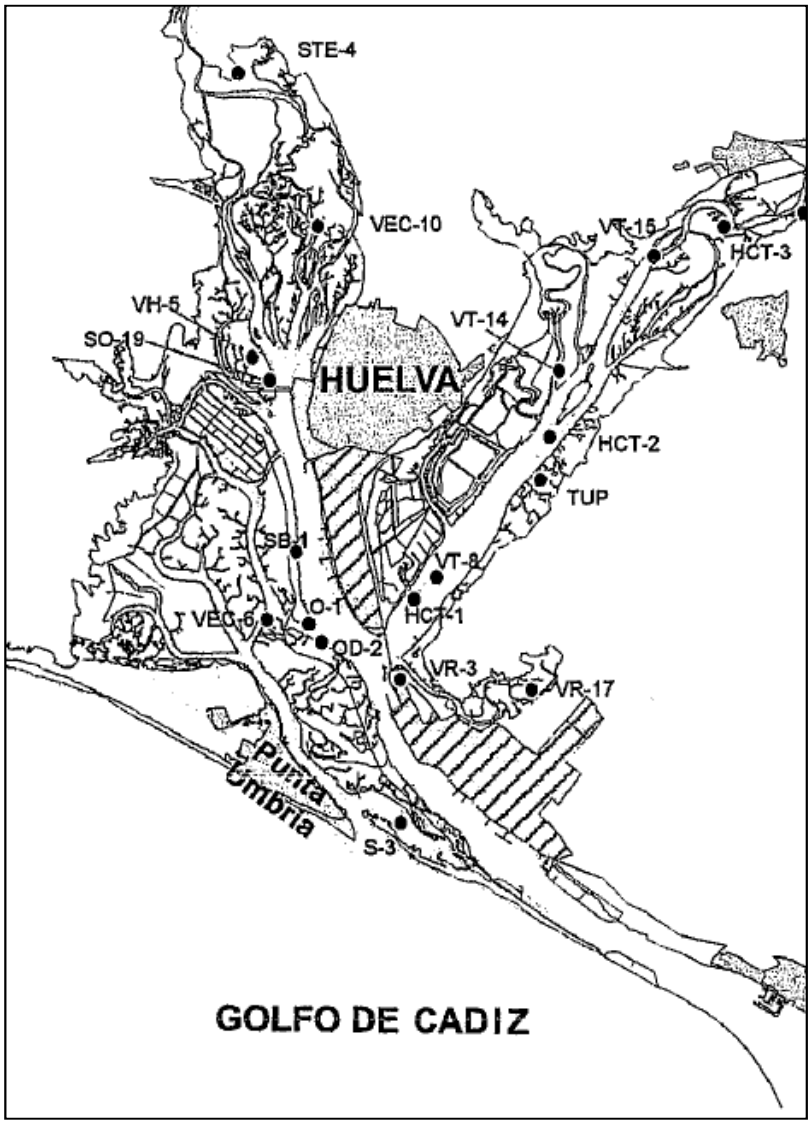

Figure 2.9 Location of the sediment core sites in the Odiel-Tinto estuary. [Source: Morales *et al.*, 2003]

Table 2.1 Published accretion rates in different environment of Odiel saltmarsh

Site	Rates (cmy^{-1})	Width	Environment*	Reference
HCT-1	0.26 +- 0.55	0-47 cm		
HCT-2	0.39 +- 0.01	0-32 cm	Channel edge	(Davis *et al.* 2000)
HCT-3	0.30 +- 0.01	0-41 cm		
S-3	0.10 +- 0.01	0-18 cm	Tidal flat	
OD-2	0.45 +- 0.01	0-15 cm	Channel edge	
OD-2	1.06 +- 0.02	0-36 cm	LM	
O-1	0.18 +- 0.01	36-45 cm	Channel edge	(San Miguel *et al.* 2001)
TUP	1.21 +- 0.03	0-40 cm	LM	
TUP	0.40 +- 0.01	40-80 cm	Channel edge	
VEC-6	0.21 +- 0.02	0-27 cm	HM	
VT-8	0.141	0-240	Channel + TF	
VT-15	0.115	0-410	Channel + TF	
-	0.033	0-130	FP	
-	0.433	130-390	Channel Edge	
ST-1	0.336	390-750	Channel	
-	0.217	750-1270	TF	
VH-5	0.436	0-565	Channel Edge+ HM	
VEC-10	0.137	0-400	Channel Edge+ HM	(Morales *et al.* 2003)
STE-4	0.177	0-1400	TF	
-	0.070	0-1000	Channel Edge +HM	
SB-1	0.671	1000-3250	TF	
-	0.240	0-1310	Channel	
SO-19	0.241	1310-2210	TF	
VR-3	0.122	0-340	Channel Edge + HM	
VR-17	1.076	0-355	Channel Edge + LM	

*TF= Tidal flat; HM= High marsh; LM= Low marsh; FP= fluvio-marine Flood Plain

The saltmarsh vegetation is characterised by Mediterranean saltmarsh species (e.g. *Salicornia ramossisima*, *Salicornia fruticosa, Arthrocnemun macrostachyum*, *Limoniastrum monopetalum* and *Suaeda vera*) with some variations due the Atlantic influences (*Spartina maritima*) (Gehu & Rivas-Martinez, 1984). The Odiel saltmarshes have been classified as 'Mediterranean-Atlantic saltmarshes' by Gehu and Martin-Rivas (1984) and as a sedimentary shore with 'barrier connected, foreland and estuarine saltmarshes' by Dijkema (1984).

In a local context, these environments provide many ecosystem services that directly benefit the local communities and in a regional context, they are of special interest for migratory birds due to its strategic location between Africa and Europe. For example, these saltmarshes are the nesting place of one of the largest spoonbill (*Platalea leucorodia*) colonies in Europe (30% of total the population in Europe). This species is cited in Annexe I of the European Directive with relation to wild birds (79/409, CEE) and it has been identified as vulnerable with less than 10,000 couples (8,900 nesting couples, *BirdLife International* 2004).

2.2. General methodology: work packages and work flow

The research conducted here incorporates a multifaceted methodology for investigating the response of the Mediterranean-Atlantic saltmarshes due to sea-level rise at local scales. This is important because the sustainability of these ecosystems is vulnerable to anthropogenic pressures and potential impacts due to sea-level rise, which are locally variable. Here, monitoring and projecting future responses in saltmarshes are crucial in order to reduce sea-level rise impacts by means of integrated management (restoration/adaptation). Thus, the developed methodology will be applied at the estuary landscape scale to understand locally the current state of saltmarshes, the recent past and the future behaviour.

To achieve the aims and objectives previously described, the programme of work has been divided into three work packages, summarised as a work flow in the Figure 2.6. Each work package follows a different approach, and in order to keep chapter unity, the methods for each work package are outlined and explained in each chapter. First, the overarching explanation of the work packages and work flow is reviewed here. The three work packages broadly reflect i) the recent past evolution (WP1), ii) the contemporary nature of the system (WP2), and iii) the future behaviour (WP3) of the Odiel saltmarshes (Figure 2.6). They are inherently interlinked through field-data acquisition and analysis, secondary data processing and validation, and modelling.

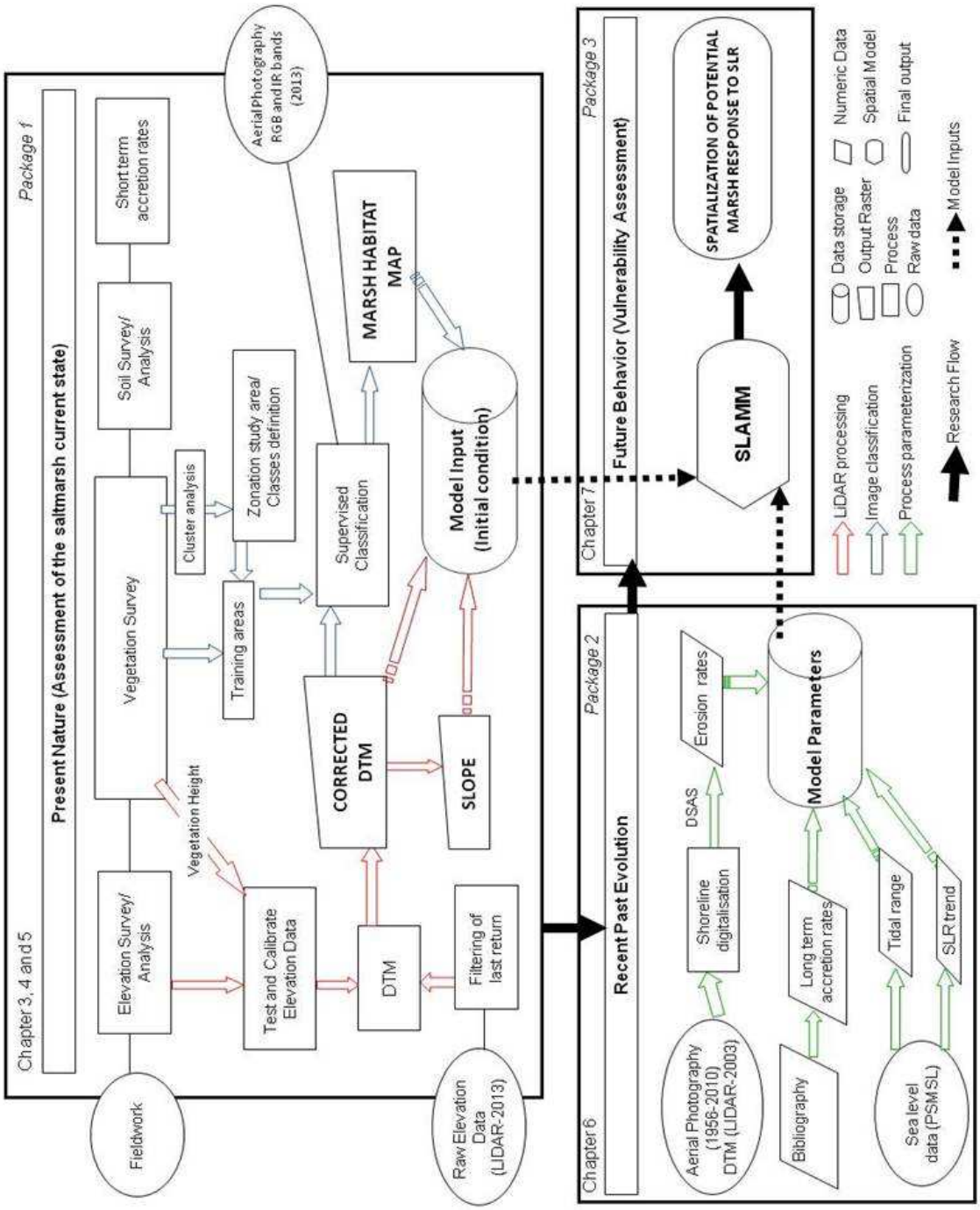

Figure 2.10Thesis work flow and work packages.

WP1 focuses on examining and improving understanding of the recent (last 50 years) geomorphological and anthropogenic evolution of the Odiel saltmarshes. This includes establishing saltmarsh development, and researching the relative importance of different forcing mechanisms on the development and dynamics of the Odiel saltmarshes. In particular, the role of sea-level rise on saltmarsh behaviour will be evaluated. These analyses also provide some of the parameters needed for running the sea-level change and saltmarsh response using model SLAMM (WP3). The centres of inquiry in this work package are:

- change analysis of environmental units to ascertain saltmarsh respond to various drivers such as sea-level change, costal defend infrastructure construction and natural processes;
- change analysis of saltmarsh shoreline delineated from recent (1956 to 2013) aerial photographs to derive saltmarsh erosion rates;
- synthesis of historical accretion rates from published data (core sediments). Long-term accretion rates are crucial for investigating the response of the Odiel saltmarshes due to sea-level rise. Previous research on the Odiel saltmarshes includes the acquisition of several cores (Figure 2.9; Table 2.1).
- synthesis of historical sea-level trends derived from gauge data and satellite altimetry. In the Gulf of Cadiz only two tide gauges have longer series which are available from the Permanent Service for Mean Sea Level (PSMSL): the Cadiz (Spain) tide gauge (1961 to 2009) and the Lagos (Portugal) tide gauge (1906 to 1990). In the study area, the Mazagon (Huelva) tide gauge has been collecting data since 1997 and is maintained by the national tide gauge network. Mean values during 1997-2003 of tidal levels from this tide gauge are shown in Table 2.2: levels have been calibrated with the Spanish hydrographic datum (Alicante).

Table 2.2 High tide data of the Mazagon tide gauge (Huelva) corrected by reference vertical Datum (Spanish hydrographic zero; zero in Alicante). The tide gauge's original data were referred to its own datum and the shown height in the table has been calculated. [Fraile, 2005]

Mean Tides in Odiel-Tinto Estuary (1997-2003)	**Tidal coefficient**	**Huelva (m)**
The Highest High Water (HAT + surge)	-	2.77
Highest Astronomical Tide (HAT) -- highest equinoctial spring tide	1.2	2.09
Mean Higher High Water (MHHW) -- mean High equinoctial spring tide	1	1.78
Mean High Water Spring (MHWS) -- mean High spring tide	0.94	1.69
Mean High Water (MHW) --mean High daily tide	0.7	1.32
Mean High Water Neap (MHWN)	0.45	0.93
(weak High neap tide)	0.2	0.55
Height difference between tide gauge mean level and reference topographic zero (Alicante)	-	0.39

WP2 focuses on assessing the present nature of the study site (the Odiel saltmarshes). This package acquires, collates and examines high resolution data to spatially characterise the current morphological, sedimentary and ecological nature of the

saltmarshes. Work undertaken in this package produces a suite of data layers (DEM, slope and saltmarsh habitat map) necessary to progress the modelling work in WP3. The centres of inquiry in this package are summarized below:

- saltmarsh habitat and species survey, including an analysis of the spatial organisation of plant species and vegetation communities, and elevation-ranges associated with;
- saltmarsh surface sedimentation rates, derived from field-based sediment trap measurements, to ascertain associations between topography, vegetation communities and deposition rates;
- saltmarsh vegetation and habitat mapping using several image classification techniques (pixel based and object based supervised classification) and remotely sensed data (satellite imagery and aerial photography), incorporating evaluation of these approaches to find the most suitable method for mapping and monitoring Odiel saltmarsh habitats in the context of available data.
- topographic surveying, and analysis of saltmarsh morphology using LiDAR data to thoroughly characterise saltmarsh structure and eco-geomorphology;
- The final work package (WP3) is based on the application of a sea-level change saltmarsh response model to the Odiel saltmarshes. Here, the SLAMM model (Clough *et al.* 2010) has been applied. All data compiled and processed in WP1 and WP2 are integrated into the progression of this modelling. This work package is focussed on understanding SLAMM and undertaking a suite of different scenarios that address uncertainty in both sea-level rise projections and data resolution.

2.3. Data description

2.3.1. Andalusian Vegetation map

The digital vegetation map of Andalucia (at a scale of 1:10,000) provides the only site-wide vegetation data that includes the whole of the Odiel saltmarshes. The surveys that underpin the map were undertaken by Environmental Ministry of Andalucia between 1993 and 2003 for Andalucía, and specifically 2003 for the Odiel saltmarshes. Data was derived through photo-interpretation (based on aerial photography from 1993 and 2003) and digitisation of homogeneous polygons *at 10,000 scale* supported with ground truth surveys by means of vegetation quadrats (0.5 x 0.5 m). The resulting geodatabase is detailed and provides percentage vegetation cover of the dominant species in every polygon. This map is published by the Environmental Ministry of Andalucía and is available by request. The primary use of this data is in the selection of training areas for the image classification processing and validation during previous years.

2.3.2. Airborne LiDAR

A combined LiDAR sensor and photogrammetric camera flight (Table 2.3) was carried out on 29th January 2013 specifically for this study and has been funded by the project '*Detail mapping and web dissemination of demographic, tourist and environmental data for vulnerability assessments linked to beach erosion in the Andalusia Coast (sea level rise associated to climate change)*' (Department of Geography, University of Seville). Data were collected for the whole Odiel saltmarshes during the low tide (-1.1 m; tidal coefficient= 89) to minimize the amount of water on the marsh surface. Reported vertical and horizontal accuracies for the LIDAR sensor are 0.07-0.10m and 0.15-0.17m respectively. A high resolution aerial photograph (R, G, B, IR, and panchromatic bands) was also taken with 0.15 m spatial resolution. The final products of this flight were: raw LiDAR data ('LAS' files), multispectral aerial photographs (102 photograms), digital surface model (DSM) and digital elevation model (DEM).

Table 2.3 Details of the LiDAR flight carried out in February 2013

LiDAR Flight	
Sensor name	ALS50 II
Flight height	1450 m – 1600 m
Pulse frequency	Until 145.3 kHz (145,300 pulses/s)
Altimetry precision expected	10cm
Number of Collected returns	4
Recorded intensity	Once per pulse
Multiples Pulses in Air	Yes
Points density	2 points*m^{-2}

2.3.3. Aerial photography

Aerial photography is the primary geospatial imagery used here to explore the evolution of the study area during the last 50 years, from which shorelines can be digitised and erosion rates calculated. Additionally, they are used as the basis for past habitat mapping. There are several aerial photographs available for the study site from the last few decades. Aerial photographs available range between 1956 and 2011 and have a spatial resolution of between 0.5 and 1 metre (Table 2.4). The oldest photography (1956) and was carried out by the military service of USA. This photography was only available as a hard copy, but between 2005 and 2006 was georeferenced and converted into a digital orthophoto and thus now is also available in digital format. This is important as the data provides information about the saltmarshes before the significant anthropogenic modification that

occurred during the seventies. A range of other post-1970s orthophotos is available for the study area, accessible through inter-operable services[9].

Table 2.4 Aerial photographs available for the study area [Source: www.idendalucia.es]

Year	Resolution (m)	Type	Source
1956/57	1	B/W	Military service USA
1977/83	0.5	B/W	Spanish National Photogrametric flight
1984/85	1	B/W	Spanish National Photogrametric flight
2001/02	0.5	B/W	Spanish National Photogrametric flight
2007	0.7	Colour	Spanish National Photogrametric flight
2008/09	0.5	Colour(R, G, B, IR)	IECA - PNOA
2010/11	0.5	Colour	Spanish National Photogrametric flight
Feb-2013	0.15	Colour(R, G, B, IR)	Dept. Geography (University of Seville). It was acquired in combination with a LiDAR flight

2.4. Field campaigns

Fieldwork undertaken for this research was organized into seven campaigns (Table 2.5). The first campaign was mainly exploratory (for familiarisation purposes) to establish access points for saltmarsh and to review the vegetation species presence. This campaign helped plan the other campaigns. During the second campaign, a random vegetation and sediment survey were carried out, and ground truth data for image classification purposes were also collected. The third campaign focussed on deployment of sediment traps across the saltmarsh systems, selecting different saltmarsh habitats. The fourth was a continuation of the vegetation survey and ground-truth data collection. During this campaign, elevation surveys were also carried out. Two elevation surveys were undertaken: the first one on the boundaries of the marsh (over roads), and the second one within the saltmarsh. Finally, the fifth campaign was a continuation of the elevation survey within the saltmarsh.

Table 2.5 Campaigns overtaken for field data acquisition

Campaign	Starting date	Finishing date
1	05/09/2011	09/09/2011
2	13/09/2011	25/09/2011
3	28/12/2011	07/01/2012
4	03/09/2012	22/09/2012
5	26/08/2013	30/08/2013

[9] http://www.ideandalucia.es/index.php/en/visualizacion-wms/44-servicios-de-ortofotos-y-ortoimagnees-generales

3. Historical evolution of the Odiel saltmarshes (Tinto-Odiel estuary)

The coastal zone is subjected to a dynamic equilibrium especially sensitive to any alteration (natural or anthropogenic). In order to assess the potential impacts of sea-level rise, it is crucial to understand the parameters that control the current behaviour of a particular coastal site and their recent evolution. The aim of this chapter is to analyse and quantify the anthropogenic and the geomorphological changes in the Odiel estuary (incorporating the Odiel saltmarshes and the lower reaches of the Tinto-Odiel estuary) over recent decades. The response of the system is evaluated in the context of key driving mechanisms, such as sea-level rise, and broader environmental changes. To address this aim, decadal geomorphological and anthropological changes within the estuary and across the saltmarsh are explored through spatial analysis of available aerial photography. The results presented here provide context information to assess future sea-level rise impacts in a human-modified saltmarsh such as the Odiel saltmarshes in Chapter 7, as well as medium term horizontal erosion rates that are required for modelling those impacts.

3.1. Methods

3.1.1. Data

The data availability limits the time frame available for analysis to the last 60 years. The earliest aerial photography available is from 1956 (1 m spatial resolution) and the most recent 2013 (0.15 m spatial resolution); the interval between surveys is approximately decadal, although no surveys were undertaken in the 1960s leaving a gap of 20 years in the early part of the dataset. Landsat imagery is also available for the study area since 1983, but the spatial resolution (30 m) of these images does not allow a fine quantitative analysis of the saltmarsh, in particular small infrastructures such as dikes/sea walls or the horizontal saltmarsh retreatment or growth. Furthermore, there is not LandSat imagery available for the 1950s and 1960s during the period when major anthropogenic changes occurred. Thus LandSat imagery has not been used for this study. Previous to this time there are several published historic maps and charts of this area for the following years: 1862 (Spanish Royal Navy; Figure 3.1), 1875 (Hydrographical Agency), 1936 (Spanish National Geographic Institute) and 1946 (Cartography Institute of Andalucía; Figure 3.2). These maps are the only information source that shows the geomorphogy of the estuary before the 1960s, and have been used here for obtaining qualitative information only. They have not been used for calculating quantitative habitat change and erosion rates, due to the lack of information about the indicator used for shoreline drawing and resolution.

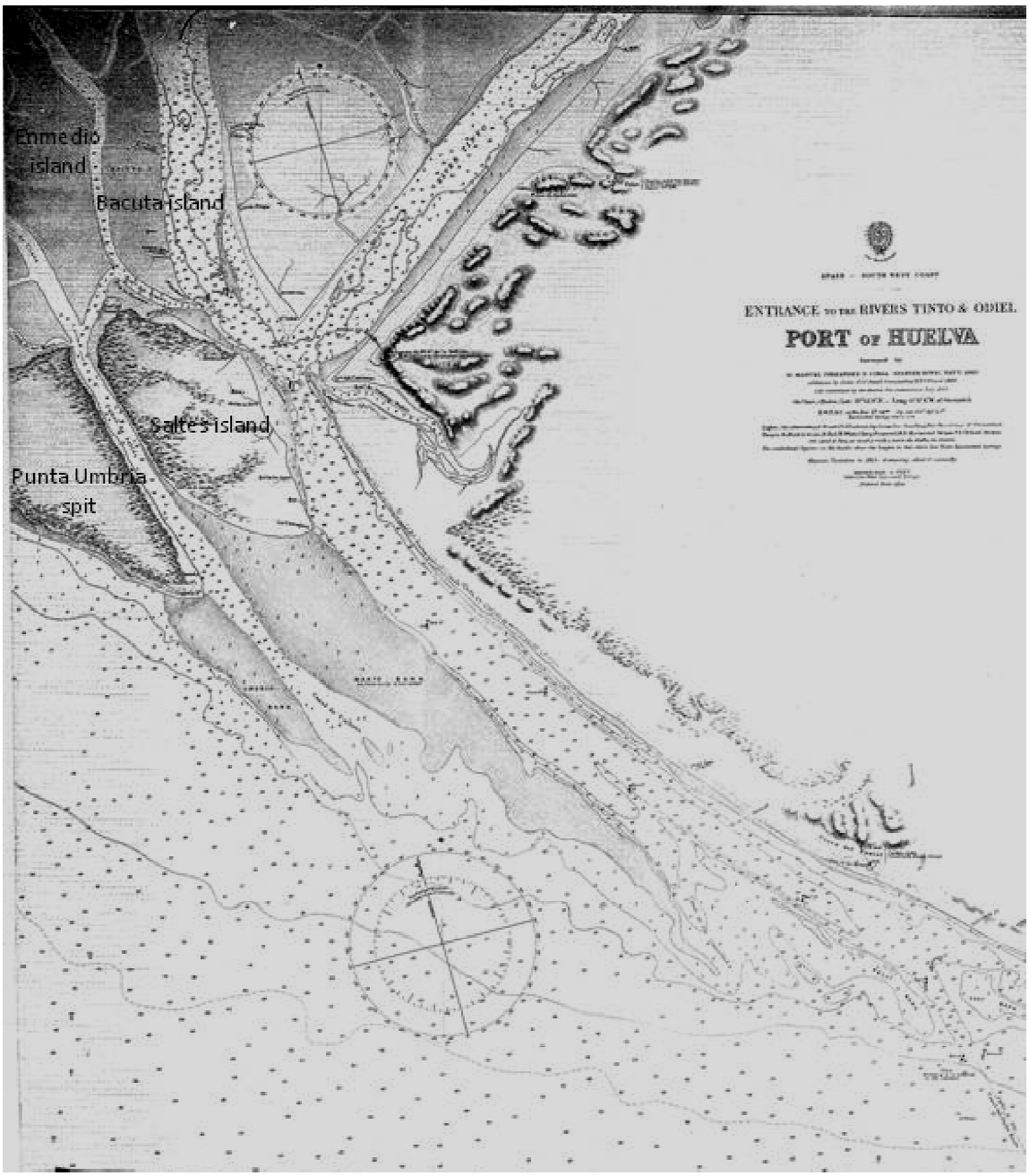

Figure 3.1 Configuration of the Tinto-Odiel estuary mouth in 1862 [Source: map surveyed by Fernandez y Coria; and published by Spanish Royal Navy (1862)]

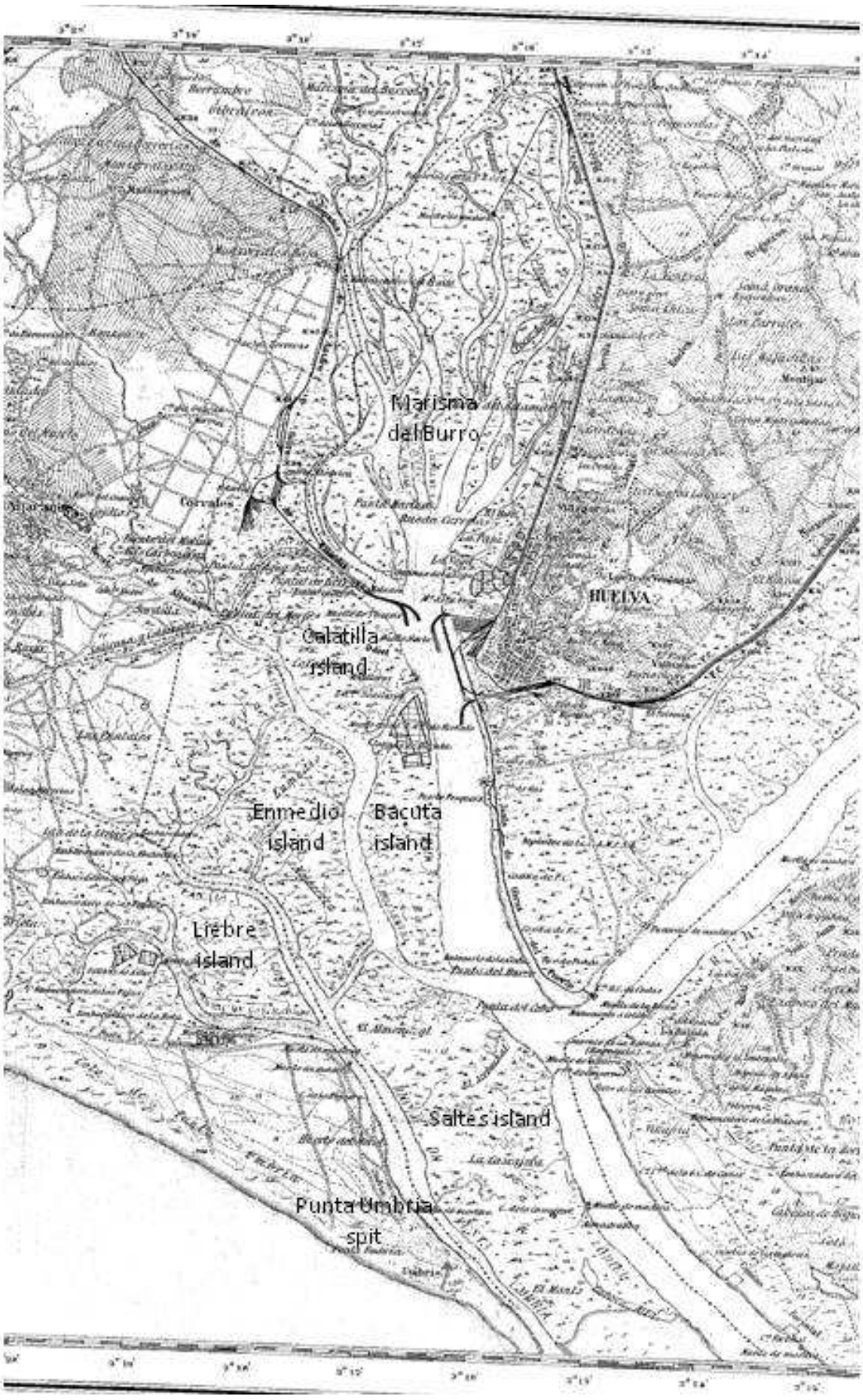

Figure 3.2 Configuration of the Tinto-Odiel estuary in 1946 [Source: map published by Cartography Institute of Andalucía, 1946]

3.1.2. Decadal estuarine changes

The investigation of decadal estuarine changes has been carried out through the digitisation of geomorphological and anthropogenic features at different points in time from aerial and satellite imagery (between 1956 and 2013). The change detection analysis was based on the geospatial mapping from these resources for years: 1956, 1979, 1984, 2001, 2007 and 2013. The features recognised on the aerial photos were digitised and on completion of this task for all coverages, the features were rationalised to 9 classes:

- *Backshore*: the unvegetated supratidal zone
- *Hard infrastructure*: hard coastal structures such as dikes, sea walls and embankments.
- *Harbour*: marinas, fishing and industrial ports
- *Saltmarshes*: high density and low density saltmarsh vegetation
- *Reclaimed area*: areas modified by humans where the natural functions have been modified. For example, saltmarsh environments transformed into salt factories or dried up for agriculture or other activity
- *Sand dune*: this category refers to active and stable barrier island and sandy spits that have been colonised partially or completely by vegetation
- *Tidal channel*: sub-tidal channel
- *Intertidal mud*: muddy intertidal flats and channels
- *Intertidal sand*: sandy intertidal flats and bars

The digitisation process was undertaken at the scale of 1:2,000 within an ESRI geo-database (ArcGIS 10.2), using the indicators shown in Table 3.1. Firstly, all polygons were created across the 2013 aerial photography (after visual photo-interpretation), producing the '2013 *layer'* (spatial resolution). The aerial photography for other years were not digitised from scratch but modified from previous layers. For example, polygons included in the '2013 *layer'* were modified (down-dated) for generating the '2007 *layer'*; the '2007 *layer'* was used for generating the '2001 *layer'* and so on. Only polygons that experienced changes between years were modified. Thus, the unchanged polygons will have the same boundaries in all years, reducing potential manual error in polygon delimitation or data entry in the attribute table. This approach also reduces the execution time. In addition, the final layers were submitted to a quality control through the topology error tool in ArcGIS 10.2, where the following rules were used: "polygons must not overlap" and "polygons must not have gaps". In total, more than 1000 topology errors were corrected.

Table 3.1. Indicators used for the digitalisation process

Class	Indicator	
	Lower limit	Upper limit
Backshore	The wet mark visible from the high tide	The vegetation boundary
Hard infrastructure	The outer limit of the coastal infrastructure	
Saltmarshes	The saltmarsh vegetation boundary facing tidal flats or channel	The saltmarsh vegetation upper boundary
Reclaimed area	Outer limit of the sea wall or the visible transformation	
Sand dune	The backshore or tidal flat	Urban areas/ other cover class
Tidal channel	Permanently flooded zone	The lowest low tide found
Intertidal mud	Tidal channel	Other cover class
Intertidal sand	Tidal channel	Other cover class

The change detection analysis was carried out in Microsoft access, analysing the geo-database tables produced during the digitisation process. The surface area of each class per year was calculated and compared over the studied time period. The percentage of change (PoC) between years was also calculated for pair of years for the whole period following equation 5. The PoC is the absolute change experienced by one class when the class surface area in the initial year is compared with the final year of a certain time interval. The PoC values can be positives or negatives, indicating the change direction: negative values means loss of area and positive gain of area.

$$PoCi = \frac{(Cf - Co)}{Co} * 100 \quad (5)$$

where, Co is the surface area (ha) of the class i in the initial year of the time interval, and Cf is the surface area (ha) of the same class in the final year.

3.1.3. Saltmarsh patch analysis

The procedure followed for analysing saltmarsh patches at landscape scale has been based on the principles of landscape fragmentation using the Land Fragmentation Tool[10] (LTF v2.0). Although this tool has been developed following the forest fragmentation classification described in Vogt *et al.* (2006), and using equivalent procedure, it can be applied to any land cover type of interest (saltmarshes in this case). LFT is a python script that runs out of ArcToolbox in ArcGIS 9.3 or 10.0, and enable to perform patch analysis in an intuitive and efficient manner.

[10] developed by Jason R. Parent and James D. Hurd with the support of the Center for Land use Education and Research, and the Department of Natural Resources and the Environment at the University of Connecticut

LFT classifies a land cover (raster format) into four categories based on a specified edge width: *patch* (pixels that form small fragments of the land cover of interest), *edge* (outer perimeter of the core), *perforated* (inner perimeter of gaps in the core) and *core* (Figure 3.3). In the particular case of tidal marshes due to the spatial distribution of channels and creeks that perforate saltmarsh habitats, it has been noted that inner and outer *core* perimeter has been classified as *perforated.* Thus *edges* and *perforated* are considered the same for this analysis and have been named *edge*. Due to the lack of literature related to "edge effect" in saltmarshes, an edge width of 20 m has been considered suitable for this study based on the Odiel saltmarshes size and the results presented by Benoit and Askins (2002) (where they reported that small anthropogenic (<10 m) and natural (<30m) barriers affect different saltmarsh birds distribution and nesting in Connecticut saltmarshes). The input data used to run this analysis were raster files with two classes: 'non saltmarsh' (cell value=1) and 'saltmarsh' (cell value=2). The inputs raster were derived from the digitised layers (1956, 1977 and 2013) in the change detection analysis, where the 'shapefiles' were converted into raster files (5m cell size) and reclassified using ArcGIS 10.2.

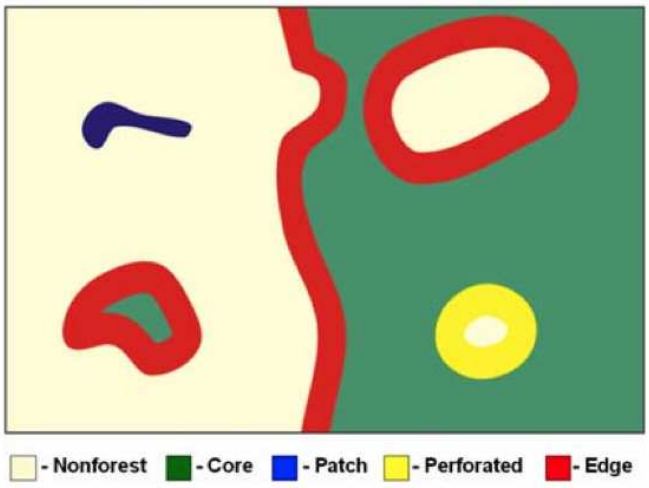

Figure 3.3 Four classes of spatial pattern exhibited within land cover data [Source: Vogt *et al.,* 2006]

The analysis carried out here has been adapted and interpreted based on saltmarsh patch analysis. The purpose of this analysis is to identify those saltmarsh zones that are potentially more sensitive to sea-level rise. These zones include saltmarsh patches (pixels that form small fragments of saltmarsh) and edges (pixels that occur along the perimeter of core zones) originated naturally or by human pressures. Patches and edges are assumed to be less resilient to new pressures than cores due to the smaller size and the proximity to others land cover types ("edge effect"). The pixels classified as core are outside the

"edge effect" and are assumed to be more resilient. Core pixels are sub-divided into three categories: *small core* (<100 ha), *medium core* (100-200 ha) and *large core* (>200 ha).

3.1.4. Shoreline changes: horizontal erosion and sedimentation rates

In order to investigate shoreline changes in the Odiel saltmarshes, shorelines were digitised as polylines for the following years: 1956, 1979, 1984, 2001 and 2013 (Figure 3.4). The digitisation of the shorelines was carried out under the same specifications explained in section 3.2.1. The indicator used for the shoreline digitisation was the saltmarsh vegetation boundary. This indicator was selected due to its stability over time (Pajak & Leatherman, 2002) and because it was a feature clearly visible in all images.

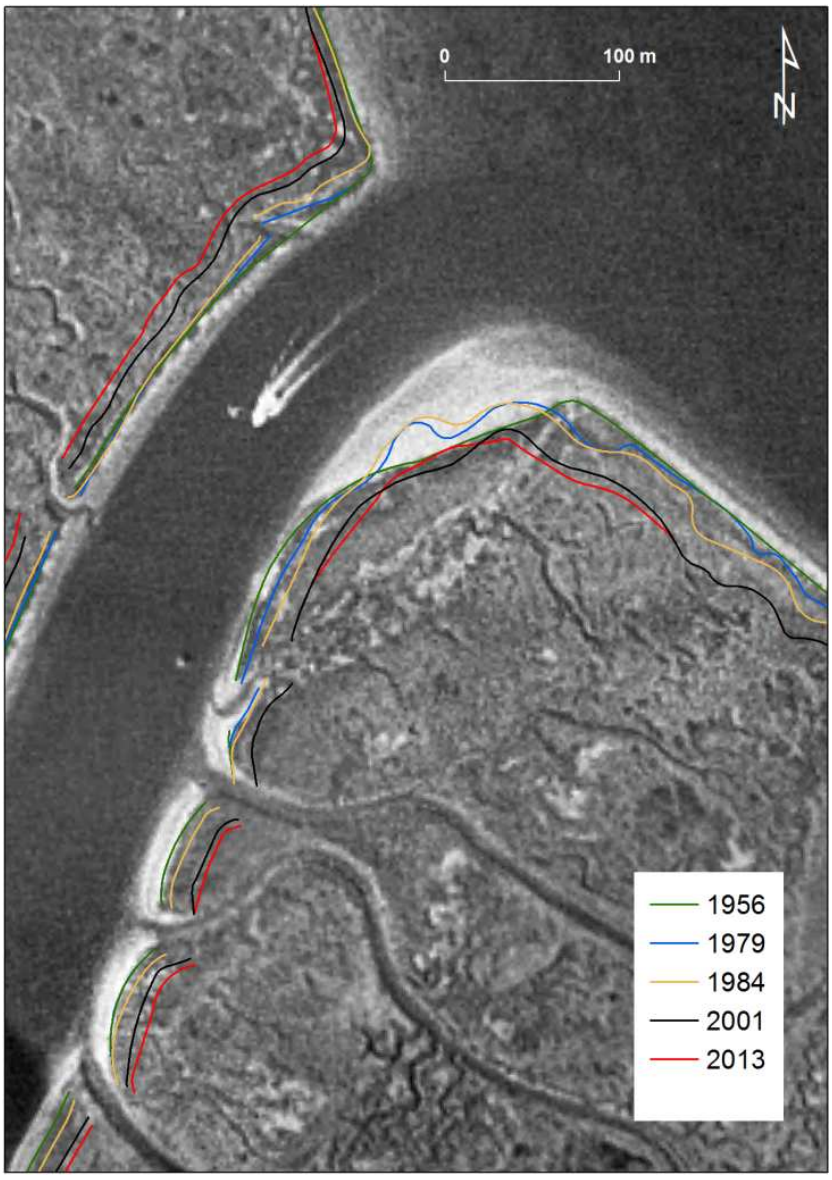

Figure 3.4 Shoreline digitalisation for calculating rate-of change in the Odiel saltmarshes. The shorelines are displayed over the 1956 aerial photography

Decadal shoreline change in the Odiel saltmarshes was analysed using the Digital Shoreline Analysis System (DSAS v4.0). DSAS is a freely available extension for ESRI ArcGIS that enables the calculation of shoreline rate-of change statistics from a time series of multiple shoreline positions (Himmelstoss, 2009). DSAS works by generating orthogonal transects from a given baseline at a user-defined separation. For this work 100 m separation was given and 782 transects were generated (Figure 3.5). The generated transects are used to calculate retreat or advance of the shoreline for each of the time intervals. Then, DSAS calculates rates-of-change and associated statistics that are reported in an attribute table. The DSAS tool requires user data to meet specific field requirements. DSAS produces several shoreline change measures within the transect output layer. The measurement used here is the end point rate (EPR) and linear regression rate-of-change (LRR). The EPR is calculated by dividing the net distance of shoreline movement by the time elapsed between the earliest and latest measurements (*i.e.* the oldest and the most recent shoreline); the LRR statistic can be determined by fitting a least squares regression line to all shoreline points for a particular transect (the rate is the slope of the line) (Himmelstoss, 2009). The EPR reflects the net rate of change, in this case from 1956 to 2013; the LRR expresses a rate of change that takes into account all time steps across the available data.

In order to characterise saltmarsh shoreline behaviour, a cluster analysis was performed using the relative shoreline distance at each time interval for each transect (N=782). Different clustering approaches were carried out including average (mean distance) and Ward's hierarchical method. The clustering approach used was the average method (in 'R' v.2.15.1), which gave the best cophenetic correlation (CC = 0.98) when compared with other methods (for example Ward's method CC = 0.37). Cluster analyses have been proved to be a suitable method for classify coastal areas as it was reported by Scott *et al*., (2011).

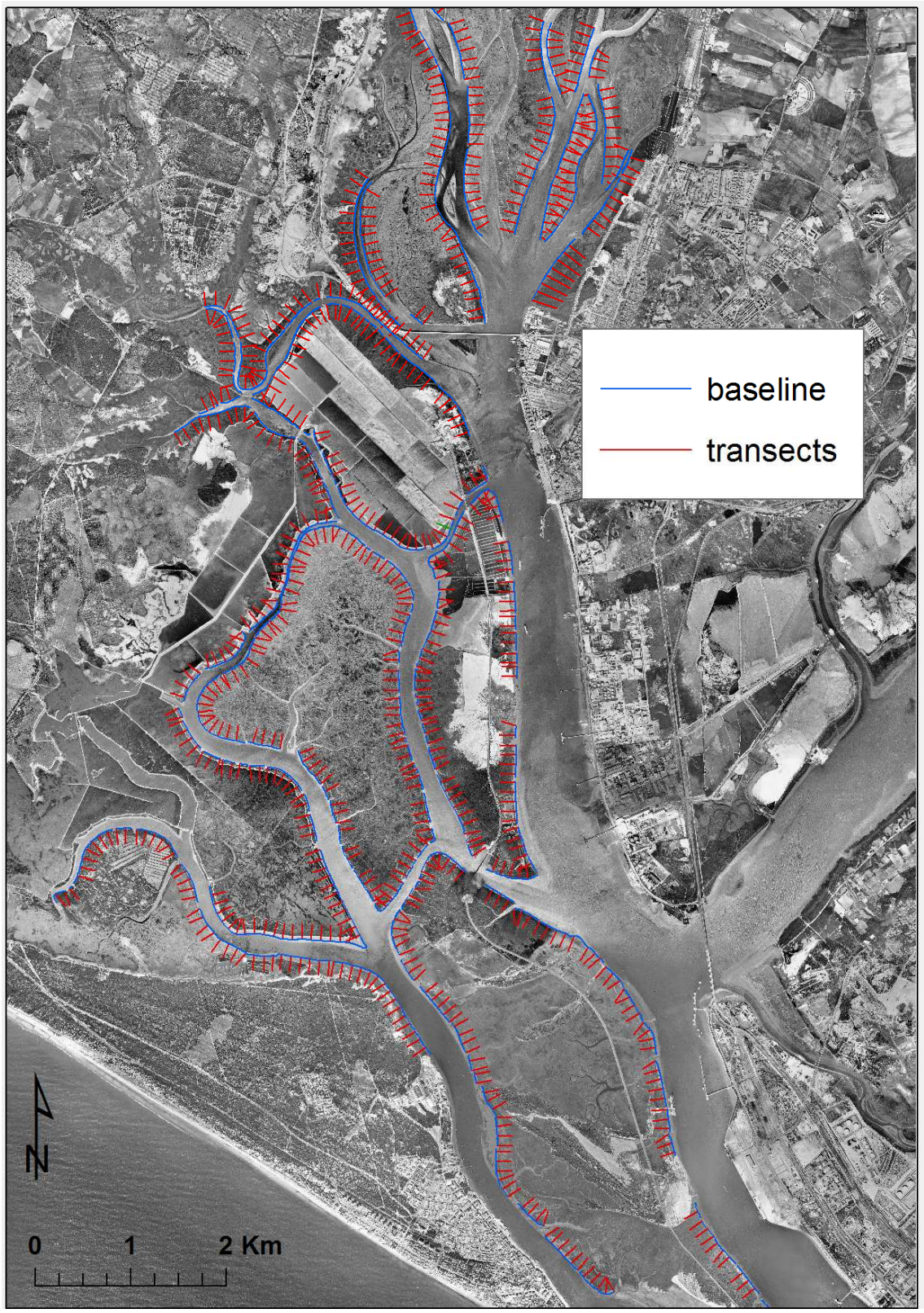

Figure 3.5 Orthogonal transects generated by DSAS (ArgGIS 10.2) from a digitised onshore baseline for shoreline change analysis in the Odiel saltmarshes.

3.2. Decadal geomorphological and anthropologic changes

Odiel saltmarshes have experienced important changes during the last decades in the studied area (Table 3.2; Figure 3.6; Figure 3.7). The results derived from the change detection analysis by class show that during the time period 1956-1979, the total *saltmarsh* surface area was dramatically reduced roughly 1,000 ha (Table 3.2), which is closely related to the increase in the *reclaimed area* (~ 1,000 ha). The *saltmarsh* class experienced a loss of more than 25% between these years (Table 3.3), while the *reclaimed area* class increased its total surface by >100% for the same time interval. The surface area of the *harbour* / *hard infrastructure* classes also increased between 1956 and 1979: the PoC for *harbour* is 18.1% (surface area increase of 0.35 ha) and >100% for *hard infrastructure* (surface area increase of 16.5 ha). The PoC for the classes *backshore*, *intertidal mud* and *intertidal sand* were-40.3, -16.8 and -89% respectively, reducing their surface area by 27, 176 and 448 ha approximately. The reduction of these three classes is closely related to the expansion in the *tidal channel* (> 540 ha).

Table 3.2 Surface area in hectares computed per class and year of the Odiel saltmarshes

	1956	1979	1984	2001	2007	2013
Backshore	67.7	40.4	71.5	55.8	52.9	50.2
Hard infrastructure	15.8	32.3	49.8	69.2	69.6	68.9
Harbour	1.9	2.3	2.8	3.0	3.1	3.2
Saltmarshes	4147.6	3083.9	3190.2	3303.2	3347.0	3362.3
Reclaimed area	978.4	2146.4	2125.6	2138.6	2153.7	2135.6
Sand dune	228.5	229.5	210.0	328.6	355.7	361.4
Tidal channel	2315.6	2844.9	2402.9	2307.5	2267.6	2253.6
Intertidal mud	1048.8	872.8	1052.6	955.3	925.5	930.6
Intertidal sand	503.2	55.1	202.1	146.4	132.6	141.9
TOTAL (ha)	9307.6	9307.6	9307.6	9307.6	9307.6	9307.6

These results indicate that the Odiel saltmarshes experienced high anthropogenic pressure between 1956 and 1979 that caused a reduction in saltmarsh habitat due to land reclamation and the construction of the Juan Carlos I dike (and associated road). The land reclamation process was due to the development of large industrial salt factories from 1960 in the central section of the studied area (Figure 3.7), which also explained the growth in coastal defences such sea walls and embankments. However, the main factor that has caused the *hard infrastructures* growth in this time interval is the construction of the Juan Carlos I dike.

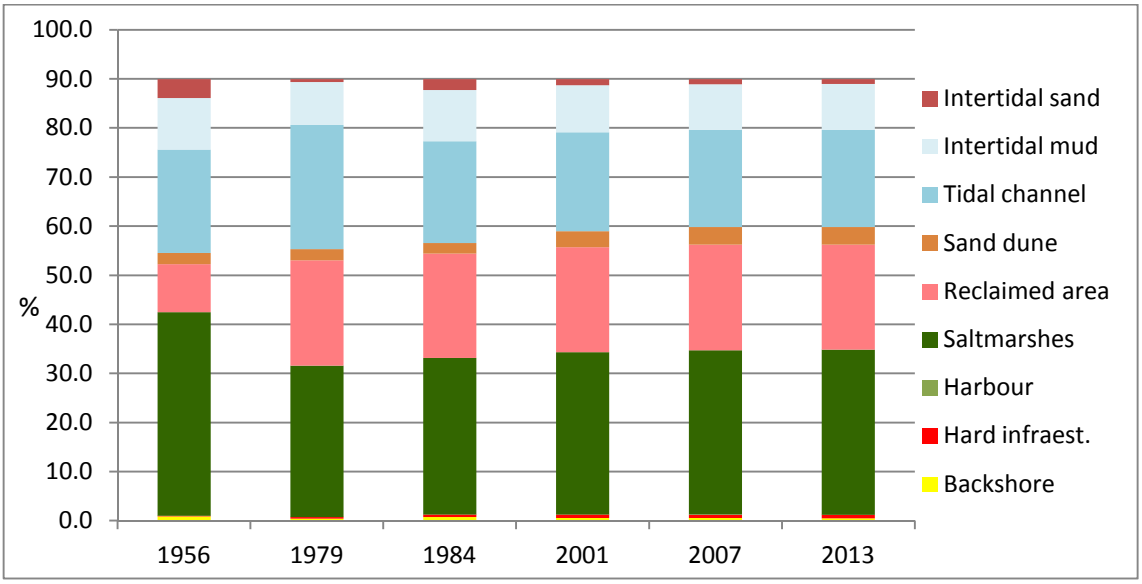

Figure 3.6 Percentage of surface area computed per class and year of the Odiel saltmarshes

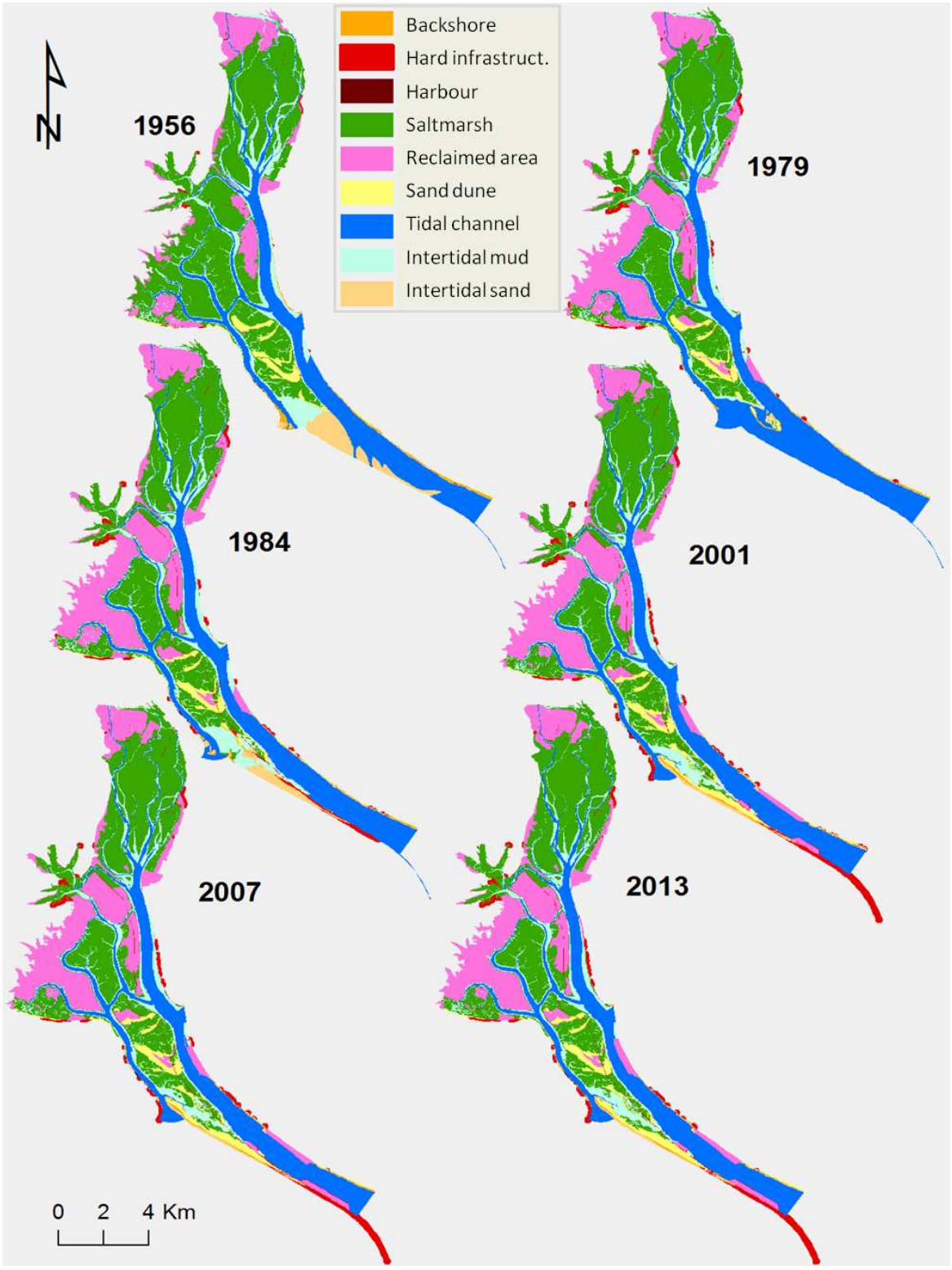

Figure 3.7 Decadal changes of the Odiel Saltmarshes between 1956 and 2013

Table 3.3 Percentage of change (PoC) per period analysed. This percentage represents the relative surface loss or gain experienced per class during each period. Negative values state percentage of surface loss and positive values percentage of surface gain in the final year respect the initial year

	1956-1979	1979-1984	1984-2001	2001-2007	2007-2013	1956-2013
Backshore	-40.3	76.9	-22.0	-5.2	-5.2	-25.95
Hard infrast.	104.1	54.1	39.0	0.5	-0.9	335.66
Harbour	18.1	22.3	8.2	2.2	3.2	64.80
Saltarshes	-25.6	3.4	3.5	1.3	0.5	-18.93
Reclaimed area	119.4	-1.0	0.6	0.7	-0.8	118.28
Sand dune	0.4	-8.5	56.5	8.3	1.6	58.09
Tidal channel	23.6	-15.5	-4.0	-1.7	-0.6	-2.12
Intert. mud	-16.8	20.6	-9.2	-3.1	0.5	-11.27
Intert. sand	-89.0	266.5	-27.6	-9.3	7.0	-71.80

At the estuary mouth, the most notable geomorphological changes between 1956 and 1979 are observed across the tidal flats (mud and sand), tidal channel and backshore. This part of the estuary is very dynamic owing to its exposure to strong tidal currents and high energy swell, in addition to receiving large volumes of sediment from further along the coastline through longshore drift. The composition of the estuary mouth in 1956 is completely different to the one observed in 1979 (Figure 3.8). In 1956, a large amount of sediment occupies the nearshore and mouth forming sand bars, spits and extensive sandy tidal flats. Multiple tidal channels cut through the mouth sand bars, with morphologies comparable to ebb-tidal deltas (Fitzgerald, 1984). By 1979, these sediments amalgamated with one long sand spit growing north toward Saltes Island, between the Punta Umbria Ria (west) and Huelva Ria (east) and favouring the saltmarsh formation in the sheltered area (1979 map; Figure 3.11).

During 1979 and 1984 time period all the classes increased their surface except the *reclaimed area*, *sand dune* and *tidal channel*. The *reclaimed area* decreased by c. 20 Ha, related to the cease and abandonment of some traditional salt flats (e.g. some plots in Salinas de Astur). Natural tidal flooding returned to these areas resulted in some initial colonisation by saltmarsh vegetation. This recovery is shown in the PoC for the *saltmarsh* class: 3.4% (total surface increase in 1984 was ~106 ha). The area of *sand dune* shrank by 8.5% (19.5 ha), explained by a growth in the *backshore* (~31 ha), while the *tidal channel* shrank in nearly 15% (~440 ha) which it is related to the increase in the *tidal flat* classes (sand and mud). *Harbour* and *hard infrastructure* also increased their surface area during this period: more than 20% (~0.5 ha) and 50% (~17.5 ha) respectively. The growth in the *harbour* class is due to the expansion of the industrial area and the creation of the New Port infrastructures at the west shore of the Huelva Ria. The great increase in the *hard*

infrastructure surface on the other hand is due to the continuation of the Juan Carlos I dike construction that in 1984 was roughly 9 km longer than in 1979. The construction of this coastal infrastructure has produced geomorphological changes in the estuary mouth, retaining and stabilising sandy sediments, and creating sheltered areas that have favoured saltmarsh creation (Figure 3.9).

During the next time period (1984-2001), the *backshore*, *tidal channel*, *intertidal mud* and *intertidal sand* reduced their surface area by 21.9, 3.9, 9.2 and 27.6 % respectively (Table 3.3). These changes are relate to the net increase in *sand dune* area by more than 50% (~118 ha), which mainly occurred within the developing spits at the estuary mouth. The combination of spit development and extension of the Juan Carlos I dike promoted stabilisation and vegetation colonisation across much of the intervening tidal flat, leading to conversion into *sand dune* (Figure 3.10). Likewise, saltmarsh surface area within the estuary mouth increased (~113 ha) in this period, mostly a product of vegetation colonisation and hence loss of *mud flat* (by ~86 ha). The *hard infrastructure* also increased in this time interval (~19.5 ha) through further extension of the Juan Carlos I dike, which is roughly 3.5 km longer in 2001 than in 1984, and the construction of a new dike at the Punta Umbria Ria mouth (Figure 3.10).

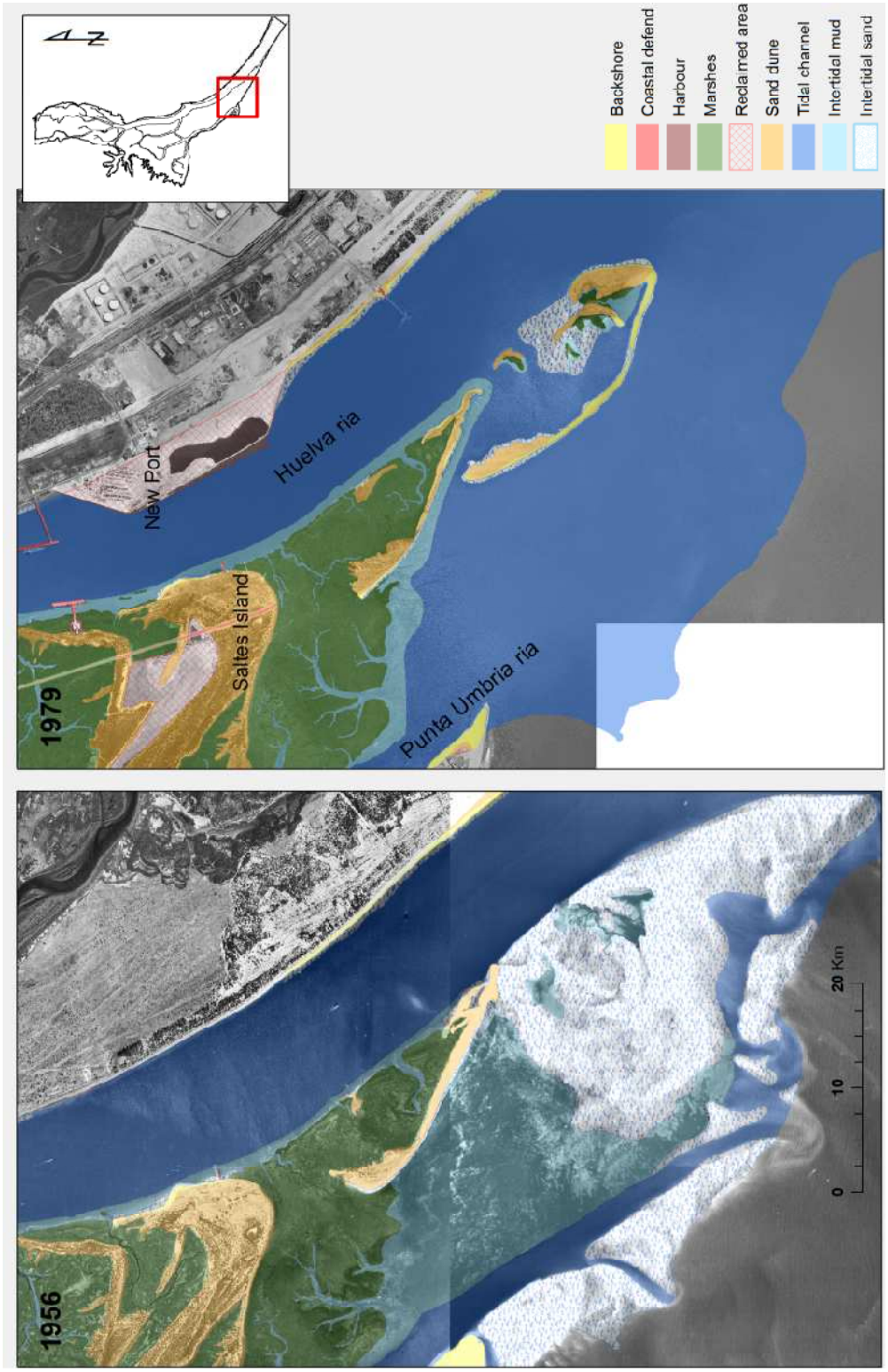

Figure 3.8 Geomorphological changes at the Tinto-Odiel estuary mouth between 1956 and 1979. It should be noted that some sandy bars approaching the Punta Umbria Ria mouth in 1956 are out of the study area

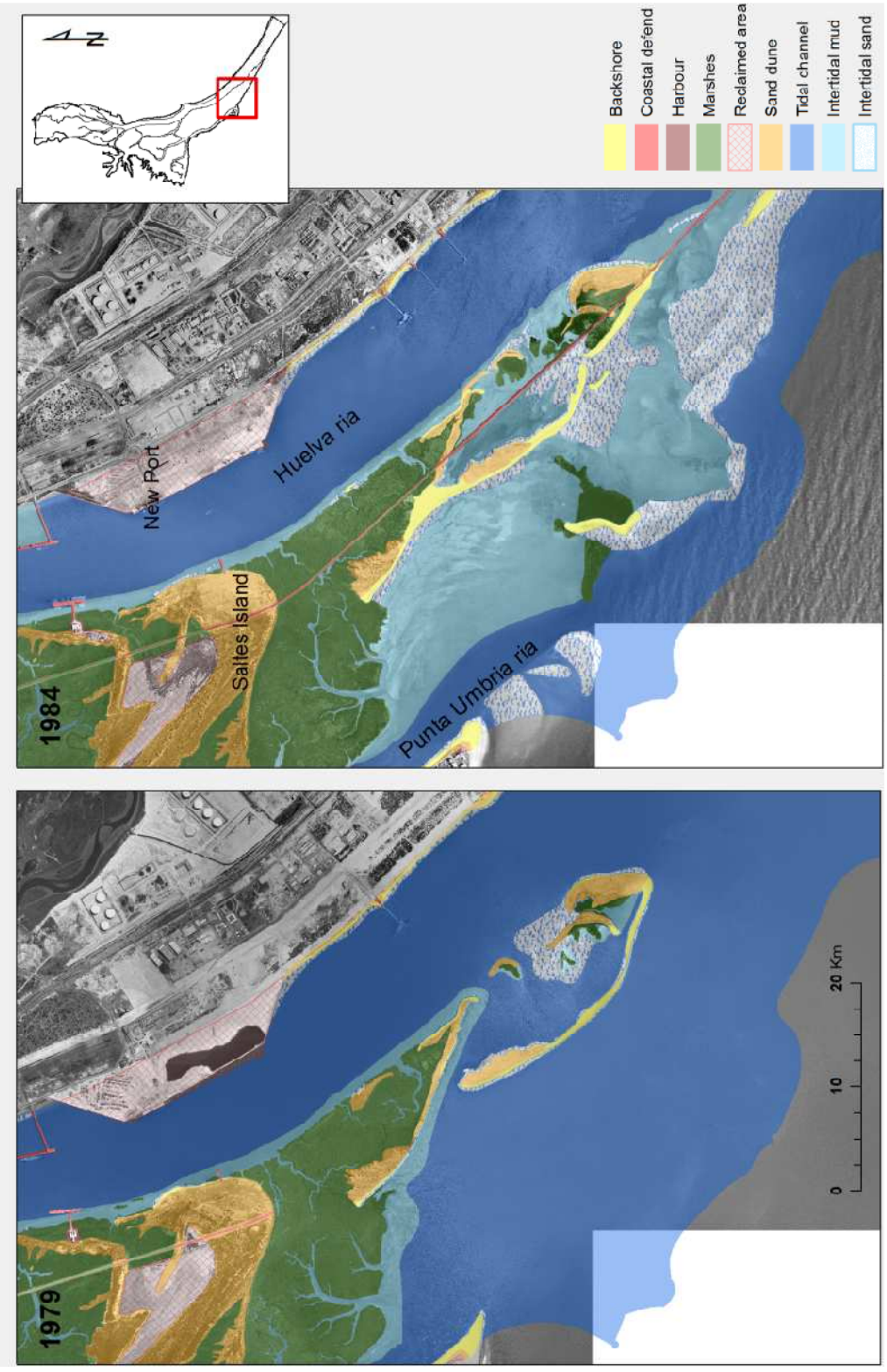

Figure 3.9 Geomorphological changes at the Tinto-Odiel estuary mouth between 1979 and 1984. The Juan Carlos I dike construction created a barrier between both Ria mouth (Punta Umbria and Huelva) favoured sandy sediment retention and sheltered environments

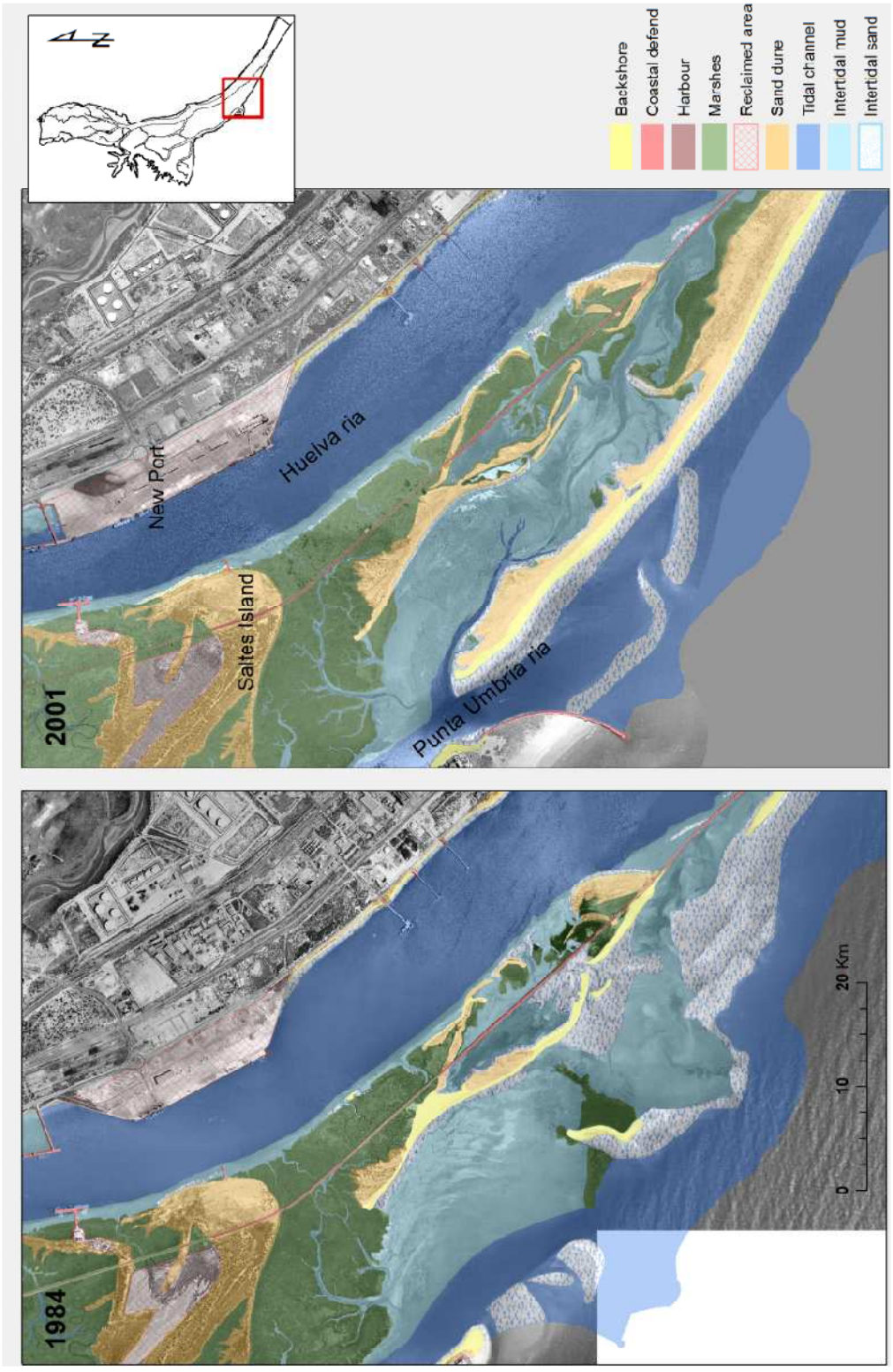

Figure 3.10 Geomorphological changes at the Tinto-Odiel estuary mouth between 1984 and 2001

Between 2001 and 2007, the changes are less pronounced and the percentages of change (PoC) values are lower as it shown in Table 3.3, which in part reflects the shorter time frame covered between these surveys. The *backshore* and *intertidal sand* areas reduced by 2.9 and 13.7 ha respectively, while the *sand dune* area increased in 27.1 ha. The total *saltmarsh* surface area also grew during this period: 43.8 Ha, reducing the total surface of *intertidal mud* by 3 % approximately (~29.8 ha). The geomorphological composition of the estuary mouth in 2007 remains similar to 2001 (2001 map; Figure 3.10). A similar story is evident from the final time interval (2007-2013), with PoC <10% for all the classes. The most significant changes in this time period are related to increases in *sand dune* (5.6 ha), *mud* (~5 ha) and *sand* (~9 ha) *intertidal*, and *saltmarsh* areas (~15 ha). Much of this change reflects stabilisation and sedimentation, particularly enhanced by vegetation growth of habitats created within the complex of developing spits within the estuary mouth. The *hard infrastructure* surface area is reduced by 0.5 Ha, which it is related to the removal of some sea wall sections and small dikes.

Estuary evolution over recent decades has been greatly affected, directly and indirectly, by the construction of the Juan Carlos I dike. This hard infrastructure divided the Calatilla, Bacuta and Saltes islands in two sections, causing division of the saltmarsh habitat and tidal channels. Figure 3.14 illustrates how three tidal channels located in the Saltes Island were impacted by dike construction, particularly in terms of introducing a new topographic divide to the east of the pre-existing natural drainage divide. The channels and creeks located at the eastern part of the natural drainage divide have been greatly modified as it shown in 1979 map. In 1979, the creek sections located to the west of the dike, but to the east of the natural drainage divide, were not able to drain toward the main channel, allowing standing water to accumulate (these creeks were no longer receiving regular tidal incursion by 1979). Creeks to the east of the dike maintained tidal connectivity, but likely experienced some changes due to the decrease in creek length imposed by the barrier.

The evolution from 1979 to 2013 of these fragmented channels (1, 2 and 3) is shown in Figure 3.14. Between 1984 and 2001, the fragmented channels on the west side of the dike were artificially connected to some of the pre-existing channels that drained to the west of the natural drainage divide. Some of the management work on this site during the 1980s and 1990s was focussed on reconnecting these channels to the tidal influence again (Natural Park Office, pers. comm.). Although these interventions have greatly improved the drainage and tidal connectivity across the eastern portions of the saltmarsh, channels 2 and 3 still do not fully drain to the west, and they retain water closer to the dike, thereby effectively acting as deep salt pans.

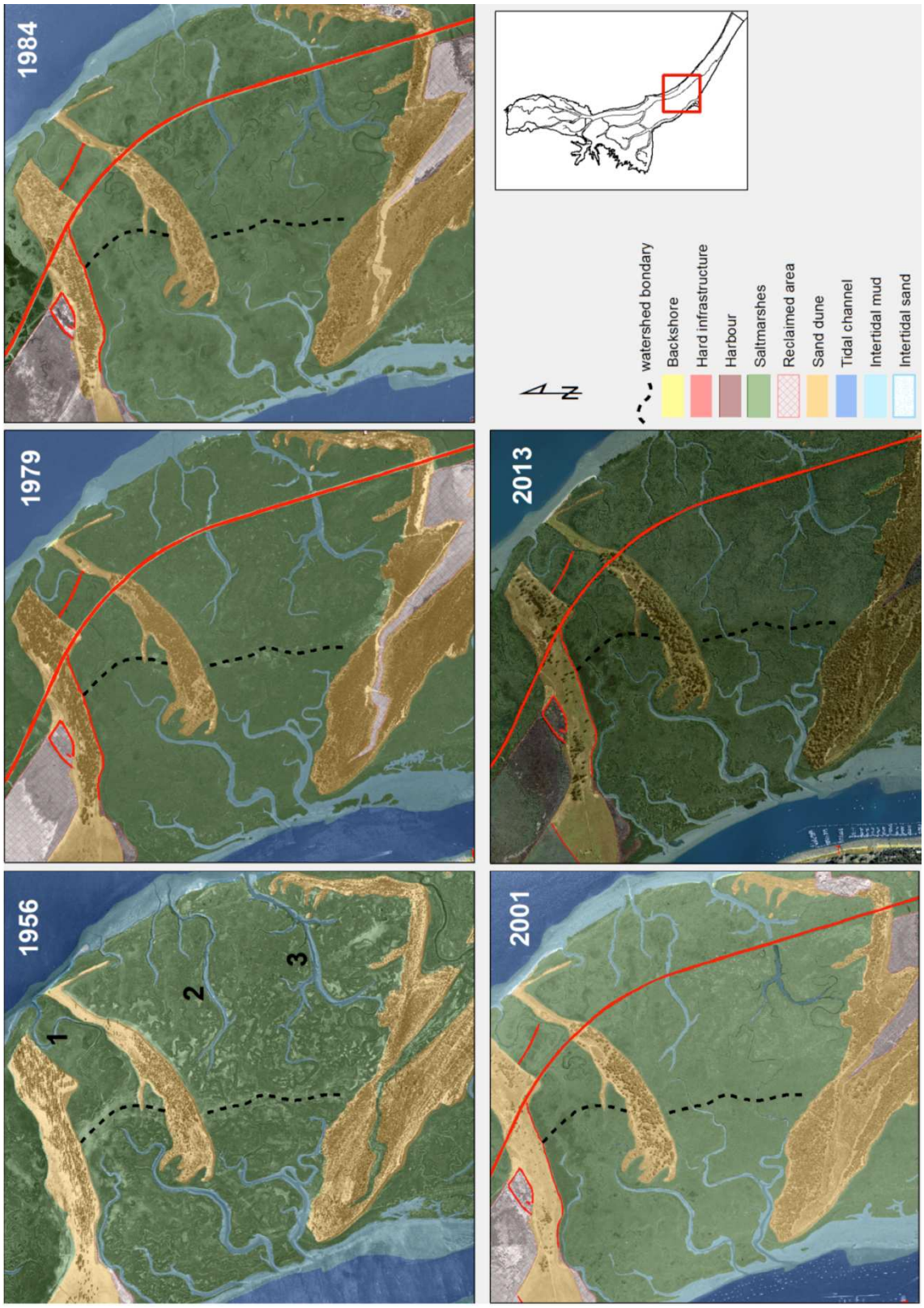

Figure 3.11 Habitat and tidal channel fragmentation of the Saltes Island caused by the Juan Carlos I dike construction (shown as red). The black dash line represents the watershed boundary in this area. As it shown in the 1979 map, two tidal channel sections have been isolated, and the dike is preventing drainage through the natural watershed drainage

3.3. Saltmarsh patch analysis at landscape scale

The results of the patch analysis are shown in Table 3.4 and Figure 3.12. Between 1956 and 1979 the Odiel saltmarsh patch area increased from 7.06 ha to 15.86 ha. The growth in small saltmarsh fragments is mainly due to reclamation processes carried out during this period (~25% of the saltmarsh surface in 1956 was converted into industrial salt factories by 1979). At this time many sea walls were built to control the flooding leaving some saltmarshes patches along the outer perimeter sea walls. The increased patchiness in 1979 coincides with a reduction of the core surface area. For example, large and medium core areas lost 1013.31 and 177.62 ha respectively. Edge areas decreased by c. 120 ha in 1979, mainly due to the reclamations.

By 2013, the patch surface area increased by a further 4 ha. This growth is related to an increase in saltmarsh division in some zones, but also by new habitat creation (of small fragmented areas) in other zones (mainly at the river mouth). The core surface area increased reflecting efforts taken by the Natural Park managers over the last decade (Natural Park pers. comm.) to reconnect divided zones and the promote new saltmarsh growth. As expected, the *edge* surface area has also increased due to new saltmarsh creation.

Table 3.4 Variation of saltmarsh patch, edge and core surface area (ha) per year (1956, 1979 and 2013)

	1956	**1979**	**2013**
Patch	19.60	44.07	48.78
Edge	1930.03	1810.93	2054.30
Small core (<100 ha)	277.41	270.91	306.74
Medium core (100-200 ha)	1820.25	806.94	955.59
Large core (>200 ha)	493.69	316.07	317.24

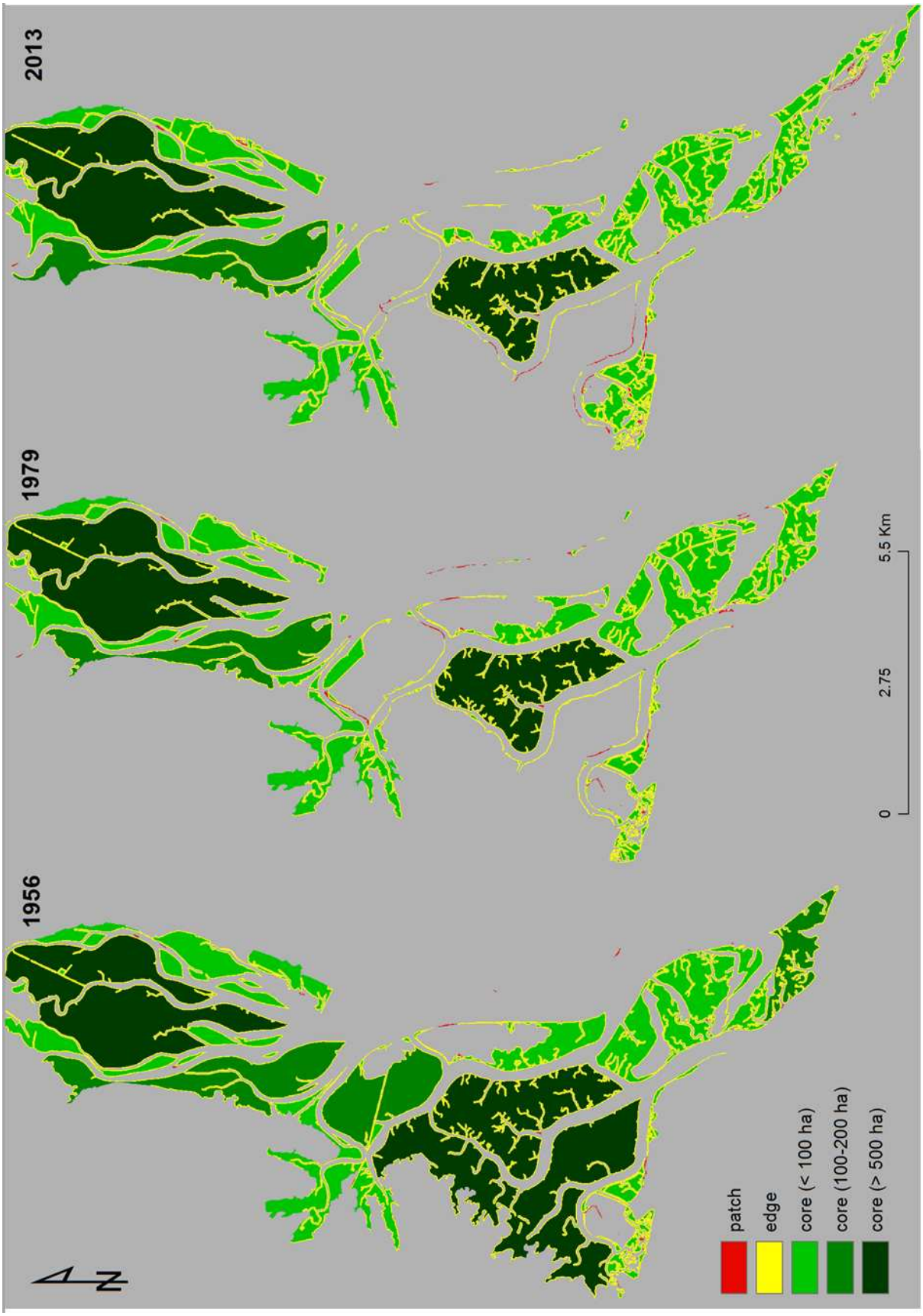

Figure 3.12 Patch type present in the Odiel saltmarshes in 1956, 1979 and 2013

3.4. Decadal shoreline change: horizontal erosion and sedimentation rates

The most striking result in the analysis of saltmarsh shoreline change is the significant difference in behaviour between the northern and southern marshes over recent decades (1956-2013). The Odiel saltmarshes in the mid/lower estuary have mostly retreated whereas those in the upper estuary have mostly advanced (Figure 3.13). Within the upper estuary, the greatest growth is experienced on the east shore of the Retamal creek, where the horizontal growth rate is > 2.5 my^{-1}. Saltmarsh shorelines associated with the islands within the mid/lower estuary show recession over the same time frame: Enmedio Island for example has eroded at a rate of 0.5-2.5 my^{-1}. Although the results using EPR (map A, Figure 3.13) and LRR (map B, Figure 3.13) statistics show similar tendencies, some differences are evident. These are particularly associated with stretches experiencing smaller rates of change where calculation of the EPR (which only uses the initial and final years) masks some inter-decadal variability that is picked up in the LRR statistic.

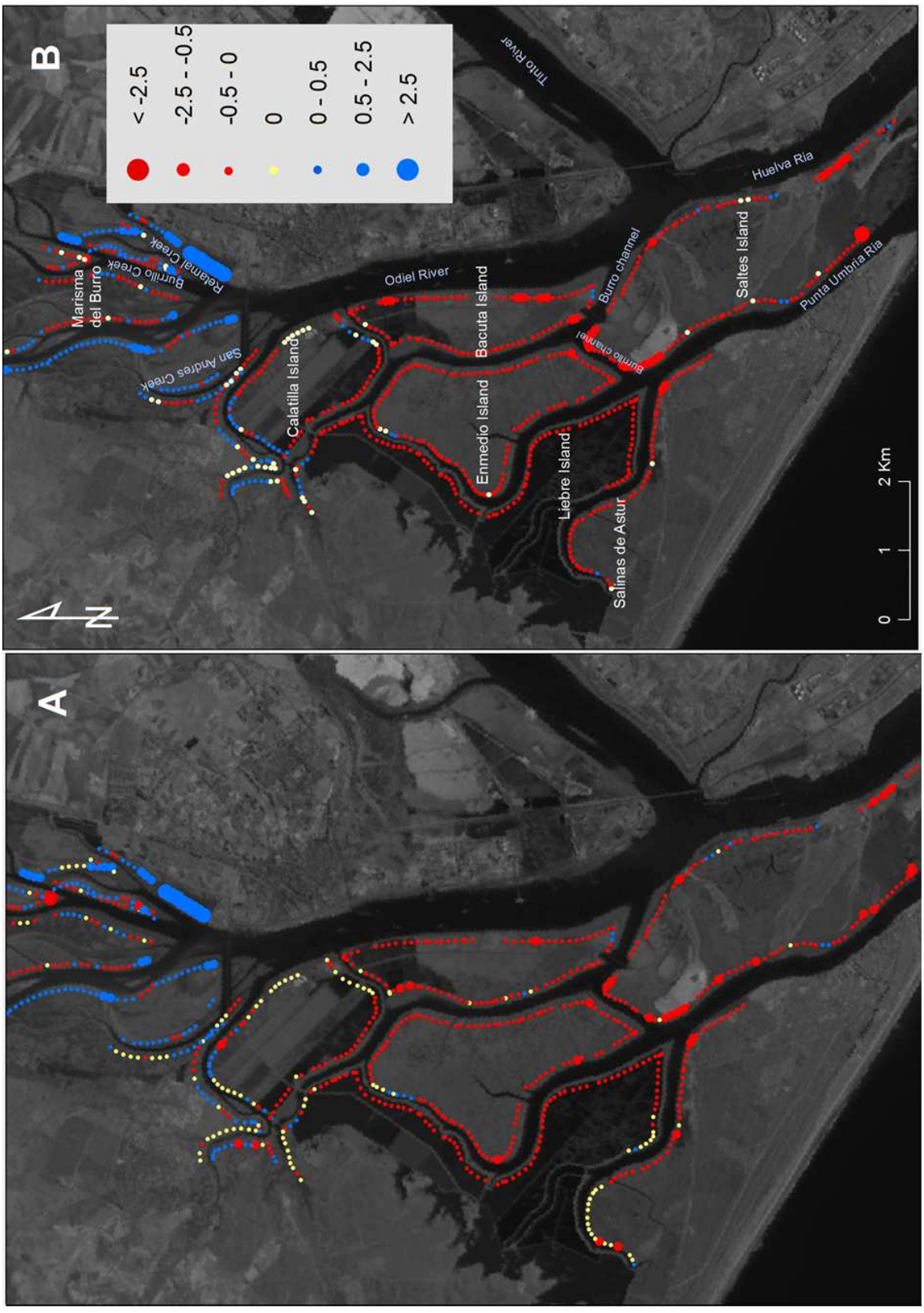

Figure 3.13 Erosion and sedimentation rates (in my^{-1}) in the Odiel saltmarshes between 1956 and 2013 (displayed over 1987 spot image). The variable the end point rate (EPR) is represented in map A, and linear regression (LRR) in map B; where red dots mean erosion rates (retreatment), blue dots sedimentation rates (horizontal growth) and yellow dots no shoreline changes

Further testing was carried out to determine if the rate statistics appropriately represented shoreline evolution. Transects showing different behaviours were selected and the relative shoreline position (with respect to earliest year: 1956) was calculated and plotted. EPR and LRR statistics do not comprise sufficient information to explain the behaviour of different sectors of the saltmarshes over the time, although they were suitable to quantify the erosion and sedimentation rates during the total studied time period. An example time series of relative change in shoreline position is shown in Figure 3.14. The EPR and LRR statistics assume a linear behaviour (EPR=0.04 myr^{-1} and LRR=0.05 myr^{-1}) whereas the real shoreline tendency of this transect is more complicated: advancing during the first 20 years, maintaining the same position for the next 18 years and retreating during the last 13 years.

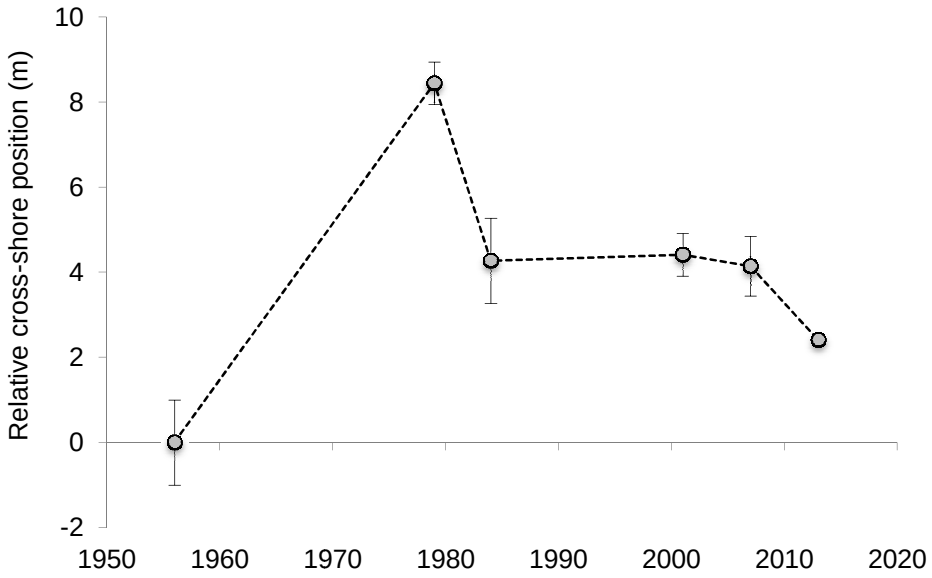

Figure 3.14 Shoreline position relative to the 1956 location (in metres) from 1956 and 2013 at transect 348

In order to characterise saltmarsh shoreline behaviour, a cluster analysis was performed using the relative shoreline distance at each time interval for each transect (N=782). The clustering approach used was the average method (in 'R' v.2.15.1), which gave the best cophenetic correlation (CC = 0.98) when compared with other methods (for example ward method CC = 0.37). Results from the cluster analysis divided the dataset into 7 groups representing types of shoreline tendency (between 1956 and 2013). The shoreline tendency at each transect represented by each group is shown in Figure 3.15 and the characterisation of the saltmarsh shoreline by group is shown in Figure 3.16. Most of the transects (N=740) were classified as group 1, and only 40 transects as other groups, highlighting that most of the saltmarsh margins are behaving similarly.

Shorelines classified as group 1 are characterised by an initial growth or retreat followed by a general stabilisation, with a small net change in position. Shorelines distributed in the north and northwest (e.g. Calatilla Island and San Andres creek) showed very small changes over time. Rates of change increase slightly between 1979 and 1984, but the last 30 years is characterised by a stabilisation of the shoreline. The rates of change within this area are mostly ±0.1 my^{-1}. In the west (e.g. Salinas de Astur and Liebre Island), shorelines are characterised by an initial growth followed by retreat and then stabilisation. The growth at the beginning lasted 20 - 30 years, but after 1984 all transects experienced retreat until 2001. Since then, the shorelines seem to be relatively stable with only minor variations (positive or negative) of ±0.1 my^{-1}. Shorelines within the mid estuary (mainly Enmedio Island and Liebre Island) have a general recessional tendency with some evidence of stabilisation over the last decade. During the first two decades some of the transects showed a small advance to 1979 followed by retreat. The shoreline retreat in these areas ranged between 1 and 30 m approximately, where large areas of the marsh environment have been converted in industrial salt production. The remaining saltmarsh here seems to have been adjusting to the new conditions.

Group 2 and 6 represent shorelines with a general recessional tendency, where erosion rates are slower in the first decades followed by an increase between 1984 and 2001 and a more recent period of stabilisation when the changes are less pronounced. The main differences between these two groups is that, during the last 6 years, the first group maintains a decreasing tendency and the second one shifts to an increasing tendency. The recession in group 6 reaches up to 110 m, but far less in group 2 (< 50 m) for most of the transects. This group is distributed across Punta Umbria ria. Shorelines in group 3 and 5 showed a tendency for shoreline growth followed by stabilisation during the last couple of decades. However, during the first two decades some transects in group 3 show retreat, but this ceases after 1979 following the growth tendency of the other transects. The main difference between these two groups is that the final stabilisation started in 1984 in group 5, and in 2001 in group 3. These groups are exclusively found in the north estuary.

Group 4 and 7 presented a growth tendency, but with some differences. Shorelines in group 7 are characterised by significant advance (up to ~ 200 m) during the first decades followed by a decrease in rate of change, and then stabilisation in latter decades. Unlike group 7, shorelines in Group 4 maintained the same position between 1956 and 1984, which was then followed by rapid advance (up to ~ 80 m) during the 1980s and 1990s. During the last 12 years, shorelines in group 4 were stabile and no major changes were observed. These groups are found only in one sector of the Odiel saltmarshes: along the east shore of the Retamal and Burrillo creek.

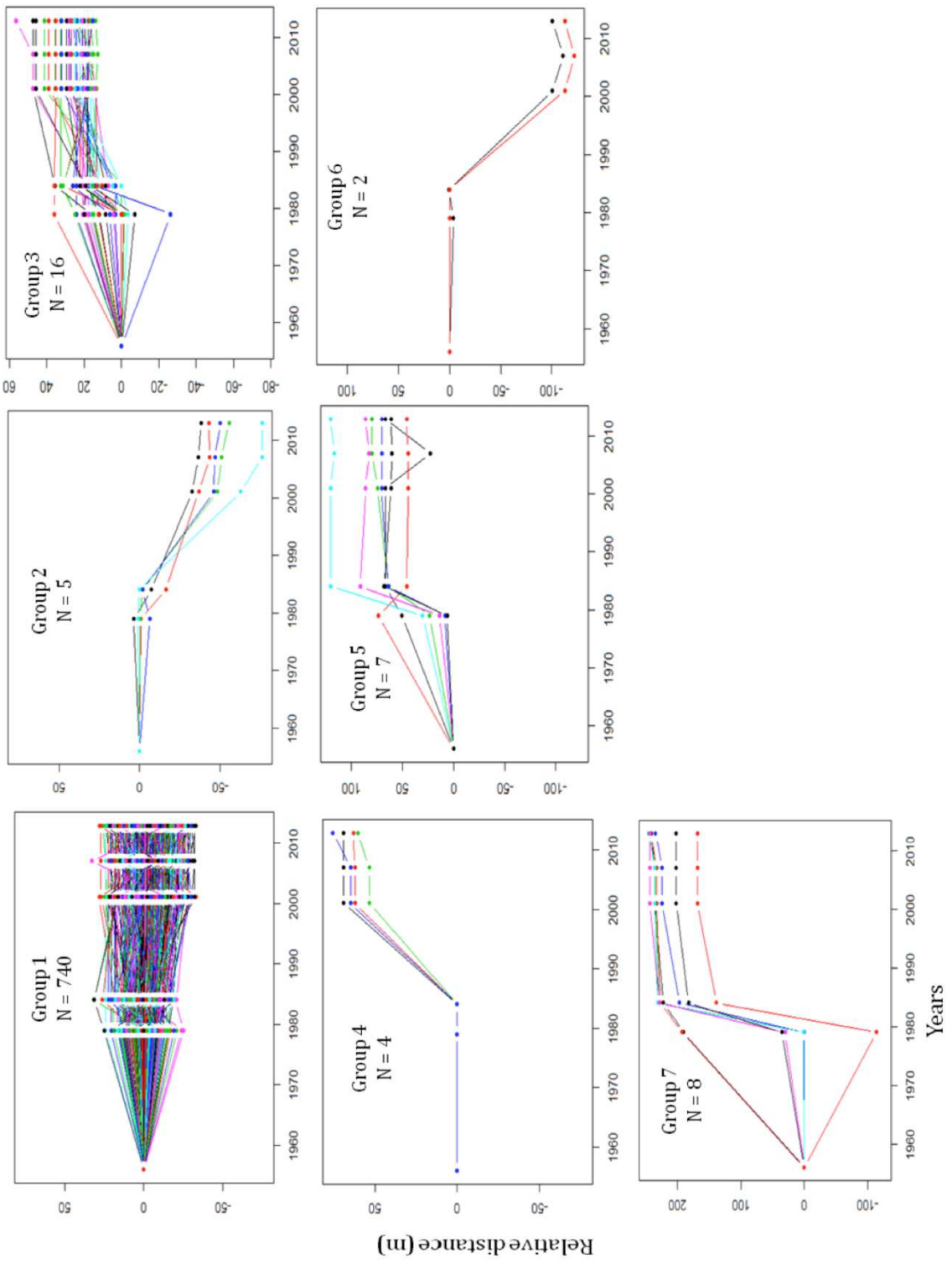

Figure 3.15 Relative shoreline distance (in metres) relative to 1956 for each transect in the Odiel saltmarshes. Transects were grouped based on cluster analysis (Average Hierarchical Clustering), and each group represents some similarities in shoreline behaviour over time (1956-2013), where N indicates the number of transects in each group

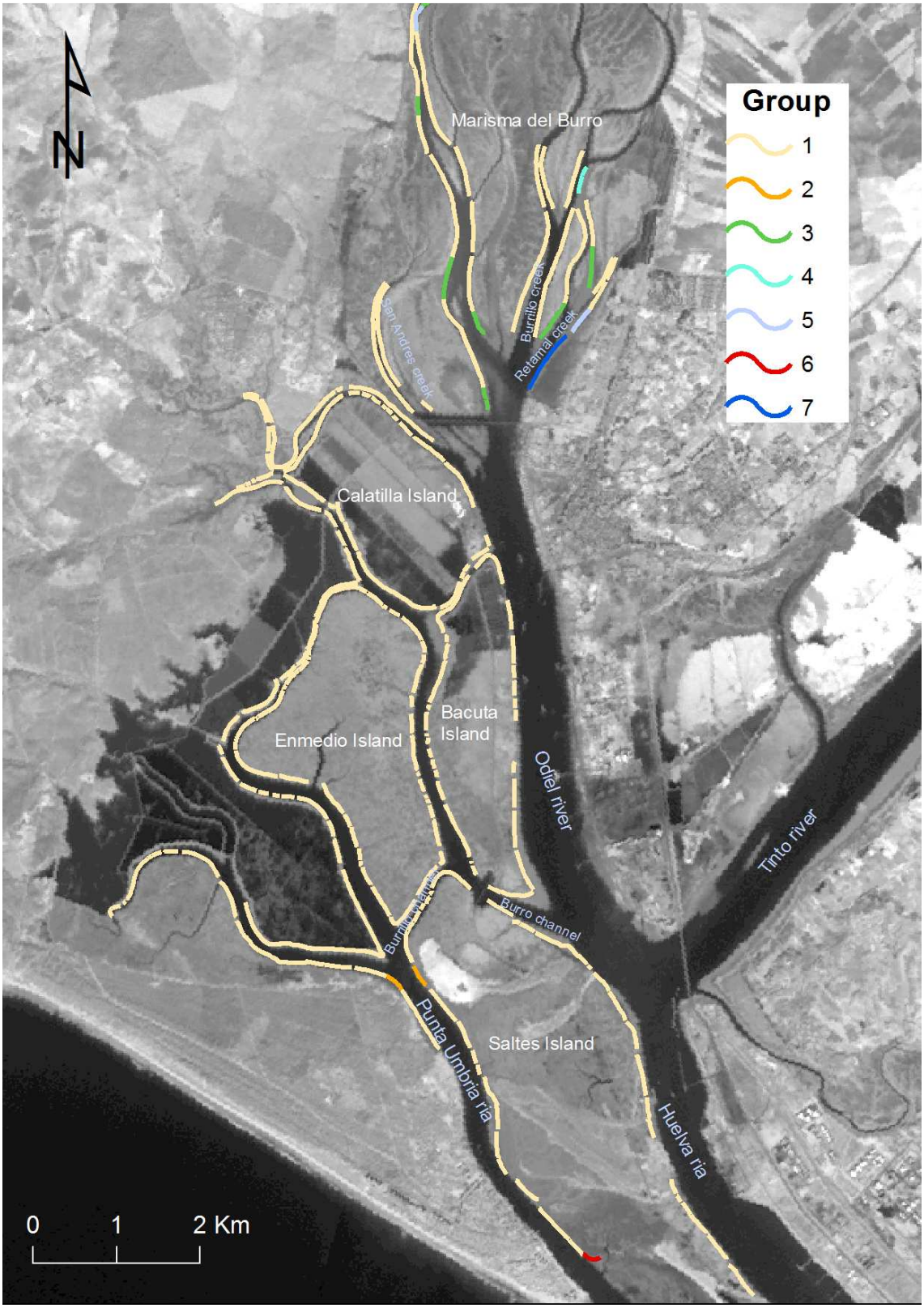

Figure 3.16 Characterisation of the shoreline changes in the Odiel saltmarshes based on cluster analysis. The legend indicates the group of each shoreline sector; where red/orange colours state a retreatment tendency and blue/green colours progradation.

3.5. Forcing of coastal change

3.5.1. Wind speed and wave climate

The climate of the Huelva coast is mild, characterised by low-mid energy wind and swell (Figure 3.17). The wind regime at the Tinto-Odiel estuary mouth is dominated by southwest to north-westerlies, and the dominant swell comes from the south-west (Figure 3.17, A). Mean wind speed ~ 17 km south from estuary mouth is 4.6 ms^{-1} (for the period 1958 and 2015). Wind at gale force speeds and above (>34 knots (~17.5 ms^{-1})) represents ~0.02% of the wind speed record and higher wind speeds are generally from the south-west. Monthly variation in wind and wave climate over the last 50 years comprises a seasonal pattern whereby winter months experience higher wind speeds and larger waves in comparison to summer months (Figure 3.18).

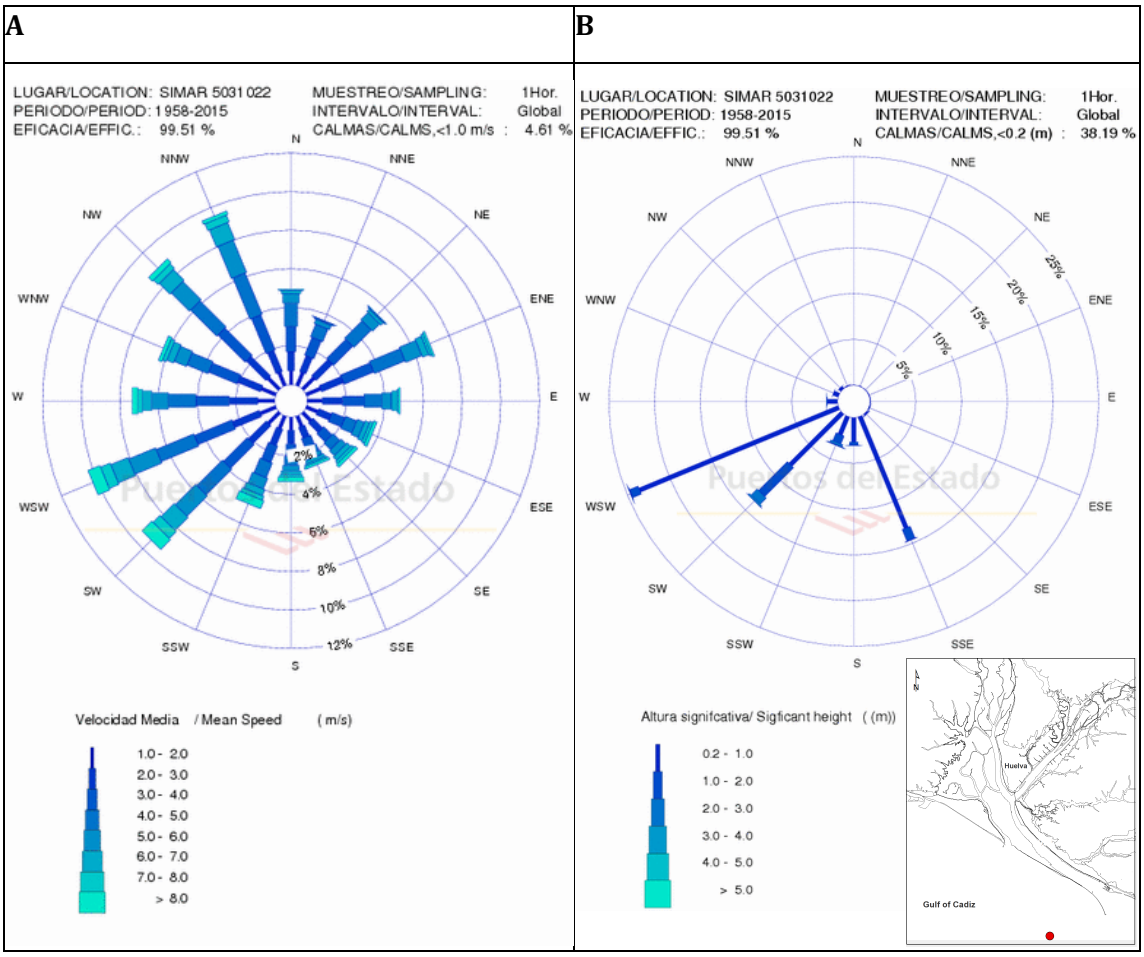

Figure 3.17 Wind (A) and wave (B) roses (1958-2015) for the Huelva coast (6.92° W, 37.08° N; SIMAR model point 5031022 in red). [source: http://www.puertos.es/en-us/oceanografia/Pages/portus.aspx]

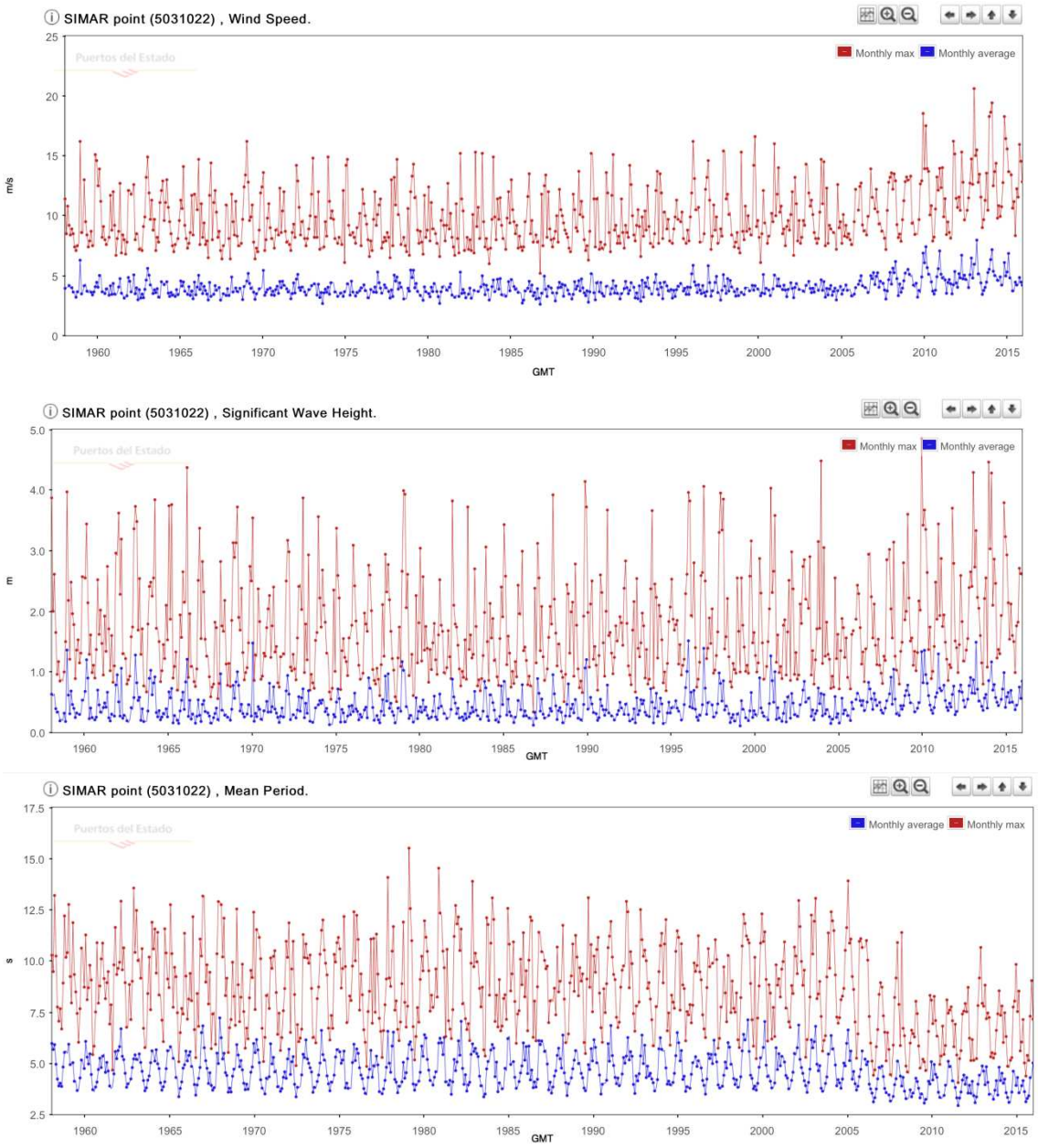

Figure 3.18 Review of time series (1958 – 2015) wind and wave climate for the Huelva coast (6.92° W, 37.08° N; SIMAR model point 5031022). From top showing monthly mean and max wind speeds, significant wave height and mean period. [source: http://www.puertos.es/en-us/oceanografia/Pages/portus.aspx]

The time series data imply some change in wind and wave climate in the late 1990s and 2000s, but this is more likely a product of changes in the modelling approach used to derive this data (Puertos del Estado, 2015). These time series products are fused from SIMAR-44 numerical modelling product (1958-1999) and WANA prediction data (2000 to present), the latter of which incorporated a significant change in model resolution in 2006 (Puertos del Estado, 2015). These timings are clearly visible as distinct changes in time series structure in Figure 3.21. Reliance on simulated climate data is not ideal, but instrument (observed) data for this region is limited spatially and temporally. For

example, data recorded by the Gulf of Cadiz weather buoy only extends back to 1996 (Figure 3.19) and data has only been recorded at the Huelva weather station (Figure 3.20) since 1984. These shorter-term datasets reinforce the seasonal nature of the wind and wave climate across this region, but helpfully clarify that there is limited evidence for a change in these climate metrics around 1999 and 2006. Some longer-term patterns are evident in the Gulf of Cadiz data that implies a lull in wind and wave energy from 2003 to 2008, but this is partly due to data gaps during this time period that might have preferentially removed higher wind speed/wave height records.

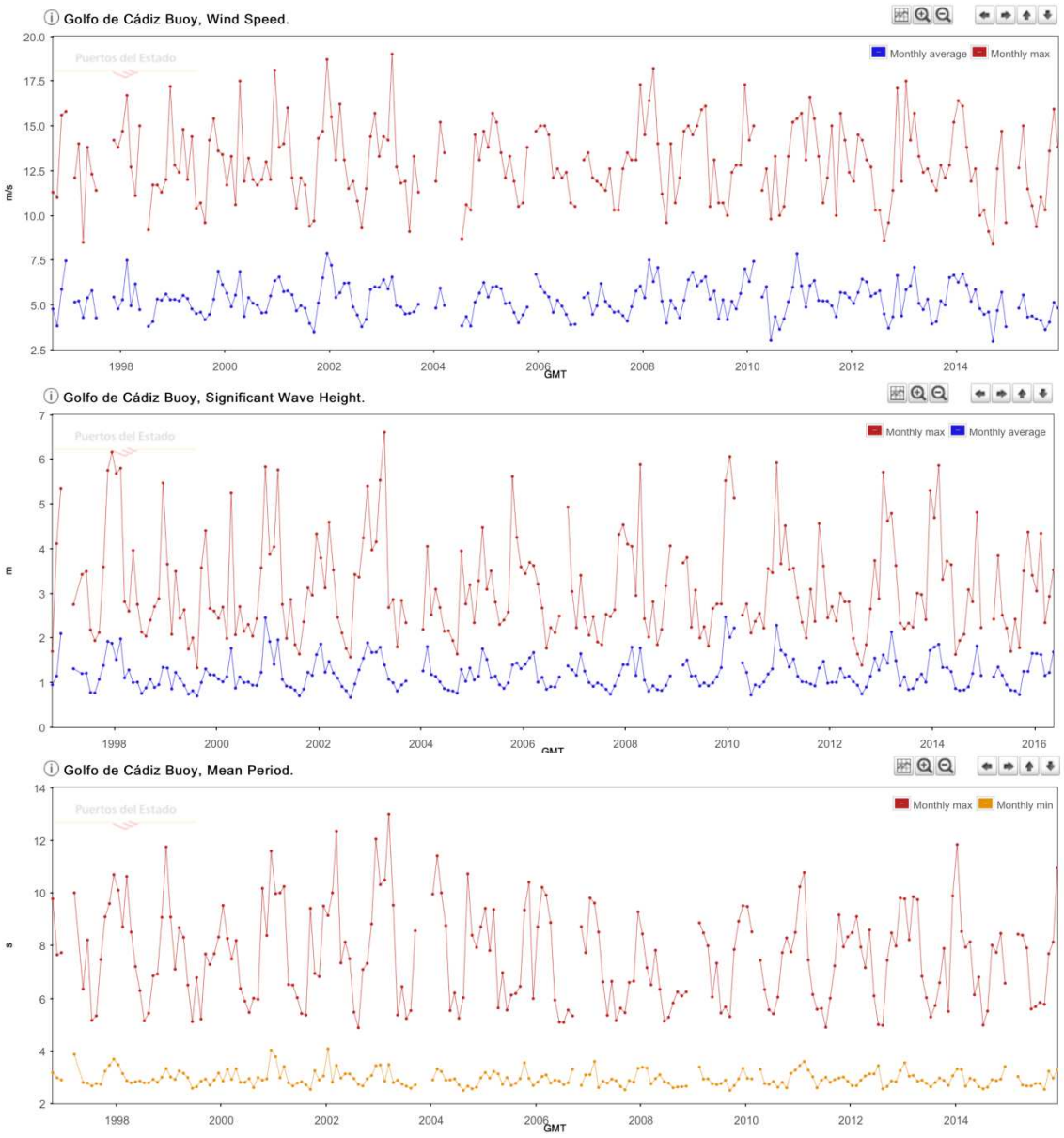

Figure 3.19 Review of time series (1996 – 2015) wind and wave data for the Gulf of Cadiz wave buoy (6.96° W, 36.48° N). From top showing monthly mean and max wind speeds (ms^{-1}), significant wave height (m) and mean period (s). [source: http://www.puertos.es/en-us/oceanografia/Pages/portus.aspx]

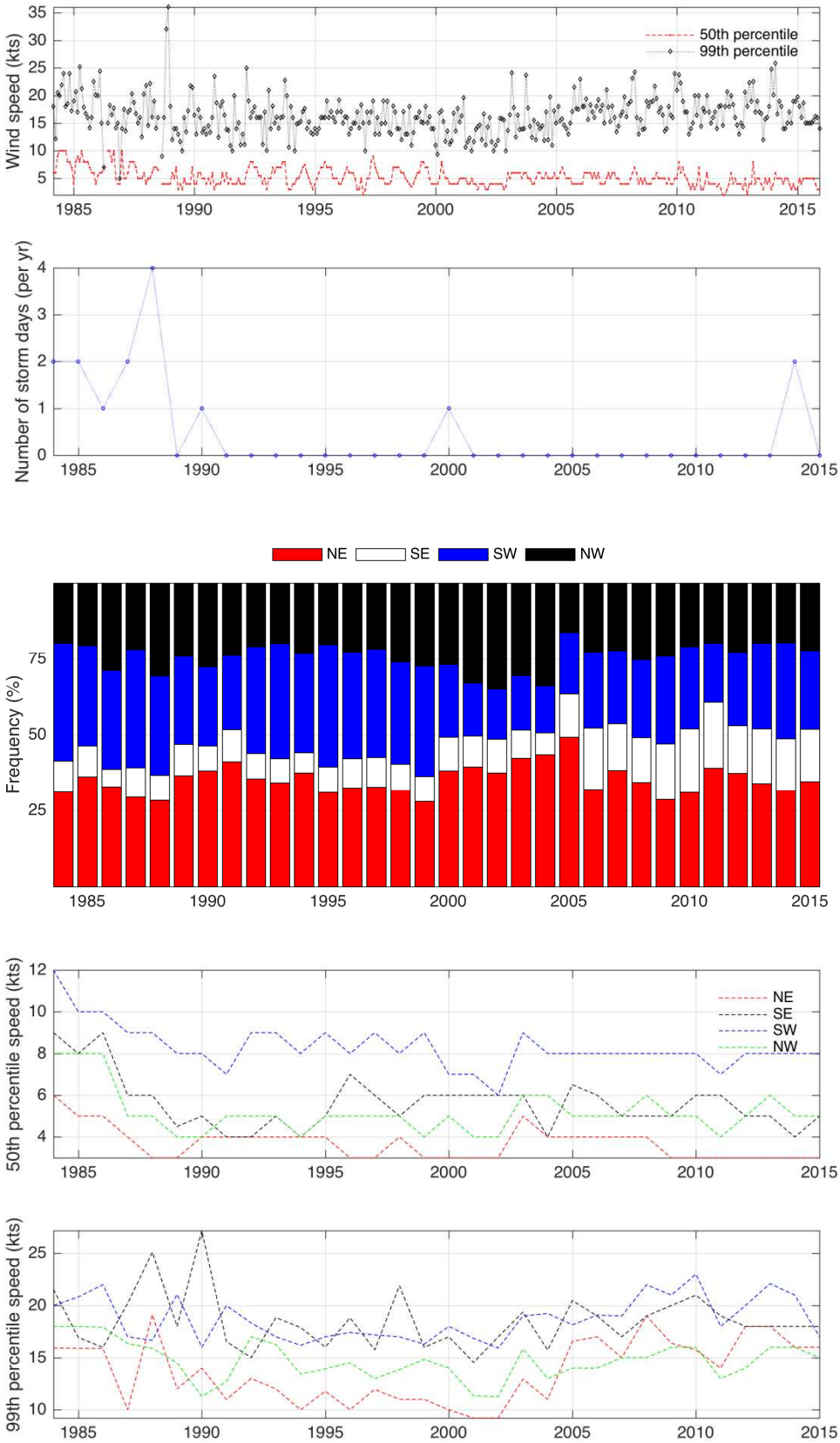

Figure 3.20 Review of time series (1984 – 2015) wind data recorded at the Huelva weather station (6.92° W, 37.28° N; WMO station code 08383). From top showing monthly median and extreme wind speeds, annual wind direction frequency and annual median and extreme wind speed from each wind direction quadrant. [data source: http://www.badc.ac.uk]

The Huelva weather station wind record is more complete, and suggests some change in the degree of seasonality through time. The records imply that higher energy conditions characterised the mid-late 1980s and that there was a slight decrease in median wind speed during the late 1990s and early 2000s. Overall however, the evidence for distinct shifts in wind energy through time is limited, but the frequency distribution of wind direction suggests that the last 10 years has experienced an increase in wind from the southeast, with relative decreases in the frequency of wind from the southwest and northeast. In 2005, there was a peak in wind from the northeast with an associated drop in the frequency of wind from the northwest. After this time, northeasterlies returned to their long-term average (~35%), but southeasterlies increased from a long-term average of ~10% to 18%. The shifts in wind direction were not associated with any specific change in median speed, but there is some indication in the data that extreme wind speeds from a northeasterly direction have increased.

3.5.2 Rainfall and river discharge

Rainfall in Huelva is very seasonal and the annual precipitation may occur in a few days a year (torrential rain). Rainfall records from the Huelva weather station were analysed monthly and annually within the studied time period (Figure 3.21) in order to investigate if there was any relevant change. A monthly standard deviation greater than the mean suggests a great variability in the monthly rainfall for all the time periods analysed. Annual rainfall also varies between years, presenting differences in the annual mean with standard deviation greater than 100 mm for all time step periods, but again any relevant change was observed between periods.

For example, from August 1996 to July 1997, 67 % of the annual rainfall occurred in 21 days of December and January (Castillo *et al*., 1999). Periods of torrential rain coincide with increases in the flow of the Odiel River (Castillo *et al.*, 2000). Rainfall also varies greatly between years, presenting great differences in annual sums (Figure 3.21). In 1996 the total precipitation in the Odiel saltmarshes was nearly 1100 mm, and less than 300 mm in 1966 for instance.

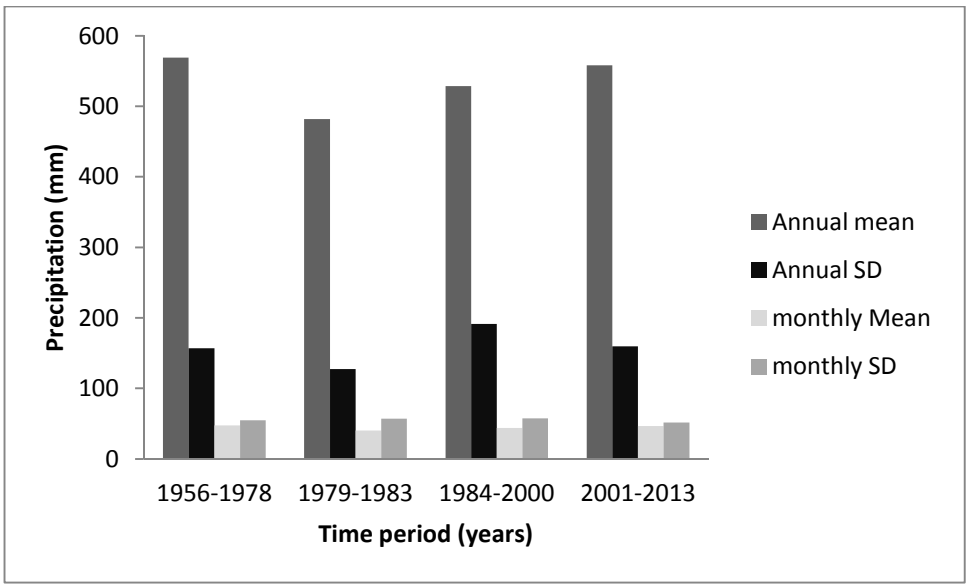

Figure 3.21 Monthly and annual rainfall (mm) from 1956 to 2013 in Huelva, where SD is the standard deviation [data source: http://catalogue.ceda.ac.uk/uuid/3f8944800cc48e1cbc29a5ee12d8542d]

There are few gauge stations in the Odiel river basin. However, these stations lack complete discharge datasets due to the shortage of new gauge stations or the malfunctioning of old ones (Gibraleon and Calaña stations). One of the oldest stations is the Gibraleon gauge station located at the upper Odiel estuary (Figure 3.22, B). The historical discharge data for this station are summarised in Figure 3.22 (1969-1994) and Figure 3.23 (1980-2006). Figure 3.22 and Figure 3.23 showed the great inter- and intra-annual discharge variability of the Odiel River. The annual flux for some years was greater than 500 hm^3, while for other years was less than 50 hm^3. For example, flux values smaller than 200 Hm^3 were recorded in 1973-1975 and 1980-1982, and values between 500 and 800 hm^3 in 1969, 1970, and 1977-1979. The maximum value (1800 hm^3) recorded during the period 1969-2006 was reached in 1989. This peak value suggests that the greater erosion rate estimated for the period 1984-2000 could have been influenced by greater river discharge during this period.

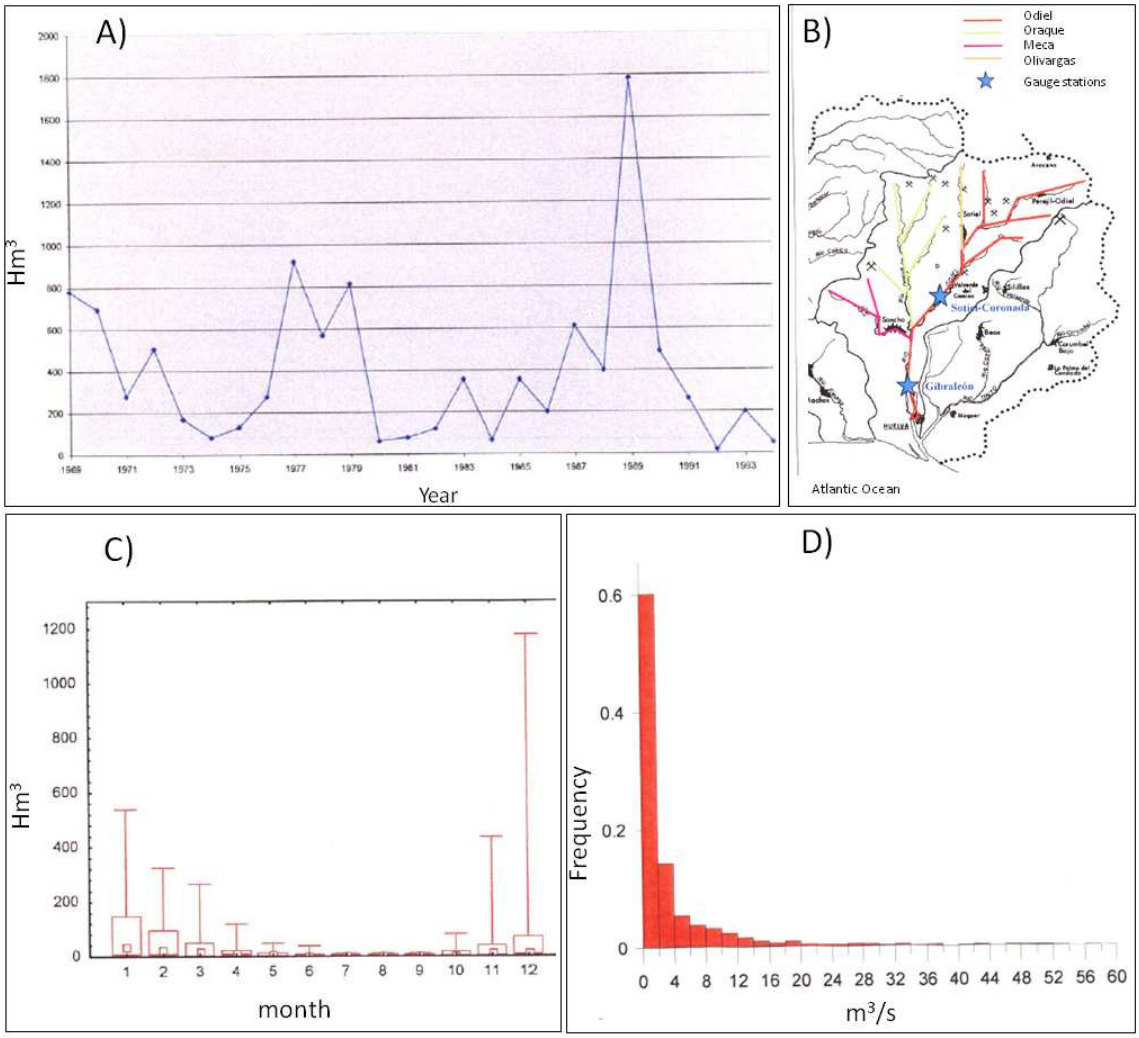

Figure 3.22 Discharge data for the Odiel River at the Gibraleon gauge station between 1969 and 1994 showing: (A) annual discharge; (B) location of the gauge stations and Odiel sub-basins; (C) monthly discharge; and (D) frequency [Source: Lopez *et al.*, 2006]

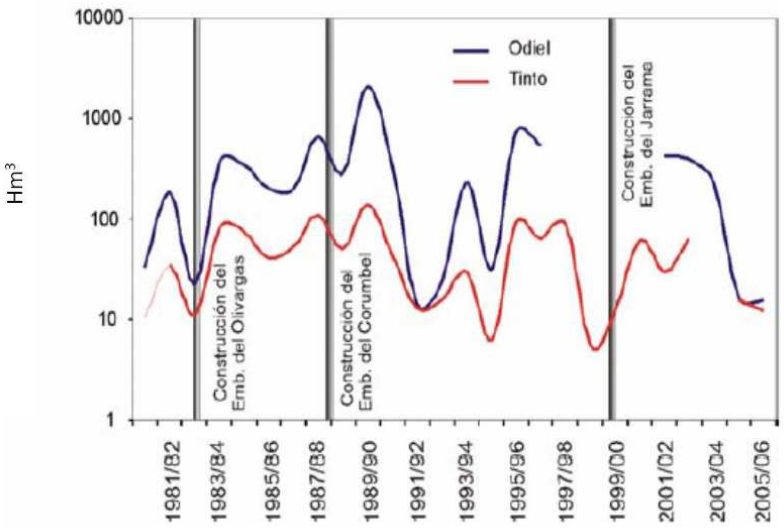

Figure 3.23 Annual discharge of the Odiel River in blue (at Gibraleón gauge station) and Odiel River in red between 1980 and 2006, stating the construction of three water reservoir (black lines) [Source: Olias Alvarez *et al.*, 2010]

However, discharge data recorded at Gibraleon station are not complete due to the malfunctioning of the gauge during flood events (usually in autumn and winter) (Galván *et al.* 2016), leaving a gap between 1997 and 2002. Data for these years are not available and thus the relation between discharge and horizontal erosion is difficult to assess for the whole time period. Although rainfall data are available at the estuary, this variable usually does not well explain discharge data (Galván *et al,.* 2016). In the Odiel river basin rainfall varies greatly from North (upper River basin) to South (low River basin and estuary). For example, the average rainfall is ~500 mm y^{-1} near the coast, and ~1000 mm y^{-1} at the upper river basin (Olias Alvarez *et al.*, 2010). Rainfall is not considered a good indicator of discharge values (Galván *et al,.* 2016) for covering the gap between 1997 and 2000. Galván *et al.* (2016) approached this issue by modelling daily water balance based on soil type, slope, land-use and weather data. The measured and simulated data at the Gibraleon station is shown in Figure 3.24. Overall, the period 1982-2000 seems to reach higher values in discharge than for the period 2001-2010.

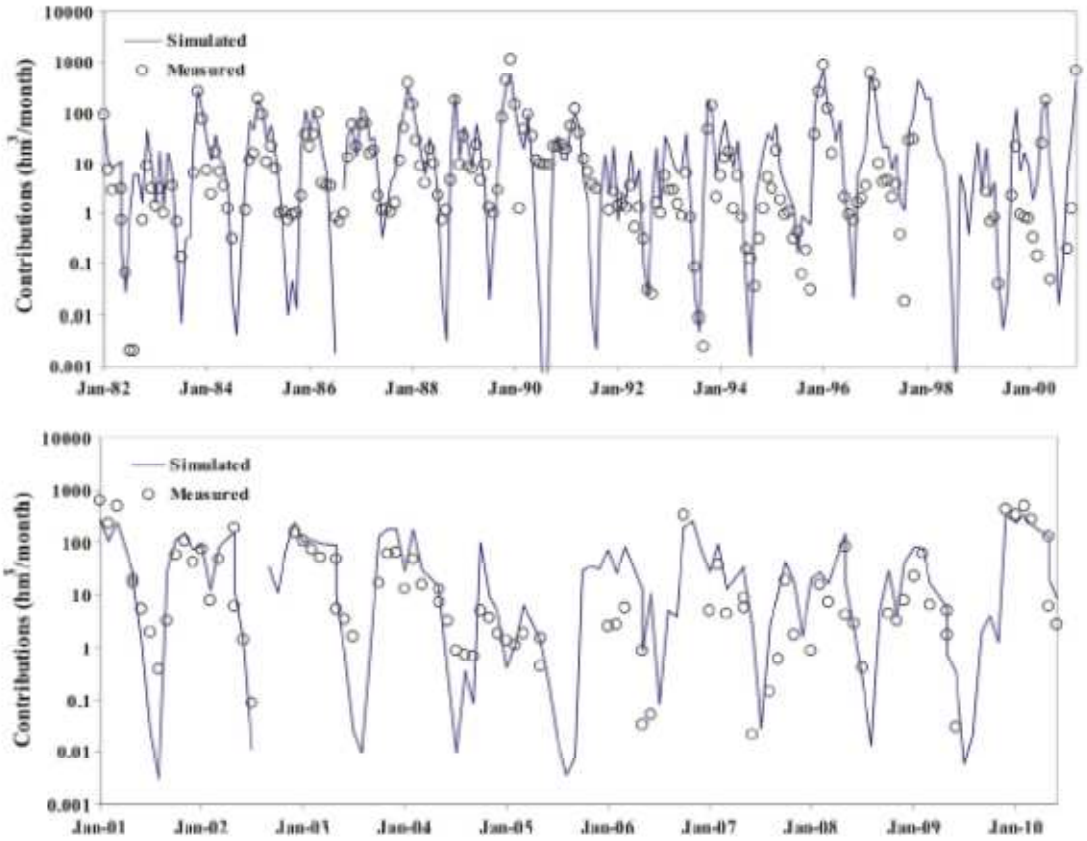

Figure 3.24 Monthly discharges (measured and simulated) of the Odiel River at the Gibraleon gauge station between 1982 and 2010

3.5.3. Local mean sea-level change

The only tide gauge located near the Odiel saltmarshes with more than 10 year data is the "Huelva tide gauge", located at the estuary mouth in the Mazagon marina (location shown in Figure 3.25). This is one of the tide gauges that the PSMSL uses to estimate mean sea level. The monthly data downloaded from the PSMSL data set is display in Figure 3.25. The data showed that sea level in the Odiel saltmarshes is rising 3.33 mmy^{-1}. However, short time series could be influenced by other factors (e.g. tide cycles). Thus, in order to understand the evolution of the local mean sea level in the Odiel saltmarshes several mean sea level data set from different tidal gauges in the Gulf of Cadiz have also been explored.

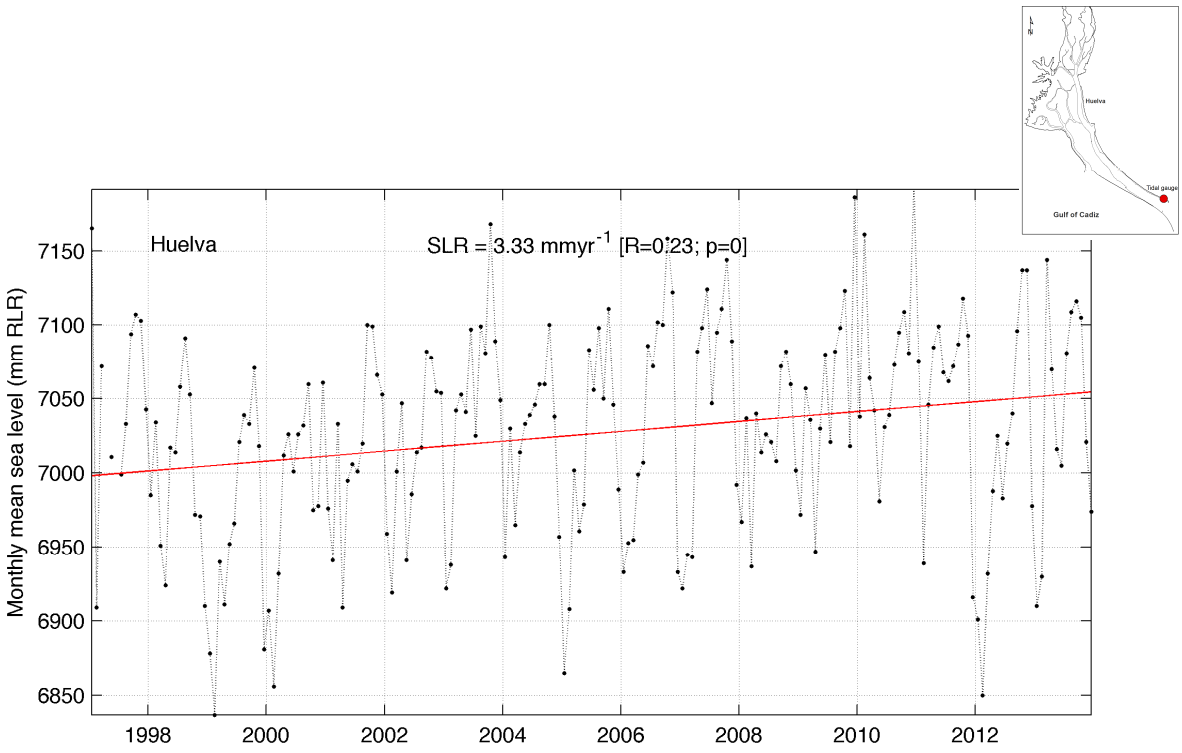

Figure 3.25 Monthly mean sea level (mmRLR) from 1997 to 2013 at the Huelva tide gauge (location shown as red dot) [source: PSMSL]

The evolution of mean sea-level at different stations in the Gulf of Cadiz is displayed in Figure 3.25 and their location in Figure 3.26. All the stations showed an increasing tendency in mean sea-level. However, the rates varied depending on location, it should be noted that the time series of different locations do not cover the same time period and some stations presented gaps. Lagos and Cadiz II station covered the oldest time dataset but they presented long gaps. For example, in the Lagos stations the data collection ceased in 2000 presenting gaps in between and at the end of the series. Cadiz III presented data from 1960 without important gaps. The rate of sea-level rise in this station was of 3.81 mmy^{-1} showing similar rates to the Huelva station.

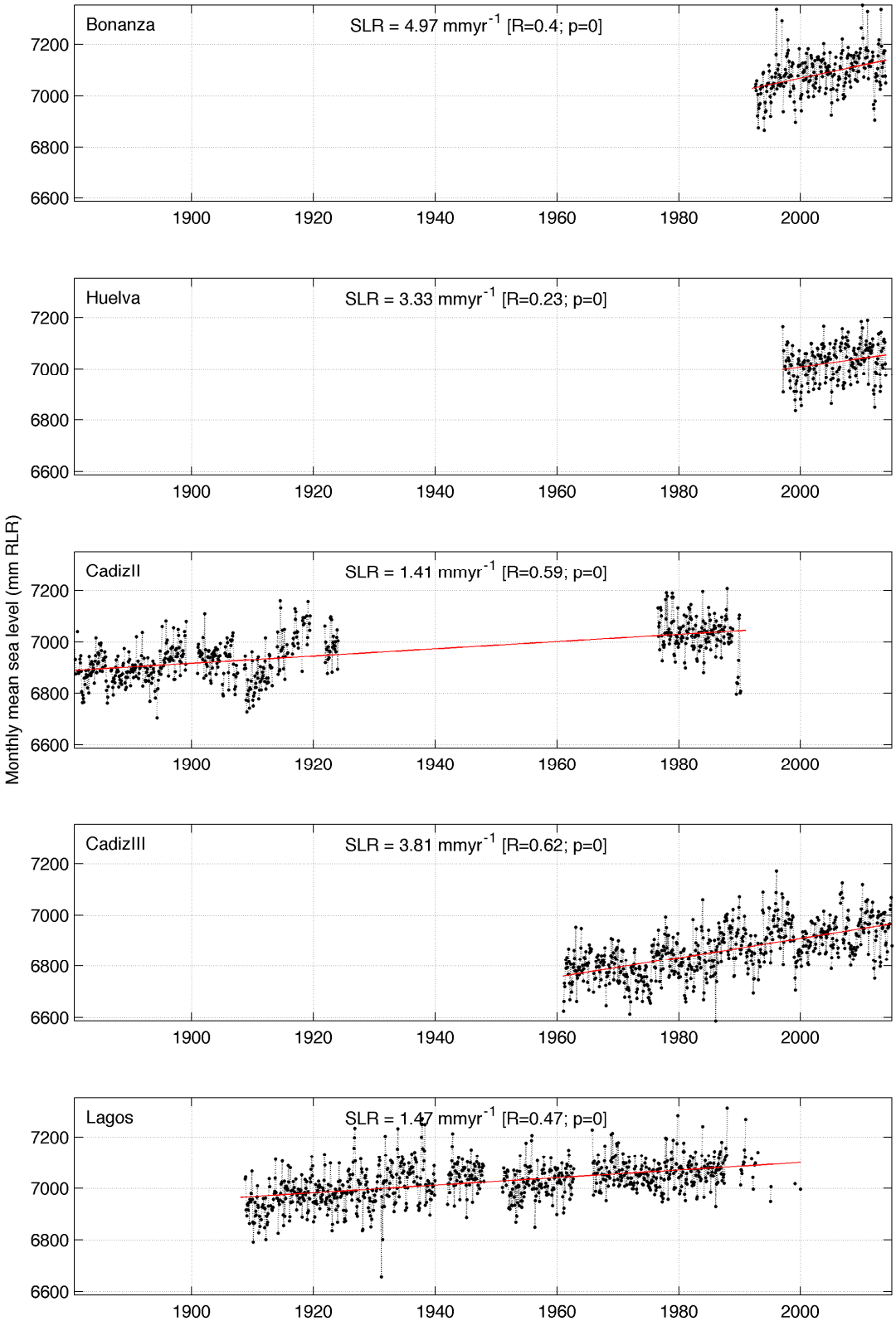

Figure 3.26 Monthly mean sea level (mmRLR) at different stations in the Gulf of Cadiz (Bonanza, Huelva, Cadiz (I and II) and Lagos (Portugal) tide gauges) [Source: PSMSL]

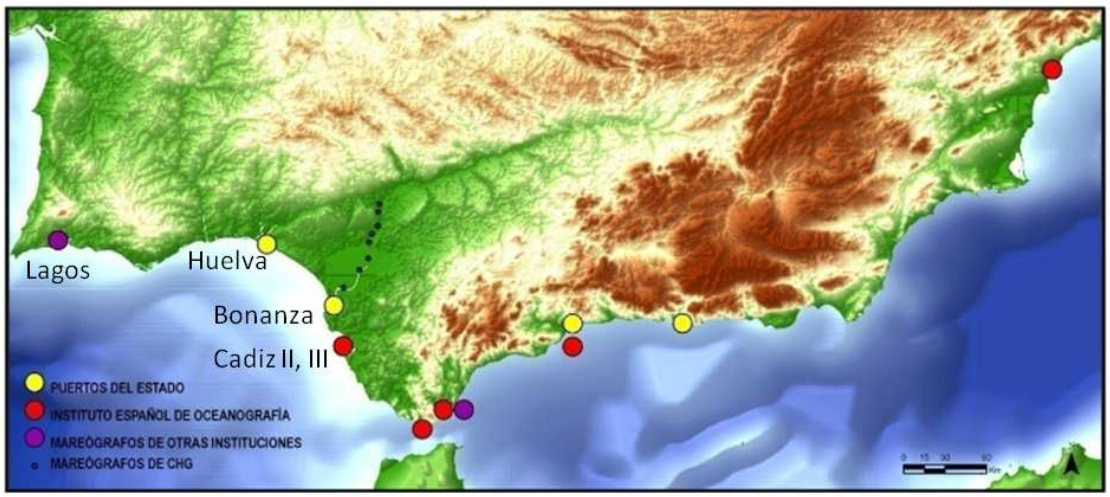

Figure 3.27 Tidal gauge location at different stations in the South of the Iberian Peninsula, specifying those found in the Gulf of Cadiz (Bonanza, Huelva, Cadiz (I and II) and Lagos (Portugal) tide gauges) [Source: Fraile (2011)]

3.6. Summary and discussion

The spatial distribution and tendency of change in the Odiel saltmarshes during recent decades is shown in Figure 3.28 and Figure 3.29 respectively. The most dramatic changes occurred between 1956 and 1979, when the Odiel saltmarshes suffered a great transformation (Figure 3.28). This transformation was the consequence of industrial development of the city of Huelva and adjacent towns, and conversion of marsh areas for industrial salt production during the 1960s and 1970s, resulting in large-scale loss of saltmarsh habitat (Figure 3.29), and an increase in saltmarsh patches. With the growth of the green policies in Spain during late 1970s and early 1980s, the study area was covered by several nature conservation designations (Biosphere reserve, Paraje Natural, special protection area and RAMSAR place). This led to a cessation of the destructive processes of earlier decades and initiation of new growth in saltmarsh area (Figure 3.29), which also increased the core surface area shown in the patch analysis (Table 3.4). During the 1980s and 1990s, the system re-adjusted to these new conditions, which has induced new habitat creation at the lower estuary (increasing the saltmarsh surface) and possibly some increase in the erosion rates at mid estuary. In addition, during this time conservation measures began to be applied over the remaining saltmarsh habitats, reducing greatly the habitat loss and favouring habitat recovery in the most recent decades.

The human activities identified in the Odiel saltmarshes (e.g. industrial development and hard structure construction) have also been the cause of saltmarsh loss in other saltmarshes worldwide such as in the USA (Kennish, 2001). Direct impacts such as physical habitat modification or habitat loss result from the construction of hard structures such dikes, piers, levees or water control embankments (Turner & Rao, 1990;

White & Morton, 1997; Bryant & Chabreck, 1998). However, long-term indirect impacts are also associated with these anthropogenic perturbations. For example, Kennish (2001) states that the construction of hard structures (e.g. water control embankments and dikes) as well as canals and their associated damaged banks modifies the saltmarsh hydrology, interfering often with the natural tidal flooding and drainage. Consequently, the water flow over the saltmarsh surface is also altered, reducing sediment supply and connectivity, thereby affecting vertical accretion and vegetation colonisation.

In the Odiel saltmarsh, water control embankments for instance have been extensively built during the latter half of the 20th century for large-scale modern industrial salt production installations. These structures in addition with the Juan Carlos I dike construction have modified the hydrology of the system, altering the tidal flooding and drainage in some creeks and across the marsh surface. These new conditions have possibly induced erosion processes around the Enmedio Island as is highlighted in Figure 3.30. For example, between 1956 and 1979, the Enmedio Island shoreline showed small changes and growth in some sectors; however, from 1979 this tendency changed showing saltmarsh retreat and rates of retreat reached a maximum between 1984 and 2001.

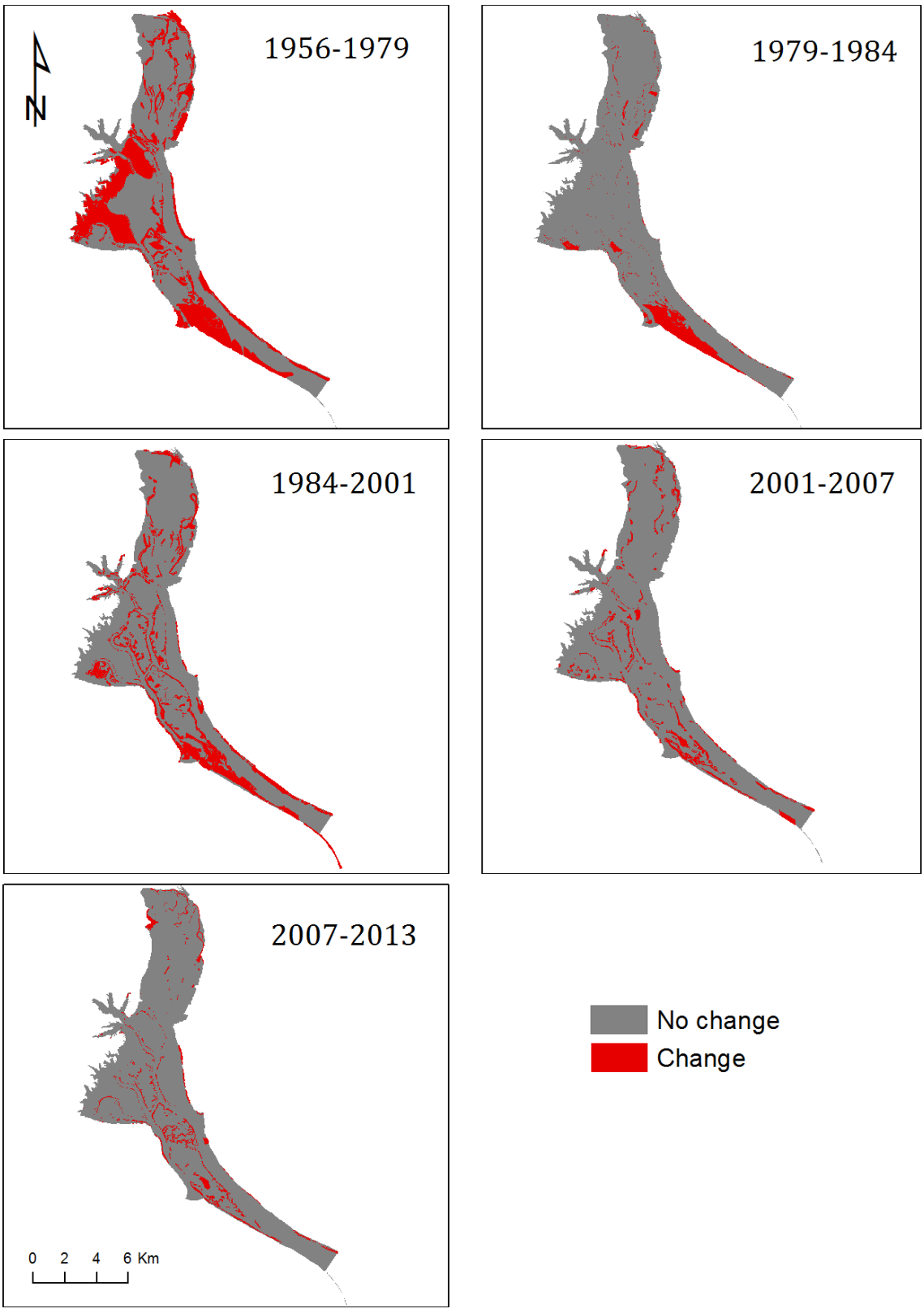

Figure 3.28 Changes experienced the Odiel saltmarshes per time interval. Grey represents areas that did not change within the time interval; red identifies areas that changed cover class.

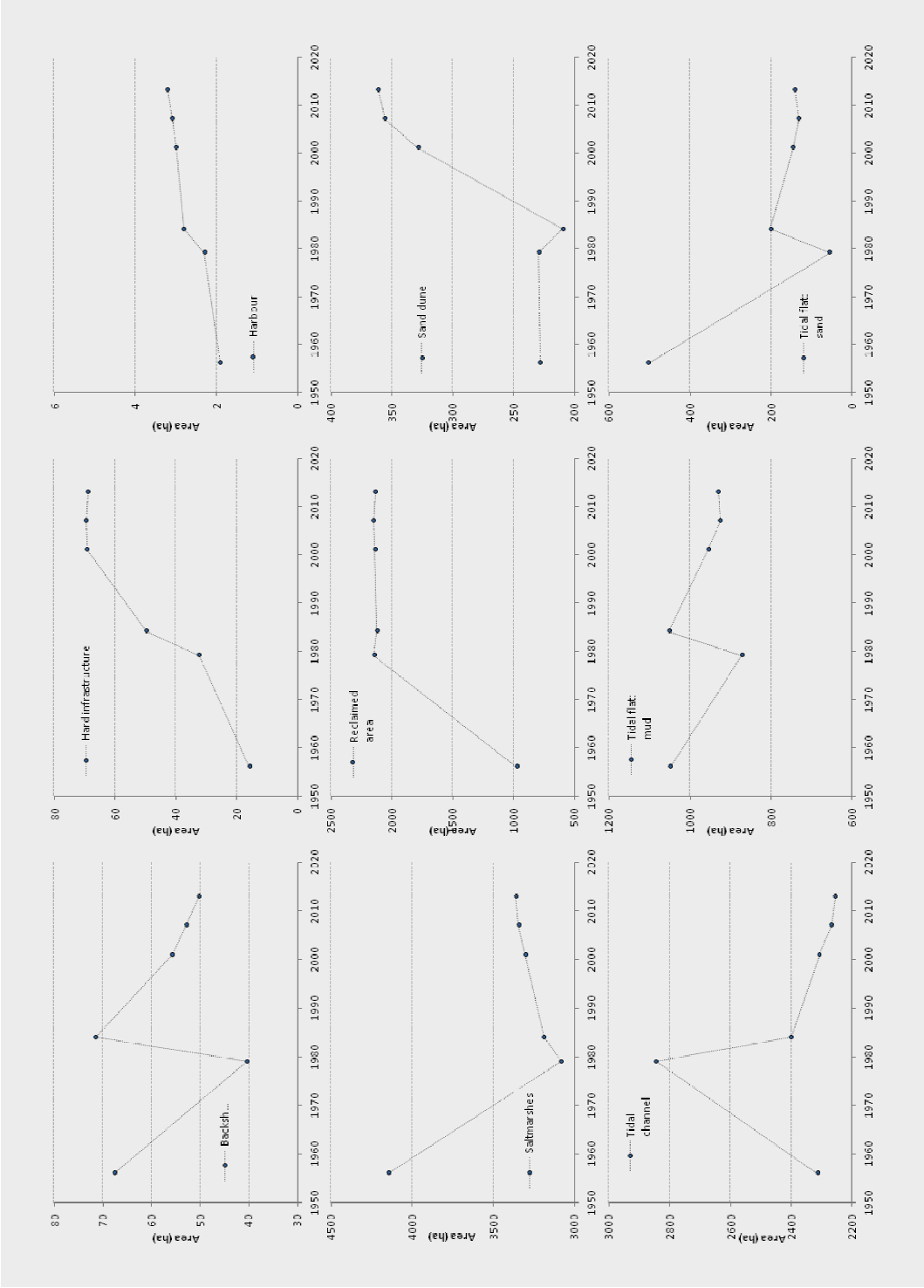

Figure 3.29 Variation and tendency followed by each cover class in the Odiel saltmarshes over the time. The Y axis represents the surface area (ha) occupied by each class and the X axis the year.

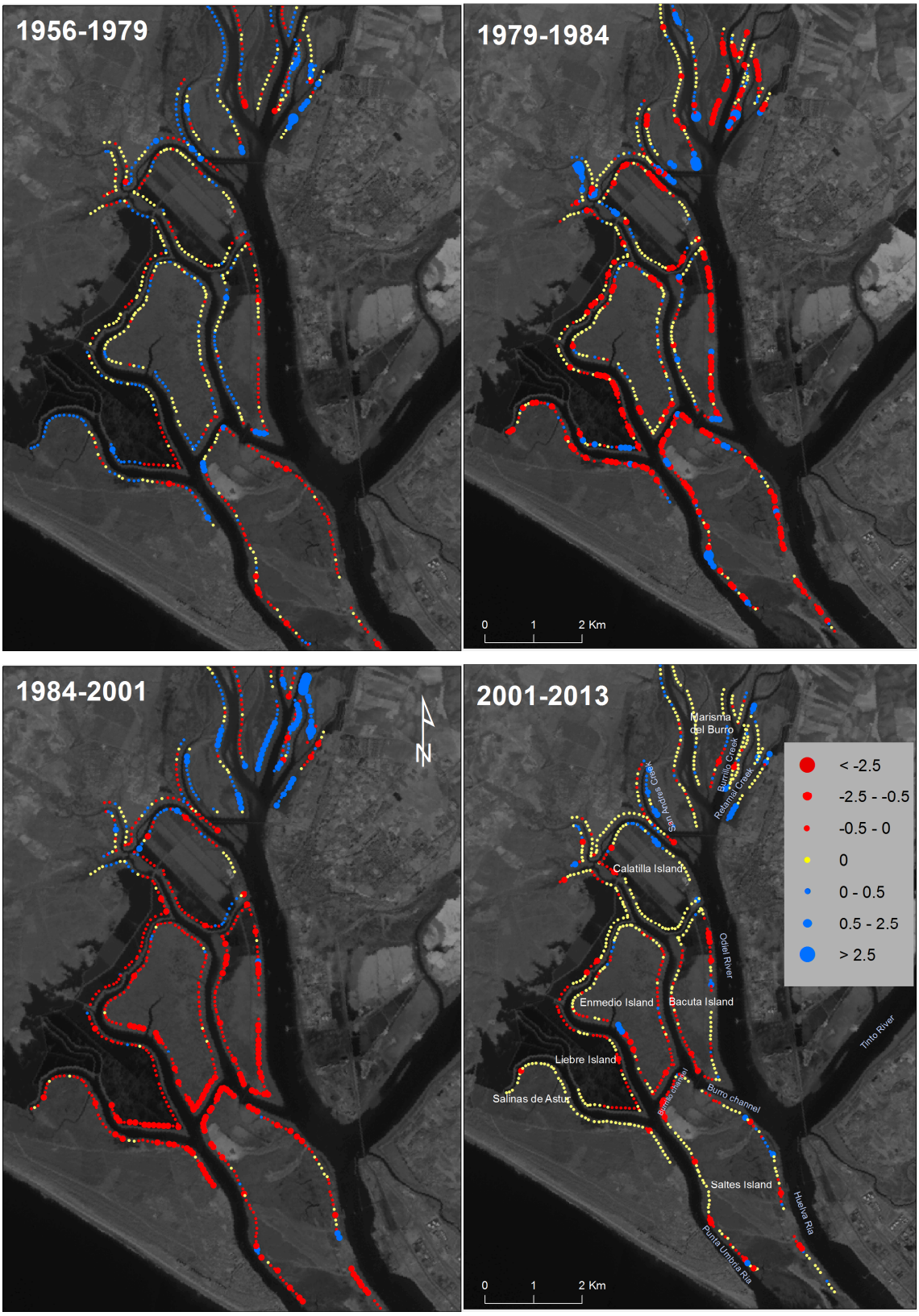

Figure 3.30. Horizontal Erosion and sedimentation rates (End Point Rate in my^{-1}) at different time periods in the Odiel saltmarshes

Castillo *et al.* (1999) reported severe horizontal erosion along the Enmedio Island, sampling 25 sites from July 1996 to July 1997 using 84 iron poles (1.7 m height) as markers. On average, they identified a saltmarsh cliff retreat of -29 cm yr^{-1} stating 3000 m^2 of saltmarsh loss that had led to 1850 m^3 of sediment remobilisation and consequent deposition on the channel bed. They also suggested a possible correlation between rainfall and erosion rates through the year indicating that although the mid-estuary hydrodynamics was mainly dominated by tidal forces, the seasonal tendencies were modulated by fluvial discharges. Similar findings relating erosion/sedimentation processes and climatic factors were reported by other authors (e.g. Barros, 1996; Cahoon *et al.,* 1996) in Mediterranean climate saltmarshes. But further work on erosion patterns (between 1956 and 1996) led Castillo *et al*. (2000) to dismiss the idea of a correlation between erosion and rainfall due to lack of ongoing evidence. In this work, the erosion patterns are analysed in a longer period (1956-2013), showing some evidence that the greater erosion rates at the mid estuary between 1984 and 2001 were probably exacerbated by greater river discharges during this time period. However, it should be noted that this relationship was not clear when rainfall data were analysed.

Although gradual saltmarsh cliff erosion is a natural process, particularly along channel margins, caused by tidal flow and ebb and fluvial currents (Chapman, 1974), the results presented here showed that the anthropogenic modifications of the Odiel saltmarshes also played an important role in the erosion processes during the 1980s and 1990s along the Enmedio Island. Here, severe erosion processes were induced due to saltmarsh retreat that was initiated by reclamation processes and dike construction (Figure 3.30). Between 1984 and 2013, erosion rates were possibly reduced due to system adjustment to the new conditions and some conservation measurements carried out by the Natural Park office (e.g. wooden revetments along the Enmedio Island south shore) in combination with lower values of river discharge.

The constructions of the Juan Carlos I dike modified the maritime connection between Huelva and Punta Umbria Ria, increasing the boat traffic in two marsh creeks (Burro and Burrillo channels). Ojeda *et al*. (1995) describes that the Burro and Burrillo channels have different hydrodynamics within the estuary due to their role as the only navigable channels connecting the Huelva Ria and Punta Umbria Ria after the construction of the Juan Carlos I dike. Over the decadal scale considered here, post- dike construction erosion rates in the Burrillo channel were greater than in the rest of the channels around the Enmedio Island, and this could be related to an increase in maritime traffic. Castillo *et al.* (1999) also identified greater erosion rates along the Enmedio Island shore facing the Burrillo channel than along other shorelines of the island. They highlighted that the waves created by the passing boats are possibly increasing the erosion rates at this location

simply due to the increase in maritime traffic. Erosion processes induced by passing boats have also been indentified in other saltmarshes in the U.S.A. (Schwimmer, 2001; Houser, 2010).

In the Tinto-Odiel estuary, the system response to anthropogenic and natural drivers has been observed in geomorphological and habitat changes, as well as in shoreline change described along the Odiel saltmarshes. Here, different system responses have been identified within the estuary that is expressed in a north-south spatial pattern. Thus, three zones have been identified within the estuary: upper, mid and low estuary.

In the upper estuary, although saltmarsh habitats were lost due to hard structures and harbour construction, the saltmarsh shows growth over recent decades (groups 3, 4, 5 and 7 in the cluster analysis). This growth tendency is also related to the saltmarsh restoration projects carried out by the Huelva port office as compensation measurements to reduce the impacts of port and harbour construction. Shorelines included in groups 5 and 7 showed behaviours that are directly related to these compensation measurements (e.g. plantation of *Spartina maritima* on mud flats (Castillo & Figueroa, 2009)). In the context of sea-level rise, the local mean sea-level in the Tinto-Odiel estuary has been rising at a rate of around 3.3 mmy^{-1} (between 1996 and 2013). However, the sedimentation rate estimated for this part of the estuary is 4.36 mmy^{-1} (VH5 in Figure 2.9) (Morales *et al*., 2003). Thus, apart from the restoration actions taken in some areas, the saltmarsh growth shown in the results seems to be logical due to these conditions. Greater river flooding during the late 80s did not increased erosion in this part of the estuary, possibly due to the in this part of the estuary dominate sedimentation processes and the fluvial sediments (sand) are usually deposited here during winter/autumn.

In the mid estuary, human modifications have caused harmful effects over the saltmarsh, resulting in large scale saltmarsh retreat and loss over time. The recessional tendency is related to natural processes (e.g. tidal flow and ebb and fluvial currents) exacerbated by human impacts (e.g. hydrological changes and waves generated by passing boats) and possibly by sea-level rise. For example, the accretion rate for the marsh platform in the Enmedio Island has been estimated at 2.1 ±0.02 mmy^{-1} (San Miguel *et al.* 2001). This value is smaller than the local mean sea-level rise rate (3.3 mmy^{-1}). Thus, it is quite possible that sea-level rise is outpacing sedimentation at this site, which is another factor adding to the erosive tendency in this part of the estuary. As in other estuaries, the sedimentary dynamic here is primarily controlled by tidal regime. The tidal current velocities in relation to tide height and the number of periods of flooding and exposure are important factors controlling sedimentation processes across these intertidal habitats and estuarine channels (Swinkbanks and Murray, 1981). In this sense, the industrial salt production, which needs 65 tonnes of seawater to produce one tonne of sodium chloride

(Adam, 2002), may have altered sedimentation patterns in the area through modifications to the water regime and sediment supply. Overall, shorelines included in groups 1, 2 and 3 seem to be responding to hydrodynamic changes caused by the saltmarsh reclamation, and shorelines in groups 5 and 6 to the effect of the passing boats in navigable channels. However, all the mentioned impacts in combination with the irregular annual fluvial discharge and rising rate in sea-level make difficult to identify and quantify the contribution of each phenomenon to these erosion process.

In the lower estuary, close to the mouth region, the sedimentary dynamics are controlled by a combination of tide and swell (Morales *et al.,* 2003). The dominant waves come from the southwest, influencing a long-shore drift that transports sediment west to east, from the main source of sandy sediments - the Guadiana River at the border between Spain and Portugal, along the Gulf of Cadiz shoreline. This explains the formation and development of spits along river mouths within the region. The long-shore drift reaches up to 300,000 m^3y^{-1} (Ojeda *et al.* 2011), and in combination with strong tidal currents and persistent swell, these natural conditions explain the dynamic the estuary mouth, where significant morphological changes have occurred over the last 50 years. However, the Juan Carlos I dike and the Punta Umbria dike construction greatly influenced the dynamics of this part the estuary.

The great accumulation of sediments at the estuary mouth retained by the Juan Carlos dike has also reduced the marine influence in this sector. These new conditions have induced new habitat creation such as saltmarshes, beaches and sand dunes during the last decades. In particular, creation of new saltmarsh has been favoured due to the conversion of previously high energy environments into low energy, back-barrier environments. Additionally, the Juan Carlos I dike has divided the tidal low-lying sediments at the south of the Saltes Island changing the geomorphology of this sector and creating two lagoons with different drainage conditions. The west part due to the great sediment retention has a slower drainage than to the east (Castellanos *et al.*, 1999). Furthermore, sea-level rise at this sector may have influenced some of the processes related to sediment transport but its impact is difficult to assess due to change the configuration of the lower estuary resulting from dike construction.

Overall, based on the analysis of the climate data, it is not possible to identify any significant climatic shifts that fully explain the changes observed in the Tinto-Odiel estuary, suggesting that the role of sea-level plays an important role. However, the effect of the sea-level rise is also manifested in different ways in different parts of the estuarine system depending on their natural features and anthropogenic history.

4. Contemporary baseline assessment of the saltmarsh bio-geomorphology

The aim of this chapter is to investigate the contemporary plant communities and vegetation structure across the Odiel saltmarshes, looking at relationships with some environmental factors (mainly ground elevation) and (short-term) sedimentation rates for understanding saltmarsh response to sea-level rise. The definition of saltmarsh habitat types based on vegetation surveys was crucial for mapping saltmarsh habitats later on (Chapter 5) using supervised image classification techniques. This map is used for improving LiDAR-derived DEM (in Chapter 6) and it is one of the input layers for running spatial landscape models such as SLAMM (Chapter 7). Short-term sedimentation rate is a key variable to understand the contemporary sediment availability within this saltmarshes, and the ability to grow vertically as the sea level rises. This information is mainly contextual and it is used to assess the current state of the Odiel saltmarshes.

4.1. Introduction: environmental factors controlling saltmarshes

Spatial patterns in saltmarsh ecology are not governed by a single feature such as tidal forcing or salinity, and multiple factors are required to explain them. Saltmarsh ecosystems are largely controlled by 10 major environmental factors: tides, salinity, soil, drainage, aeration, water table, rainfall, evaporation, temperature and biota (Chapman, 1941). These environmental factors are interrelated, affecting saltmarsh functioning, processes and plant zonation (Figure 4.1). For example, subtle gradients in elevation can be associated with variations in other factors such as oxygen availability (Mitsch & Gosselink, 2000), soil moisture/soil water salinity (Adam, 1990; Gray & Brunce, 1972), soil redox potential (Armstrong & Beckett, 1985; Pezeshki. 2001), availability of nutrients (Levine *et al*., 1998), and concentrations of organic matter (Mudd *et al.,* 2009; Morris & Haskin, 1990; Groenendijk, 1987), all of which contribute to the characteristic patterns of spatial and vertical zonation found in saltmarsh macrophytes (Crain *et al.,* 2004; Bertness & Hacker, 2013).

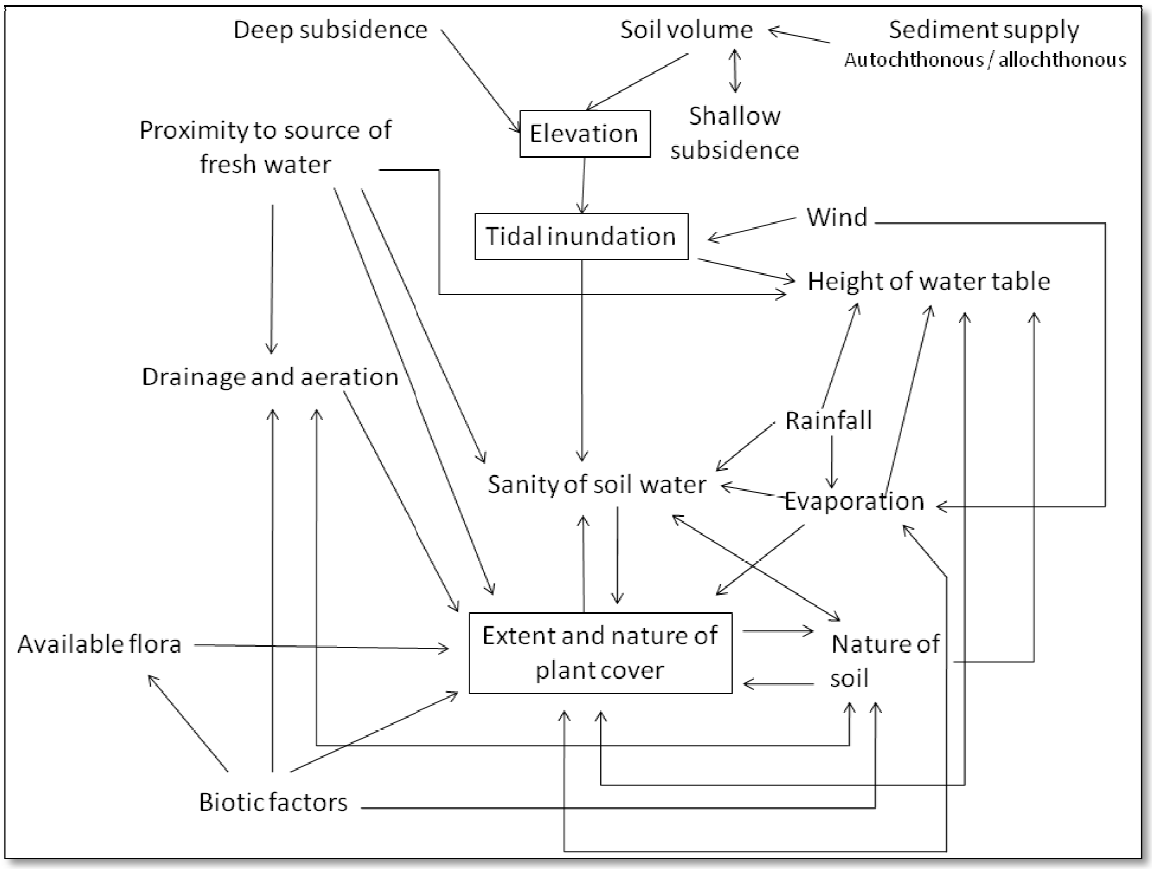

Figure 4.1 Interrelation of environmental factors affecting saltmarshes [modified from Nibbakeb and Bertness, 2001]

Key to saltmarsh ecomorphological development are tidal range and the submersion (inundation) period (Long & Mason, 1983; Adam, 1990; Doody, 2008; Chapman, 1974; Frey & Basan, 1978). These impart significant controls on saltmarsh functions such as accretion, plant zonation and development of creek networks. Timescales of inundation (the hydroperiod) relate to the period of time that the marsh substrate is covered by seawater (number of floodings) and sediment supply. They are strongly related to saltmarsh accretion (Long & Mason, 1983; Adam, 1990; Allen & Pye, 1992; Allen, 2000; French, 1993), which in combination with shallow and deep subsidence control saltmarsh elevation.

Apart from the direct flooding effect that the rise and fall of the tide can cause over saltmarshes, the water level variation notably influences other factors such as aeration within the marsh soil, salinity of the soil solution and the soil texture (Hinde, 1954; Chapman, 1974). Salinity in saltmarshes can vary significantly due to rainfall, temperature, evaporation, freshwater discharges and the proximity to the open sea. While the flux of salt varies with elevation, decreasing in higher positions due to the reduction in flooding frequency, the interstitial soil water salinity does not seem to follow any pattern (Adam, 1990). Lower saltmarshes have low variation in soil salinity, showing a strong correlation

with fluctuations in inundation water salinity regardless of precipitations or droughts (De Leeuw *et al*., 1993; Rozema & Diggelen, 1991). In contrast, at higher elevations other factors such as temperature and rainfall can raise or lower salt concentration resulting in greater spatial and temporal variation in marsh soil salinity (Adam, 1990; Smith, 2009; Pratolongo *et al*., 2009). For example, in drier periods with higher temperatures and low rainfalls, evaporation will increase and therefore the soil salinity concentration will also increase. This process is more evident in arid and semi-arid climates.

Salinity can be a major factor in controlling vegetation distribution, although other soil factors also must be taken in account (Chapman, 1974). The relationship between soil salinity and vegetation cover has been discussed by several authors based on local studies (Crain *et al*., 2004; Redondo *et al*., 2004; Huckle *et al*., 2000; Tyler, 1971), which conclude that high salinity levels can influence plant distribution on saltmarshes due to physiological tolerance. Additionally, soil salinity also affects other variables such as primary production and plant growth. For example, Curco *et al.* (2002) showed that primary production increases as soil salinity decreases in a Mediterranean saltmarsh, and experiments by Rozema *et al.* (1991) indicated that high salinity reduces growth of the species tested (*Scirpus maritimus* and *Puccinellia maritima*). Hence, soil salinity on high marshes, which can strongly depend of temperature, rainfall and evaporation, can influence plant zonation and growth.

Edaphic characteristics such as aeration, soil texture, redox potential, nutrient levels and drainage can also be important in controlling vegetation type (Gray & Brunce, 1972; Chapman, 1974) and plant growth (Rozema *et al*., 1991). Early studies of saltmarsh soil aeration (Teal & Kanwisher, 1961; Howes et al., 1981) showed that oxygen was only found in the upper few centimetres with reducing conditions elsewhere, except for well-drained areas. More recent studies (e.g. Rozema *et al.*, 1991; Rozema, 1993) investigate plant growth at different CO_2 concentrations (at 340 p.p.m. CO_2 (ambient) and 580 p.p.m. CO_2) in aerobic and anaerobic conditions, concluding that the growth of grass species such as *Scirpus maritimus* and *Puccinellia maritima* is greater under anaerobic solution and elevated CO_2 conditions. The soil aeration in saltmarshes is strongly related to the frequency and duration of tidal flooding (Adam, 1990). Higher elevations are increasingly aerated due to the reduction in hydroperiod; soils across lower elevations are prone to being water-logged. Therefore, topography and elevation may create significant temporal and spatial differences in soil aeration within the marsh (Armstrong *et al.,* 1985). This variable is also related to texture and drainage properties of the soil. For example, soils with high content of clay will have less aeration due to their structure which also leads to poor drainage. In contrast, sandy soils are more free-draining and aerated than clay soils.

Finally, flora, fauna and microorganisms (such as fungus and bacteria) are important biological factors controlling saltmarshes. Halophytes are very important in saltmarsh development (Erfanzadeh, 2010; Long & Mason, 1983; Cahoon *et al*., 2000), promoting vertical accretion. The presence of vegetation reduces water flow speeds, favouring sediment deposition (Boorman *et al.*, 1998; Boorman 2003). Microorganisms and fauna also play an important role in saltmarsh functions, most specifically in terms of nutrient cycles (Lillebø *et al.*, 1999). Odum (1971) considers microorganisms the primary consumers in detritus-based systems such as saltmarshes. Furthermore, transport of nutrients is controlled by both benthic animals (e.g. bivalves, crabs) and water circulation within estuaries (Levin *et al*., 2001; Pratolongo *et al.*, 2009). Other herbivores such as water birds can consume and then export the biomass to others saltmarshes or wetlands (Pratolongo *et al*., 2009).

4.2. Methods

4.2.1. Vegetation survey design and analysis

Quadrats are an effective sampling unit for vegetation surveys, particularly those associated with grassland communities such as saltmarshes (Kent & Coker, 1992; Roman *et al.*, 2001; Elzinga *et al.,* 1998). The Odiel saltmarshes do not follow a clear zonation within parallel belts to the shoreline and thus the use of transects was deemed inappropriate. Two campaigns in September 2011 and 2012 were carried out, where vegetation was surveyed using a 1 × 1 m quadrat (Figure 4.2, Figure 4.3). In total, 156 sites were sampled across the Odiel saltmarshes. Quadrats were located using a semi-random positioning process. First a 200m x 200m grid was generated to cover the study site using Arcmap (ArcGIS); a spreadsheet-based random number table (Microsoft Excel) was used to select the grid cells to sample. On the ground, 1 x 1 m quadrats were semi-randomly positioned within each grid cell (the final location was limited by difficult access and creek network). In each quadrat, plant species presence and abundance (percentage cover), vegetation height (sward height following (Van der Graaf *et al*., 2002)) and soil strength (using a Pilcon shear vane (Brown *et al*., 1998)) were measured.

In order to explore plant species assemblages on the Odiel saltmarshes and investigate community zonation, the plant species data were analysed using TWINSPAN (version 2.3). TWINSPAN is a top-down clustering approach that performs a hierarchical division of species and samples (Lepš & Šmilauer, 1999; Hill & Šmilauer, 2005). TWINSPAN performs a two-way classification, which effectively groups samples and species, using ordinations (Correspondence Analysis) to inform the divisions in terms of identifying the main gradients in the data. TWINSPAN also expresses 'indicator species'

that provide some criterion for the communities defined in the division process. In addition, elevation data were extracted for every quadrat using 2013 DEM in ArcGIS (v10.2).

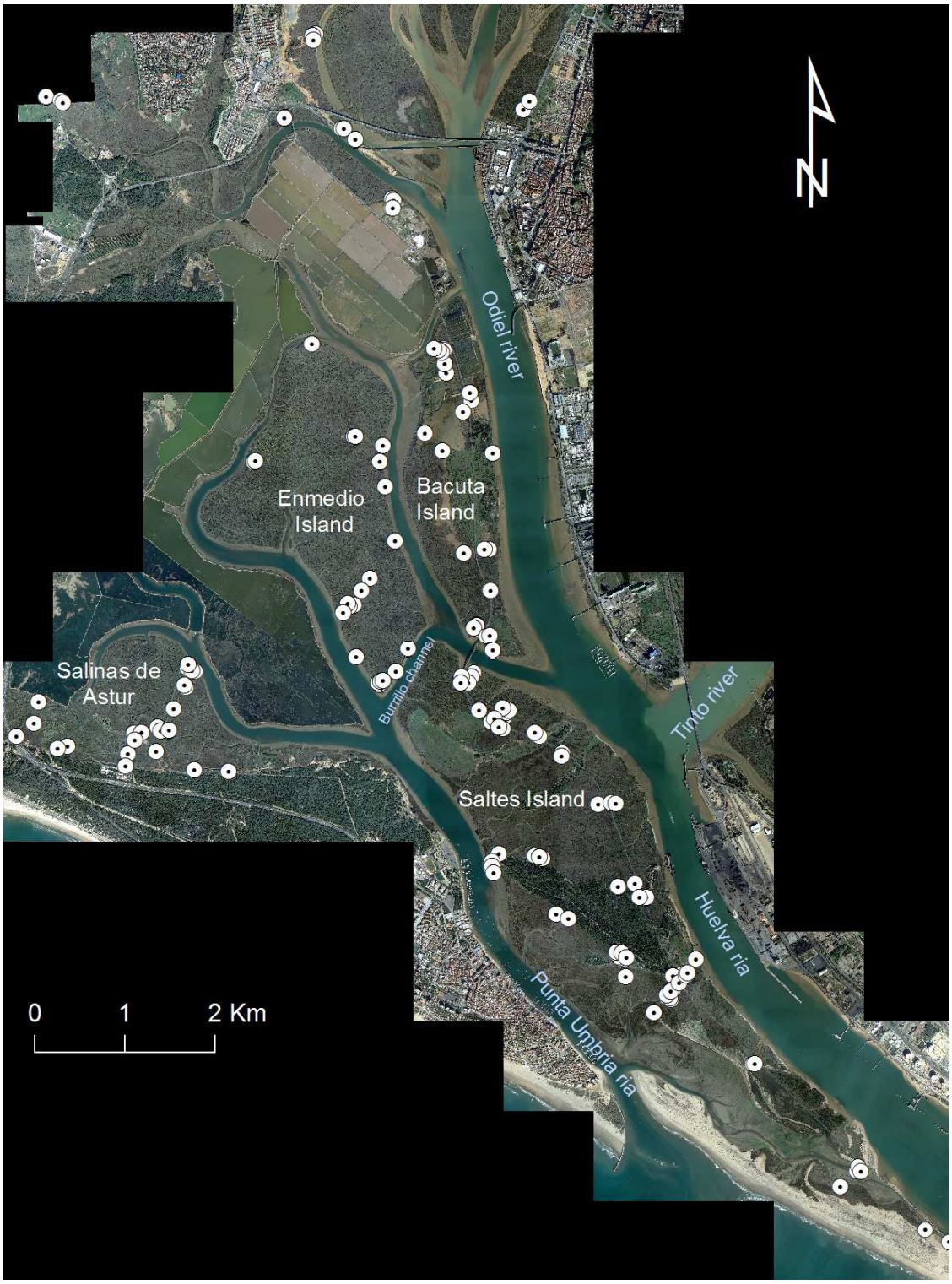

Figure 4.2 Quadrat location of the vegetation survey undertaken in the Odiel saltmarshes.

Figure 4.3 Example of the 1x1m quadrat used for the random vegetation survey.

4.2.2. Soil survey and analysis

Sediment samples were collected from 1 in 3 quadrats to explore broad relationships between basic soil properties and plant species assemblages and to provide contextual information. The transportation of the soil samples from the study site (Huelva, Spain) to the laboratory (London, UK) in cool boxes was the main reason to collect 1 soil sample in 3 quadrats. As this thesis is not focused on analysing soil properties, the chosen size sample was considered suitable to provide contextual information. Additionally, Euclidian distance to the nearest main creek was also estimated in ArcGIS (v10.2) using the quadrat location (points) and a digitised creek network layer (based on 2013 aerial photography).

The soil samples, collected in plastic bags, were stored in a cool box, and then returned to the laboratory and stored at 4°C until they were processed. Samples were then analysed for moisture content (loss on drying), and organic and carbonate content (loss on ignition). Sequential loss on ignition (LOI) is a simple approach for estimating the organic matter and inorganic carbon content in sediments using linear relations between LOI and organic and inorganic carbon content (Santisteban *et al*., 2004). This approach is easy to implement in the laboratory, which makes this method widely used (e.g. Korsman *et al*., 1999; Dodson & Ramrath 2001; Heiri *et al*., 2001; Boyle, 2004). In saltmarshes, this methods has also been widely used (e.g. Temmerman *et al*., 2003; Ashley & Zeff 1988; Curco *et al*., 2002; Sousa *et al*., 2010; Vranken *et al*., 1990). The procedure followed for this work was:

a-Loss on drying was use to estimate moisture content. For each sample, 2 g of wet sediment was weighed into an empty crucible of known weight. All crucibles were placed in the oven overnight at 105°C and then placed in a desiccator for cooling to prevent re-absorption of moisture. The crucibles were weighed again and the

sample weight remaining after drying was calculated. As a proportion of the original 2g sample weight, this provided percentage moisture content

b-Loss on ignition was undertaken at 550°C (LOI_{550}), a method for estimating organic content. The previously dried subsamples of sediment were placed (in their crucibles) in a 550°C furnace for 2 hours. When the crucibles were cooled slightly they were placed in a desiccator, to fully cool before being weighed. Percentage organic content was calculated as the proportion of the dry weight lost on ignition.

c- Loss on ignition was undertaken at 925°C (LOI_{925}), a method for estimating carbonate content. The remaining ash samples were returned to a 925°C furnace for 4 hours. The crucibles were removed and placed in a desiccator and re-weighed when cooled. The difference between the ash weight and the weight lost at 925°C was multiplied by 1.36 (the difference between the molecular weights of CO_2 and CO_3) to derive the carbonate content which is then expressed as a percentage of the dry weight.

4.2.3. Sediment traps design and analysis

Sediment traps were deployed for 4-6 month periods (from Jan 2012 to March 2014) to estimate annual measures of sediment deposition rates within different habitats across the Odiel saltmarshes (tidal flat, vegetated tidal flat, low marsh, and middle-high marsh) (Figure 4.4). Ceramic tiles (20 x 20 cm) were placed glazed-side up and levelled with the soil surface (as described in Darke & Megonigal (2003) and Pasternack & Brush (1998) with 15 - 20 cm wire pins to secure them (Figure 4.5) In order to estimate sediment bulk density, sediments were also collected using a 'density ring' for each site. Sediment traps have successfully been used to estimate short term accretion rates in marshes in USA (e.g. Neubauer *et al*., 2002; Darke & Megonigal, 2003), Spain (e.g. Lopez-Gonzalez *et al*., 2006) and Canada (e.g. Robert *et al*., 1991). Initially, 18 sample sites were set along the marshes with two tiles at each site. However, due to problems with access, 8 of the sample sites (located on Enmedio Island) had been discarded. Thus, 6 new sample sites were set in locations with easier access in 2013.

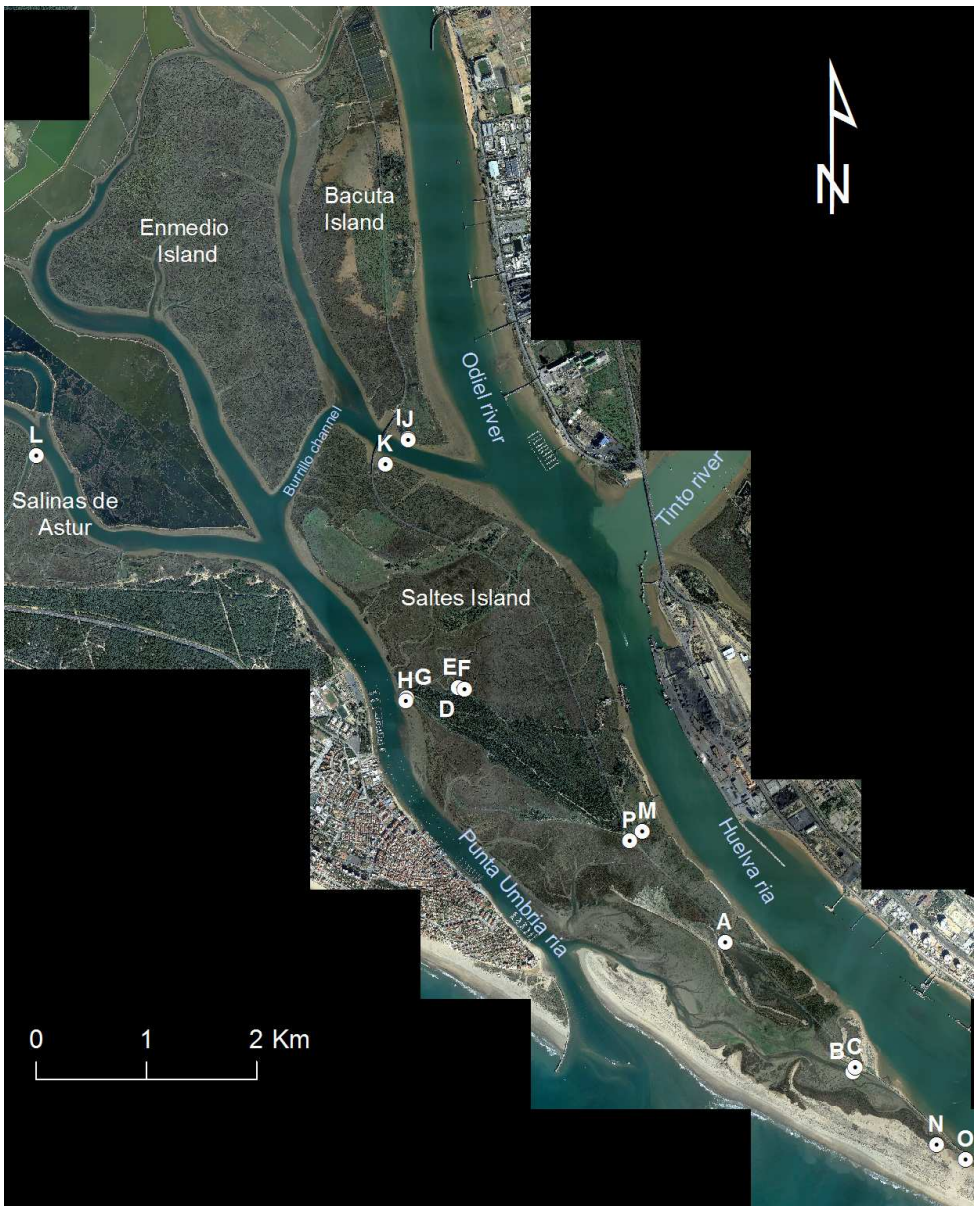

Figure 4.4 Location of the sediment traps.

Figure 4.5 Ceramic tile located at mid-low saltmarsh habitat.

Sediment deposited on the tiles was collected in large plastic bags (previously weighed in the laboratory): sediment was removed from the tile using a spatula and washing with water (using a spray bottle) when necessary (which was also collected in the bag). These samples were stored in cool bags for transportation (from Spain to the UK), and then returned to the laboratory and stored at 4°C. The samples - both those collected from the tiles and those collected in the density rings - were later processed to measure wet and dry weights. The wet sediments were weighed, dried (at 105°C) and weighed again. Wet and dry bulk densities (ρ_w and ρ_d respectively) were calculated for each site based on the known volume of the density ring (15.5 cm^3) (Equation 4.1):

$$\rho_w = \frac{M_w}{V} \qquad \rho_d = \frac{M_d}{V} \qquad (4.1)$$

where M_w and M_d are wet and dry masses for a known volume V. Deposition rates were calculated as a bulk mass deposition for each time frame (4-6 month time period), and these were converted to accretion rates using the bulk density to calculate sediment volume deposited on every tile which equated to a vertical rate when tile area and time period were accounted for (Neubauer *et al.*, 2002; Bricker-Urso*et al.*, 1989). These calculations provide an estimate of accretion rates, but do not take into account post-deposition compaction.

4.3. Characterization of Odiel saltmarsh vegetation

The results obtained from the vegetation survey showed the diverse plant community that occur within the tidal frame of the Odiel saltmarshes. Here (within the tidal frame), the halophytes are represented by 5 families and 10 genera (*Atriplex, Inula, Salicornia, Puccinellia, Limoniastrum, Limonium, Spartina, Suaeda, Salsola* and *Scirpus*) comprising 17 species Table 4.1.

Table 4.1 Plant species found on the Odiel saltmarshes.

Family	***Species***
Amaranthaceae	*Atriplex portulacoides* *Salicornia fruticosa* *Salicornia perennis* (subesp.) *perennis* *Salicornia perennis* (subesp.) *alpini* *Salicornia ramosisima* *Salicornia macrostachyum* *Salsola vermiculata* *Suaeda maritima* *Suaeda vera*
Asteraceae	*Inula crithmoides*
Cyperaceae	*Scirpus maritimus*
Plumbaginaceae	*Limoniastrum monopetalum* *Limonium vulgare* *Limonium algarvense* *Limonium ferulaceum*
Poaceae	*Puccinellia maritima* *Spartina densiflora* *Spartina maritima*

The spatial distribution of species surveyed is shown in Figure 4.6. Some species exhibit an extensive spatial distribution whilst others have a localised distribution. For example, *Atriplex portulacoides* is a 'generalist' species and is found throughout the estuary. Species such as *Salicornia perennis*, *Salicornia fruticosa*, *Salicornia ramosissima*, *Salicornia macrostachyum, Limoniastrum monopetalum*, *Limonium sp.*and *Suaeda sp*. are mainly distributed at the central part of the estuary. *Spartina densiflora*, however, tends to be found in larger patches in the inner (far north) estuary. There are some species that are mainly found nearer the estuary mouth (southern extent) such as *Puccinellia maritima* and *Spartina maritima*.

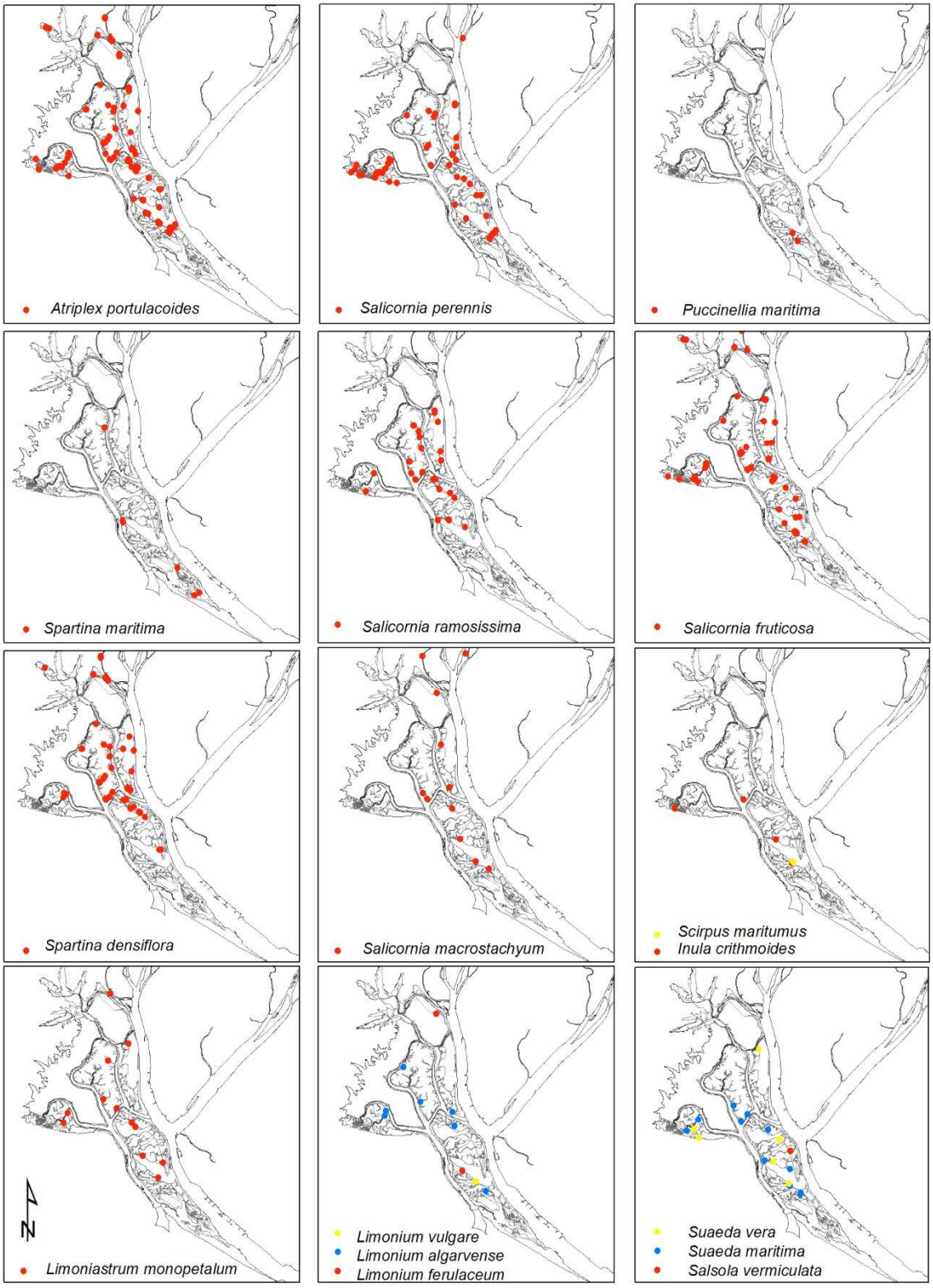

Figure 4.6 Spatial distribution of plant species in the Odiel saltmarshes based on vegetation survey (quadrats).

Plant species data were analysed using two-ways indicator species analysis (TWINSPAN) to divide the species and samples into groups to explore possible classes of plant communities. The analysis highlights the most common plant associations and a

potential organisation of species assemblages in the Odiel saltmarshes (Figure 4.7). The first division in the TWINSPAN results splits the data into two groups. *S. perennis* subsp. *perennis* and *S. ramosissima* are the indicators of one group, which are associated with the low marsh. *S. fruticosa*, *A. portulacoides*, *Sp. densiflora* and *S. perennis* subsp. *alpini*, which are associated with the mid- and high marsh, were indicators for the second group. Further divisions split these groups into more specific communities that can be described as low marsh, salt pan, mid marsh and high marsh habitats (Figure 4.7). Within the high marsh community further divisions in TWINSPAN results (4th division; 23 quadrats) showed *Sp. densiflora* as a separate community. This specific community was observed in the field forming large homogeneous patches of *Sp. densiflora* along the upper-mid estuary, and it was quite different to others high marsh communities at the mid- and low estuary. The field evidences supported by the TWINSPAN results led to consider this community as a different habitat type referred to as Spartina marsh. Furthermore, the canopy height of this community was also quite distinct to the other communities (Figure 4.8). Thus, the Odiel saltmarshes habitats can be best described as comprising low marsh, salt pan, mid marsh, high marsh and Spartina marsh. General floristic characteristics of the key plant communities found in the Odiel saltmarshes are summarised in Table 4.2.

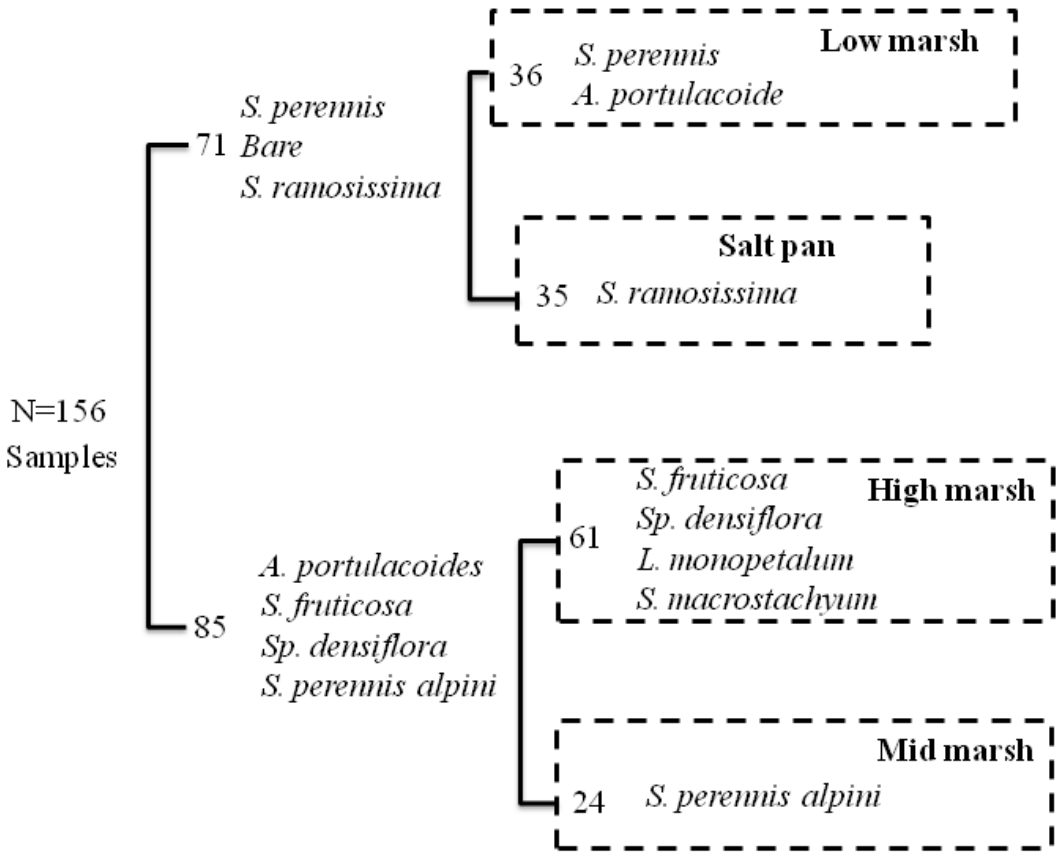

Figure 4.7 Summary of the cluster analysis obtained in TWINSPAN. The numbers refer to number of quadrats that contain the species mentioned.

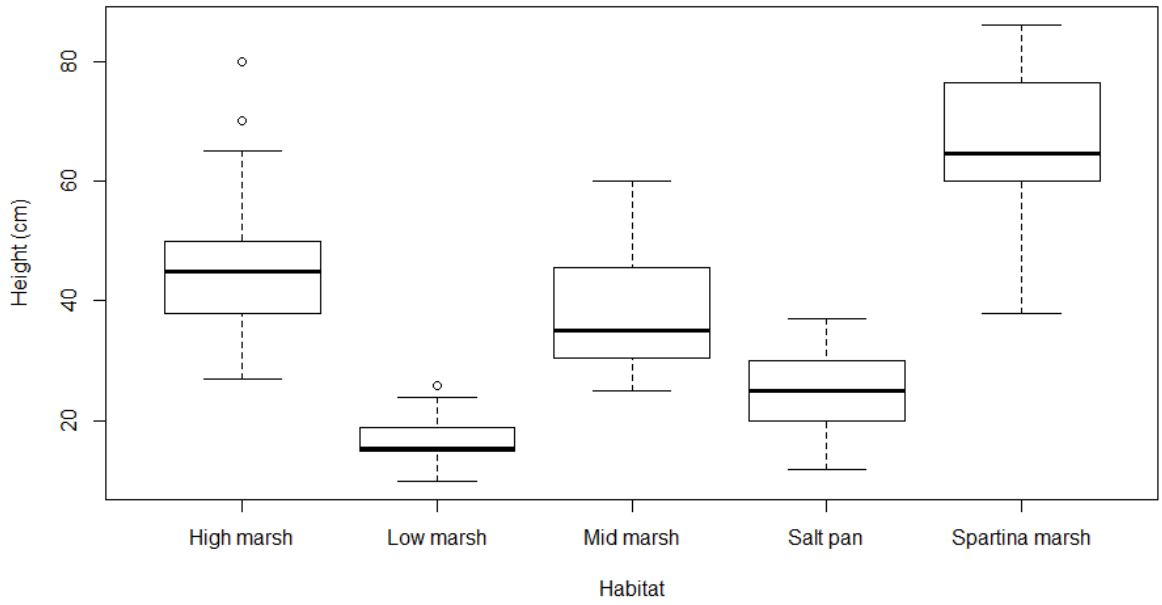

Figure 4.8 Canopy height for different saltmarsh habitats at the Odiel saltmarshes.

Table 4.2 Summary of floristic characteristics of the key plant communities in the Odiel marshes.

Community	Key species	Diversity	Structure
Low marsh	*S. perennis* (subsp. *perennis*); *A. portulacoides*,	Low	Continuous sward
Salt pans	*S. ramosissima*	Low	Low spatial density
Mid marsh	*S. perennis* (subsp. *alpini*); *A. portulacoides*,	High	Continuous sward
High marsh - Salicornia	*S. fruticosa*	High	Mixed
High marsh - Spartina	*Sp. densiflora*	Low	Homogeneous and tall

Of particular note, pioneer saltmarsh (*Spartina maritima*), which occurs on the tidal flats, is not well represented in the TWINSPAN analysis because the surface area of the pioneer marsh in the Odiel saltmarshes is relatively small compared with other habitats. Additionally, these species are usually found forming little islands over unconsolidated, sparsely-vegetated tidal flats, which complicate the access for vegetation surveys.

Broadly, the low marsh is mainly represented by *S. perennis* (subsp. *perennis*) and *A. portulacoides*, although others species such as *Li. vulgare*, *Pu. maritima, Su. maritima, S. ramosissima* and short *Sp. densiflora* can also be found with less frequency and abundance. The average canopy height of this habitat ranges between 15 and 24 cm, with an average of roughly 17 cm. The distribution of the low marsh community is related to younger saltmarshes closer to the estuary mouth and more centrally along channel and creek

edges. Some differences in diversity are evident across this community depending on its location within the estuary. Closer to the estuary mouth, the low marsh patches cover large surface areas and more plant diversity (up to 7 species) can be found, while those patches located along channels and creeks across the mid and upper estuary cover smaller surface area and the diversity is lower (up to 2 or 3 species). Figure 4.9 (A) displays different sites of low marsh habitats found in the low estuary.

The mid-marsh community mainly comprises *S. perennis* (subsp. *alpini*) and *A. portulacoide,* although others species such as *S. fruticosa* and *Sp. densiflora* can also be found with less frequency and abundance. These communities usually present a dense canopy, which form a tortuous root system of roughly 20-30 cm above ground. The mid-marsh habitats in the Odiel saltmarshes are mainly found across the mid and low estuary. The average height canopy for this community is 38 cm approximately, presenting a wider range of heights than the low marsh communities. Figure 4.9 (B) shows different examples of mid-marsh environments within the low estuary.

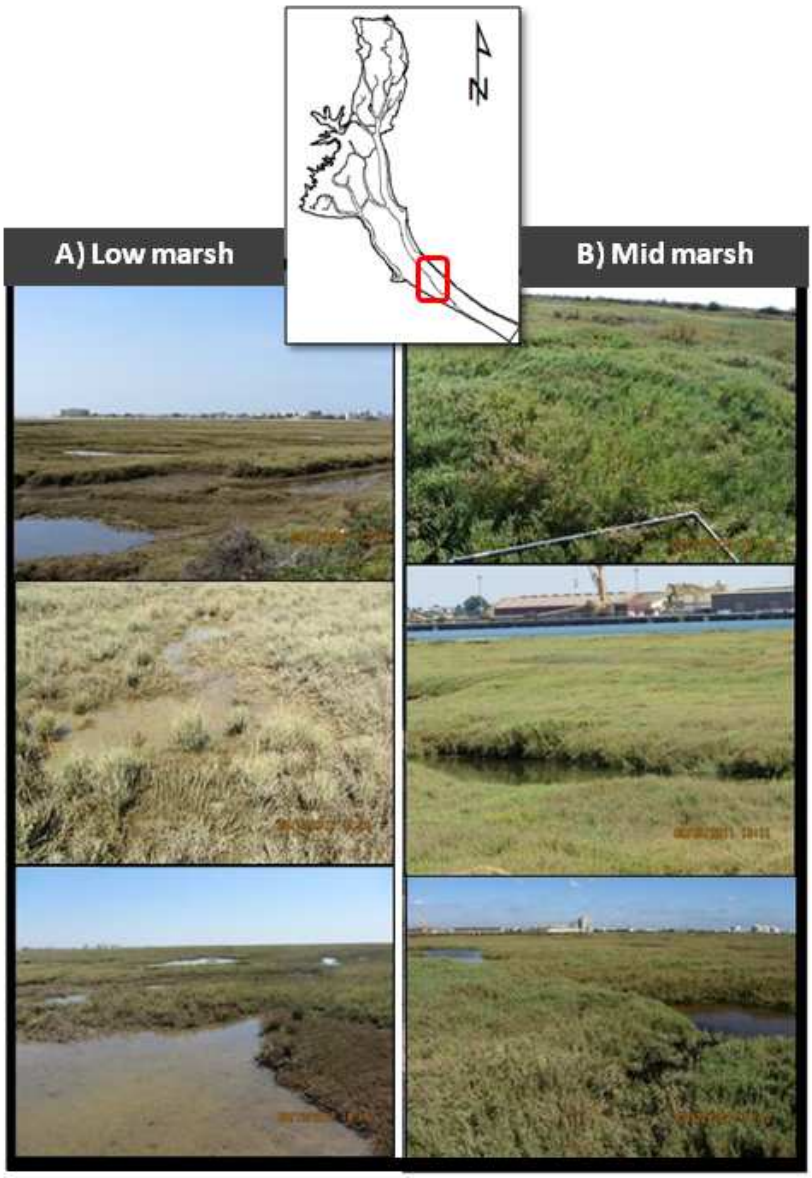

Figure 4.9 Examples of low (A) and mid (B) marsh habitats in the Odiel saltmarshes.

The salt pan habitat mainly comprises bare mud and *S. ramosissima* (Figure 4.10), which are recognised as a single group in the TWINSPAN analysis. Plant diversity in this habitat is quite low due to the hypersaline conditions, and only *S. ramosissima* was found covering the salt pans (*S. ramosissima* was the only annual species found within the saltmarsh vegetation). The growth structure of this habitat (mainly represented by one species) is characterised by low plant density (notable spacing among single plants) and average height of 25 cm. The structure of individual plants is characterised by a jointed vertical main stem and erect lateral branches. This habitat is found across lower elevations within the mid-high marsh platform. In summer, bare mud in salt pans is usually covered by a layer of salt when the estuarine water is evaporated. In pans located across lower elevations, which are more frequently flooded, *S. perennis* (subsp. *perennis*) was also

found. The plants covering the perimeter of the salt pans are adapted to very high salinity conditions and *S. macrostachyum* was usually found covering those areas.

Figure 4.10 Salt pan habitat in the Odiel saltmarshes. *Salicornia ramosissima* appears in the front over the salt pan (pink colour) and *Salicornia macrostachyum* in the back (green colour).

With regard to the high marsh, two main sub-groups are found (based on field observations): one is dominated by *S. densiflora* (Figure 4.11A) and the other is characterised by *S. fruticosa* and *A. portulacoides* (Figure 4.11B). These habitats are the most frequent in the Odiel saltmarshes. Most of the saltmarsh platform located at the mid and outer estuary is dominated by *Salicornia* marsh and at the mid-upper estuary by *Spartina* marsh. In the high marsh, other species such as *A. portulacoides, A. macrostachyum, L. monopetalum, L. ferulaceu, I. crithmoides, S. vera, S. Vermiculata*, *L. algarvense*[11] and *S. densiflora* are also found, whereas the Spartina marsh is mainly formed of large *Spartina*-only areas (often referred to as 'Spartina Sea') with less than 10% of other species such as *A. macroshtachyum*.

[11] *L. algarvense* is endemic to the South-Atlantic Iberian saltmarshes and it is considered vulnerable species in the Iberian Peninsula.

Figure 4.11 (A) Spartina marsh and (B) high marsh habitat in the Odiel saltmarshes.

4.4. Habitat environmental characterisation

To provide contextual information, the influences of environmental factors on different habitat were explored by looking at 6 parameters: % dry weight, % moisture loss, shear strength, % carbonates, % LOI and distance from creeks. Results showed (Figure 4.12) that low marsh and mid marsh habitat have similar range values in parameters such as % moisture loss, % dry weight and % carbonates, suggesting similar soil properties for these two habitats. The first two parameters covered a broad range from 15 to 70 % approximately, and the third one covered a narrower range (1.6 - 3 % in low marsh and 1.3 – 2.8 % in mid marsh). High values in moisture loss state low infiltration capacity suggesting high content in clay and frequent flooding, which are features representative of low and mid marsh habitats. However, these habitats were also found in parts of the saltmarsh (at the low estuary) with higher content in sand, which may explain the high values in dry weight and low values moisture loss. For % LOI, mid marsh (~13%) presented slightly higher mean than low marsh (~11%), and covered a broader range values than low marsh. This means that the organic content in the mid marsh is slightly higher than in the low marsh. Leaf litter was found in both habitats, but in the mid marsh higher root density was observed which may explain the higher values. Mean carbonates values were higher than high marsh and salt pan habitats possibly due to

higher shell content. This can be explained by the presence of grazing gastropods, which is usually higher in lower parts of the saltmarshes. On average, shear strength in the low marsh presents lower values than the mid marsh, reaching values down to 8 KPa (the lowest value of the dataset), which was expected due to higher water content in the soil and lower density root system.

High marsh covers a narrower range for % dry weight and % moisture loss than the mid and low marsh; between 62 and 79.5 % for dry weight and between 21 and 37 % for moisture loss. These values suggest lower content in clay and less frequent tidal floods, which is a feature of high marsh habitats. Conversely for % LOI and % carbonates, the high marsh covers a broad range of values overlapping with low and mid marsh at the bottom values. However, this habitat includes much higher values of both these parameters than other parts of the system. The average carbonate content is lower than in other habitats suggesting less shell content in the sediments, which is expected for higher soil elevations in saltmarshes due to the decrease in gastropods. However, the high values of the carbonate range are possibly explained by residual shell deposits found across the high marsh. Low values in organic matter are probably due to the high sand content in the soil samples, which get higher near the sandy barrier islands. The distance from creeks and the shear strength (KPa) parameters for high marsh also have a broad range of values, reaching higher values than other habitats as it was expected. The micro-topography characteristic of saltmarsh environments leads to complex spatial patterns where high marsh can be found near or far from creeks. In the case of the shear strength, high values are also characteristic of high marshes, showing more developed soils with more dense root systems and with less water content. However, lower values of this parameter are possibly showing once again higher content in sand in some parts of the high marsh.

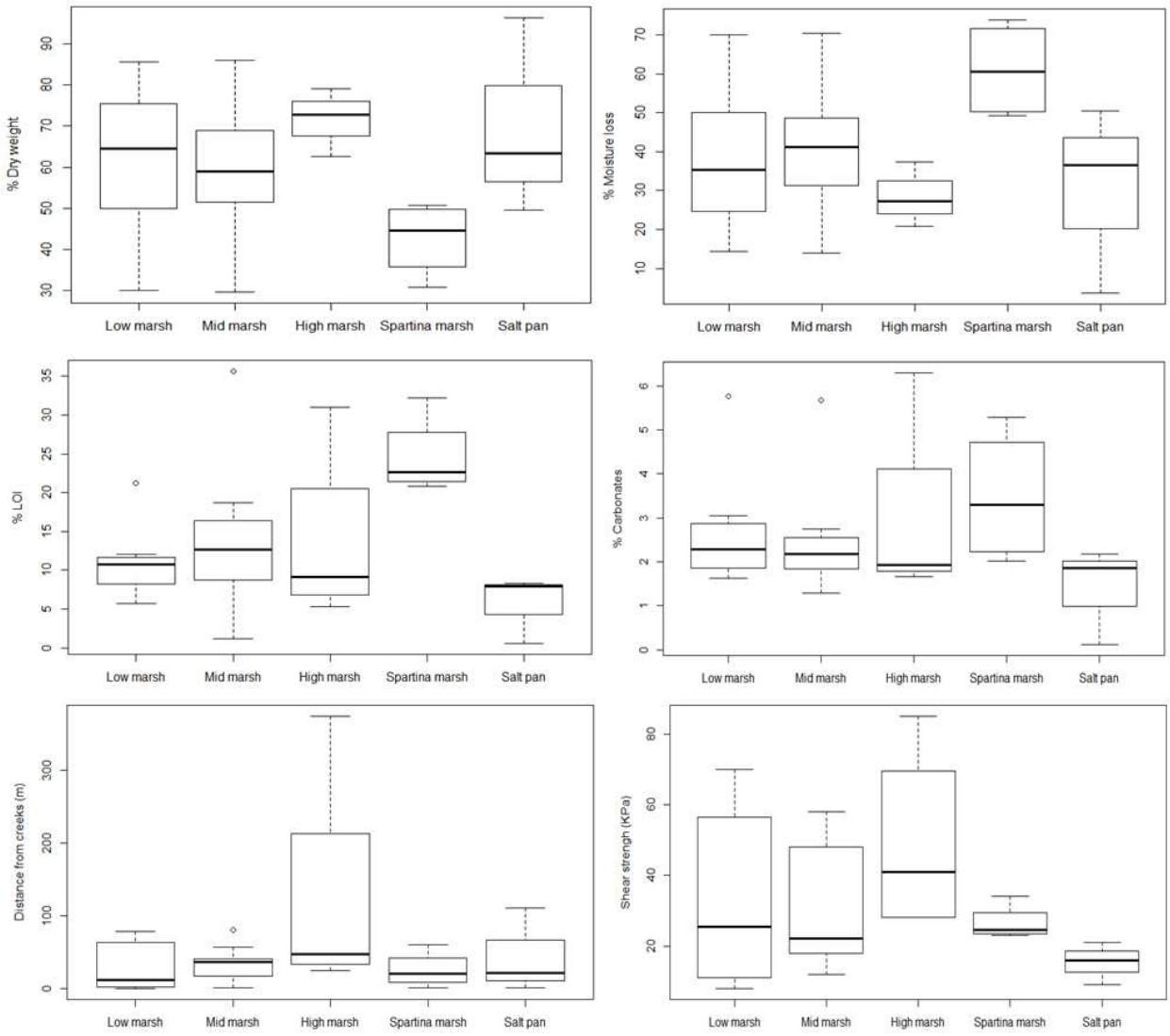

Figure 4.12 Environmental parameters box plots for each habitat type.

The results showed that the Spartina marsh has high values in parameter such as % moisture loss, % LOI and % carbonates, and low values for % dry weight and distance from creeks. In comparison with other habitat types, the Spartina marsh covered the highest values of the data set for % moisture loss (max. value = 74 %) and LOI (max. value = 32 %). Higher values in moisture loss and low dry weight state soils with higher content in clay and low infiltration capacity, showing the tolerance of this species to anoxic sediments. Across the mid-estuary, this habitat type was usually found near ponds and/or surrounding ponds. The high values in soil organic matter are possible due to root rhizome production and leaf litter deposition. The higher carbonate contents suggest higher shell content in the soil samples that could be related to gastropods found in salt ponds. For shear strength and distance from creeks, this habitat showed lower and

narrower range of values than high marsh for instance. This is showing once again the preference and tolerance of *Spartina densiflora* to anoxic/clay soils.

Finally, salt pan habitats showed low values for % LOI, % carbonates and shear strength and a narrower range than low and mid marsh. For example, this habitat reached the lowest value of the data set for % LOI (0.6 %) and carbonates (0.1%). Additionally, salt pans also reached the lowest value of the data set for moisture loss (3.7 %) and the highest value for % dry weight (~ 96 %). These results show that salt pan sediments have less organic content than other habitats and that sediment moisture can reach lower values as they are more susceptible to desiccation processes. These results were expected as the extreme salinity conditions in these habitats determine the low biocoenoses, limiting the presence of gastropods and vegetation. For example, very low plant density or bare soil is characteristic of this habitat type, and leaf litter was not usually found on the ground surface. Low values in moisture loss were also expected as these habitats are located in higher elevations where tidal floods are less frequent. Furthermore, evaporation reaches high values due to high temperatures and low precipitation during summer periods, and soil can dry up very quickly leaving a thin salt layer over the pans.

In order to investigate the ground elevation distribution per habitat, elevation values were extracted from the LiDAR-derived DEM for each quadrat location (Figure 4.13) and represented within the context of the tidal frame. The analysis of habitat types and the associated elevation values as expected shows a strong dependence of habitat presence on soil elevation in pioneers, low, mid and high marsh/Spartina marsh. However, salt pan elevations overlap with mid, high and saltmarsh habitats. The results revealed that saltmarsh vegetation in all habitats were found above mean high water neap (MHWN) except for low marsh vegetation and pioneers that were found below this tidal level. The mean ground elevation of high marsh and Spartina marsh was found between the high astronomical tide (HAT) and mean high water spring (MHWS), and the mean elevation of the mid- marsh and the salt pan between MHWS and mean high water (MHW). The salt pan soil elevation was expected to overlap other habitats because these pans are depressions over mature saltmarshes with lower elevation than the habitats surrounding them.

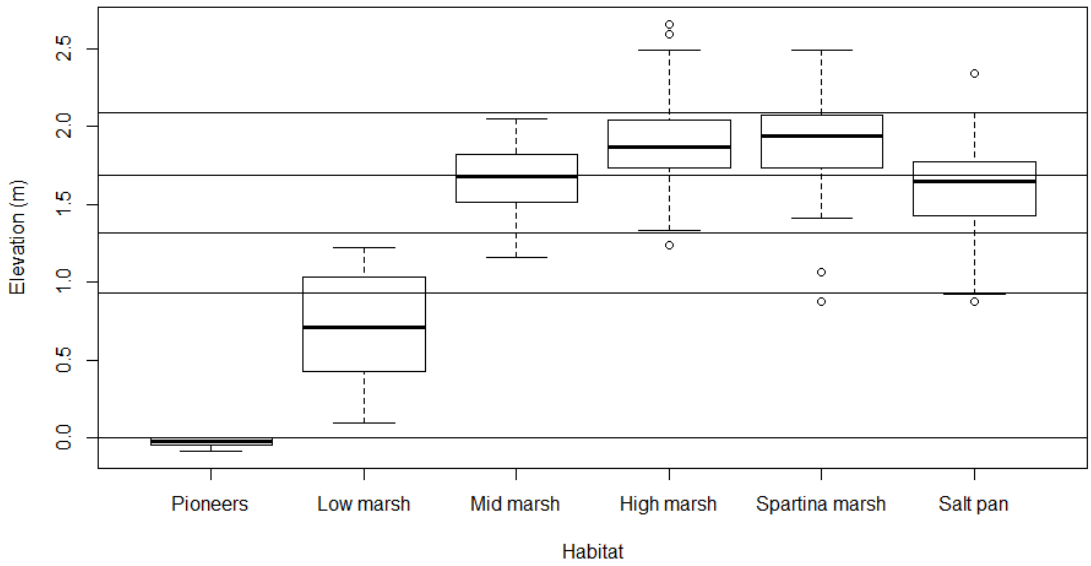

Figure 4.13 Ground elevation above mean sea level (m) of each habitat type in the Odiel saltmarshes. Elevation is referred to the Spanish vertical datum (zero in Alicante). Pioneers elevation (*Spartina maritima*) has been included

4.5. Short accretion rates

The results of the short accretion rates are shown in Table 4.3. These results revealed that the highest mean accretion rate (~15 cmy^{-1}) was found within vegetated tidal flat habitat (site H) and the lowest (~2 cmy^{-1}) was in the high marsh habitat (site L), located on the saltmarsh platform with 1 m height cliff at the edge of the platform (Table 4.3). Results were examined by comparing accretion rates across the main sampling period (spring/summer or autumn/winter, where accretion rates might reflect changes in productivity) and by habitat type (Figure 4.14). Accretion rates did not show differences between sampling period, but the rates by habitat type decrease from a maximum over the tidal flat, through the low marsh to a minimum in the mid-high marsh. Additionally, in order to check if there were significant differences between sampling period and between habitats, a Kruskal Wallis test was carried out. Results revealed that there is no significant difference in median accretion rate between sampling period, but did show significant differences between habitat (at the 95% level: p=0.04).

Table 4.3 Short accretion rates for each site; where D is dry density (cm^3y^{-1}), T total time surveyed, M mean accretion rates (cmy^{-1}), SD standard deviation Dshore distance from shore (m), and Z soil elevation (metres above the Spanish hydrographic zero).

Site	DD (cm^3y^{-1})	T (days)	Mean (cmy^{-1})	SD	DShore (m)	Z (m)	Habitat description
F	0.79	1012	5.65	2.62	1	1.34	High marsh (~0.5m height marsh cliff)
L	0.19	550	1.98	0.78	10	1.86	High marsh (~1m height marsh cliff)
N	0.41	679	2.74	0.28	30	1.22	Mid marsh (lagoon)
M	0.22	802	3.3	1.28	80	1.31	Mid marsh
A	0.67	1123	3.74	4.32	0.3	0.82	Low marsh (lagoon)
O	0.34	679	9.97	3.23	10	0.97	Low marsh (lagoon)
C	0.74	413	5.2	2.66	0.5	1.01	Low marsh (lagoon)
I	0.4	362	7.8	4.46	5	1.23	Low marsh
K	0.19	125			0.5	1.32	Low marsh
P	0.23	189	6.89	2.34	15	1.35	Low marsh
B	0.63	1003	7.23	5.98	0	0.45	Vegetated tidal flat (lagoon)
H	0.93	373	14.99	6.96	0	0.93	Vegetated tidal flat
D	0.49	1012	14.31	5.84	0	0.43	Tidal flat
E	0.85	1012	7.64	2.19	0	0.6	Tidal flat
G	0.75	610	5.93	3.2	0	0.73	Tidal flat
J	0.4	487	5.52	1.98	0	0.92	Tidal flat

Although habitat type influenced the accretion rates, the results showed that site features and location also influenced the rate values. Within the same habitat type differences were found depending on location and geomorphology. For example, those tiles located at saltmarsh sites facing a lagoon (e.g. site B; ~7 cmy^{-1}) showed smaller accretion rates than those facing channels (e.g. site H; ~15 cmy^{-1}). The accretion rates within the equivalent habitats decrease when the distance from shore increases. However, the distance from shore for sites within a lagoon does not seem to show any pattern within the same type of habitat. For example, distance from shore in site A is lower than in site O, but the accretion rate is higher in site O than in site A.

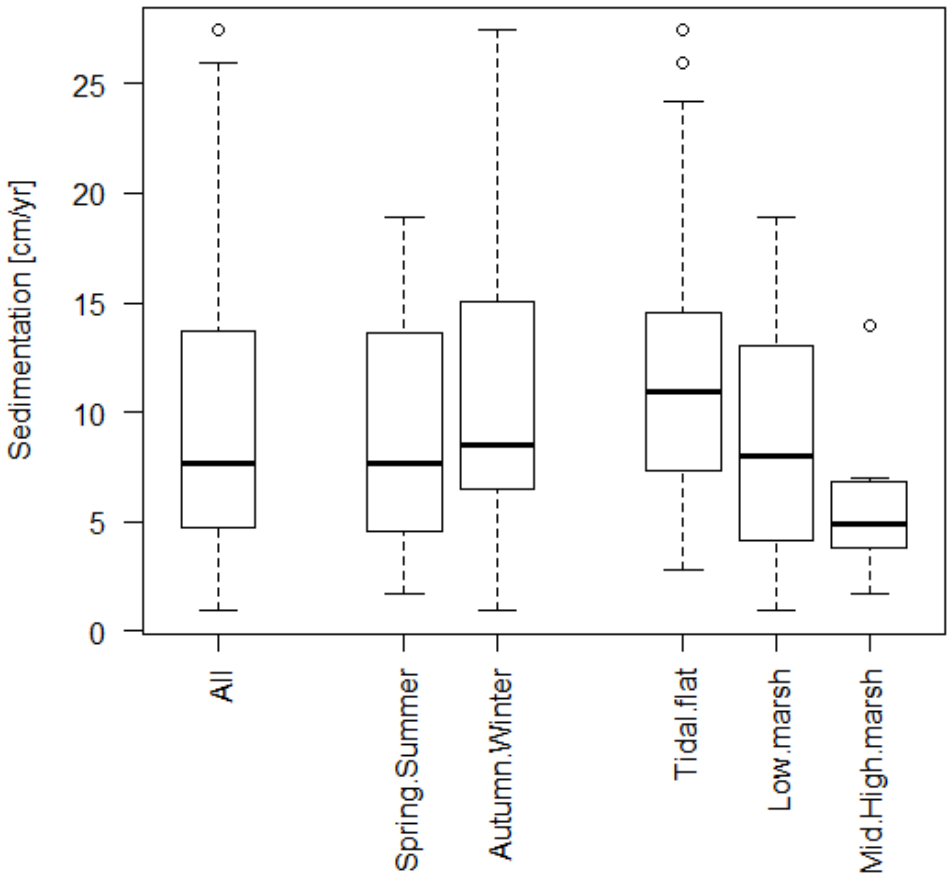

Figure 4.14 Accretion rates in the Odiel saltmarshes per habitat type and two main sampling (spring/summer and autumn/winter) seasons between 2012 and 1014.

4.6. Summary and discussion

Habitat zonation within the Odiel saltmarshes can be best described as comprising low marsh, salt pan, mid- marsh, high marsh and Spartina marsh. Although some of the species tend to be found in the same type of habitat within the saltmarsh, there are some species that do not follow any pattern and occupy a diverse range of elevations and situations within the saltmarsh. The species identified with these features are *A. portulacoides* (low, mid and high marsh) and *Sp. densiflora* (low, mid and high marsh; although the latter is the most frequent habitat where it has been found in large homogenous patches). *A. portulacoides* is a species with a great environmental adaptability (Cott *et al*., 2013) and its broad distribution within the Odiel saltmarshes is not surprising. *Sp. densiflora* has been previously identified as a species with broad tolerances to grow beyond its optimum environment (Snow & Vince, 1984) and has been shown to exhibit a wide ecological range, and thus it is expected to find it throughout the Odiel saltmarsh (Castillo *et al*., 2010). This species is originally from South America and it is spreading throughout the estuary and it is hybridising with the local *Spartina sp*. (*Sp. maritima*). It has been found everywhere in the Odiel saltmarsh but was spread mainly in homogeneous patches across the upper

estuary. However, it seems to be colonising the mid estuary slowly, reducing the plant diversity. The great environmental adaptability of these two species makes them more resilience to environmental changes and they could be used as key species to monitor changes over the time within the Odiel saltmarshes. The increase in their distribution within the estuary could be an indicator of environmental changes. In the case of the *Sp. densiflora* and its hybrid, the broad colonisation of low, mid and high marsh habitats throughout the estuary is already affecting the biodiversity of the Odiel saltmarshes (Nieva *et al.*, 2001), decreasing saltmarsh plant diversity. This colonisation is likely to be accelerated in a context of sea-level rise.

Another species that was found in different types of habitat was *S. ramossisima*, but it is not found everywhere like *A. portulacoides* and *S. densiflora*. In this study, it was found in low marsh habitat forming homogeneous meadows of this species or with *S. perennis* subsp*. perennis*, and in a higher topography within salt pans. Figueroa *et al.* (1987) reported the distribution of this plant species in the Odiel saltmarsh between MHW and LLW within low marsh habitats and in higher topography salt pans (where the tidal flood occurs during high tidal coefficient of high water or equinoctial tides). In this work, this species was also found in salt pan located between the MHWN and the HAT.

With regard to plant distribution based on elevation in the Odiel saltmarsh, other authors have reported similar findings to the results presented here. For example, Castellanos *et al.* (1994) indicated that lower elevations are dominated by *Sp. maritima* (pioneers) (although sometimes *Sp. densiflora* can also be found), and that higher elevations are usually occupied by shrubby species such as *A. macrostachyum*, *L. monopetalum* and *Su. vera*. They also indicated that in mature saltmarshes, the vegetation commonly found in the creek embankments are *Sp. densiflora*, *A. portulacoide* and *I. crithmodey*. Previously, Rubio & Figueroa (1983) had documented that the dominant species at intermediate levels (between mud flats and high marsh) are *S. perennis*, *A. portulacoides* and *Sp. densiflora*, and in salt pans, *S. ramossisima*, *S. fruticosa* and *A. macrostachyum* (Rubio & Figueroa, 1983). In this study, *S. fruticosa* for example was also found in high marsh habitats, but within transition zones (at higher locations) *A. macrostachyum* was found instead.

The role of elevation in determining distribution of plant communities depends on two factors: the tolerance of individual species to physical and chemical factors associated with submergence and the interactions (competition) between species with potentially overlapping tolerances (Castillo *et al.*, 2000). The vertical elevation of some halophytes seems to cover a relatively wide range (Silvestri *et al.*, 2005; Castillo *et al.*, 2000) as it has been identified in this work, and their distribution across the saltmarsh could also be related to biotic interactions (Ungar, 1998). Although the elevation range for different

habitats overlapped in the vertical, the average values presented differences (Figure 4.13) among high/Spartina, mid and low marsh, showing their tolerance to tidal submergence and salinity.

Previous work in the Odiel saltmarsh showed a correlation between salinity and elevation due to the high evaporation in Mediterranean climate, where salinity tends to increase with elevation (Castillo *et al*., 2000). For example, *Sp. maritima* is the species that showed more tolerance to tidal flooding and less tolerance to salinity. This species was found forming homogenous patches over unconsolidated mud flats at lower elevations and with *S. perennis* (subsp. *perennis*) at slightly higher elevations. On the other hand, *A. macrostachyum* within the high marsh was found in the highest elevation of the saltmarsh, showing high tolerance to high levels of salinity.

Another example of vegetation differences based on elevation (which determine tidal submergence and salinity tolerance) is the two sub-species of *S. perennis* (subsp. *alpini* and *perennis*). These species were found at different elevations overlapping only around half a metre in the vertical. The subspecies *perennis* was found at lower elevations primarily in low marsh habitats and the subspecies *alpini* at higher elevation covering mid marsh habitats.

Redondo-Gómez *et al.* (2007) carried out an experiment to explain the distribution of these two sub-species of *Salicornia perennis* (*perennis* and *alpini*) in the Odiel saltmarshes. Their results revealed that subsp. *perennis* was distributed at lower elevations and failure to survive above its limit was related to hypersalinity and water stress in summer; and that subsp. *alpini* was found at higher elevations and the failure to survive above its limit was associated with its intolerance of increasingly hypoxic (reducing sediments). These preferences may explain the growth differences of these two sub-species observed during the field work. For example, *S. perennis* subsp. *alpini* was usually found in a very dense canopy, forming a tortuous root system of roughly 20-30 cm above ground when it was found at lower elevations. Furthermore, the division of the tidal low-lying sediments at the south of the Saltes Island by the Juan Carlos I dike has created two lagoons at both sides of the dike with very different drainage conditions. Saltmarshes located at the west side of the dike have a slower drainage than those located to the east due to the sand accumulation retained in the west by the dike and also due to the slightly higher elevation in the west side (Castellanos *et al.*, 1999). These two subspecies could be key species to identify changes due to sea-level rise due to *S. perennis subsp. alpini* intolerance of increasingly hypoxic conditions as shown by Redondo-Gómez *et al.* (2007). The swap of the *subsp*. *alpini* by *subsp*. *perenni*, and the above-ground root system observed during the field work could be indicators of the current sea-level rise at the Odiel saltmarshes.

With regard to environmental factors, only a few seem to explain habitat type and the presence of different vegetation. For example, salt pans are characterised by low organic content possibly related to degraded organic matter, low and mid marsh by low/intermediate organic content mainly related to leaf litter and root density, and Spartina marsh by high values mainly related to root rhizome production and leaf litter deposition. However, high marsh habitats appear to have a broad range of values that could be related to its presence in sandy and muddy soils. With regard to moisture loss, the salt pan and high marsh habitats presented the lowest average values and Spartina marsh the highest value which is not surprising due to the broad ecological range of this species. However, mid and low marsh showed intermediate values, which is not expected for low marsh habitats. Low marsh habitats are usually characterised by high soil moisture, low dry weight and low shear strength (Ponnamperuma, 1972). These results could be explained by the presence of low marsh (*S. perennis* subesp. *perennis* and *A. portulacoildes*) in sandy sediments with higher porosity (less capability to retain water) and higher dry weight. It also should be noted that vegetated tidal flats (*S. maritima*) are classified by other authors as low marsh (Castellanos *et al.,* 1994) and here they have been considered as a separate habitat that it has not been included in this analysis due to the low number of samples collected.

Overall, Spartina marsh and salt pans were more different to the other habitat types. In the case of Spartina marsh, the unexpected narrower range values in some of the analysed parameters could be related to the fact that this plant species was not usually found in very sandy soils in the survey undertaken here. The similarities between low marsh and mid marsh are possibly related to the fact that these two types are dominated by the same species (*S. perennis*) but different subspecies.

Broadly, soil properties such as soil texture, aggregate stability, infiltration capacity, organic or chemical content and shear strength play an important role in erosion processes (Morgan, 2005). These properties largely define the resistance of a soil to be eroded by an erosion agent (e.g. water). Some authors (Watts *et al.* 2003; Teisson & Fritsch, 1988) have used shear strength to explain erosive events, suggesting that erosion occurs once a critical shear stress is exceeded (exerted by the moving fluids over a bed of sediments). Particularly in saltmarshes, the analysis of soil shear strength can provide some information to explain the mechanics of erosion processes in generally weak saltmarsh clays and cohesive sands (Boudreaux, 2009). The improvement of this parameter in areas with erosion problems could play an important role in preventing or reducing erosion in saltmarshes. Plant roots for example can improve soil shear strength, and can act to reinforce a mass of soil against shear failure (Zhang *et al*. 2009), increasing soil stability and surface erosion resistance (Nugent, 2011; De Baets *et al*. 2005).

The zonation in the Odiel saltmarshes is mainly driven by elevation and salinity. Soil texture (sandy to silt-clay) is possibly playing an important role in zonation as it has also been identified in other Mediterranean saltmarshes (Landi & Angiolini, 2015); although it has not been shown in the Odiel results here, it could be an interesting question to follow in future studies. For example, other authors (Ayyad & El-Ghareeb, 1982; Conesa *et al*., 2011; Ihm *et al*., 2007) reported that zonation in coastal saltmarsh vegetation near sand dunes are greatly influenced by texture and salinity gradients, as well as soil-water relationships and soil texture. Thus, although the Odiel saltmarshes is greatly influenced by elevation due to its meso-tidal regime, in higher elevations (apart from salinity) plant zonation could be related to soil texture. This has been clearly observed in *Limoniastrum monopetalum* that was found broadly in sandy soils.

Short-term accretion rates can greatly vary spatially and temporally in saltmarshes. Accretion rates across saltmarsh habitat types largely depend of the tidal flood duration, where sites that are more frequently flooded for longer tend to show higher rates (Reed, 1990; Cahoon *et al*., 1995; Leonard, 1997). Spatial and temporal variations of flooding frequency across the saltmarsh are subjected to seasonal or interannual sea level variations, influencing spatial and temporal deposition rates (Neubauer *et al.,* 2002). In the Odiel saltmarshes, a relationship between deposition rates and habitat type was observed, where lower elevation habitats showed higher deposition rates. Furthermore, deposition rates within the same habitat type showed a spatial pattern depending on site location and geomorphology. This behaviour makes sense as interior sites are usually further from the sediment sources (e.g. main creeks) as sediments are deposited while they are transported across the saltmarsh first through small creeks and then across the inner saltmarsh flat (French & Spencer, 1993; Leonard, 1997).

Previous work (Castellanos *et al*., 1998) undertaken in the Odiel saltmarshes showed similar relationship between accretion rates and habitat type, indicating dependence between accretion rates and saltmarsh geomorphology. Castellanos *et al*. (1998) in their work also showed a seasonal pattern. In this work, a significant dependence between deposition and sampling seasons was not observed. This could be caused by the fact that the sampling period in this work covered two seasons, while Castellanos *et al*. (1998) recorded accretion rates monthly. Also, the interannual variation of Mediterranean climates could be playing an important role when different years are compared.

Finally, it is important to bear in mind that the short accretion rates do not take into account shallow and deep subsidence, thus these data are not suitable for modelling the potential respond of saltmarshes due to sea-level marsh. For this purpose, long term accretion rates should be used as the rates presented by Morales *et al.* (2003) (Table 2.1).

However, the results obtained here are used qualitatively for investigating the sediment availability within the saltmarsh. The results showed that there are sediments available within the Odiel saltmarshes, enabling the vertical growth of these saltmarshes. For example, accretion rates in mud flats and vegetated mud flats located near main channels shown much higher values than other habitats and locations. This information is crucial in a context of sea-level rise, and it will help to assess potential impacts in Chapter 7.

5. Remotely sensed data for saltmarsh habitat classification

The aim of this chapter is to examine different remote sensing techniques for mapping saltmarsh habitats at fine scales (1:2,000), and the suitability of these techniques for monitoring saltmarsh habitats. Pixel-based and object-based image analyses are examined for mapping saltmarsh habitats accurately using a sub-site. The best approach is then used for mapping the entire Odiel saltmarshes. The final map is used for improving LiDAR-derived DEM in Chapter 6 and as one of the input layers for running landscape models in Chapter 7 (SLAMM).

5.1. Introduction

Image classification is one of the most common image processing techniques for translating remotely sensed data into useful geographical information such as vegetation or habitat maps. Image classification is defined as "*the aspect of image processing in which quantitative decisions are made on the basis of the data present in the image, grouping pixels or regions of the image into classes representing different ground-cover types*" (Rees, 1999). Classifying remotely sensed data into a thematic map is challenging because the classification process may be affected by many factors such as the complexity of the landscape, characteristics of the remotely sensed data, image processing and classification approaches (Lu & Weng, 2007). In saltmarshes, accurately mapping detailed features within saltmarshes from remotely sensed data is an even greater challenge due to the low spectral contrast between plant species and the small scale of vegetation patterns. These are well recognised as the main limitations in saltmarsh mapping (e.g. Silva *et al.*, 2008; Adam *et al.*, 2009; Kelly *et al.*, 2011) that complicate the classification process more than in other coastal or terrestrial environments.

The selection of a suitable classification approach for a specific study can be difficult. Generally, this is so because many factors such as data characteristics (e.g. spatial resolution and source), classification technique and availability of classification software play an important role in the classification results (Lu and Weng, 2007), and the use of different data or classifiers may result in different outputs. In addition, a wide range of classification approaches now exists, which may complicate the selection process further. Rees (1999), Tso and Mather (2009) and Horning *et al.* (2010) review techniques and classifiers, and in general, approaches can be grouped by specific criteria (Table 5.1) such as type of pixel information, whether training areas are used or not (i.e. supervised or unsupervised), or whether parameters are used or not.

Saltmarsh classifications reported in the literature fall into four main categories of image classification (Table 5.2). Sub-pixel based analysis (SPBA) (e.g. He *et al.*, 2010) has

been applied to satellite imagery such as LandSat in order to capture information within the pixel (e.g. water, mud and vegetation). Application of pixel based image analysis (PBIA) is more common and diverse, and is used at several spatial scales due to the different nature of remotely sensed data (e.g. aerial photography and very high resolution satellite images). Studies at habitat (e.g. Thomson *et al*., 2004; Chust *et al*., 2008) and plant species level (e.g. Belluco *et al*., 2006) are common. Use of object based image analysis (OBIA) is rather more limited and has been applied to specific saltmarsh features (e.g. Kim *et al*., 2010), a few plant species and identification of mud (Ouyand *et al.*, 2011).

Table 5.1 Types of image classification approaches based on different criteria. It should be noted that the inclusion in one category does not exclude a classification to be grouped into other categories. [Source: modified from Lu and Weng, 2007]

Criteria	Categories	Characteristics	Example of classifiers
Whether training samples are used or not	Supervised classification	Land cover classes are defined. Sufficient reference data are available and used as training samples. The signatures generated from the training samples are then used to train the classifier to classify the spectral data into a thematic map.	Maximum likelihood, Minimum distance, artificial Neural network, decision tree classifier.
	Unsupervised classification	Clustering-based algorithms are used to partition the spectral image into a number of spectral classes based on the statistical information inherent in the image. No prior definitions of the classes are used. The analyst is responsible for labelling and merging the spectral classes into meaningful classes.	ISODATA, K-means Clustering algorithm.
Whether parameters such as mean vector and covariance matrix are used or not	Parametric classifiers	Gaussian distribution is assumed. The parameters (e.g. mean vector and covariance matrix) are often generated from training samples. When landscape is complex, parametric classifiers often produce 'noisy' results. Another major drawback is that it is difficult to integrate ancillary data, spatial and contextual attributes, and non-statistical information into a classification procedure.	Maximum likelihood, linear discriminant analysis.
	Non-parametric classifiers	No assumption about the data is required. Non-parametric classifiers do not employ statistical parameters to calculate class separation and are especially suitable for incorporation of non-remote-sensing data into a classification procedure.	Artificial neural network, decision tree classifier, evidential reasoning, support vector machine, expert system.
Which kind of pixel information is used	Per-pixel approach	Traditional classifiers typically develop a signature by combining the spectra of all training-set pixels from a given feature. The resulting signature contains the contributions of all materials present in the training-set pixels, ignoring the mixed pixel problems.	Most of the classifiers, such as maximum likelihood, minimum distance, artificial neural network, decision tree, and support vector machine.
	Sub-pixel approach	The spectral value of each pixel is assumed to be a linear or non-linear combination of defined pure materials (or endmembers), providing proportional membership of each pixel to each endmember.	Fuzzy-set classifiers, subpixel classifier, spectral mixture analysis.
	Object-oriented approach	Image segmentation merges pixels into objects and classification is conducted based on the objects, instead of an individual pixel. No GIS vector data are used.	Most of the classifiers used in per-pixel approach (to see ecognition for more details).
	Per-field approach	GIS plays an important role in per-field classification, integrating raster and vector data in a classification.	GIS-based classification approaches.

SPBA is most appropriate for middle spatial resolution data (between 10 and 30 m) such as LandSat imagery. This approach has been used for mapping features within the marshes and plant species. For example, He *et al.* (2010) explored the feasibly of spectral mixture analysis of LandSat TM for monitoring estuarine vegetation. They conclude that this technique with appropriate endmembers (or pure material) had relatively

satisfactory accuracy for monitoring vegetation. However, this technique shows some limitations because the endmember selection is very complicated in mosaic vegetation structures of saltmarsh environments (Silvestri *et al.,* 2003).

The more widely applicable PBIA method allows use of different data types, and low to high spatial resolution. Yang and Liu (2005) argue that spectral confusion is the major limitation for reaching adequate accuracy using this approach when medium spatial resolution data and broad spectral bands are used in mapping saltmarshes. The majority of the recent studies reviewed in the literature used high spatial resolution images for performing PBIA (Table 5.2), which it is consistent with Yang's arguments. In addition, Beluco *et al*. (2006) state that high spatial resolution data benefit the classification results for two main reasons: i) smaller pixel size increases the number of pixels per each training area, and ii) heterogeneity within the pixel is reduced. This means that there are more pixels available for training the classifier, and the distinction between classes may improve.

Table 5.2 Summary of the main classification approaches used in saltmarsh mapping

Categories	**Classifier**	**Classified features**	**Data used**	**References**
Pixel based Supervised classification	Maximum likelihood	Vegetation, water, mud	LandSat; Photo	Ramsey & Laine (2013)
		Vegetation zones, sand, mud and stone	CASI; CASI+Lidar	Thomson *et al.* (2004)
		Five plant sp. and soil	ROSIS,CASI, MIVIS and QuickBird	Brown (2004) Belluco *et al.* (2006)
		Unvegetated/vegetated	Photo	Van der Wal *et al.* (2008)
		Coastal land-cover	Photo+Lidar	Chust *et al.*(2008)
		Plant communities	Lidar	Collin *et al.*(2010)
	Spectral angle mapper	Four plant species and soil	ROSIS,CASI, MIVIS, QuickBird	Marani *et al.* (2006) Belluco *et al.* (2006)
	Neural network	Vegetation zones, mud and water	CASI	Brown (2004)
Pixel based Unsupervised classification	K-means	Four plant species and soil	ROSIS,CASI, MIVIS, QuickBird	Belluco *et al.* (2006)
Object based	Several classifiers available in eCognition	Two plant species, mud	Landsat	Hurd *et al*. (2006)
		Vegetation zones	Landsat	Tian *et al*. (2008)
		Vegetation, mud ,water	Photo	Kim *et al*. (2011)
		Two plant species, mud	QuickBird	Ouyang *et al.* (2011)
		Segmentation		Moffett & Gorelick (2013)
Sub-pixel based	Spectral mixed analysis	Few plant species, mud and water	Landsat	He *et al.* (2010)

PBIA is increasingly used to map saltmarshes, usually for identifying whole wetlands from other land-cover classes (e.g. Chust *et al.*, 2008; Ramsey & Laine, 2013) and for identifying features or plant zonation within the saltmarsh (e.g. Belluco *et al.*, 2006; Marani *et al.*, 2006). Nevertheless, the studies that attempt to classify features within the saltmarsh through supervised techniques seem to be applied to relatively small study

sites. This is so because the classifiers are very sensitive to the quality and quantity of training areas selected, and in small sites it is easier to gather representative and spatially distributed ground data for selecting suitable training areas (Thomson *et al.,* 2004).

OBIA has been tested with LandSat images (Hurd *et al*., 2006; Tian *et al.,* 2008), however high spatial resolution imagery has been used more recently to successfully distinguish small objects within the saltmarshes (Moffett & Gorelick, 2013) such as ponds, small creeks and vegetation patches. This is an emerging research area; published examples are few and quite recent, focused on evaluating segmentation parameters and environment-specific methods (Kim *et al.,* 2011; Moffett & Gorelick, 2013), which at present show little consensus within saltmarsh applications. The low spectral contrast of tidal saltmarsh vegetation has limited the OBIA-studies to distinguish between water, mud and water combined (Hurd *et al*., 2006; Kim *et al.,* 2011) and few plant species (Ouyang *et al*., 2011). However, as it has been reported that the low contrast of vegetation may depend on the specific nature and structure of local vegetation and that differentiation between species can therefore vary geographically; i.e. the rules defining specific species and habitats likely vary from saltmarsh to saltmarsh.

Regardless of the classification method, some authors (Gilmore *et al.,* 2008; Chust *et al.,* 2008; Arroyo *et al.,* 2010) have included elevation data within the classification process for distinguishing species of low spectral contrast located at different elevation within the marsh due to the complications for separating saltmarsh plant species or communities,. This is possible because there is a tight relationship between species and elevation that underpins zonation and habitat patches within saltmarsh environments (Sanchez *et al*., 1996; Bockelmann *et al*., 2002; Silvestri *et al*., 2005). Elevation data has been used to improve the classification process of both PBIA and OBIA approaches.

Overall, the success in saltmarsh mapping strongly depends on the particular characteristics of each site, including vegetation species present at each site. Thus, it is important to explore different approaches for a particular site in order to maximise the possibilities of selecting the most suitable approach for that site. Here, two image classification approaches were analysed using a representative smaller site (the Saltes Island). Then, the best approach was applied to classify saltmarsh habitats across the entire study area. The results obtained were combined with the vector information digitised in Chapter 3 to map the entire Odiel saltmarshes protected area. The resulting classification is a primary input describing the estuarine environment in the SLAMM model applied in Chapter 7 to examine the impact of future change in sea level.

5.2. Class definition and preliminary data processing

The analyses undertaken focus on the saltmarsh environment and thus all the defined classes for image classification were orientated towards saltmarsh habitats. During the class selection process, it was also important to consider the limitations of the method, and available sources for distinguishing among the classes. The class selection is not an easy task, and it can influence the degree of successful classification results later on. The saltmarsh species-assemblages used to define the habitat classes were previously derived from field-based vegetation survey data (Chapter 4). The vegetated saltmarsh environment was thus represented by low marsh, salt pans, mid marsh, high marsh and *Spartina* (high) marsh.

However, some of these species-assemblages are composed by similar species making difficult their spectral recognition as a single class. A spectral separability analysis was applied in ENVI (v 4.6) using training areas and the 2013 aerial photography (red, green, blue and IR bands) before performing the supervised classifications. After testing the separability among classes, some of the previously defined classes were merged. *Mid marsh* and *high marsh* were spectrally confused due to both are characterised by tall *salicornia* species (*S. fruticosa* and *S. perennis subsp. perennis*); and *low marsh* and (vegetated) salt pan were also confused due to both are characterised by short *Salicornia* species (*S. perennis* subesp. *perennis* and *S. ramossisima*). Thus, *mid marsh* and *high marsh* were merged into *Salicornia marsh* as they mainly contained *Salicornia sp.* with similar height/structure; and *low marsh* and (vegetated) salt pan were combined into *low marsh* class. However, some of the classes that showed spectral confusion were kept when these classes occurred at different topographic elevations and were form by different species characterised by different vegetation height such as *Spartina marsh* and *low marsh*. The following 5 classes were established for performing supervised classifications (Figure 5.1):

- *Low marsh*: *Salicornia perennis perennis*, *Salicornia ramossisima* and *Atriplex portulacoide.* This class usually have a darker colour than *Salicornia marsh* due to this vegetation is flooded during the high tide and the vegetation is usually covered by thin layer of mud
- *Salicornia marsh*: >90% of *Salicornia fruticosa* and *Salicornia perennis subsp. alpini,* and <10 % of other species such as *Arthrocnemum macrostachyum, Atriplex portulacoide, Limoniastrum monopetalum* or *Spartina densiflora*
- *Spartina marsh*: >90% *Spartina densiflora and* <10% of other species such as *Salicornia fruticosa, Atriplex portulacoide* and *Arthrocnemum macrostachyum.*
- *Mud*: bare mud
- *Water*: ponds

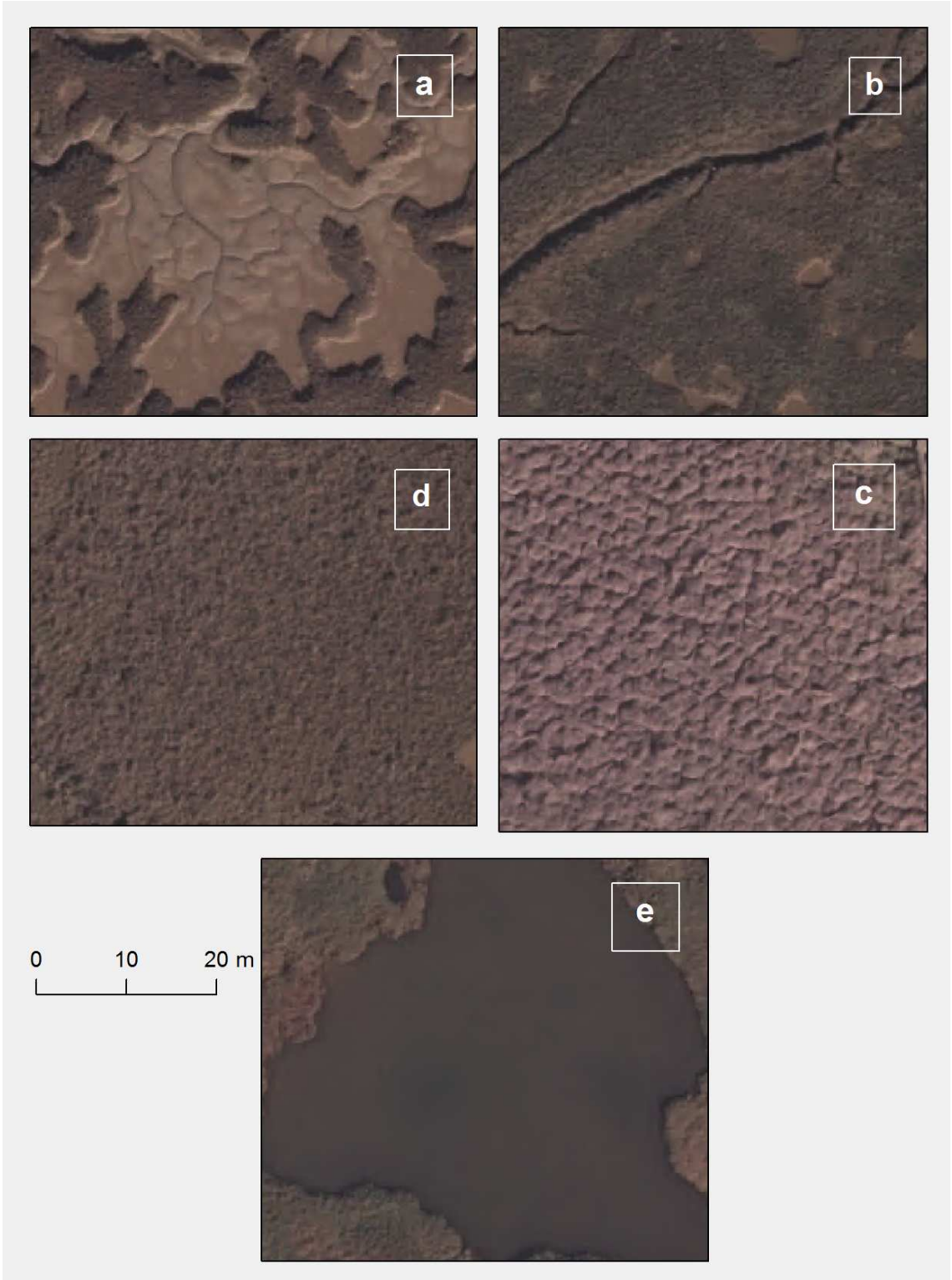

Figure 5.1 View of the 5 classes defined from the 2013 aerial photography (0.16 cm resolution), where each letter refers to the following class: (a) Mud, (b) Low marsh, (c) Salicornia marsh, (d) Spartina marsh, (e) Water

5.3. Training and validation areas sampling design for image classification

Training areas and validation areas are a very important part of the image classification process. Training areas enable supervised classifications to be undertaken, whilst validation areas are used to assess the results of the classification. The quality of these areas, as well as the algorithm used to perform the classification, determine the overall classification accuracy. Hence the selection of these areas was planned thoroughly before undertaking field surveys.

Training areas should be located on those places where homogeneous samples of known cover class are found (Tso & Mather, 2009). Training areas are ground-controlled data or information regarding the nature of study area and should accommodate the intra-class variability within the study site. Thus, the selection of these areas was based on the diversity of each class during fieldwork undertaken in September 2011 and 2012. However, in order to prevent positive biases for estimating the classification accuracy, training areas of each class must be different and relatively far apart from the validation areas (Belluco *et al*., 2006). For example, if both areas are neighbours, the probability of similarity is higher, resulting in overestimates of the accuracy. The number of training areas collected ranged from 40 to 60 areas (polygons) per class.

Validation areas are ground-truth data that have been collected randomly for assessing the results of the classification. A stratified sample method was performed for validating selected areas by class and generating random points within a pre-defined classified layer (using the 2003 Andalusian vegetation map; see section 2.3.1). This was undertaken in ArcGIS - ArcToolbox 10.2 (*Management tool – Feature class – Create random points*). The sample size is very important because it provides information about the classification accuracy (confusion matrix) and assists in validating classification results. Therefore, the sample size should be representative of the population, and it should give enough random information for training the statistical classifiers. Based on similar studies (Canovas, 2012), a minimum number of 20 validation areas per class should be considered.

The training and validation areas were digitised over the 2013 aerial photography in ArcGIS 10.2 at 1:2.500 scales. The training areas were photo-interpreted using information from field surveys, a geo-referenced photograph catalogue (Figure 5.2) generated for this work, elevation data and the pre-existing vegetation map (2003). In the case of validation areas, the ground-truth data (field-based vegetation survey) was used. The GPS points were converted into 'shapefiles' containing the ground-truth data information, then this information was used to digitise homogeneous polygons over the 2013 aerial photography.

Figure 5.2 Sites of the ground-based photography integrated in the photo catalogue.

5.4. Method

In order to explore the best classification approach, PBIA and OBIA were performed over the 2013 aerial photography using the four spectral bands (Blue, Green, Red and IR), and then these four bands plus LiDAR-derived elevation data (DSM). In order to reduce processing time and to explore the different classifications and data, a sub-site was selected: the Saltes Island a central part of the Odiel-Tinto estuary with an area of 665 ha approximately (Figure 5.3). Due to the low spectral contrast among saltmarsh classes, the main channels and non-saltmarsh habitat were masked in order to avoid spectral noise and focus on the saltmarsh-specific habitats. Based on the results obtained in the OBIA and PBIA classifications, the best approach was then applied to the saltmarsh environments over the entire study area using a saltmarsh mask Figure 5.4.

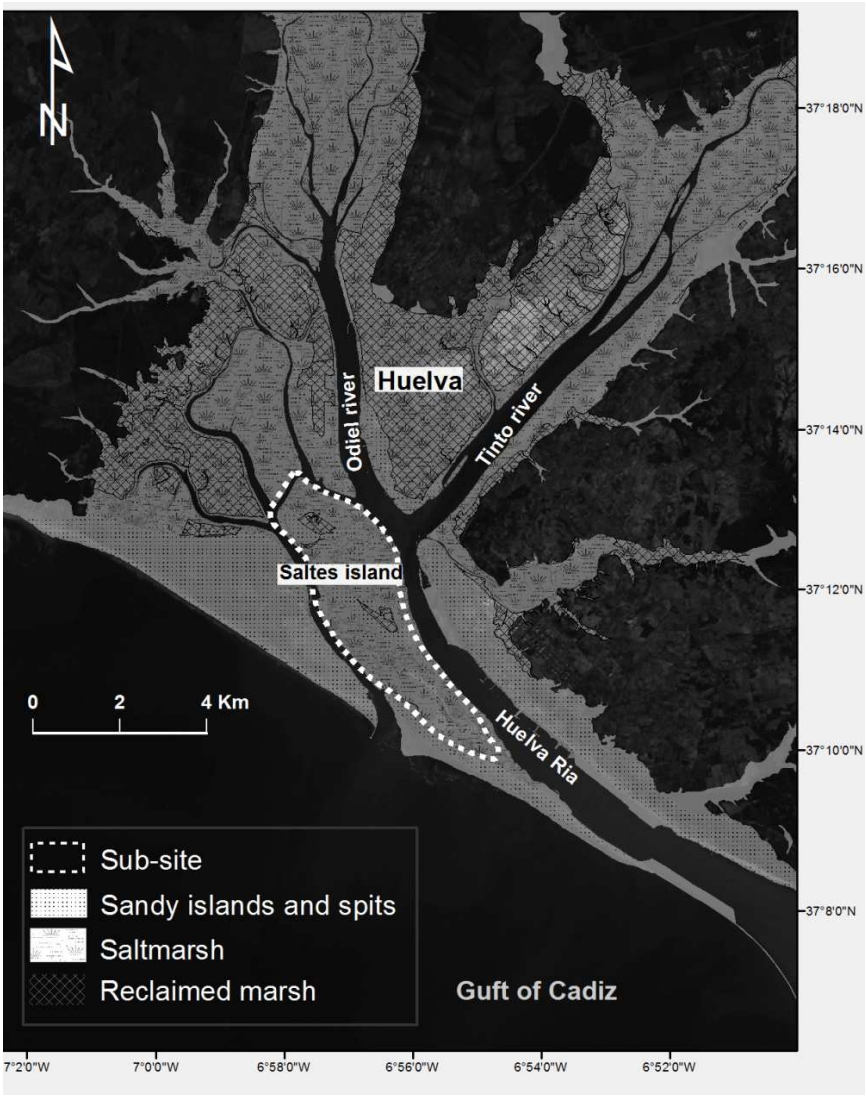

Figure 5.3 Location of the sub-site for performing different image analysis approaches: the Saltes Island (The Odiel saltmarshes, SW Spain)

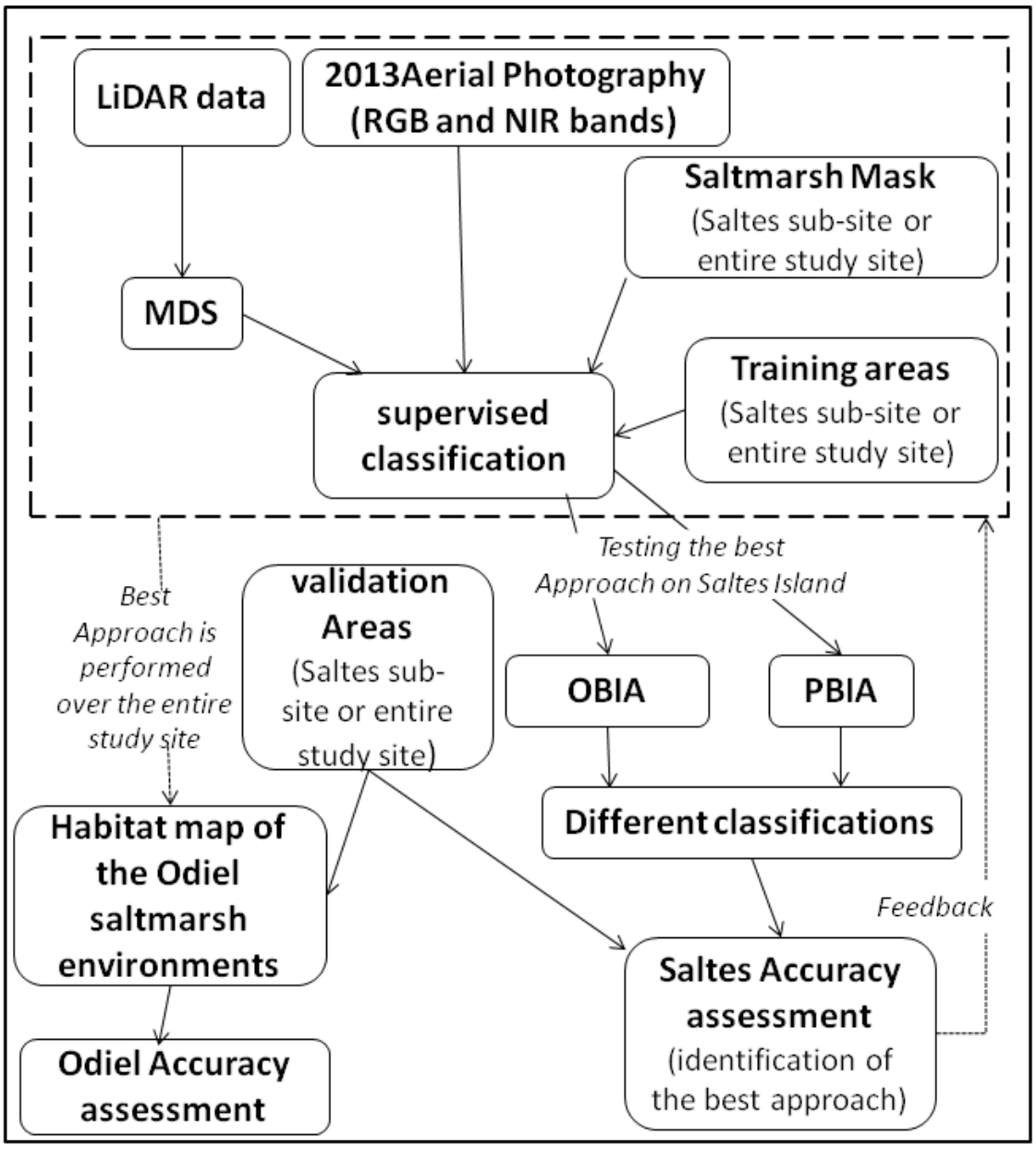

Figure 5.4 Workflow diagram of the method used

5.4.1. Pixel Based Image Analysis (PBIA)

Maximum likelihood (ML) algorithm was applied to perform two supervised classifications using ENVI (v 4.6): one with only four spectral bands (Blue, Green, Red and Infrared); and the other one with four spectral bands plus elevation data (DEM). This algorithm performs statistical supervised pattern recognition calculating the probability of a pixel belonging to each predefined class. In this approach, a pixel is associated to the class to which the probability is the highest and it is based on Bayesian probability (for more details see: Tso and Mather (2009: 58)). The post-classification was based on majority/minority analysis implemented in ENVI, where a kernel matrix with size 3x3 was

used. The calibration of the classifier was performed through training areas digitised in ArcMap (ArcGIS 10.2).

5.4.2.Object Based Image Analysis (OBIA)

5.4.2.1. Image segmentation

The segmentation process was performed in two main steps. The first step was to apply the Multi-Resolution Segmentation (MRS) algorithm integrated in eCognition Developer software (v 8.7) (Baatz & Schäpe, 2000; Benz *et al.,* 2004; Moffett & Gorelick, 2013) to the 2013 aerial photography. As described in Benz *et al.* (2004), MRS is a region-growing method that groups randomly selected pixels in a scene into objects by automated merger decisions based on a homogeneity criterion and scale parameter. The homogeneity criterion of the MRS algorithm measures how homogeneous or heterogeneous a pixel (or object) is based on a combination of colour and shape properties of both the initial and the potential resulting image object. The segmentation process is based on the following settings that must be defined by the user:

- **Spectral value (or colour) versus shape heterogeneity weights**: this controls the importance of the spectral and shape information within the segmentation (from 0 to 1, it must be specified how much weight is given to each property, which must then sum to 1). The colour homogeneity is based on the standard deviation of spectral bands (which can also be also weighted). In this analysis, it was given double weight to the NIR band than to the other bands. The shape homogeneity is based on the deviation of a compact or smooth shape.
- **Smoothness versus compactness weights**: this controls the object shape information and determines how much the object shape is spatially compact versus spectrally homogeneous and less compact (Moffett & Gorelick, 2013), which also must sum to 1.
- **Scale parameter**: this is the threshold that limits overall object colour and shape complexity. Higher scale parameters means less restriction for merging pixels (or objects) and therefore the resulting object will be bigger, while smaller scales will result in smaller resulting objects.

All this information is computed to determine whether to merge a pair of adjacent pixels (or objects) or not. For example, a pair of objects is merged when the shape and spectral heterogeneity does not exceed the defined scale parameter (Moffett & Gorelick, 2013). Here, different scale parameters were previously applied to a selected subset in order to investigate the optimal parameter. The optimal scale parameter for this analysis was 10. This scale parameter lets us distinguish small creeks and ponds at object level, which are the smallest objects to be recognised in the image.

In order to merge partially small objects previously created, the second step was to perform the same segmentation process to the brightest objects in the scene (which are related to vegetation patches and salt pans that usually form bigger patches than small creeks and ponds). The brightest objects were merged using a larger scale parameter (15).

5.4.2.2. Image classification

Image classification is then applied to the objects previously created. The K-nearest neighbour (KNN) classifier (Kim *et al.,* 2011) was the algorithm used for performing the classification. First, the classifier was trained with training points obtained by following the below steps (for avoiding user intervention in the object creation):

1. Training areas in shapefile format (ArcGIS) used in PBIA were imported to eCognition and used in a intial segmentation with the parameters specified above and specifying that the resulting objects respect the training area boundary. This means that one training area could be divided into smaller objects, but the outside border will remain unchanged in the new objects.
2. The new training areas (now forming smaller polygons) are exported into ArcMap, where the polygon layer is converted into a layer of points, where every point is located within a polygon (object) and contains class information (code and name).
3. The point layer is then used for training the resulting objects from the segmentation process in the OBIA (this time without specifying to use the training areas layer in the segmentation process).

5.4.3. Accuracy assessment

The accuracy assessment of the image classification is evaluated through visual comparisons with information obtained from field campaigns and *confusion matrices* using validation areas. The evaluation process used mostly direct information on the spatial vegetation distribution obtained in Chapter 4, although the pre-existing vegetation map (2003) and information reviewed in from the literature (Castellanos *et al*., 1994) were used to support this field data. Here, a coefficient agreement for nominal scales, called the Kappa index (Cohen, 1960), was also calculated.

5.5. Exploring the best approach for mapping saltmarsh habitats

The results of PBIA and OBIA obtained using i) the four spectral bands and ii) the four spectral bands plus the DEM layer are shown in Figure 5.5 and the confusion matrices in Table 5.3. Overall, the classifications using OBIA presented better results than PBIA. The overall accuracy was 54.5 % for PBIA and 70.1 % for OBIA. Additionally, there were

significant increases in classification accuracy (Table 5.3) when the additional DEM layer was added to the classifier used in PBIA (71.8 %) and OBIA (83.1 %).

The gain in accuracy achieved using the DEM was greater for PBIA (+17 % corresponds to a 32 % improvement) than OBIA (+13 % relates to an 18 % improvement). Part of the increase in overall accuracy in PBIA and OBIA when the DEM layer was added appears to be due to an increase in discrimination between the *low marsh* and S*partina marsh*, and *Salicornia marsh* and *Spartina marsh* (Table 5.3). For example, the *Spartina marsh* accuracy increased from 5.7 % to 67.1 % in PBIA (Table 5.3; A and B) and from 31.7 % to 74.1 % in OBIA (Table 5.3; C and D) when the DEM layer was added. The accuracy of this class has increased due to a reduction in the areas of *low marsh* and *Salicornia marsh* misclassified as *Spartina marsh*. The accuracy (in both PBIA and OBIA) was not affected for the *water* class when the DEM layer was used, and it was slightly affected for classes such as *mud*, *low marsh* and *Salicornia marsh*. Overall, the classification using OBIA was more accurate than the classification using PBIA. All classes except *mud* were better classified using OBIA than PBIA. Thus, OBIA including DEM layer was considered the best approach for mapping the entire study area.

Figure 5.5 Image classification of Saltes Island using different data and image analysis techniques: (A) Pixel-based image analysis with only spectral data; (B) Pixel-based image analysis adding elevation data (DEM); (C) Object-based image analysis with only spectral data; and (D) Object-based image analysis adding elevation data. [B, C and D results overleaf]. Note: only intertidal and saltmarsh environments are considered here, and all other habitats have been masked

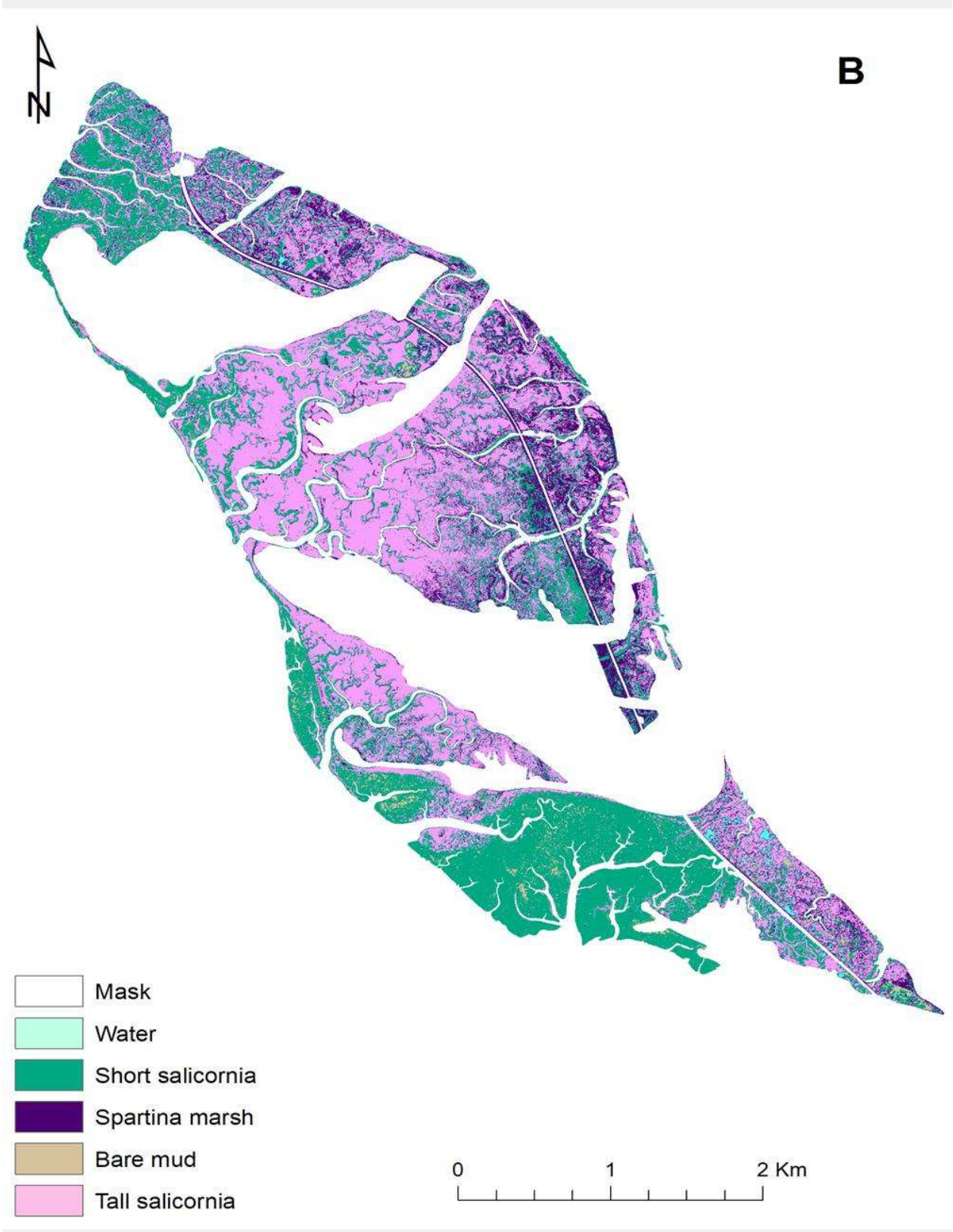

Figure 5.5 cont. Image classification of Saltes Island using different data and image analysis techniques: (A) Pixel-based image analysis with only spectral data; (B) Pixel-based image analysis adding elevation data (DEM); (C) Object-based image analysis with only spectral data; and (D) Object-based image analysis adding elevation data.. Note: only intertidal and saltmarsh environments are considered here, and all other habitats have been masked

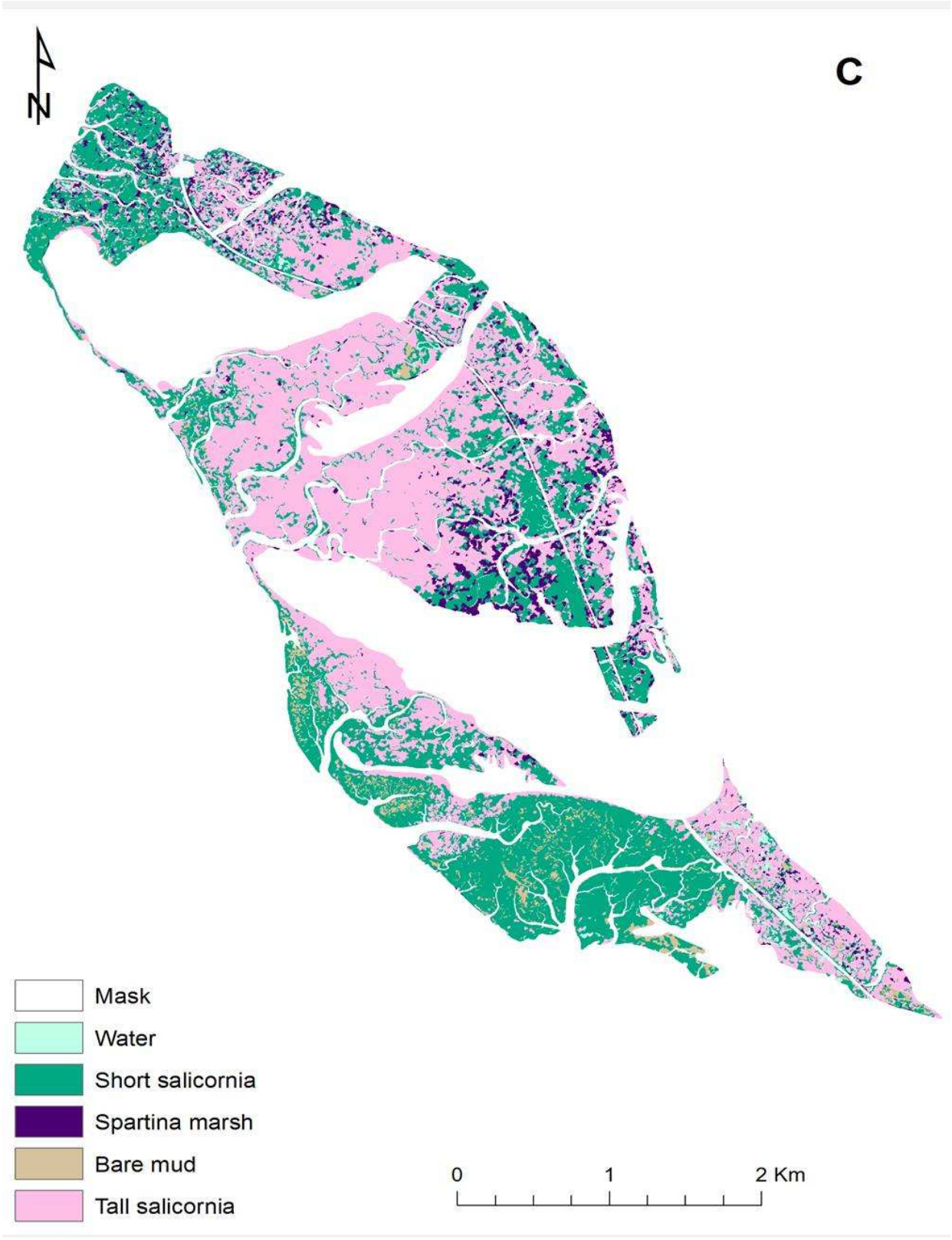

Figure 5.5 cont. Image classification of Saltes Island using different data and image analysis techniques: (A) Pixel-based image analysis with only spectral data; (B) Pixel-based image analysis adding elevation data (DEM); (C) Object-based image analysis with only spectral data; and (D) Object-based image analysis adding elevation data.. Note: only intertidal and saltmarsh environments are considered here, and all other habitats have been masked

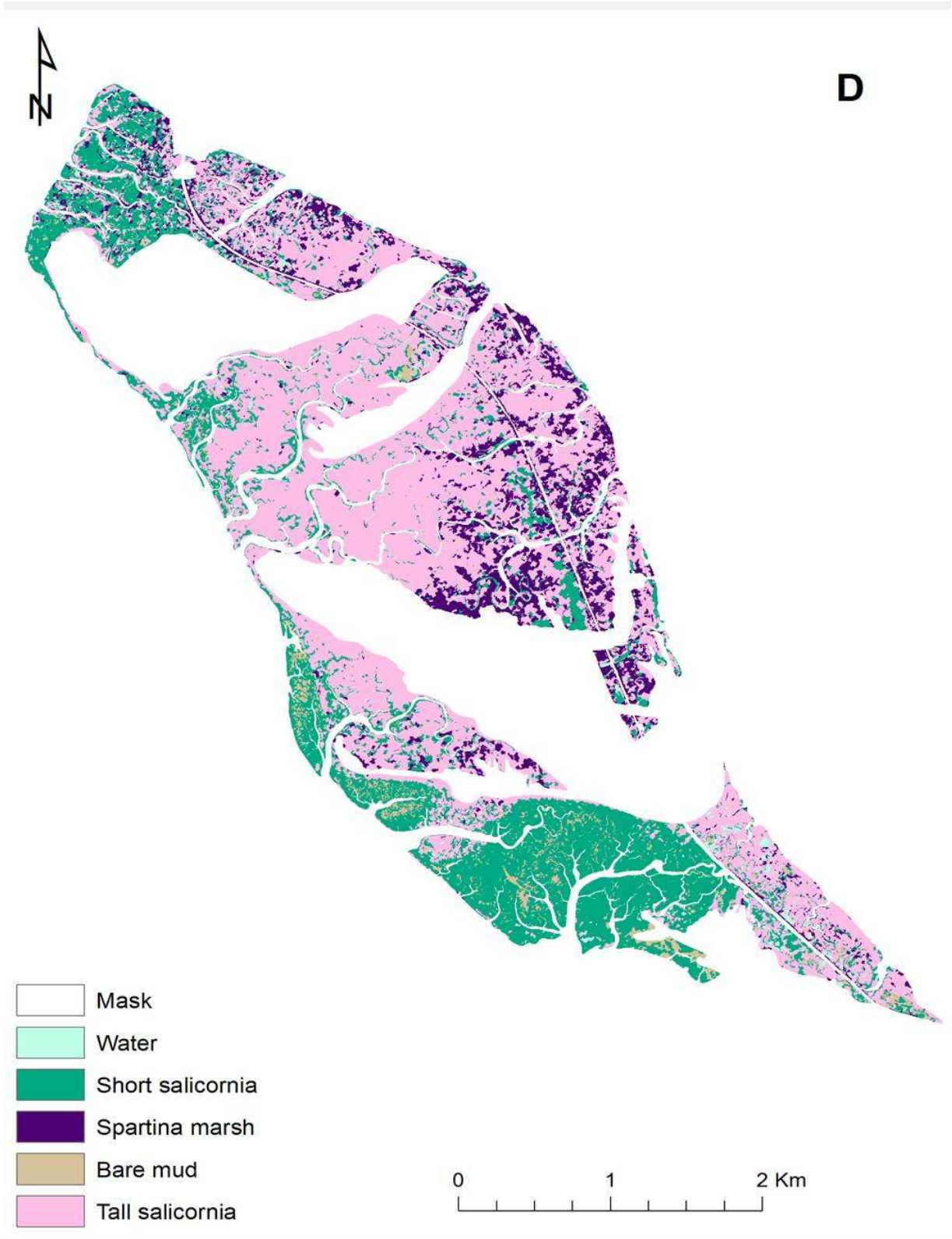

Figure 5.5 cont. Image classification of Saltes Island using different data and image analysis techniques: (A) Pixel-based image analysis with only spectral data; (B) Pixel-based image analysis adding elevation data (DEM); (C) Object-based image analysis with only spectral data; and (D) Object-based image analysis adding elevation data.. Note: only intertidal and saltmarsh environments are considered here, and all other habitats have been masked

Table 5.3 Confusion matrices and kappa indices of different classification approaches and data at the Saltes Island (2013). The values in the confusion matrices are in percentage and represent the producer accuracy (which highlights how well the map objects have been classified)

(A) Pixel - based classification: multispectral data					
Classif/Ground data	Water	Mud	Low marsh	Salic. marsh	Spart. marsh
Water	**92.3**	0	0	0	0
Mud	0	**87.5**	0	0	0
Low marsh	7.7	12.5	**89.6**	36.5	52.9
Salic. marsh	0	0	10.3	**61.2**	41.4
Spart. marsh	0	0	0	2.4	**5.7**
Total accuracy (%)= 54.5				Kappa Index = 0.49	

(B) Pixel - based classification: multispectral data + DEM					
Classif/Ground data	Water	Mud	Low marsh	Salic. marsh	Spart. marsh
Water	**92.3**	0	0	0	0
Mud	3.8	**88.9**	0	0	0
Low marsh	0	11.1	**96.5**	22.3	13.2
Salic.marsh	0	0	3.4	**69.6**	19.8
Spart. marsh	3.8	0	0	12.5	**67.0**
Total accuracy (%)= 71.8				Kappa Index = 0.65	

(C) Object - based classification: multispectral data					
Classif/Ground data	Water	Mud	Low marsh	Salic. marsh	Spart. marsh
Water	**97.6**	0	0	0	0
Mud	0	**77.7**	0	0	0
Low marsh	2.4	22.3	**92.6**	3.9	55.0
Salic. marsh	0	0	7.4	**81.5**	13.3
Spart. marsh	0	0	0	14.6	**31.7**
Total accuracy (%)= 70.1				Kappa Index = 0.59	

(D) Object - based classification: multispectral data + DEM					
Classif/Ground data	Water	Mud	Low marsh	Salic. marsh	Spart. marsh
Water	**97.6**	0	0	0	0
Mud	0	**78.3**	0	0	0
Low marsh	2.4	21.7	**93.1**	0.2	6.3
Salic. marsh	0	0	6.9	**83.7**	19.6
Spart. marsh	0	0	0	16.1	**74.1**
Total accuracy (%)= 83.1				Kappa Index = 0.76	

5.6. Odiel saltmarsh mapping

The classification results for the saltmarsh habitats in the Odiel saltmarshes are shown in (Figure 5.6). The habitat map reveals a complex pattern in the spatial distribution of these habitats. The *Spartina marsh*, which is characterised by dense and dominant coverage of *Sp. densiflora*, and the *Salicornia marsh*, characterised by *S. perennis* subsp *alpine* and *S. fruticosa* (mid-high saltmarsh habitats), are most abundant. The *Spartina marsh* is mainly distributed in the upper-mid estuary, and the *Salicornia marsh* in the mid- and low estuary.

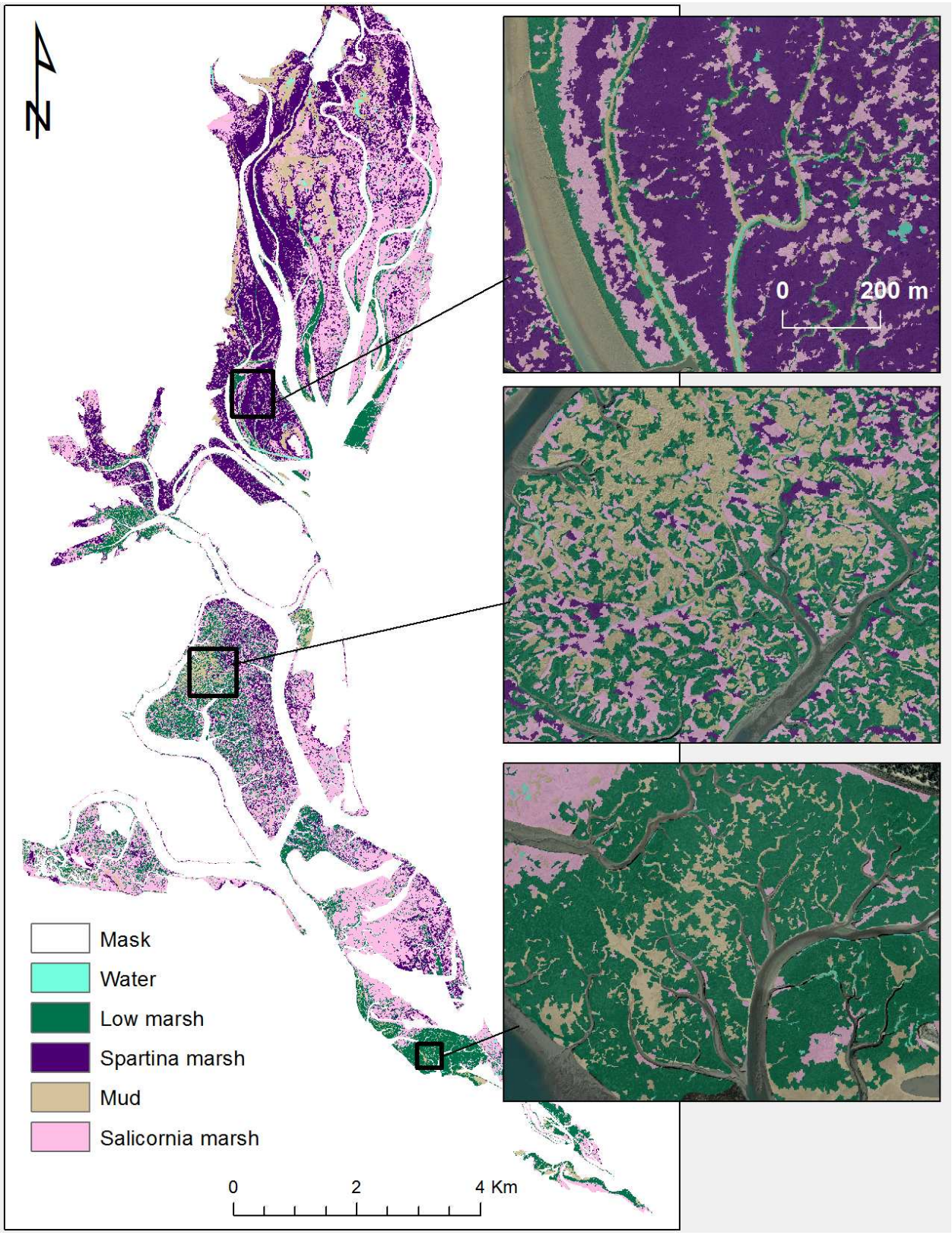

Figure 5.6 Odiel saltmarsh habitat mapping using object-based image analysis (multispectral data and elevation data derivate from a combined photogrammetric and LiDAR flight)

The *low* and *mid saltmarsh* are closely associated in terms of their plant species communities, characterised in the main by *S. perennis* and *A. portulacoides*, but distinguished by growth structure where plants are notably shorter in the low marsh (*S.*

perennis subsp *perennis, S. ramosissima*) areas than in the mid- saltmarsh areas (*S. perennis* subsp *alpini)*. Very low density vegetation, bare mud (intertidal flats and salt pans) and water (small creeks and ponds), are found throughout the estuary, but the salt pans are a more prominent feature of the upper estuary. Zonation is strongly influenced by the creek network, and patterns of habitat distribution closely follow this network.

The overall accuracy of the classification was 85% and the Kappa coefficient 0.79 as it is shown in the confusion matrix (Table 5.4). As this information does not show how well individual classes have been classified, the user[12] and producer[13] accuracy was also estimated. Focusing on the producer accuracy, which highlights how well the map objects have been classified, all the cover classes have reached values over 80%. *Mud* and *low marsh* were classified with producer accuracy greater than 90% (95 and 92% respectively), while *water*, *Salicornia marsh* and *Spartina marsh* were slightly less (84, 83 and 82% respectively). The average height canopy (DSM) between low marsh and the rest of vegetation classes played an important role in the classification results, enabling high accuracy values for this class.

Table 5.4 K-nearest neighbour confusion matrix for the 5 saltmarsh habitat cover classes. The columns represent the reference data derived from validation areas and the rows the user data derived from the classification results

User/Ref. class	Water	Mud	Low marsh	Salic. marsh	Spart. marsh	Total
Water	**5966**	0	0	0	0	5966
Mud	933	**5273**	112	0	0	6318
Low marsh	121	0	**9389**	800	640	10950
Salic. marsh	0	0	613	**18807**	2053	21473
Spar. marsh	0	0	87	2991	**17118**	20196
Total	7100	5557	10201	22598	20924	
Accuracy						
Producer (%)	84	95	92	83	82	
User (%)	100	83	86	87	85	
Overall (%)	85					
Kappa Coefficient	0.79					

5.7. Discussion and summary

To map saltmarsh habitats with high accuracy is a challenge due to the low spectral contrast between plant species and the small scale of vegetation patterns (Adam *et al*., 2009; Kelly *et al*., 2011; Silva *et al*., 2008). In this sense, the combination of spectral and elevation information significantly improved saltmarsh mapping, allowing higher accuracy values. The results obtained in this work have shown the improvements of adding

[12] It refers to the probability of that a certain class on the ground is classified as such.
[13] It refers to the probability of a pixel labeled as a certain class in the map is really this class.

elevation data to the image analysis of saltmarsh habitats (Table 5.3) using two approaches: OBIA and PBIA.

Using multispectral and elevation data, OBIA showed a higher overall accuracy and Kappa coefficient than PBIA. However, when the accuracy values are considered per class, some classes were well classified in both OBIA and PIBIA, while others classes were better classified in one approach than in the other one. The classes that were classified with very high accuracy values in both approaches were *water* and *low marsh*. However, classes such as *Salicornia marsh*, *Spartina marsh* were better classified using OBIA (obtaining higher accuracy values). Unlike other classes, *mud* was classified better in PBIA than OBIA, although in both cases reached high accuracy values (> 78%). The better results in OBIA is probably so because in OBIA adjacent pixels with similar features were merged before performing the classification reducing the 'salt and pepper' effect characteristic in PBIA classifications. Apart from the influence of working with pixel or objects on the classification results, the classifiers used in PBIA and OBIA were different. This fact can also influence the classification results.

High overall accuracy (85%) was also obtained over the entire study site integrating a large expanse of saltmarsh. This result is comparable to the values obtained by Brown (2004) and Belluco *et al*. (2006). However, they applied a pixel-based classification (maximum likelihood classifier) to a smaller saltmarsh area using hyperspectral satellite images (CASI) and elevation data. The overall accuracy obtained by them were 79 (Brown, 2004) and 92 % (Belluco *et al*., 2006). The high spectral resolution of these images provided more information to discriminate between saltmarsh plants with low spectral contrast. Interestingly, results from the Odiel saltmarsh present a higher accuracy for bare mud (95%) than in the Brown (2004) study (75%). The segmentation process previous to the classification has helped in saltmarsh feature recognition in classes such as water and mud, resulting in high individual accuracy values: 84% water (ponds and small creeks) and 95% for mud (tidal flats and salt pans).

The application of PBIA approach in saltmarsh environments has some advantages and drawbacks. This is a useful approach for its broad spatial coverage, repeatability, analytical speed and automation potential (Adam *et al*., 2009; Moffett & Gorelick, 2013). However, there are also some drawbacks when high resolution imagery is used due to complex spatial patterns in saltmarsh at the fine scale and the low spectral contrast in vegetation classes (Ouyang *et al.*, 2011). Ouyang *et al.* (2011) state that high resolution images in saltmarshes may produce 'salt and pepper' effect, resulting in noisy maps. The spectral contrast level in saltmarsh may distinct in different sites depending mainly on species presence (Silvestri *et al.*, 2003; Rosso *et al.*, 2005; Artigas and Yang, 2006; Andrew and Ustin, 2008) and season (Gao and Zang, 2006; Gilmore *et al.*, 2008). Thus, the success

of this method for mapping saltmarshes can strongly depend on remotely sensed data characteristics and time of the year acquired, as well as on plant species found at the site.

In contrast to PBIA, OBIA considers more variables that act simultaneously toward the common aim of distinguishing saltmarsh vegetation classes (in this particular case). These variables are the pixel spectrum, its relative spatial location, and the local spectral homogeneity and shape of adjacent groups of similar pixels (Moffett & Gorelick, 2013). All these variables can help to improve vegetation pattern recognition in saltmarshes, and thus to minimise the 'salt and pepper' effect typical of PBIA approaches. Several authors argue that, in general, this approach offers better results than pixel based approaches (Chen *et al*., 2006; Smith, 2009; Blumberg & Zhu, 2007; Platt & Rapoza, 2008). However, the major disadvantage of OBIA in comparison to PBIA is that it is a semi-automatic process that requires more user inputs. Thus, it is very dependent on user knowledge, which makes generalisation of the approach rather difficult.

In short, saltmarshes are generally characterised by small scale vegetation zones and low spectral contrast among plant communities, which can complicate the classification processes mixing plant species cover and therefore reduce the accuracy of results. To minimise noise and maximise accuracy, it is very important to select (where possible) the most suitable data set comprising appropriate spatial and spectral resolution and high resolution elevation data, in addition to a suitable classification approach that specifically addresses the classification needs identified. The approaches frequently used for classifying saltmarshes are PBIA and OBIA, which have showed advantages and disadvantages based on site specifications and data, but evidence from the Odiel saltmarshes shows that OBIA can handle many of the challenges of habitat classification mapping.

6. Correction and assessment of LiDAR-derived DEM

The aim of this chapter is to investigate the effectiveness of using elevation ground control points (differential GPS) and vegetation surveys to improve vertical accuracy in a LiDAR-derived DEM for modelling potential sea-level rise impacts in Atlantic-Mediterranean saltmarshes, through the application of habitat-specific correction factors in the Odiel saltmarshes (Spain, Gulf of Cadiz). Essential to this process is the availability of a high-resolution habitat map, and here the Odiel saltmarsh habitat map obtained in Chapter 5 was used for this purpose (85% overall accuracy). The resulting DEM was used in Chapter 7 as one of the main inputs that feeds the predictive model (SLAMM).

6.1. Introduction

Accurate digital elevation models (DEMs) of saltmarshes are crucial for both conservation and management goals. Light detection and ranging (LiDAR) is increasingly used for topographic surveys due to the ability to acquire high resolution data over spatially-extensive areas. This capability is ideally suited to saltmarsh environments, which are often vast, inaccessible systems where topographic variations can be very subtle. Derivation of surface (DSMs) versus bare ground elevation models (DEMs) relies on the ability of the LiDAR sensor to accurately record multiple returns. In saltmarshes however, the dense stands of low (< 1 m) vegetation commonly found precludes the acquisition of more than one return, and the resulting DEM is no different to the DSM. Establishing the offset between ground and vegetation surface in order to correct the LiDAR-derived DEM can be challenging due to the spatial variability in saltmarsh habitats.

Under the physical limitations mentioned in Chapter 1, LiDAR-derived DEMs covering high-density vegetation saltmarshes are generally not accurate enough to distinguish topographic structure at the resolution that is used to determine tidal flooding or vegetation patterns (Hladik and Alber, 2012). Thus, a corrected DEM becomes essential for certain applications (e.g. tidal flooding and sea-level rise assessments) in saltmarshes characterised by dense evergreen vegetation, such those found in southern Europe. Previous works in saltmarshes have investigated and applied the minimum bin gridding method (e.g., Ewald, 2013; NOAA, 2010; Schmid *et al*., 2011), analysis of airborne infrared photography taken during a rising tide (Andrade *et al*., 2014) and species-specific correction factors (e.g. Hladik and Alber, 2012; Hladik *et al*., 2013; McClure *et al*., 2015) for 'user-modified' DEM creation. In the case of using species-specific correction factors for correcting LiDAR-derived DEM, the work carried out by Hladik and Alber (2012) and Hladik *et al*. (2013) in a saltmarsh in Georgia (Atlantic coast, USA), and by McClure *et al*. (2015) in a saltmarsh in San Francisco bay (Pacific coast) showed that the DTM mean

errors can be significantly reduced using this method. However, accurate vegetation maps are required for its appliance over large areas.

6.2. Method

This methodology employed a multi-layered approach to develop and apply a habitat-specific correction factor (HSCF) for a semi-automated adjustment of LiDAR-derived DEMs (Figure 6.1) with application to the Odiel saltmarshes. Although similar approaches have previously been applied (e.g. Hladik and Alber, 2012; Hladik *et al.,* 2013; McClure *et al*., 2015) to reduce mean vertical error in LiDAR-derived DEMs, all previous studies were conducted in the USA. Saltmarsh habitats in the US, especially those found in the Atlantic coast present dissimilarities to those located in Europe due to a range of differences in, for example, extent, vegetation type and structure. For example, saltmarshes in the Gulf of Cadiz comprise complex creek networks compared with the broad coastal tidal plains of the Atlantic US coast (Phinn *et al*., 1996). Saltmarshes found on the Pacific US coast, particularly in California, present more similarities to Atlantic-Mediterranean saltmarshes in the Gulf of Cadiz (Peinado *et al*., 1995) than those found in the Atlantic US coast, although species composition is distinctly different (e.g. *S. pacifica* vs *S. perennis*; *Sp. foliosa* vs *Sp. densiflora* and *S. emerisi* vs *S. ramosissima* are respectively associated with Pacific US and Gulf of Cadiz coasts). Thus, the success of this method applied to those saltmarshes found in the Gulf of Cadiz could vary based on these dissimilarities due to the difficulties related to saltmarsh species and habitat mapping. Thus, it is still unknown whether the use of habitat-specific correction factors can effectively reduce DTM vertical errors in all saltmarsh environments.

Unlike other approaches, the method undertaken here used remote sensed data acquired in a combined photogrammetric and LiDAR flight, with random vegetation surveys and object-based image analysis (OBIA) to apply the correction over the entire Odiel saltmarsh system. The production of a high-resolution habitat map was central to this approach in terms of facilitating the spatially-variable application of the habitat-specific correction factor (HSCF) to the input (unmodified) LiDAR-derived DEM. The habitat map was derived from high resolution multispectral aerial photography (using RGB and NIR bands) and LiDAR-derived DSM (final result in Chapter 5). Due to vegetation height within Salicornia class was found to greatly vary depending on location; this class was divided into tall and short salicornia based on vegetation height (modified saltmarsh map). The acquisition of field data, comprising measurements of precise ground elevation, vegetation structure and height provided the information needed to calibrate and validate the correction factor.

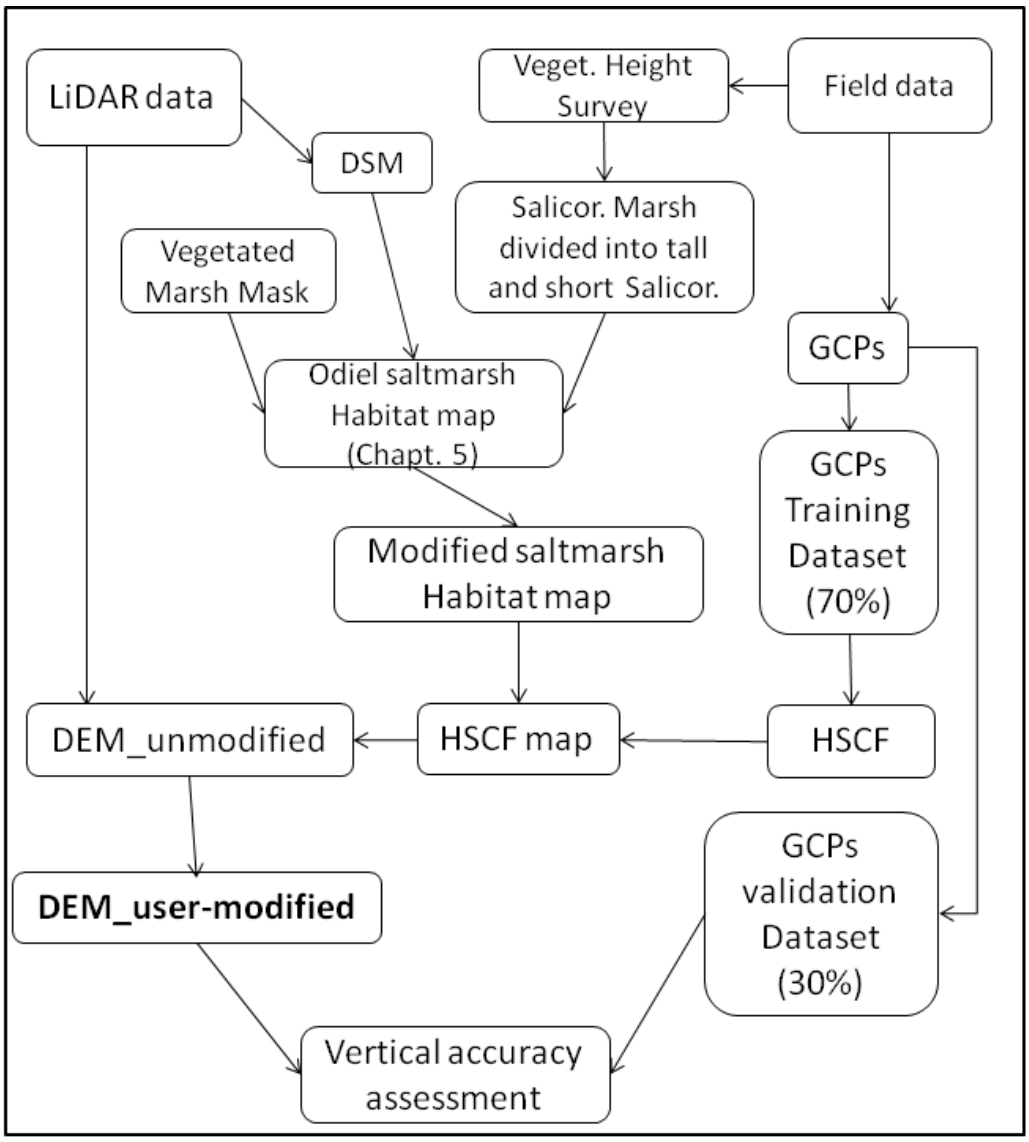

Figure 6.1 Workflow diagram of the method used

6.2.1. Study sites

Two sites within the Odiel saltmarshes were selected to develop and test the method, although canopy height data were collected across the entire saltmarsh for exploring height similarities within the same habitat type, and the potential of this method for its application over the whole study area (the Odiel saltmarshes, Figure 2.7). The sites selection was based on covering all habitat types previously defined (Chapter 4) for the Odiel saltmarshes. The first site (Site 1) is approximately 10 ha and located in Saltes Island (Figure 6.2). Habitats here are typical of those found throughout the mid-high and lower Odiel estuary saltmarshes with a dominance of *Salicornia* species: high marsh (*S. machrotaschyum*, and *S. fruticosa*), mid marsh (*S. perennis subsp. alpini* and *Atriplex portulacoide*), low marsh (mixture of *S. perennis subsp. perennis, Atriplex portulacoide and Limonium sp.*), creeks and intertidal flats. The second site (Site 2) covers nearly 4 ha and is

located in the upper estuary, near the town of Corrales (Figure 6.2). This site provides good examples of salt pans and mid- and high marsh habitats dominated by *Spartina densiflora*, which it is poorly represented in Site 1.

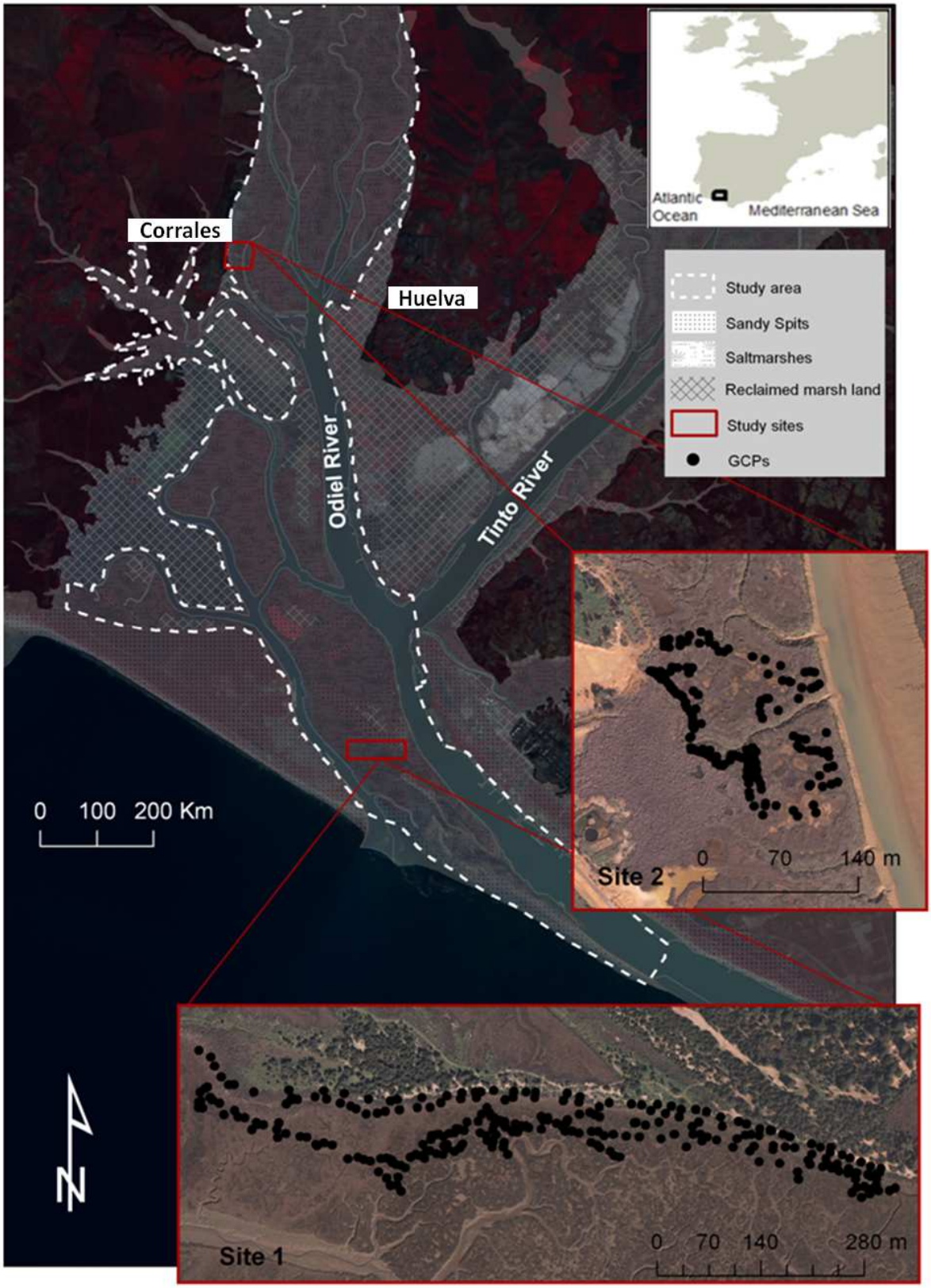

Figure 6.2 Study area and site locations at the Tinto-Odiel estuary (Huelva, Southwest Spain). Ground control points (GCPs) collected for both sites are represented by black dots

6.2.2. Field data

Using the habitat classes defined for the Odiel saltmarsh habitat map (Chapter 5), a vegetation height survey was undertaken to ascertain the variance in canopy height across habitats within the entire Odiel saltmarshes and . Here, 12 representative sites covering different habitat types were sampled, where vegetation canopy height was surveyed at 100 randomly located points within a 10x10 m quadrat. Canopy heights measured in each habitat type from different sites were compared using one-way analysis of variance (ANOVA). Additionally, a Tukey's Honest Significant Difference (HSD) test (confidence level = 0.95) was also used. Statistical analyses were performed using the software R (version 2.15.1).

A topographic survey of the saltmarsh was also undertaken at the testing sites. For this, ground control points (GCPs) - 260 within Site 1 and 132 within Site 2 - were established, at which ground elevation, canopy height and plant species presence were recorded (Figure 6.2). Ground elevation at the GCPs was surveyed using a Real-Time Kinematic (RTK) Leica-1200 (base station) GPS and two rovers with 0.02 m vertical and 0.01 m spatial accuracy. The RTK Rover foot was placed flush with the marsh surface for ground elevation points. Orthometric heights (Zero in Alicante - the equivalent of mean sea level) were calculated from RTK elevations using the Spanish Geodetic Survey GEOID (as used for LiDAR elevations) EGM08-REDNAP ("*Red Espanola De Nivelacion de Alta Precision*", Spanish High Precision Positioning Network). The total data set of 392 GCPs collected within the study sites were divided into training (70% of the GCPs; N=282) and validation data sets (30% of the GCPs; N=121). In addition, 20 GCPs were also collected over bare areas (bare ground and roads) for assessing the accuracy of the LiDAR data.

6.2.3. Remote sensed data

A LiDAR dataset was acquired in a combined LiDAR sensor and photogrammetric camera flight carried out in January 2013. Data were collected for the whole Odiel estuary during low tide (tide level = -1.1 m relative to MSL; tidal coefficient = 89) to minimize the amount of water on the marsh surface. Reported vertical and horizontal accuracies for the LiDAR sensor are 0.07-0.10 m and 0.15-0.17 m respectively. The sensor collected up to 4 returns on upland areas (mean point density = 2 points per square metre), but across the saltmarsh and intertidal environment, only one return was recorded, meaning the 'LAS' files provided little further information for modelling the ground surface in this system. Thus, the DSM and the DEM are identical across the saltmarsh: the unmodified elevation dataset is henceforth referred to as the LiDAR-derived DEM, and was resampled to 1 m

resolution. Elevations were positioned in the Spanish vertical reference frame (Cero in Alicante) and projected onto the UTM (WGS-1984) coordinate (zone 29N) system.

A discordance between ground elevation and LiDAR survey dates arose due to weather conditions: the LiDAR flight had been planned to coincide with the field survey (which was undertaken in October 2012), but was delayed to January 2013(when weather and low tide conditions were next optimum). The tide coefficient was similar to that of the ground survey. Although not ideal, both surveys were still undertaken within the same winter period, thereby reducing the potential for significant change between surveys. Furthermore, except *S. ramosissima* most of the saltmarsh plant species found in Odiel saltmarshes such as *S. fruticosa*, *S. perennis*, *A. macrostashyum* and *S. densiflora* are perennial (Figueroa *et al*., 1987), which enables a stable evergreen vegetation canopy over the saltmarsh through the whole year. This has been checked and confirmed during the field campaigns.

6.2.4. DEM corrections based on HSCF

The habitat-specific correction factor (HSCF) was based on the vertical bias, or mean error, of the LiDAR-derived DEM with respect to the ground-truth data (the training GCPs). Ground elevations surveyed at 70% of the GCPs were compared to the DEM elevation values for the same locations. The difference between these two values at each GCP was used to first compute the vertical bias, and second, summarised as a mean correction factor for each habitat type. The vertical bias (CF_i) has been previously used to compute correction factors for saltmarshes in Hladik and Alber (2012) and it is calculated as:

$$CF_i = Z_{DEMi} - Z_{GCPi} \qquad (6.1)$$

where Z_{DEMi} is the elevation derived from the LiDAR-derived DEM, and Z_{GCPi} is the elevation measured by RTK-dGPS, at each GCPi. For each habitat type j, a habitat-specific correction factor ($HSCF_j$) is then computed from the arithmetic mean of all CF_i that relate to each habitat type.

Application of these habitat-specific correction factors to the Odiel study sites was undertaken using the high resolution saltmarsh habitat cover map (derived from the OBIA classification in Chapter 5). This facilitated the spatialisation of all $HSCF_j$ into a new layer $HSCF_{map}$ (at 1m spatial resolution), and the correction of the LiDAR-derived DEM to a user-modified DEM (mDEM) where:

$$Z_{mDEM} = Z_{DEM} - HSCF_{map} \qquad (6.2)$$

The GCP validation dataset (30% of the collected GCPs) was use to validate mDEM and assess the difference between the LiDAR-derived DEM over vegetated environments (the true accuracy of the original LiDAR product). The vertical accuracy assessment of both elevation models was carried out using two error metrics: mean error and Root Mean Square Error (RMSE).

6.2.5. Saltmarsh habitat map

A high resolution habitat map was produced (Chapter 5) through the application of OBIA on a combined data product covering just the saltmarsh region (Figure 5.6). Water and non-marsh habitats (supratidal spits, reclamations) were masked. The source layers were multispectral aerial photography (January 2013) comprising panchromatic, near-infrared, red, green and blue bands and the raw (unmodified) LiDAR-derived DEM (equivalent to a DSM of the saltmarsh environments). This habitat map produced was used to apply a habitat-specific correction factor, within which the *Salicornia marsh* class was divided into *tall Salicornia* and *short Salicornia* (a modified habitat map). This decision was made based on the plant height survey undertaken for this work, which showed significant height differences within *Salicornia* dominated saltmarsh. One of the advantages of using OBIA in eCognition is the possibility of hierarchical structure of cover classes (Figure 6.3). This is particularly useful in order to divide or merge different classes within the final classification (e.g. saltmarsh habitat map) based on a rule set without running the whole process again. The resulting map is shown in Figure 6.4.

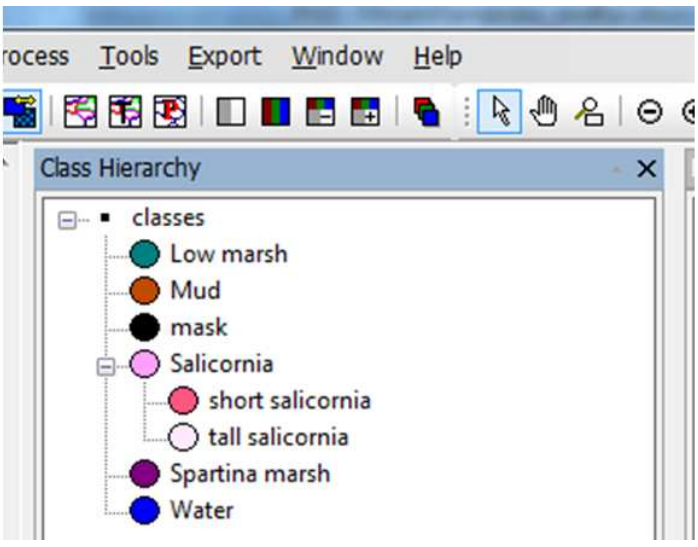

Figure 6.3 Hierarchical structure of cover classes used in eCognition.

6.3. Results

6.3.1. Ground survey

Results from the saltmarsh ground survey showed significant plant height differences within *Salicornia marsh*. Thus, this class was divided into *short Salicornia* and *tall Salicornia*. Figure 6.5 highlights the variance in canopy height across habitat types in the Odiel saltmarshes. Canopy heights measured in the different habitats (2 sites in *low marsh*, 3 in *short Salicornia*, 3 in *tall Salicornia* and 3 in *Spartina marsh*) were compared using one-way analysis of variance (ANOVA), which proved that there were significant differences in height means between habitats ($p < 0.001$). Additionally, the Tukey's HSD (confidence level = 0.95) clarified that the height means were significantly different between different habitats (results were considered significant when $p < 0.05$) but were similar among the same habitat type.

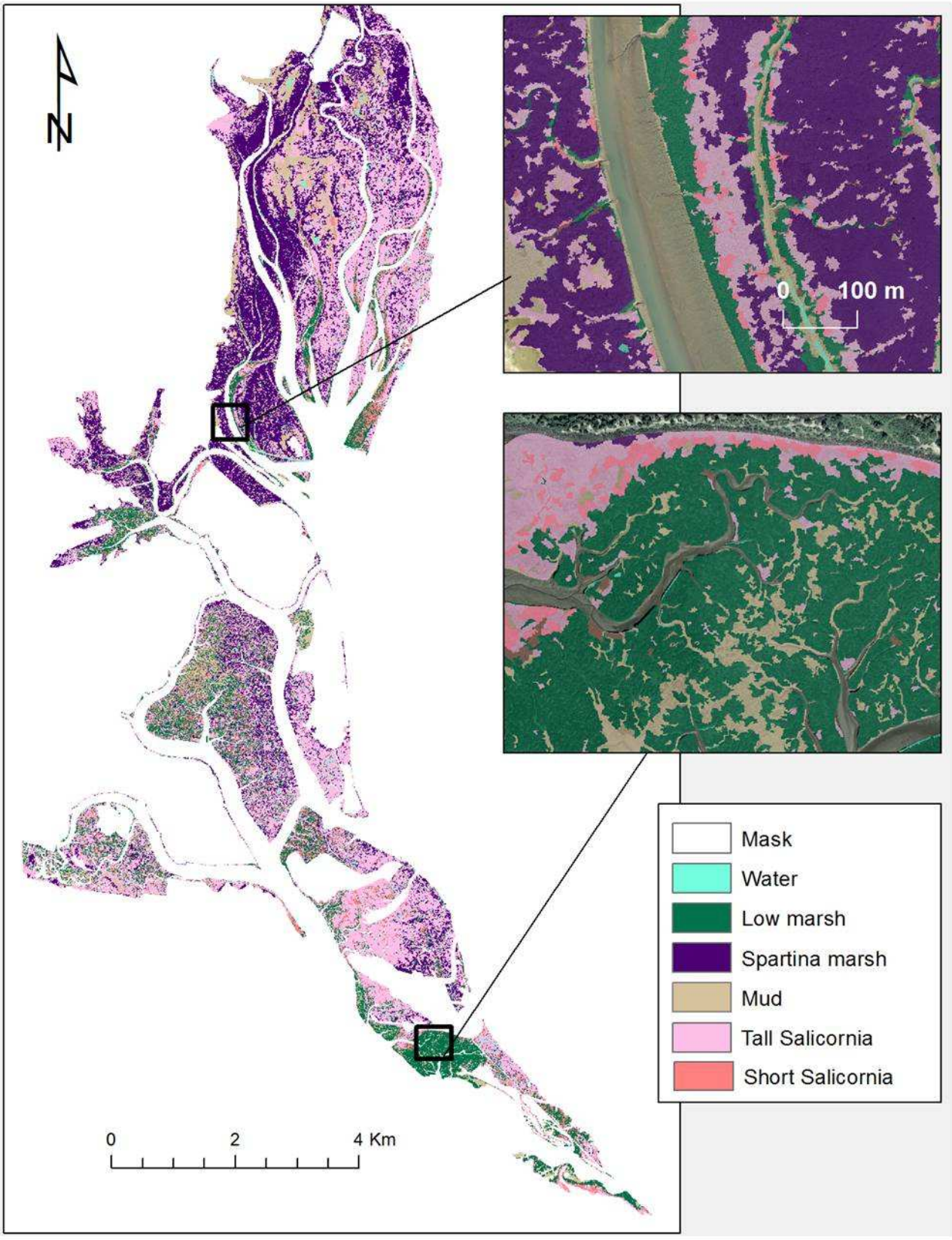

Figure 6.4 Marsh habitat map of the Odiel saltmarshes (SW Spain) for applying the habitat-specific correction factor

Results from the RTK survey at Site 1 and Site 2 showed that ground elevation ranged from 0.03 to 3 m in Site 1 and from 1.2 to 2.4 m in Site 2, and vegetation height from 0.03 to 0.61 and 0.05 and 1.07 m respectively. The GCPs were classified by habitat type, divided as 41 points within *low marsh*, 153 in *short Salicornia*, 102 in the *tall Salicornia* and 96 in the *Spartina marsh*. Ground elevation measured at each GCP in these different habitats was also compared using one-way analysis of variance (ANOVA), which proved that there were significant differences in ground elevation means between habitat types ($p < 0.001$). Additionally, the Tukey's HSD clarified that the elevation means were significantly different between these cover classes.

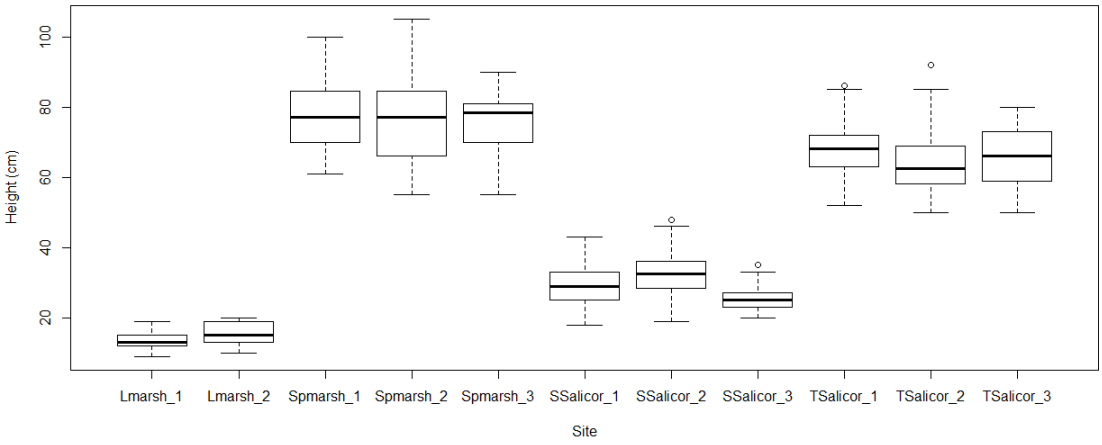

Figure 6.5 Vegetation height per habitat type at different sites, where "Lmarsh" means low marsh, "SSalicor" *short Salicornia*, "TSalicor" *tall Salicornia* and "Spmarsh" spartina marsh. The numbers state different sites within the Odiel saltmarshes.

6.3.2. DEM production and accuracy assessment

The HSCFs were only computed for vegetated saltmarsh habitat classes (Table 6.1) and the unvegetated classes (mud and water) were added to the mask layer (with a HSCF value of zero) to avoid negative bias. The results highlight that the *Spartina* marsh has the highest canopy and the largest standard deviation compared with the other classes. The variability in canopy height (reflected in the standard deviation) is explained by the structure of this plant, which grows in erect clumps of slender stems with long and narrow leaves. Other saltmarsh vegetation is distinctly shorter and less variable.

Table 6.1 Habitat-specific correction factors (HSCF), the associated standard deviation (SD) and the root mean square error (RMSE).

Habitat class	HSCF values (m)	SD (m)	RMSE
Low marsh	0.15	0.067	0.104
Short Salicor.	0.25	0.066	0.068
Tall Salicor.	0.32	0.088	0.142
Spartina marsh	0.55	0.16	0.292
Mask	0	-	-

The HSCF for each habitat class were converted to a spatially-distributed HSCF map using the habitat classification (Figure 6.6). This was applied as a spatially-distributed correction layer to the unmodified LiDAR-derived DEM across the whole study area. Comparison of unmodified and corrected DEMs are provided in Figure 6.7, for the area covered by Site 1 and Site 2, which highlights the changes in ground elevation as a result of the correction.. As it was expected the changes are more pronounced in those areas where the vegetation canopy was higher (*i.e.* the *Spartina* marsh). The supratidal zone, channels and bare mud remain the same as these were masked from the analysis. The two profiles (Transect 1 and 2) shown in Figure 6.6 clearly illustrate the spatially-varying elevation differences between the LiDAR-derived DEM and the corrected mDEM.

Accuracy was assessed in both the original DEM and corrected mDEM using a selection of ground control points (distinct from those used in the derivation of the correction factors). The results show that the HSCF considerably reduced the overall vertical mean error in both sites (Table 6.2): from 0.23 to 0.13 m in Site 1 and from 0.45 to 0.09 m in Site 2. The unmodified DEM mean vertical error was greater than 0.1 m (the LiDAR reported mean error) for all habitat classes, except for low marsh. In the case of unvegetated areas the mean vertical error remained under the reported LiDAR accuracy (0.1 m): 0.09 m in bare mud areas and 0.04 in roads. In contrast, the mean vertical error in the corrected mDEM remains well within the reported LiDAR vertical mean error (0.1 m) for all habitat types except for *Spartina marsh* (that is slightly higher) as shown in Table 6.2. The mean vertical biases in the taller and usually denser habitat types (*Spartina marsh* and *tall Salicornia*) are significantly decreased from the original DEM to the corrected mDEM: the mean error was reduced from nearly 0.53 to 0.13 m in *Spartina* marsh, and from 0.35 to 0.02 in *tall Salicornia*. The surface level in the rest of habitat classes was all slightly under-predicted in the corrected mDEM due to over estimation of the correction factor: *low marsh* (-0.02 m) and *short Salicornia* (-0.06 m). In order to investigate whether

the over-estimated correction factor was caused by the averaging technique selected (the mean), the median was also applied. Nevertheless, the results were unchanged when applying a different averaging technique.

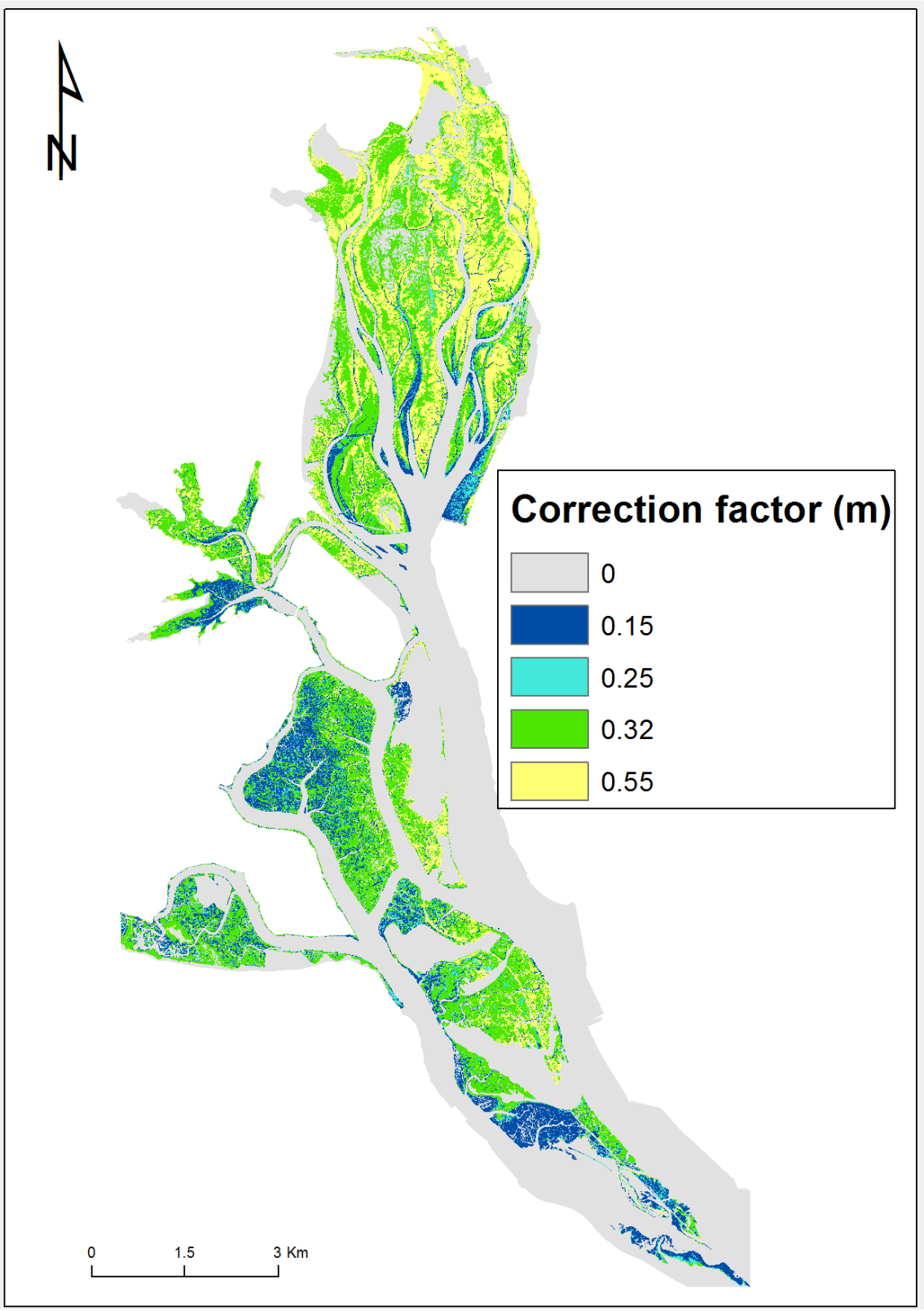

Figure 6.6 Habitat-specific correction factor (HSCF) map, where the correction factor for each habitat class has been spatially-distributed using the Odiel saltmarsh habitat map

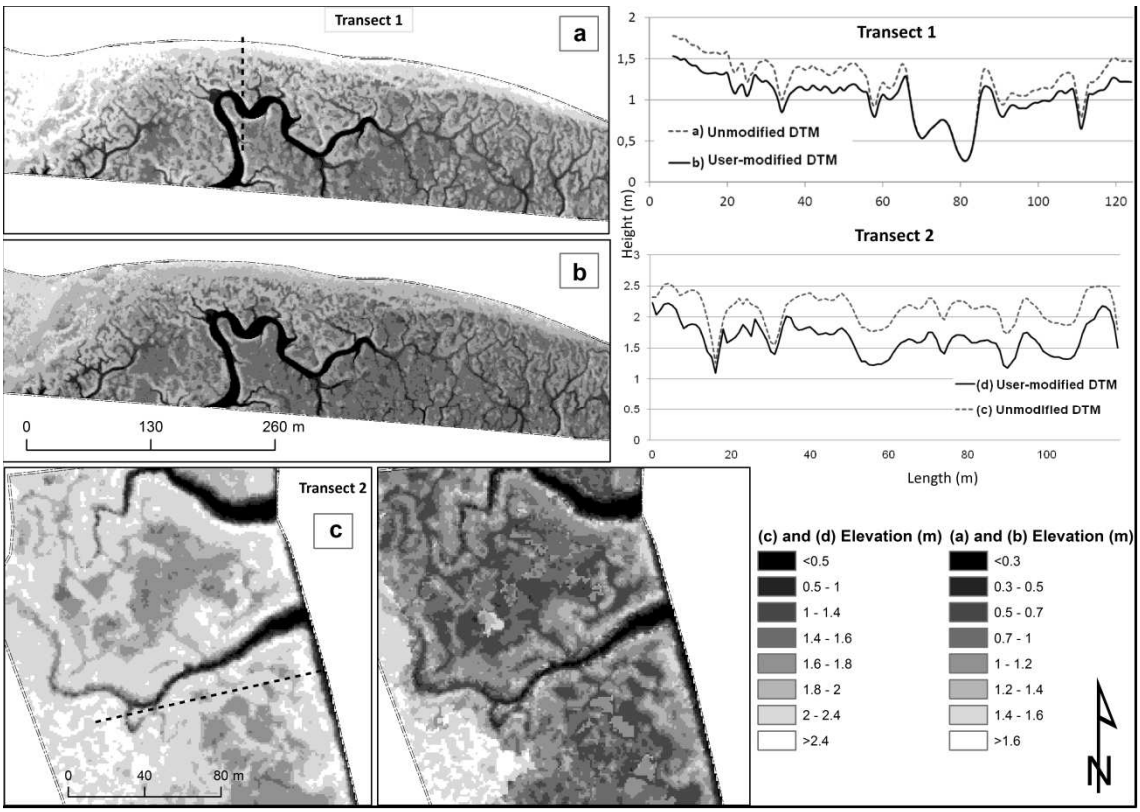

Figure 6.7 Map of the two areas used as test sites for unmodified DEM corrections showing the unmodified and user-modifier DEM for Site 1 and Site 2, where: (a) and (b) are the unmodified and the user-modified DEM respectively in Site 1; and (c) and (d) are the unmodified and the user-modified DEM respectively in Site 2. Two transects (Transect 1 and Transect 2) were selected for comparing the height profiles of both DEMs at Site 1 and 2. In the profile graphs, note the differences in canopy heights in the unmodified DEM and the user-modified DEM, and the overlapping at creeks (where a mask was used).

Table 6.2 Error statistic of the unmodified and user-modified DEM for each habitat cover class regard to GCP survey; where 'ME' is the mean error or vertical bias, 'SD' is the standard deviation and 'RMSE' the root mean square error.

	Unmodified DEM			User-modified DEM		
Habitat class	ME (m)	SD (m)	RMSE (m)	ME (m)	SD (m)	RMSE (m)
Bare mud	0.09	0.04	0.01	Not used	Not used	Not used
Low marsh	0.09	0.09	0.02	-0.02	0.08	0.06
Short Salicor.	0.26	0.11	0.08	-0.06	0.13	0.05
Tall Salicor.	0.35	0.18	0.15	0.02	0.17	0.03
Spar. marsh	0.53	0.13	0.29	0.13	0.16	0.15
Roads	0.04	0.05	0.004	Not used	Not used	Not used
Overall site 1	0.23	0.13	0.07	0.13	0.14	0.06
Overall site 2	0.45	0.19	0.24	0.09	0.18	0.16

Figure 6.8 Mean error (ME) and root mean square error (RMSE) per habitat cover class. The ME and RMSE is compared between the unmodified DEM and the User-modified DEM.

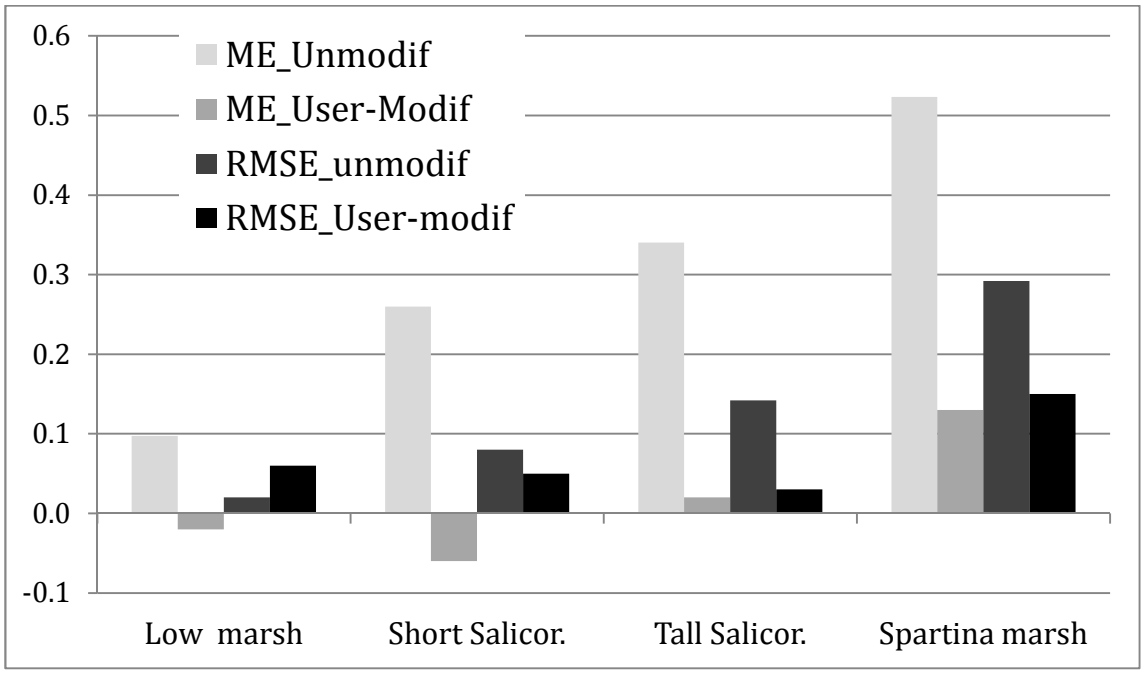

6.4. Discussion and summary

LiDAR is one of the sensors that better captures the smaller-scale structural complexity of saltmarsh topography over extensive areas. However, it is extremely important to be aware of the limitations and real accuracy of this sensor data for saltmarsh environments. Although the LiDAR sensor used for this work collected up to 4 returns, for the majority of the saltmarsh environment only one return was collected. Thus, in the filtering process, it was not possible to discriminate bare ground from saltmarsh vegetation for DEM generation. Based on the analysis undertaken for this work, a LiDAR-derived DEM (without any user modifications) can accurately represent saltmarsh elevations for only non-vegetated (e.g. intertidal flat and salt pan) or low density, short (< 0.2 m) plant habitats. The accuracy calculated for these habitats remained below 10 cm, which is the vertical resolution of the LiDAR-derived data. However, the accuracy of the unmodified DEM decreases significantly in habitats characterised by dense, tall vegetation (> 0.2 m height). Similar findings have been reported by other authors (Hladik and Alber, 2012; Schmid, Hadley and Wijekoon, 2011; Wang *et al.*, 2009).

LiDAR-derived DEM accuracy in saltmarsh environments can be improved by user modifications. For example, minimum bin-gridding from LiDAR data has been shown to decrease vertical errors in vegetated environments (Ewald, 2013). However, in open areas such as mud flats, it can produce elevations below the true ground surface (negative bias) (Rosso, Ustin, and Hastings, 2003). This technique can also reduce the resolution, and

hence possibly lose small scale topographic features in the process. It is here where the user must balance the importance of resolution over accuracy (Schmid *et al*., 2011).

The development and application of spatially variable correction factors has been shown clear benefits. Application of a correction factor that varies depending on vegetation characteristics reduces vertical errors in vegetated saltmarshes without reducing the spatial resolution. Furthermore, this technique does not compromise the accuracy in open areas such as mud flats if unvegetated areas are masked (where the correction is zero, and therefore no change is made). Masking is often considered an arduous process as it frequently relies on manual digitisation. But habitat classification through an object-based image analysis approach has the added benefit of including the identification of small features of unvegetated classes (ponds and salt pans), which can then be assigned to a mask. Thus, negative bias in those areas is avoided.

High resolution habitat classification using object-based image analysis has been used in this work to accurately capture vegetation characteristics on the basis of distinct communities and plant structure. Specific correction factors based on high resolution habitat maps derived from canopy heights and spectral information have the benefits of being applied to broad areas with less effort. However, to map saltmarsh habitats with high accuracy is a challenge due to the low spectral contrast between plant species and the small scale of vegetation patterns (Adam *et al*., 2009; Kelly *et a.l*, 2011; Silva *et al.*, 2008). In this sense, the combination of spectral and elevation information significantly improves saltmarsh mapping as it has been shown in Chapter 5, allowing higher accuracy values.

The corrected DEM obtained after application of the HSCF across the entire Odiel estuary saltmarsh environment has improved the overall accuracy of the ground elevation data, obtaining comparable results to those achieved by Hladik and Alber (2012). The accuracy improvements obtained in this modified DEM provide a saltmarsh elevation dataset suitable for applications such as modelling of sea-level rise and sedimentation in these environments. Elevation accuracy is crucial for these types of modelling because subtle changes in topography affect other factors that control saltmarsh dynamics (*e.g.* flooding and soil salinity). Projections of future global sea-level rise vary from 0.18 - 0.59 m (over the period 1980-1999 and 2090-2099) based on physical models (Meehl *et al*., 2007a, 2007b). This means that the DEM accuracy has to be smaller than sea-level rise projections over these reasonable timescales in order to accurately investigate potential impacts. In the LiDAR dataset presented here, the best accuracy in elevation data that can be obtained is 0.1 m, which is the real accuracy of the elevation raw data collected from LiDAR sensor at up-land known locations. However, it has been shown that the real accuracy of the original DEM in the Odiel saltmarshes is poorer than 0.1 m (up to 0.53 m in *Spartina marsh* for instance) due to the high density of the vegetation canopy. Thus, the

unmodified DEM in this particular case would not be suitable for modelling sea-level rise effects over the Odiel saltmarsh due to the mean vertical bias in large areas of the saltmarsh is nearly the same that the top range of the future sea-level rise projections (0.59 m). However, the corrected DEM is better able to distinguish topographic structure at the resolution that is used to determine future flooding due to sea-level rise.

7. Future response of Odiel saltmarsh due to SLR using SLAMM: sensitivity analysis and uncertainty assessment

The aim of this Chapter is to assess the potential of the Sea Level Affecting Marshes Model (SLAMM) for investigating the response of Atlantic-Mediterranean saltmarshes and its use in managerial schemes, through the application of sensitivity and uncertainty analysis in the Odiel saltmarshes (Spain, Gulf of Cadiz). The spatial input data (DEM and habitat map) and some parameter (e.g. erosion) needed for running the model have been generated in previous chapters of this thesis.

7.1. Introduction

SLAMM version 6.2 (Clough *et al.*, 2010) was used to evaluate coastal wetland habitat response to sea-level rise. SLAMM simulates 6 key processes involved in wetland conversions and shoreline modifications during long-term sea-level rise: inundation, accretion, erosion, overwash, saturation, and salinity. In order to simulate these processes over a specific site in the context of sea-level rise, SLAMM uses spatial data including a DEM, slope and wetland category maps, and site specific parameters such as tidal range, accretion rates, erosion rates, historical sea-level trends and mean sea level. To represent conversion among wetland classes, SLAMM uses a flexible and complex decision tree incorporating geometric and qualitative relationships (Clough *et al.*, 2010).

One of the main strengths of SLAMM is the ability to explore system responses to different sea-level rise scenarios, but uncertainties in predicted response will also reflect uncertainties regarding the primary inputs and hence the quality of the original elevation data and wetland classification maps. This chapter first undertakes a sensitivity analysis to explore the relative importance of data quality and resolution (spatial and vertical) in the elevation data and saltmarsh habitat classification layers. Monitoring and measurement of saltmarsh habitats is time consuming and costly, and the acquisition of the SLAMM input layers can require significant resourcing. Some understanding of where surveying efforts should be focused is therefore necessary, particularly for authorities with financial constraints. An analysis of potential impacts of sea-level rise over the Odiel saltmarshes under different IPCC scenarios (A1B, A1T, A1F1, A2, B1 and B2) using SLAMM in conjunction with the input layers generated in previous chapters (e.g. the modified 2013 DEM and saltmarsh habitat map) is then presented. Additionally, an uncertainty analysis on model inputs was undertaken to identify the important input parameters that control model output uncertainty. Finally, the modelled potential sea-level rise impacts over the Odiel saltmarshes are assessed in combination with saltmarsh erosion rates obtained from Chapter 3. This is used to generate a saltmarsh classification based on sensitivity due to sea-level rise.

7.2. SLAMM model inputs

7.2.1. Elevation data

Elevation data are the most important SLAMM input data and high quality altimetry data are required to reduce uncertainties. For example, the model uncertainties are considerably reduced when LiDAR-derived DEM data are used Elevation in combination with tidal data determines the vertical and spatial extent and frequency of inundation. The input elevation data also define the base line for future predictions. In SLAMM, input elevation data must be corrected to set the mean tide level (MTL) to zero because this is the internal model vertical datum (Clough *et al.,* 2010). The required elevation data adjustment is done following equation (7.1):

$$Elev_{(MTL=0)} = Elev_{(Datum=0)} - Elev_{corr} \quad (7.1)$$

Where, $Elev_{Datum}$ is the elevation of each cell given a vertical datum (m), and $Elev_{corr}$ is the site or cell by cell correction (MTL minus datum, in metres). In the case of the Odiel saltmarshes site, the reference vertical datum is the zero in Alicante (mean sea level). When high quality elevation data are not available, SLAMM employs a tool called NWI (National Wetland Inventory), a pre-processor that estimates elevation ranges as a function of tide ranges and known relationships between wetland types and tide ranges.

7.2.2. Sea-level rise estimation

SLAMM projects future sea-level rise over the initial conditions based on historical local sea-level and global sea-level trends. The sea-level rise is estimated at each projected time step as given in equation (7.2) (Clough *et al.,* 2010).

$$SLR_{TModel} = GlobalSLR_{TModel} + \frac{(Year_{TModel} - Year_{T0})(HistSLR_{Local} - HistSLR_{Global})}{1000} \quad (7.2)$$

where:

SLR_{TModel}= Projected local sea-level rise at current model year (m);

$= GlobalSLR_{TModel}$ = Global average sea-level rise predicted in current model year (m);

$Year_{TModel}$ = Current model year;

$Year_{T0}$= Date when model started (latest NWI map date);

$HistSLR_{Local}$l= Site specific historic trend of sea-level rise (mm/yr);

$HistSLR_{Global}$ = 1.7 mm/yr global historic trend based on IPCC (2007a);

7.2.3. Processes involved in the spatial model

SLAMM integrates four factors directly involved in the fate of tidal saltmarshes in a context of sea-level rise: inundation, erosion, accretion and salinity. These are parameterised as follow:

- Inundation: the rise of water levels and the salt boundary is defined by reducing elevations of each cell as sea levels rise, thus keeping MTL constant at zero. The effects on each cell are calculated based on the minimum elevation and slope of that cell.
- Erosion: horizontal erosion is triggered based on a threshold fetch and the proximity of the wetland to estuarine water or open ocean. When these conditions are met, horizontal erosion occurs at a rate based on site. If the maximum fetch is less than 9 km, horizontal erosion does not occur.
- Accretion: vertical sedimentation due to inorganic sediment accumulation and marsh biogenic production may be specified on a spatially variable basis or a model of accretion as a function of elevation, salinity, and/or distance to channel may be specified. SLAMM accretion relationships are empirical, defined as given by equation (7.4):

$$A_{cell} = A_{elev}(D * S) \tag{7.4}$$

  where:

  A_{cell}= predicted accretion rate for a cell, (mm/year)

  A_{elev}= accretion rate for a cell as a function of elevation alone

  D= factor representing distance to river or tidal channel

  S= salinity factor representing salinity effects

- Salinity: in a location with defined fresh-water flows, land categories can migrate based on changes in salinity. This is modelled based on a relatively simple salt wedge approximation. Variable fresh-water flows may be specified.

7.2.4. Wetland conversion

SLAMM uses a decision tree, based on the information given in Table 7.1, when converting one wetland category to another in the event of inundation or erosion. Wetland conversion under sea-level change conditions occurs when sea-level rise exceeds

sedimentation or accretion rates and when the minimum elevation of a cell is below the minimum elevation for a specific wetland category. The wetland lost fraction (which it is transferred to another category) is calculated as function of the cell slope, the minimum elevation for that category, and the lower elevation boundary for that category. Thus, SLAMM assumes that conversion of a zone from one category to another is a linear function of the elevation range that is lost due to sea-level rise within the cell (Clough *et al.*, 2010). Erosion will occur for those categories adjacent to water when the maximum fetch for a certain cell is greater than 9 km.

A connectivity model is also available in SLAMM and it can be used optionally. When this model is used, an eight-sided connectivity algorithm is used to examine cells in the context of their direct neighbouring cells. At the beginning of each time-step, each cell is marked with one of the following categories: above salt bound (connectivity is irrelevant); connected to salt water source; not connected to salt water source; and diked (lack of connectivity assumed). For example, if freshwater wetlands and dry lands are not connected to salt water due to the existence of a seawall, they are not assumed to be subject to inundation due to sea-level rise.

Table 7.1 Summary of the wetland category conversions relevant for this study due to inundation and erosion [modified from Clough *et al.* (2010)].

	Inundation	**Erosion**
	Non-adjacent to open water	Adjacent to open water and fetch > 9km (erosion)
Category	Converts to	Converts to
Dry land	Transitional salt marsh, ocean beach, or estuarine beach, depending on context	
Tidal fresh marsh	Irreg. Flooded Marsh	Tidal Flat
Transitional Salt Marsh	Reg. Flooded Marsh	Tidal Flat
Irreg. Flooded Marsh	Reg. Flooded Marsh	
Reg. Flooded Marsh	Tidal Flat	Tidal Flat
Ocean Flat	Open Ocean	Open Ocean
Tidal Flat	Estuarine Water	Estuarine Water
Estuarine Beach	Open water	Open water
Ocean beach	Open water	
Backshore	Estuarine beach	
Estuarine water	If the cell is within 500m of the open ocean then it is converted into open ocean.	

7.3. Data and methods

7.3.1. SLAMM sensitivity analysis on spatial data

Sensitivity analysis on spatial data was based on the quality of the model input data using different resolution elevation and habitat maps. Sensitivity analysis based on habitat cover maps has not been explored previously. Thus, the effort here has been focussed on investigating how different resolutions of habitat map in combination with different quality elevation data will affect model results. For this purpose, different tests have been run in SLAMM using a representative site within the Odiel saltmarshes.

A smaller study site within the Odiel saltmarshes was selected in order to reduce model running time and to assess changes between tests. The selected study site to run the sensitivity analysis tests was part of the Saltes Island (Figure 7.1). This island has representative environments of the whole Odiel saltmarshes, where habitats such as beaches, tidal flats, low marsh, high marsh, transitional marsh and up-land can be found.

The input data used for this analysis are listed in Table 7.2Table 7.2 and Figure 7.2, and the combination of these data within the SLAMM sensitivity analysis is shown in Figure 7.2. The model inputs tested were the marsh habitat maps (MHM) (Figure 7.3), the digital elevation models (DEM) (Figure 7.4) and the elevation range for each habitat category. Site parameters were kept constant and are summarised in Table 7.3. The habitat map MHM_1 was derived from the combination of the saltmarsh habitat map (supervised classification performed in Chapter 5), and 2013 estuarine habitat map (digitised in Chapter 3). The resulting map was reclassified using SLAMM categories. MHM_2 and MHM_3 were derived from simplification of MHM_1 (reducing the number of creeks, and reducing the resolution of spatial pattern of different saltmarsh habitats. This means that some pixels from different habitats will be misclassified). Additionally, a habitat map based on saltmarsh habitat elevation ranges was also generated (MHM_4). MHM_4 was created by reclassifying the user-modified DEM (generated in Chapter 6) into elevation intervals, which closely related to saltmarsh habitat types (zonation) (Silvestri *et al.* 2005). On the other hand, three different DEMs were used to test SLAMM. The first one is a 1 m spatial resolution LiDAR-derived DEM (DEM_1) without corrections (in this case the DEM is identical to DSM as it has been explained in Chapter 6), the second one a user-modified DEM (DEM_2) (obtained by correcting DEM_1 using a habitat-specific correction factor; Chapter 6), and the third one is a 10 m spatial resolution DEM (DEM_3) (source: Andalusian Environmental Agency). Finally, the elevation inputs (EIN) (Table 7.4) specific for each habitat type was also tested modifying the values by (a) ±0.2 m and (b) ± 0.4 m. EIN are the site specific elevation ranges per habitat defined in the Odiel saltmarsh by Rubio and Figueroa (1983).

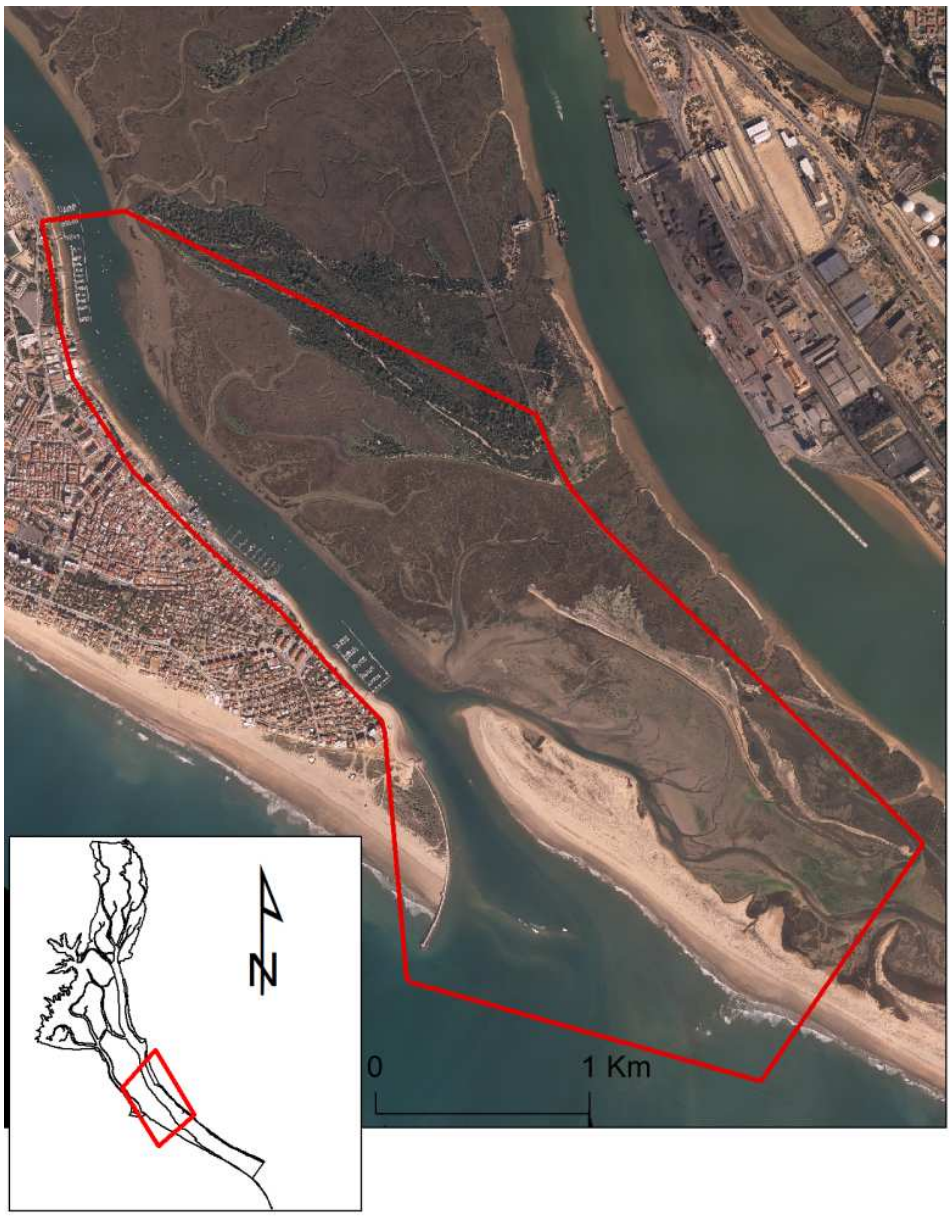

Figure 7.1 Location of the study site (red line) for testing model sensitivity

Table 7.2 Summary of data used as inputs in SLAMM

Name	Description	Source
DEM_1	Unmodified LiDAR-derived DEM (1m spatial resolution)	LiDAR flight
DEM_2	Modified LiDAR-derived DEM (1m spatial resolution)	Chapter 5
DEM_3	DEM of the Andalusian Coast (10m spatial resolution)	Andalusian Environmental Ministry
MHM_1	Marsh Habitat Map derived from supervised classification using 2013 aerial photography and DEM_2 (1 m spatial resolution)	Chapter 6
MHM_2	Manual simplification of MHM1 (5 m spatial resolution)	Derived from MHM1 (e.g. less small creeks than MHM1)
MHM_3	Manual simplification of MHM2 (5 m spatial resolution)	Derived from MHM2 (e.g. only the main channel)
MHM_4	Reclassification of DEM2 based on habitat elevation range. For Upland categories and backshore (where the height range overlaps, manual editing was carried out)	Derived from DEM2
EIN	Elevation inputs per habitat category (zonation) EIN_a (+-0.2m); EIN_b (+-0.4m)	(Rubio & Figueroa, 1983)

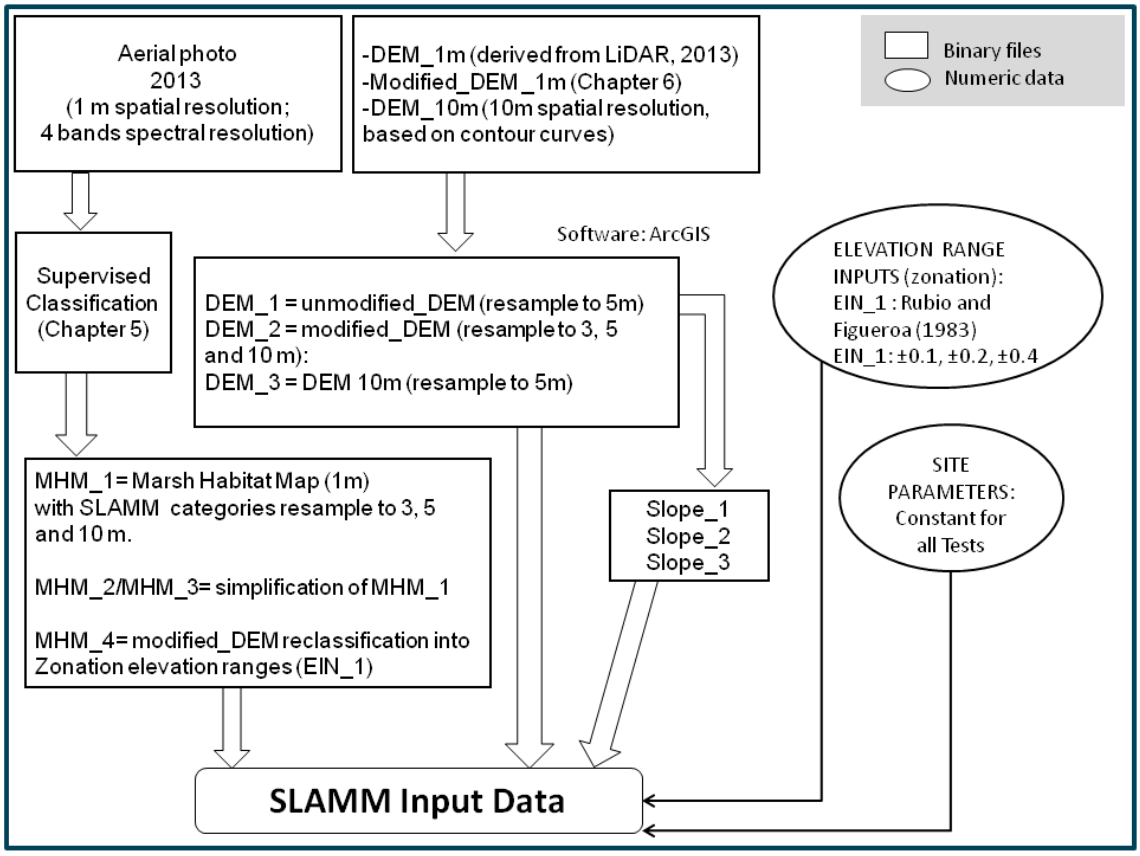

Figure 7.2 Flow chart of the input data used in the sensitivity analysis based on spatial data

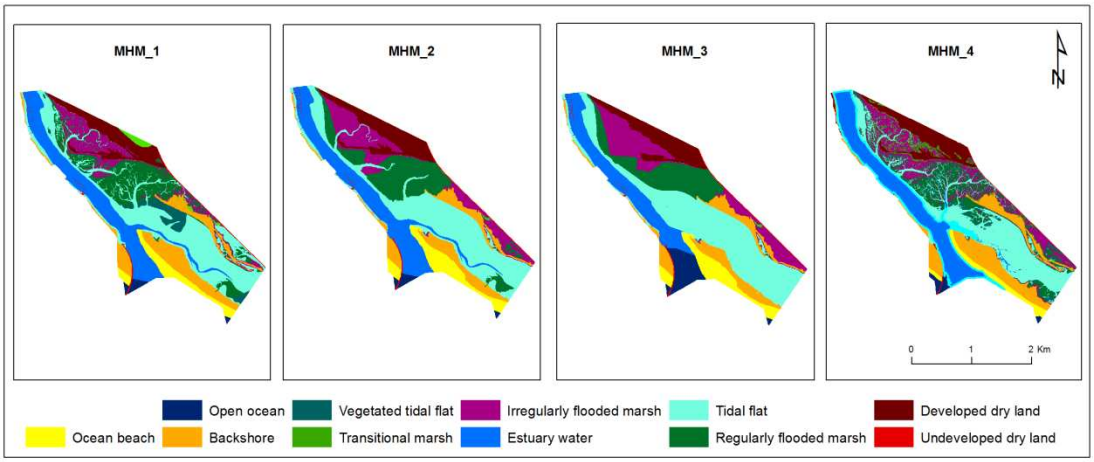

Figure 7.3 Marsh habitat maps (MHM) from Table 7.2 used as different inputs for testing SLAMM

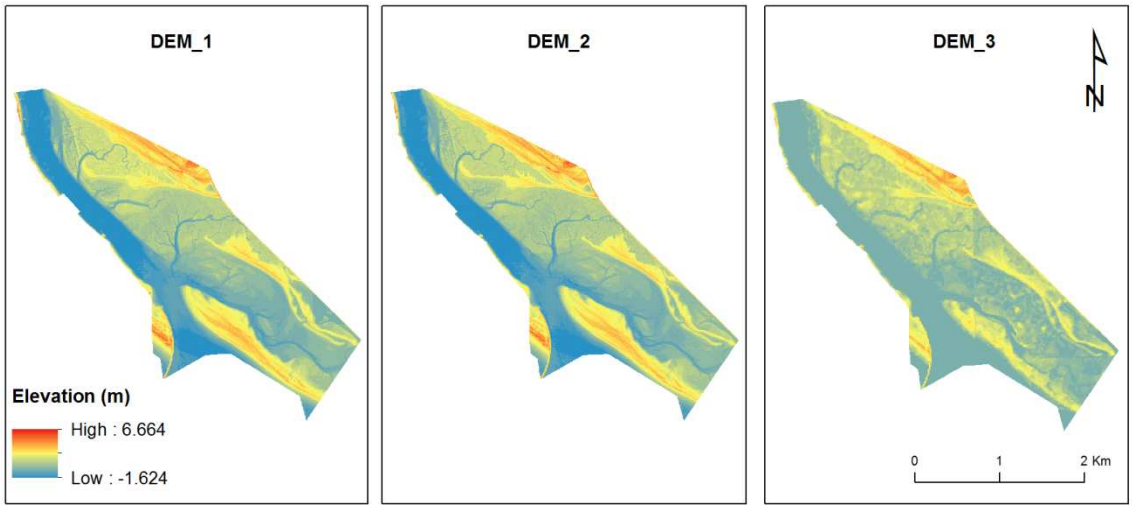

Figure 7.4 Digital elevation models (DEM) Table 7.2 used as inputs for testing SLAMM

Table 7.3 Site specific input parameters required for SLAMM

Input parameters	
Description	Punta Umbría Ria
NWI Photo Date (YYYY)	2013
DEM Date (YYYY)	2013
Direction Offshore [n,s,e,w]	South
Historic Trend (mm/yr)	3.3
MTL-NAVD88 (m)	0.39
GT Great Diurnal Tide Range (m)	3.11
Salt Elev. (m above MTL)	2.09
Marsh Erosion (horz. m /yr)	0.0105
T.Flat Erosion (horz. m /yr)	0.003
Reg. Flood Marsh Accr (mm/yr)	6.57
Irreg. Flood Marsh Accr (mm/yr)	2.5

Table 7.4 Elevation inputs (EIN) specific for each habitat type

SLAMM Category	Min Elev.	Min Unit	Max Elev.	Max Unit
Dry Land	4.05	Metres	7	Metres
Trans. Salt Marsh	3.62	Metres	4.05	Metres
Reg. Flooded Marsh	0.8	Metres	1.2	Metres
Estuarine Beach	-1	HTU	1	Salt Elev.
Tidal Flat	-0.08	Metres	0.8	Metres
Irreg. Flooded Marsh	1.2	Metres	3.62	Metres
Vegetated Tidal Flat	0.6	Metres	0.8	Metres
Backshore	1	Salt Elev.	3.048	Metres

Five tests have been run in SLAMM to perform this sensitivity analysis (Table 7.5). Test 1 explores the optimum cell size for the data available for the study area. The optimum cell size is then used for running the other tests. Test 2 investigates the model outputs using different marsh habitat maps. Here, four marsh habitat maps with different resolutions have been used, which have been defined previously (MHM_1, MHM_2, MHM_3 and MHM_4). Test 3 explores the model outputs varying habitat elevation range inputs: EIN_a (±0.2m) and EIN_b (±0.4m). Test 4 investigates the benefit of using high resolution habitat maps when only poor resolution DEMs are available. Here, the elevation pre-processor tool is also tested. Finally, Test 5 explores the differences between DEM_1 (unmodified) and DEM_2 (modified).

Table 7.5 Summary of the test specifications used for running sensitivity analysis in SLAMM

	Test 1	**Test 2**	**Test 3**	**Test 4**	**Test 5**
Cell size (m)	3, 5, 10	5	5	5	5
DEM	DEM_2	DEM_2	DEM_2	DEM_3	DEM_1 DEM_2
MHM	MHM_1	MHM_1 MHM_2 MHM_3 MHM_4	MHM_1	MHM_1 MHM_3	MHM_1
Elev. Pre-p*	False	False	False	False/True	False
Elevation ranges (zonation)	EIN	EIN	EIN EIN_a (±0.2m) EIN_b (±0.4m)	EIN	EIN

* Elevation pre-processor

7.3.2. The Odiel saltmarshes SLAMM simulation

SLAMM was run for the entire study area (The Odiel saltmarshes, see Figure 2.7) using high resolution input data: MHM_1 (Figure 7.3) and DEM_2 (see Figure 7.4). The study area was divided into sub-sites (Figure 7.5) based on published long-term accretion rates (Table 2.1) and the observed erosion tendency observed (Chapter 3). Thus, the model parameters for all sites were exactly the same as those used for the sensitivity analysis except for accretion and erosion rates (Table 7.6). The NWI elevation pre-processor was not used since high resolution data were available. In the SLAMM execution options, the *developed dry land* was protected, and the connectivity and soil saturation options were selected. The future projections were estimated for 2050, 2075 and 2100 using the mean of the IPCC sea-level scenarios available in SLAMM (A1B, A1T, A1F1, A2, B1 and B2).

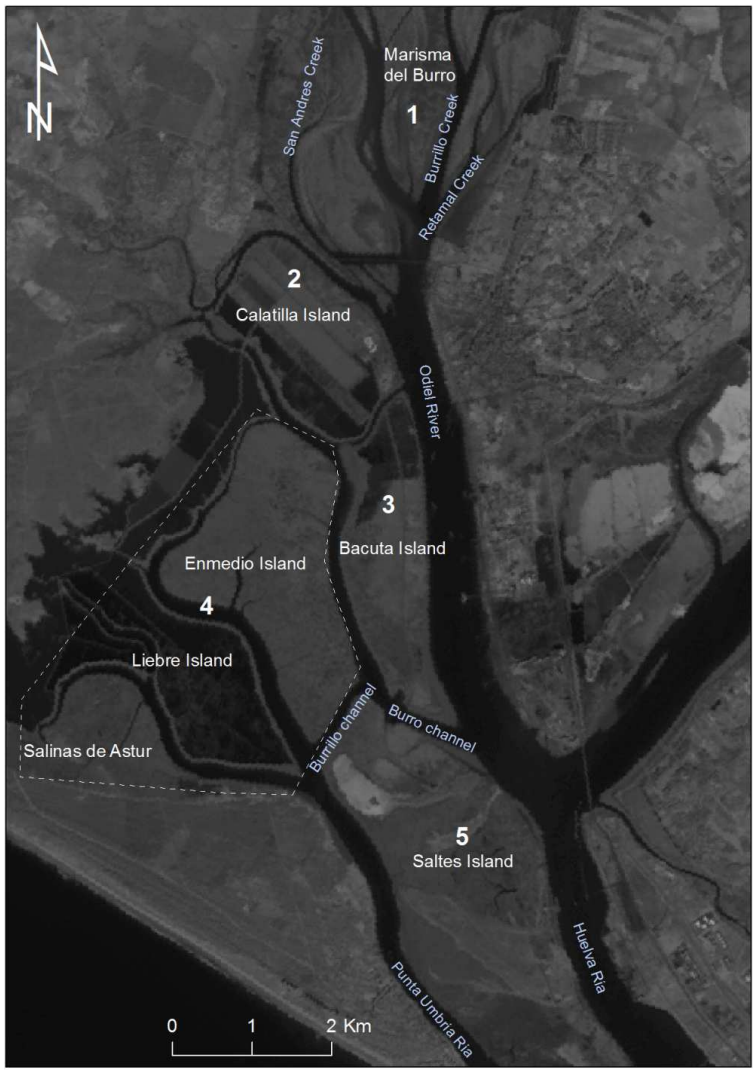

Figure 7.5 Sub-sites used for running SLAMM (in the simulation for the entire study area)

Table 7.6 Model parameters with sub-site specifications

Parameter	SubSite 1	SubSite 2	SubSite 3	SubSite4	SubSite 5
Horizontal Marsh Erosion (my^{-1})	0	0.23	0.16	0.05	0.33
*Reg. Flood Marsh Accr (mmy^{-1})	2.41	2.41	6.71	10.6	10.6
*Irreg. Flood Marsh Accr (mmy^{-1})	2.86	2.1	2.1	2.1	2.1

*Accretion rates were taken from Table 2.1

7.3.3. SLAMM uncertainty analysis

SLAMM version 6.2 has the ability to perform uncertainty analysis (Figure 7.6) thus allowing the user to see how input uncertainties affect the outputs. For example, if the user assumes the accretion rate (mmy^{-1}) of regularly flooded marsh follows a normal distribution of mean *x* and standard deviation *y*, SLAMM will randomly generate an accretion rate consistent with the distribution defined beforehand and calculate the resultant impact in hectares of the regularly flooded marsh and other marsh usage classification. Furthermore, SLAMM not only has the ability to repeat this process any number of times (for example 10,000) but also allows the user to specify many more input uncertainty distributions (say the accretion rate of irregularly flooded marsh and historical sea-level rise for instance).

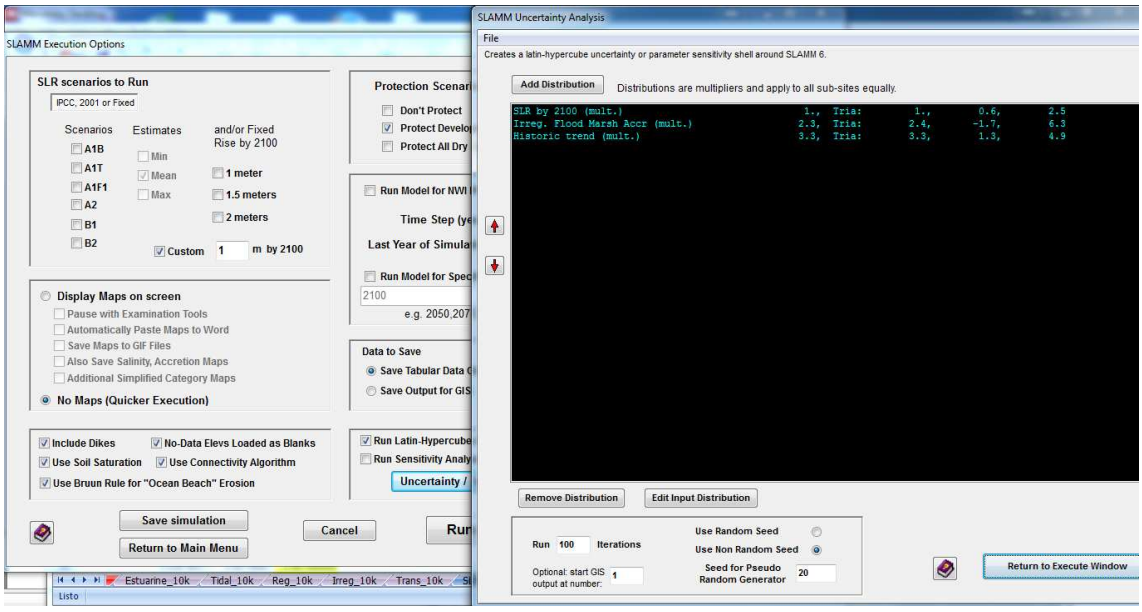

Figure 7.6 Uncertainty model integrated in SLAMM (v 6.2)

The uncertainty analysis was performed on results using a Monte Carlo approach to provide confidence statistics for model results as a function of input uncertainties. The Monte Carlo framework undertaken for this work was essentially the following:

1. To define the input uncertainty distributions (e.g. normal, triangular or uniform.)
2. To decide how many simulations/ runs lead to results which are robust (i.e. not seed sensitive) and accurate.
3. Once the number of simulations is decided, use a random generator to generate the input values which are consistent with the previously defined distributions.
4. To use these randomly generated input values to feed into the SLAMM model and to evaluate how the model outputs are affected (full calculation). If the number of simulations was set at 10,000 for example, then this process would be repeated 10,000 times, leading to 10,000 different model output outcomes.
5. To analyse the distribution of the 10,000 model output outcomes to see if there are any common patterns helping the user to understand the dynamics/ interaction of the previously defined uncertainty distributions of the model inputs.

Steps 1, 2, 3, and 5 were easy to perform, while difficulty was encountered at step 4 where one simulation took roughly 10 minutes to perform. Often, 10,000 simulations are normally deemed satisfactory (Chu-Agor *et al*., 2011) to get robust and accurate results, which would lead to a total compute time of 1666 hours or 69 days using a single computer.

Uncertainty distributions (step 1) were constructed for each of the model inputs (Table 7.7), where it was assumed that the inputs follow a triangular distribution. Triangular distributions give more importance to the extreme values that normal distributions and it was considered more suitable for this analysis. Other authors also used triangular distributions for the same parameters to perform uncertainty analysis in saltmarshes (Chu-Agor *et al*., 2010; Chu-Agor *et al*., 2011). It has been assumed that the uncertainty distributions of the accretion rates of both regularly and irregularly flooded marshes follow a joint distribution; while distributions of the sea-level rise, historical sea level rise, and accretion rates of regular/ irregular flooded marsh were assumed to be independent of each other. The values of the distributions were defined using published and observed data. The SLR_{2100} distribution values were defined using different published projections for global sea-level rise by 2100 range between 0.6 and 2.5 m (this range was based on the AR4 WG1 IPCC scenario and predictions from Vermeer & Rahmstorf (2009) and Pfeffer *et al.* (2008)); the *Htrend* used the observed local (Gulf of Cadiz) minimum, maximum and most likely (average) (Figure 3.26); and the *reg-accre* and *irreg-accre* used the published Odiel saltmarshes accretion rates: minimum (-3 standard deviation of the manifested values), maximum (+3 standard deviation of the manifested values) and most likely (average of the manifested values).

Table 7.7 Input factors for SLAMM and assumed statistical distributions for the uncertainty analysis, where 'T' means triangular distribution (minimum, most likely, maximum)

Input factor	Description	Unit	SLAMM value	Distribution
SLR_{2100}	Predicted sea-level rise by 2100	metres	1	T(0.6, 1, 2.5)
Htrend	Local historical sea-level rise trend	mmy^{-1}	3.3	T(1.4, 3.3, 5)
Reg-accre	RegFM vertical accretion/erosion	mmy^{-1}	6.5	T(-9, 6.5, 21)
Irreg-accre	IrregFM vertical accretion/erosion	mmy^{-1}	2.4	T(-1.7, 2.4, 6.3)

The next steps were to determine the number of simulations (step 2) and to use the random generator to produce random number to feed into the model (step 3). The number of simulations (N) for performing uncertainty analysis was determined using equation (7.5) (proposed in Sobol's method (Sobol, 1993)), and used by Chu-Agor *et al*. (2011) to perform uncertainty analysis):

$$N = (k + 2)\, M \qquad (7.5)$$

where k is the number of input factors and M is the sample size (usually between 500 and 1000). In this analysis, there were four input factors (SLR_{2100}, *Histtrend*, *reg-accre* and *irreg-accre*) and the value of M was 1000, leading to a total of 10,000 simulation. Random number generation was undertaken in both SLAMM and Excel.

Step 4 as defined above is the 'full calculation' approach – values of model inputs consistent with previously defined uncertainty distributions are pushed into the SLAMM which are then used by the model to calculate the final output in terms of hectares of marsh classifications by the year 2100. All the dynamics and interactions of the input variables are fully captured in this computationally intensive approach leading to an accurate output. Due to the impracticality of this approach (respect to the computing time), another approach was alternatively proposed: the 'sensitivities' approach. This approach uses a mono-factorial (once at a time) analysis by using Taylor's theorem (one variable). By using this theorem, one would be able to approximate linearly (red box below) the value of the output once the value of the input variable was known:

$$P_k(x) = f(a) + f'(a)(x-a) + \frac{f''(a)}{2!}(x-a)^2 + \cdots + \frac{f^{(k)}(a)}{k!}(x-a)^k$$

and thus a large amount of computing time would be saved in the process if f'(a) and f''(a) are known. However, the cost of the approach would be not being able to fully capture the cross effects of input variables on the final output.

In order to investigate whether the model outputs follow a linear behaviour and thus to check the suitability of the sensitivity approach, a sensitivity analysis was conducted by varying model parameters by ± 5, 10 and 15 % (one parameter was changed at a time per each SLAMM simulation), considering a 1 m eustatic sea-level rise by 2100 and the parameter defined in Table 7.3 as the base case. Additionally to determine which parameters most affect model outputs when comparing results, the screening sensitivity method proposed by (Morris, 1991) was used. The Morris method analyses the observed elementary effects (for example, changes in an output due to changes in a particular input exclusively) when random input factors are used. The input factors assessed were sea-level rise by 2100 (total projected rise in metres), site-specific historical sea-level trend, great diurnal tide range, regularly flooded marsh accretion rate, irregularly flooded marsh accretion rate, horizontal marsh erosion and tidal flat erosion. The qualitative nature of the Morris method limits its use to only identify the important inputs factors that drive model output uncertainty (Chu-Agor *et al.*, 2011).

Results from the sensitivity analysis were first assessed in terms of change in the outputs (surface area in ha) per each habitat category to check linear and non linear behaviours. Then, two sensitivity measures were calculated (the mean elementary effect, μ, and the standard deviation of the elementary effects, σ) to determine the qualitative importance of each input factor. The mean elementary effect estimates the overall effect of the inputs factors on a given output, and the standard deviation the higher-order characteristics of the input factors (such as curvatures and interactions) (Chu-Agor *et al*., 2011). These results were assessed by plotting σ on the vertical axis and μ on the horizontal axis.

The relationship between input and output variables observed in previous results seemed to be linear. This meant that for whatever inputs values generated according to the uncertainty distributions, the output would be assumed to follow in a linear fashion. However, while cross checking whether 'extreme' input values would result outputs behaving in a linear fashion was led to the fact that outputs did indeed behaved non-linearly. Non-linear behaviour must be captured in order for the sensitivities approach to work. It is possible to capture the non-linearity using the quadratic approximation highlighted in the red box (the rate of change of delta) of the Taylor series below:

$$P_k(x) = f(a) + f'(a)(x-a) + \boxed{\frac{f''(a)}{2!}(x-a)^2} + \cdots + \frac{f^{(k)}(a)}{k!}(x-a)^k$$

However, the effort required to calculate them did not justify the reward and it was decided to use the full calculation approach but with linear interpolation due to the

unfeasible model running times of the complete full calculation (~10,000 simulations), both within this study but likely experienced by other users as well.

The full calculation approach using linear interpolation was performed choosing a set of input values covering the range of the uncertainty distribution defined for each input factors (roughly 15 values were chosen for each input factor). These values were entered into SLAMM individually, changing the values of only one input factor at a time while the other inputs were held constant and equal to the base case. The computing time here was reduced to roughly 6 hours, making this approach feasible for this work.

The input – output relationship was assessed by plotting the change of the input factor (horizontal axis) and the change in the surface area (ha) of each saltmarsh habitat category (vertical axis). For example, for an input value of 0 m for sea-level rise, this would mean a 100% decrease against the base case of 1m. For input values that do not fall upon a point that was previously calculated by the SLAMM model, then linear interpolation is used (Figure 7.7). Note that extrapolation techniques were not required as the extreme values determined by the input distributions were directly used in the SLAMM full calculation run.

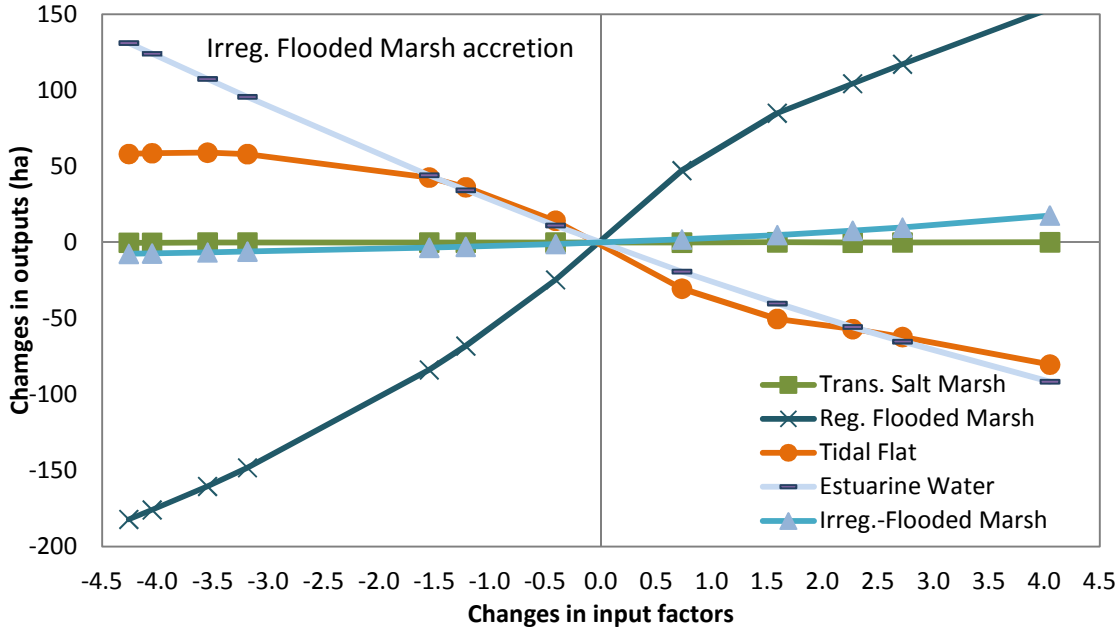

Figure 7.7 Example of the linear interpolation for *irregularly flooded marsh* accretion (for 1 m eustatic sea-level rise) using a set of inputs values that covered the full range of the uncertainty distribution. The values for the point dataset were calculated in SLAMM changing the SLR values while the other inputs were held constant.

Finally, the distribution of the 10,000 model output outcomes obtained using the full calculation with linear interpolation is analysed (step 5). With the randomly generated inputs values defined by the uncertainty distributions, coupled with the input-output relationships, it is possible to see what the approximate model output will be. Because of

the speed of this approach, it is quick to repeat the ten thousand simulation run many times (ten times) and found that the approximate model outputs were not seed sensitive. The uncertainty was then assessed in two ways. The first assessment was based on the uncertainty of the future sea-level rise by 2100 (keeping the other input factors constant), and the second one was based on the uncertainty of the important input factors for 1 m sea-level rise by 2100.

7.3.4. Classification of saltmarsh vulnerability due to sea-level rise

In order to explore the most sensitive zones of the saltmarshes due to a potential sea-level rise, the Odiel saltmarsh was classified using different information obtained from historical, present and modelled data. A saltmarsh vulnerability ranking (from very low to very high) was based on results from the entire Odiel saltmarsh simulation, saltmarsh shoreline tendency (Chapter 3) and the presence of barriers. The projected map used was the 2050 projections under the AB1 IPCC scenario. The selection of 2050 was based on the similarities of the results for all the scenarios (model projections for 2050 were practically identical), and the likelihood of the saltmarsh processes (e.g. accretion, erosion, tidal prism) to remain similar to the current conditions. The shoreline tendency was considered because SLAMM does not take into account erosion rates if the fetch is smaller than 9 km. However, in the Odiel saltmarsh it has been shown that this parameter was very important, and possibly will be exacerbated in the context of sea-level rise. Shoreline tendency was categorised as retreat, growth and stable tendency. Finally, the barrier presence was selected as barriers that would prevent saltmarsh habitats to migrate inland are present. Thus it was considered an important variable to take in account in combination with the shoreline tendencies. The barriers layer integrated the urban zones, roads, sea-walls and dikes across the saltmarsh and around the saltmarsh border in 2013.

The procedure followed for classifying saltmarshes according to its vulnerability to sea-level rise is shown in Figure 7.8. In order to compare the initial condition map (InitM) and the 2050 projected map (ProjM), both maps were reclassified into four classes: regularly flooded marsh (RegFM), tidal flat (TF), irregularly flooded marsh (IrregFM) and rest. Then, ProjM was extracted from InitM using the ArcMap raster calculator (spatial analysis tools, ArcGIS 10.2). Those zones that were projected to experience RegFM and TF loss was classified as *very high vulnerability* due to these habitats will be lost in 2050 according to the model outputs, and those zones that were categorised as RegFM in the 2050 projection were classified based on the vulnerability ranking showed in Table 7.8. Saltmarsh zones that did not experience any changes were considered to be 'not sensitive'.

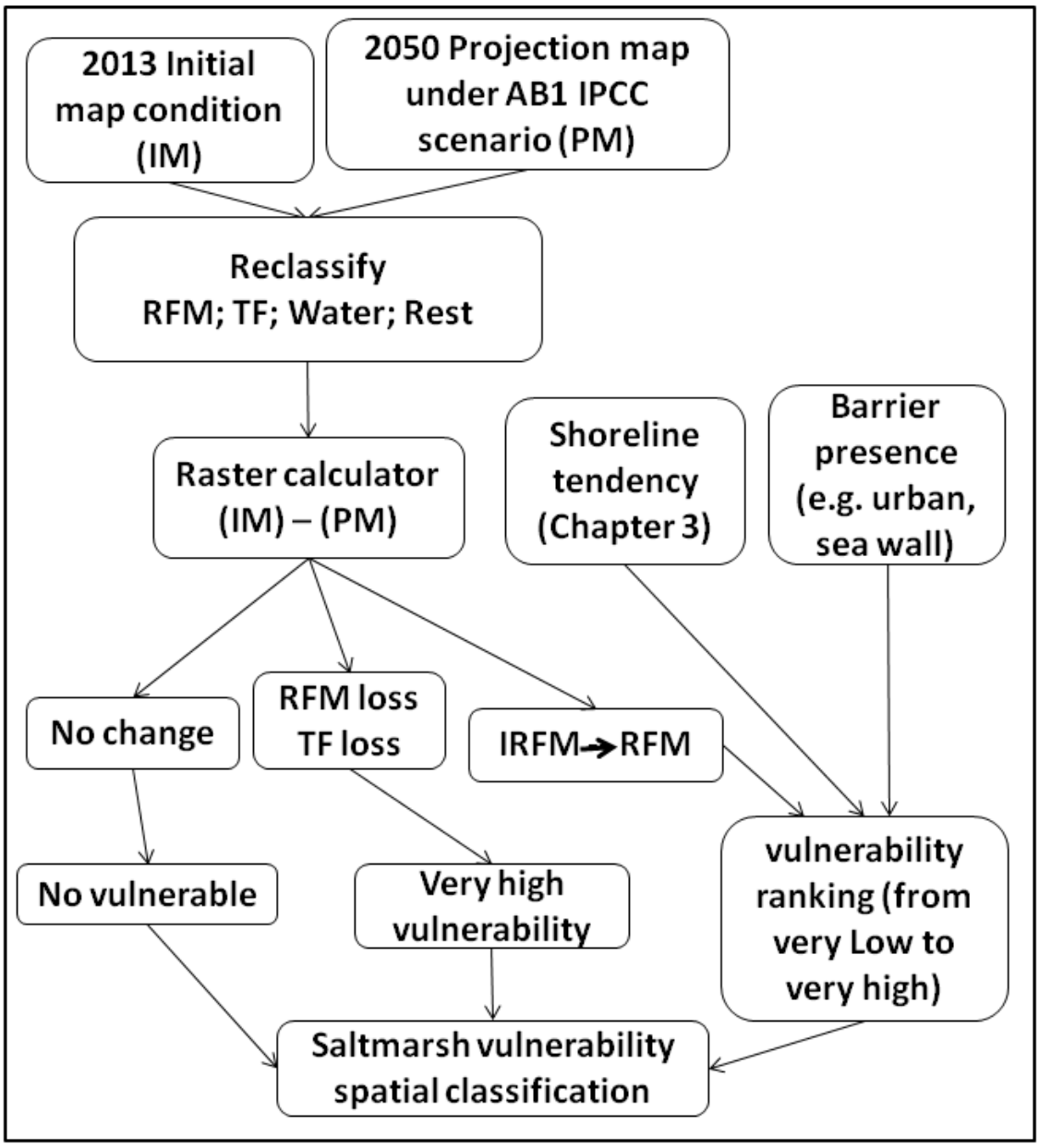

Figure 7.8 Flow diagram of the procedure for classifying saltmarsh according to its vulnerability to sea-level rise; where RegFM is regularly flooded marsh, TF tidal flat and IrregFM irregularly flooded marsh.

Table 7.8 Vulnerability ranking for classifying irregularly flooded marsh (in 2013) converted into regularly flooded marsh

	Very low	*Low*	*Medium*	*High*	*Very high*
Shoreline tendency	Growth	stable	stable	retreat	retreat
*Barriers presence (within 200 m from the shore)**	N/Y	N	Y	N	Y

*Double of the maximum retreatment tendency projected by 2050 based in the observed rate (Max horizontal erosion (96.2 m) * 2 ~ 200 m)

7.3.5. Comparison of SLAMM and UCL-modified SLAMM

The code of the SLAMM version 6.01 was modified by Pylarinou (2015) in order to suit the tidal sedimentary environments found in Europe, specifically those found in the UK. She modified the SLAMM source code to include a simplified land cover classification based on UK coastal and estuarine categories, and a set of modified habitat transition rules and amended rules specifying their relation to the tidal frame. Additionally, the modified SLAMM also runs the erosion module when the fetch is smaller than 9 Km, which it is quite normal in European saltmarshes. As this modified version of SLAMM addresses some of the initial issues found running the original version of SLAMM at the Odiel saltmarshes (erosion rates are not included if the fetch < 9Km), both models original and modified were run in order to investigate the differences between them and the importance to add a parameter such as horizontal erosion.

Table 7.9 UK default elevation ranges according to tidal ranges used in the modified SLAMM [Source: Pylarinou (2015)]

	SLAMM category No	Category Name	Default Min. Elev.	Default Min. Elev.
Estuarine Habitats	1	Dry Land	HAT	
	7	Transitional Marsh	MHWS	HAT
	20	Upper Marsh	MHW	MHWS
	8	Lower Marsh	MHWN	MHWN
	11	Tidal Flat	LAT	LAT
	17	Estuarine subtidal		
Open Ocean Habitats	12	Ocean beach	LAT	HAT
	13	Ocean flat	LAT	HAT
	19	Open Ocean		LAT

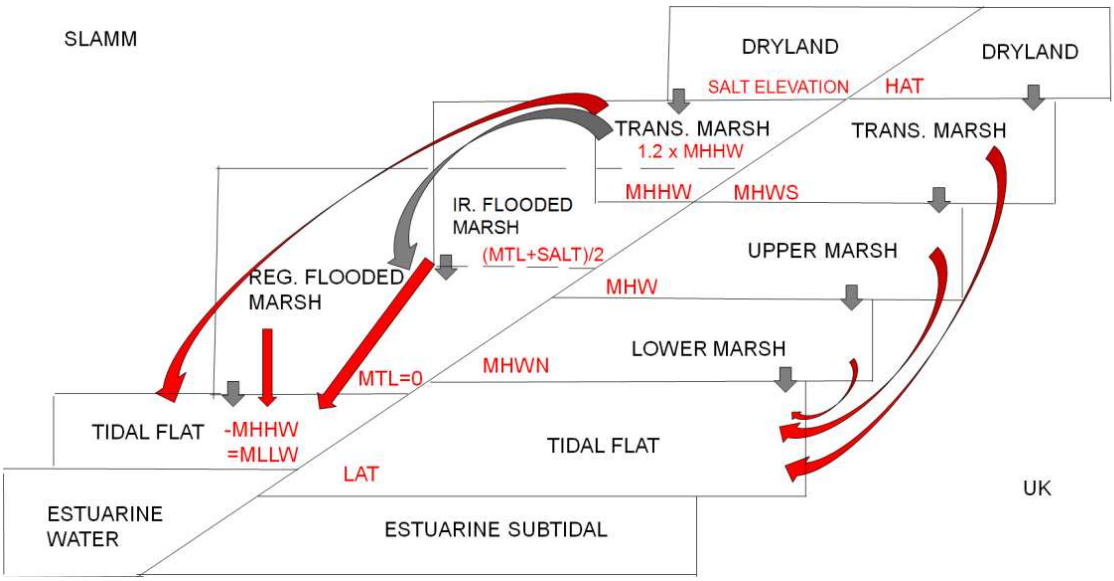

Figure 7.9 SLAMM decision tree modification including tidal ranges (where grey arrows state inundation, and red arrows erosion) [Source: Pylarinou (2015)]

Table 7.10 Site parameters for original and modified SLAMM [Source: Pylarinou (2015)]

ORIGINAL SLAMM CODE	MODIFIED SLAMM CODE
Historic Trend (mm yr^{-1})	Historic Trend (mm yr^{-1})
GT Great Diurnal Tide Range (m)	GT Great Diurnal Tide Range (m)
Salt Elevation (m above MTL)	Salt Elevation (m above MTL)
	HAT (m)
	MHWS (m)
	MHW (m)
	MHWN (m)
	LAT (m)
Marsh Erosion (m yr^{-1})	Marsh Erosion (m yr^{-1})
T. Flat Erosion	T. Flat Erosion
Reg. Marsh Accr. (mm yr^{-1})	Lower Marsh Accr. (mm yr^{-1})
Irreg. Marsh Accr. (mm yr^{-1})	Upper Marsh Accr. (mm yr^{-1})
Tidal Fresh Marsh Accr. (mm yr^{-1})	Tidal Fresh Marsh Accr. (mm yr^{-1})

7.4. Results

7.4.1. Sensitivity analysis based on spatial inputs

The results suggested that the role of elevation is the most important factor controlling model outputs. The role of the marsh habitat map is also important; however it has not the same impact on all the defined categories (Figure 7.10). The spatial model results for the tests performed are shown in Figure 7.11 and Figure 7.12. These results are reported by Test type and habitat category.

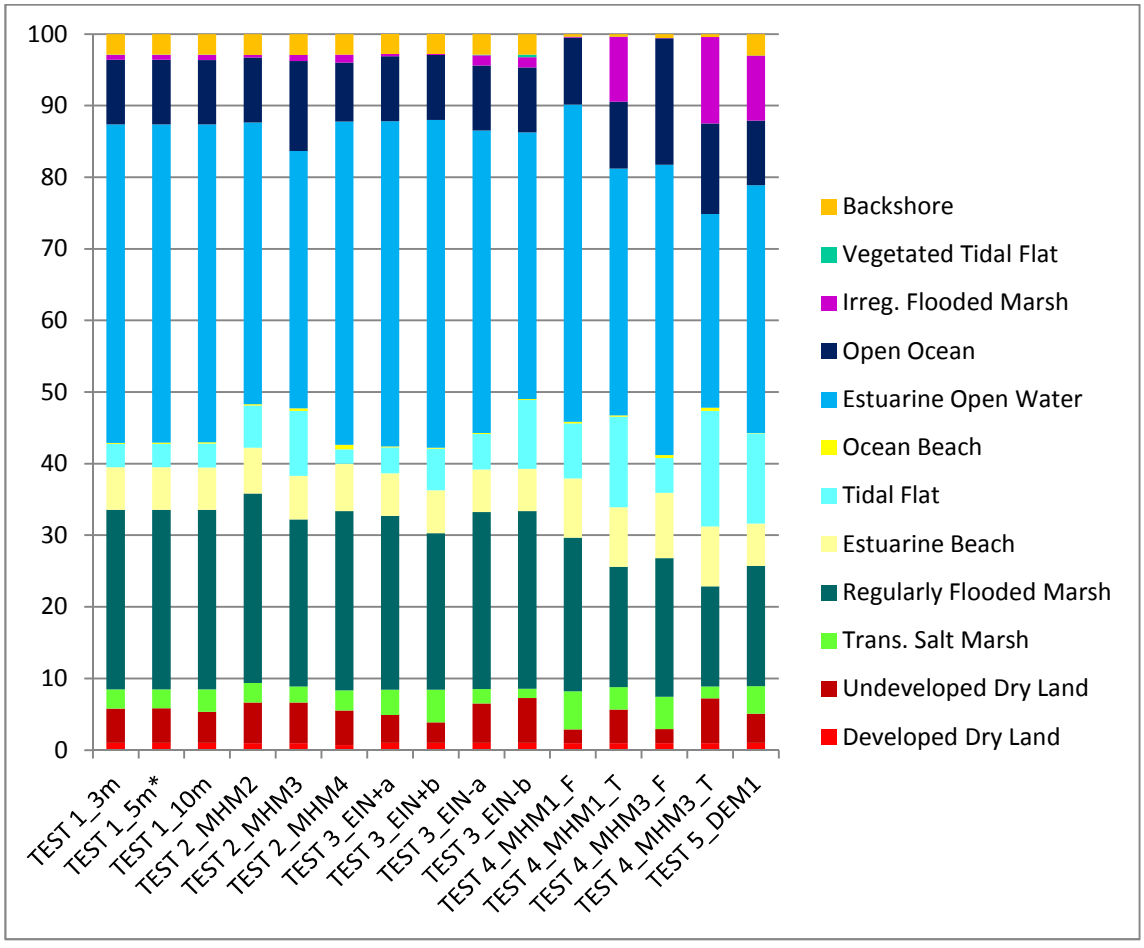

Figure 7.10 Surface area (%) of the outputs for 0.5 m sea level rise projected for 2100 and its variation per category when different inputs are used

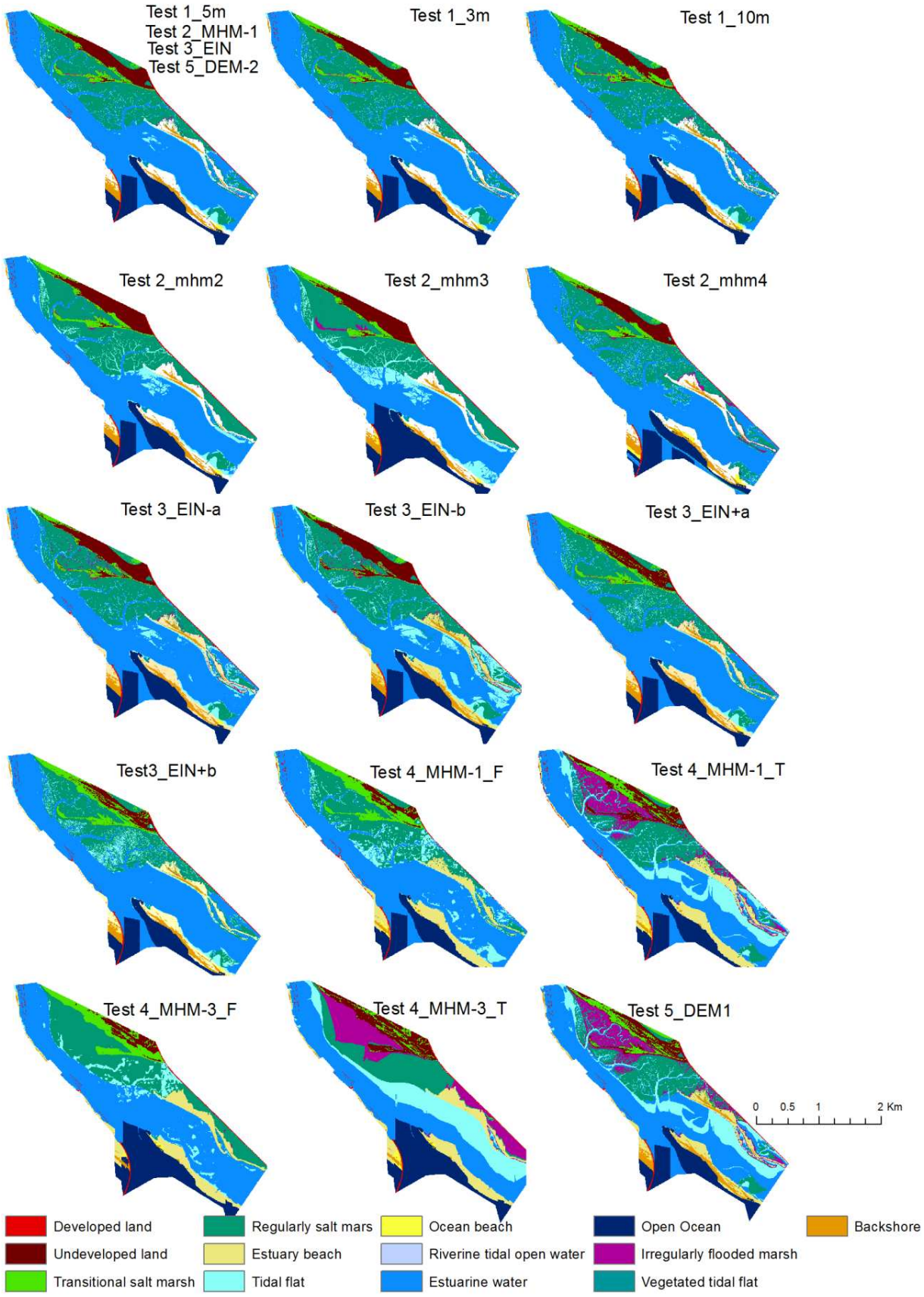

Figure 7.11 Model outputs per test for 0.5 m sea level rise projected for 2100 (see Table 7.2 and Table 7.5)

With regards to the test type, Test 1 showed that the cell size does not have a great impact in outputs when 3 m and 5 m cell sizes are used. However, the model outputs varied when 10 m cell size are used (Figure 7.12). Thus, to run SLAMM with a cell size smaller than 5 m is not recommended because it significantly increases the model execution time and only negligible change in model output. Although SLAMM is flexible with regard cell sizes, cell widths usually range between 5 m and 30 m depending on site and input data availability (Clough *et al*., 2010).

The sensitivity of SLAMM to different habitat maps is tested in Test 2 and results are compared in Figure 7.12. The results revealed that habitat map resolution considerably influences model results, highlighting the importance of the MHM, especially in open water, estuarine water and saltmarsh categories such as irregularly flooded marsh and vegetated tidal flat. The impact on the two first categories is due to elevation input ranges for these categories which are not defined in SLAMM. Thus, MHM strongly controls these two categories. For example, in Figure 7.12 creeks are highlighted in red due to in MHM3 only main channels are drawn. Thus, it is relevant to map the small creeks. In the case of MHM1 and MHM4, two maps of the same resolution are compared. The results here showed some differences as well. However, the differences are spread along the marsh area. These differences showed the importance of the habitat map on the model results. Thus, high resolution habitat maps that represent the complexity of the marsh habitats are essential.

Test 3 shows the importance of the habitat elevation range predefined within the model. Elevation inputs strongly control the model outputs, where variations of a few centimetres in the vertical influence model results (Figure 7.10; Figure 7.11). The result of this test showed the importance of correctly defining the habitat elevation ranges, which should also be site specific. Test 4 shows model output differences when the pre-processor tool is on and off using poor resolution DEM and either the high resolution or poor resolution (Figure 7.12) habitat maps. Results significantly changed when the pre-processor tool was turned on in both cases. The model is also sensitive to a change in the resolution of the habitat map when the pre-processor tool is on and a poor resolution DEM is used, showing important changes when both result maps are compared. Test 5 compares the model results when the LiDAR-derived DEM (DEM1) and modified (using a habitat-specific correction factor) DEM (DEM2) are used. The results (Figure 7.12) showed that small differences in the marsh elevation model (<0.5 m) affect model results.

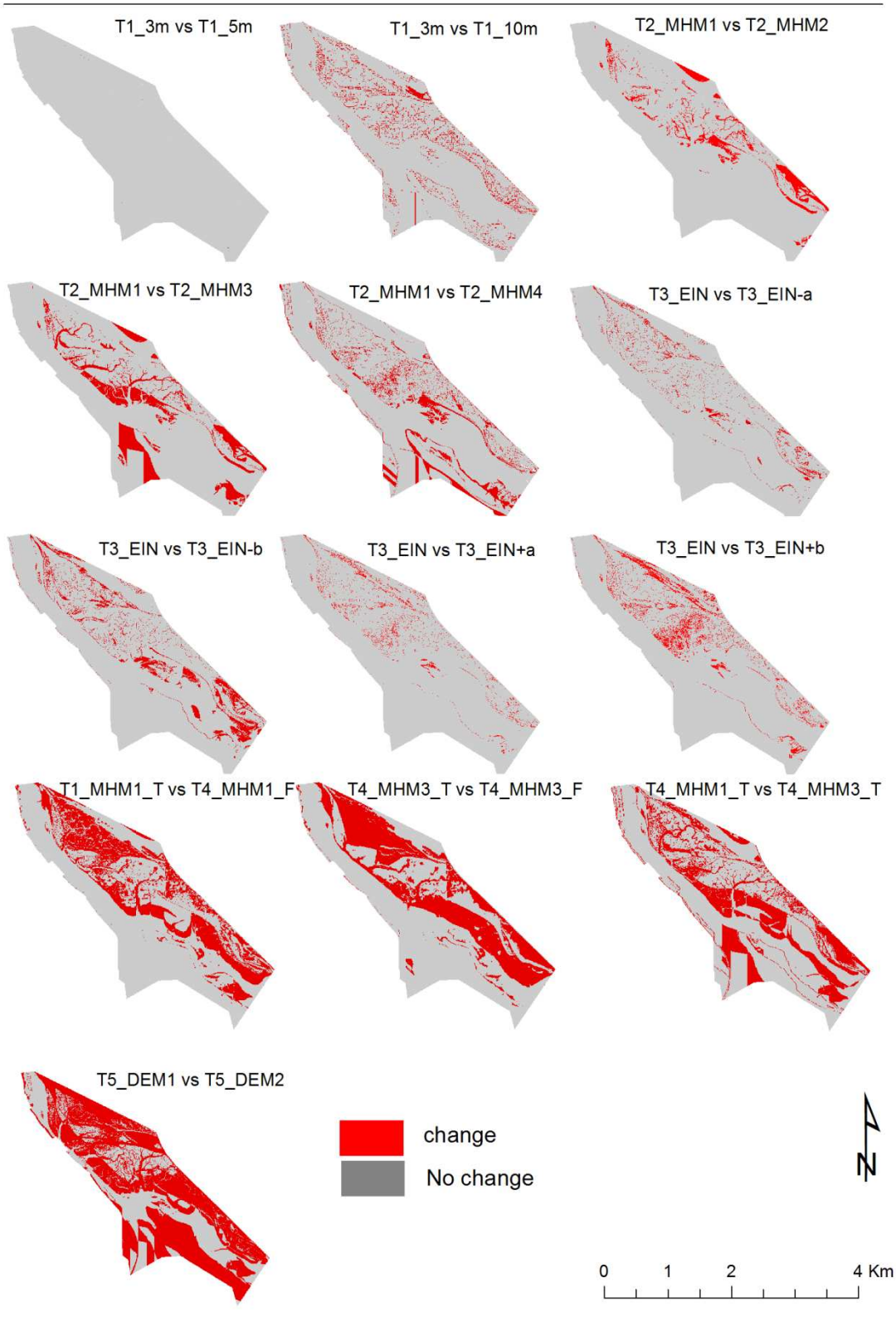

Figure 7.12 Comparison of the result obtained per test performed. T_i indicates the test carried (e.g. test 1, test 2, etc.) followed by the specific input that was modified within each test, where MHM refers to Map Habitat Map, DEM to Digital Elevation Model, EIN to elevation inputs and '5/10 m' to the cell size. The pre-processor tool was (by default) off in all the tests, and only in test 4 (T4) was on (stated by 'T') and off (stated by 'F') to compare the utility of high resolution habitat maps when high resolution DEM are not available (see Table 7.2 and Table 7.5).

With regard to habitat category, the variation in surface area by habitat type is shown in Figure 7.13 and the percentage of change respect the best estimate or base case (Test1_5m) is shown in Table 7.11. The outputs for *developed dry land* are quite stable, keeping roughly the same surface area in all tests except in Test2_MHM4 and Test4_MHM3_F. This is due to this category being protected when the model was run. The differences detected in Test2_MHM4 are due to the habitat map used (MHM4), where the area of *developed dry land* is less in the initial year (for example small dikes and jetties are not represented) and thus the surface area in the final year is expected to be less. The differences found in Test4_MHM3_F are due to the poor resolution habitat map and DEM used in this test. When the elevation pre-processor is used these differences are minimised as it is shown in Test4_MHM3_T.

The outputs *undeveloped dry land* results are less consistent between tests, and this is because this zone is not protected. Thus, habitat conversion occurs when sea level rises. Results showed that Test1_3m, Test1_5m, Test2_MHM4 and Test4_MHM1_T have similar model outputs, stating that for this category the model is not sensitive to cell size (3 m and 5 m), habitat map based on elevation and poor spatial resolution DEM (10 m) when the elevation pre-processor is used with high resolution habitat map (MHM1). This category is sensitive to poor resolution habitat maps and to DEM (when the pre-processor is not used or used with poor resolution habitat map).

For *transitional marsh*, Test1_3m Test2_MHM2 and Test2_MHM4 had similar outputs than the base case (Test1_5m); showing small variations respect the base case (0.1 % for Test1_3m and 2.3 % for Test2_MHM4). These results suggest that this category is not sensitive to cell size (when 3 m cell size was used), and is not very sensitive when MHM4 were used. However, when MHM2 and MHM3 were used the output surface was reduced 5% and 16 % respect the base case respectively. This category is also sensitive to cell size when this is greater than 5 m (~17.4 % output change respect the base case), to DEM spatial resolution (~100 % output change for T4_MHM1_F for instance) and to the elevation range predefined for this category (e.g. ~70 %. output change for EIN+b).

Regularly flooded marsh was not sensitive to cell size. Results for Test1 were almost identical to the base case and the percentage of change was 0.02% for 3 m cell size and 0.05 % for 10 m cell size (~ 1 ha). Habitat map resolution influences the model results. For example, when MHM2 and MHM3 were used, outputs differ from the best estimate (MHM1) by roughly 10 ha (~6 % and -7 % respectively). The results showed similar surface area when MHM1 and MHM4 were used (~0.2 % change respect the base case). Thus this category can be based on elevation data if a high resolution habitat map is not available. However, this category is very sensitive to DEM resolution and elevation ranges. When these variables were tested the results varied from 20 to 70 ha (from ~14 to 44 %).

	Dev. Dry Land	Undeve. Dry Land	Trans. Salt Marsh	Reg. Flooded Marsh	Estuarine Beach	Tidal Flat	Ocean Beach	Estuarine Water	Open Ocean	Irreg. Flooded Marsh	Vegetated Tidal Flat	Backshore
TEST1_3m	-0.10%	-0.06%	-0.11%	-0.02%	-0.05%	-0.55%	-0.19%	0.06%	0.08%	0.08%	-4.38%	-0.03%
TEST1_5m*	0.00%	0.00%	0.00%	0.00%	0.00%	0.00%	0.00%	0.00%	0.00%	0.00%	0.00%	0.00%
TEST1_10m	1.64%	-10.05%	17.43%	-0.05%	-0.44%	2.63%	1.52%	-0.10%	-0.56%	3.91%	20.47%	0.48%
TEST2_MHM2	-1.53%	17.21%	2.28%	5.58%	7.89%	80.02%	-0.01%	-11.47%	0.14%	-46.00%	-100.00%	2.09%
TEST2_MHM3	-1.53%	17.16%	-15.90%	-6.95%	2.80%	176.75%	124.94%	-19.04%	38.62%	23.66%	-100.00%	2.09%
TEST2_MHM4	-30.70%	0.58%	5.11%	-0.20%	11.93%	-39.88%	348.35%	1.57%	-9.20%	68.02%	-100.00%	0.03%
TEST3_EIN+a	0.08%	-19.57%	34.08%	-3.31%	0.08%	10.42%	0.08%	2.16%	0.08%	-51.72%	-75.53%	0.08%
TEST3_EIN+b	0.08%	-40.25%	70.24%	-12.70%	0.59%	77.66%	-20.40%	3.07%	0.08%	-83.42%	-97.81%	0.08%
TEST3_EIN-a	0.00%	14.19%	-23.97%	-1.45%	0.00%	51.28%	0.00%	-4.91%	0.00%	113.47%	197.54%	0.00%
TEST3_EIN-b	0.00%	29.67%	-49.80%	-1.23%	0.00%	192.87%	0.00%	-16.20%	0.00%	113.47%	917.52%	0.00%
TEST4_MHM1_F	-3.97%	-60.13%	100.36%	-14.57%	39.79%	134.74%	33.30%	-0.29%	3.13%	-82.53%	-81.79%	-86.36%
TEST4_MHM1_T	-3.97%	-2.88%	17.55%	-32.88%	39.90%	286.00%	29.09%	-22.46%	3.13%	1269.77%	-81.79%	-86.36%
TEST4_MHM3_F	-1.50%	-60.06%	70.39%	-22.78%	53.40%	49.42%	162.56%	-8.76%	94.54%	-91.74%	-100.00%	-80.23%
TEST4_MHM3_T	-2.44%	29.39%	-36.70%	-44.23%	40.84%	392.63%	201.39%	-39.20%	39.68%	1724.37%	-100.00%	-84.79%
TEST5_DEM1	0.00%	-15.45%	44.84%	-33.01%	-0.38%	284.38%	-73.06%	-22.18%	-0.01%	1271.51%	-99.73%	4.53%

Table 7.11 Percentage of change of the model outputs per category respect the base case (Test1_5m), changing one input layer at a time and keeping the model parameter constant.

Irregularly flooded marsh did not change with cell size nor when MHM2 was used. However, the results varied slightly when MHM3 (~2 ha less than MHM) and MHM4 (~2 ha more than MHM1) were used. This category was sensitive to DEM spatial resolution and elevation range. Outputs varied greatly (more than 50 ha) when the elevation pre-processor was used in Test4.

Tidal flat outputs were exactly the same when 3 and 5 m cell size were used, however they slightly changed (~1 ha) when cell size was 10 m. This category was very sensitive to habitat map variation, resulting in different outputs. For example, the surface area was approximately 20 ha for MHM1, 36 ha for MHM2, 55 ha for MHM3 and 12 ha for MHM4. The variation of surface area is due to representation: in MHM2 tidal creeks have been simplified and in MHM3 they have been deleted. In the case of MHH4 the channel system is also different to MHM1 as this map is based on elevation. This category was sensitive to DEM spatial resolution and elevation ranges. Outputs varied greatly (more than 50 ha) when the elevation pre-processor was used in Test4.

The vegetated tidal flat category in SLAMM is converted to water in the event of inundation or erosion, but it never generates new habitats within this category (menaning that reg. flooded marsh will not be converted into this category if inundation occur, but into tidal flat). Therefore this category never grows in surface area. Here, this category is only represented in MHM1 (it has not been included on the other habitat maps). Thus, there are only outputs for those tests where MHM1 was used. Outputs for different cell sizes were very similar and only slightly different when a poor spatial resolution DEM was used. The surfaces values greatly increased when the elevation habitat range was decreased.

Estuarine beach outputs are similar in all tests except for Test4, presenting variation smaller than 5 ha. The surface area of this category greatly changed (between 15 and 35 ha) when DEM3 was used. *Estuarine open water* was not sensitive to cell size and habitat elevation range; however, it was sensitive to habitat map and DEM resolution. SLAMM does not define an elevation range for this category, thus it was expected to be independent of elevation range. This category is based on DEM values and habitat map.

Open ocean outputs were very similar in all tests except when MHM3 is used. It means that this category is only sensitive to habitat maps and it only changed when MHM3 was used because in other maps the surface is exactly the same. *Ocean beach* was more sensitive to habitat maps than to DEM resolution. Outputs greatly changed in those tests where MHM3 and MHM4 were used. In contrast, *backshore* was very sensitive to DEM resolution, but was not sensitive to habitat map resolution. Outputs were very similar in

all tests except in those tests where DEM3 was used, where the surface area varied more than 13 ha (~80 % change).

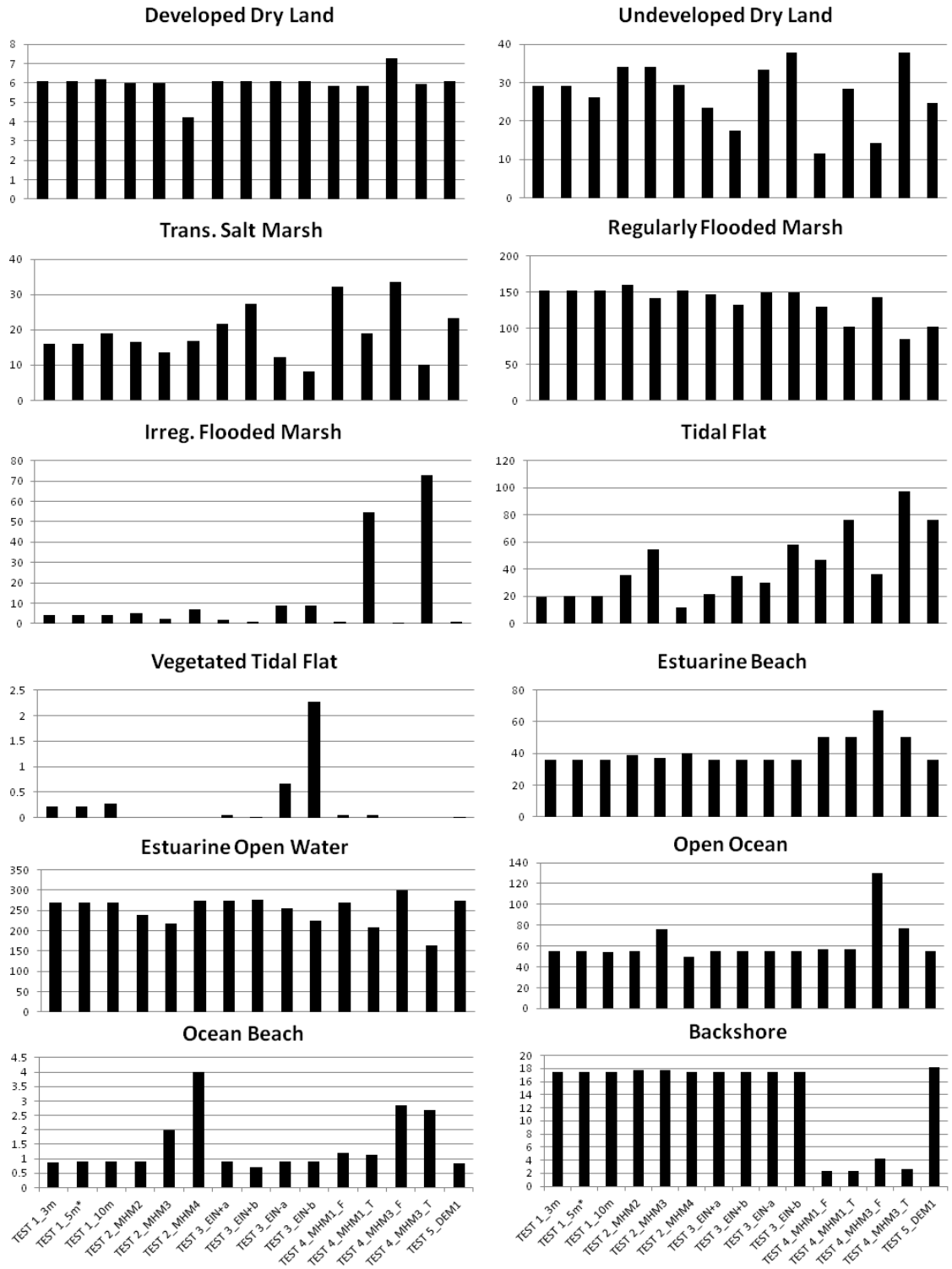

Figure 7.13 Habitat surface variation by test performed; x axis shows the surface area in hectares and y axis the different test applied. The optimum test across all categories is Test 1_5m (which uses the highest resolution input data). *This test out is the same than Test2_MHM1, Test3_EIN and Test5_DEM2

7.4.2. Potential impacts due to sea-level rise in the Odiel saltmarshes

The conversion habitat maps resulting from the Odiel saltmarshes simulation under the IPPC scenario A1B for 2050, 2075 and 2100 are shown in Figure 7.14. For A1B scenario, 2050 map showed the spatial distribution of habitats conversion projected by this time. Here, a large extension of *irregularly flooded saltmarsh* (nearly 1,500 ha; 90% of the initial surface) in 2013 is converted into *regularly flooded marsh* throughout the estuary. Only few sites in the upper estuary maintain the irregularly flooded marsh habitats. *Tidal flat* is reduced by roughly 40% (575 ha) in 2050, mainly in the main channels and creeks. However, new *tidal flat* are also predicted to occur in the mid (e.g. Enmedio Island) and low estuary (e.g. Saltes Island) due to conversion from *regularly flooded marsh*. *Undeveloped dry land* surface is also predicted to be greatly reduced by about 60%. This category is converted into *transitional marsh*. Thus, *transitional marsh* habitats are predicted to increase more 300 ha (~400%). Furthermore, *estuary beach*, *estuary water* and *open ocean* are predicted to increase roughly 40 ha, 1000 ha and 50 ha respectively. *Vegetated tidal flat*, *backshore* and *ocean flat* are predicted to be reduced by 94 % (~5 ha), 37 % (~12 ha) and 29 % (~13 ha).

The habitat conversion for 2075 sea-level rise projection under the scenario A1B were less pronounced. The surface area for all the habitats varied less than 2 ha in this year with respect to 2050 except for *tidal flat* and *regularly flooded marsh* habitats which varied in about 8 ha. *Undeveloped dry land*, *regularly flooded marsh* and *irregularly flooded marsh* increased their surface area. However, the surface area of *backshore*, *vegetated tidal flat*, *open ocean*, *estuary open water*, *ocean flat*, *tidal flat*, *estuary beach* and *transitional saltmarsh* was reduced. For 2100, the results showed that habitat conversion for this year were greater than for 2075 (Figure 7.14). *Undeveloped dry land*, *transitional saltmarsh*, *regularly flooded marsh, ocean flat*, *vegetated tidal flat*, *irregularly flooded marsh* and *backshore* reduced their surface area by 26 % (~57 ha), 96 % (~380 ha), 2 % (~51, 26 ha), 90 % (~26 ha), 80 % (~0.26 ha), 30% (~62 ha) and 30% (~6 ha) respectively. Nevertheless, *estuary beach*, *tidal flat* and *estuary open water* increased their surface area by 0.7 % (~0.5 ha), 41 % (~334 ha) and 10% (~180) ha respectively.

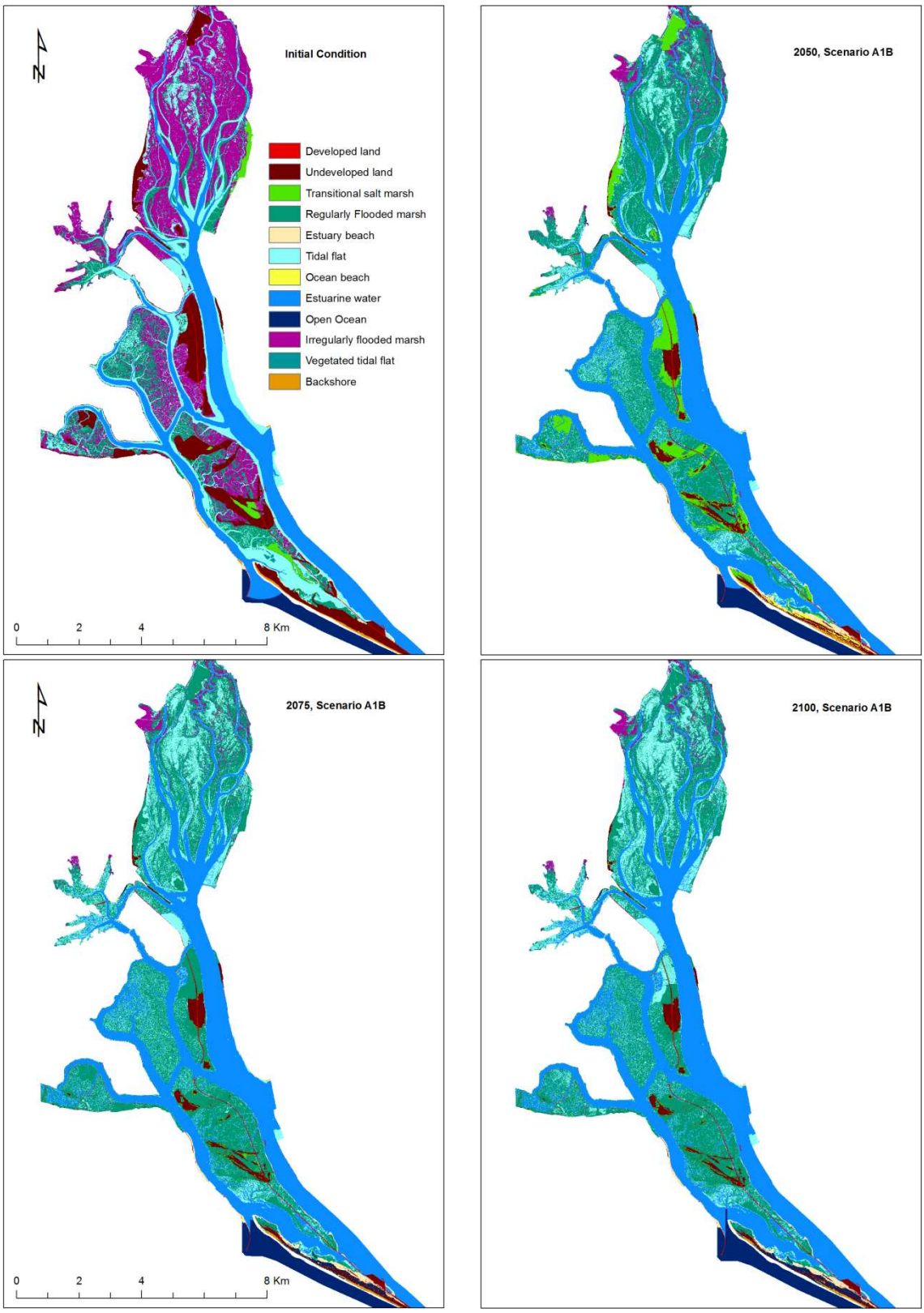

Figure 7.14 Potential habitat conversion due to sea-level rise in the Odiel saltmarshes using, using the IPCC A1B scenario

The variation found in the results under different scenarios is shown in Figure 7.15. Overall, the results for all categories were very similar for 2050 and presented more disagreement in 2075 and 2100 depending on the observed category. The surface area of the *undeveloped dry land* decreased more than 60 per cent in 2050 respect 2013 for all the scenarios as it is shown in Figure 7.15. For 2075, the results are more inconsistent revealing differences of almost 43 ha. However, not only the surface variation is different, the tendency of the predicted changes also varied. For example, in the scenario A1B the surface area for this category increased, while for the rest of scenarios this category decreased. These results revealed the inconsistency of different scenarios for 2075. For 2100, the results also varied among scenarios, showing differences of roughly 43 ha. However, for this year the tendency of this category is decreasing in all of them.

Transitional marsh increased in 2050 for all scenarios, maintaining similar values for all of them (between 395 and 399 ha). In 2075, this category dramatically decreased in all scenarios except in scenario A1B. While the transitional saltmarsh surface area was 397 ha for A1B scenario, for the rest range between 17 and 28 ha. Predictions for 2100 only varied few hectares compared with 2075 results for all scenarios except for A1B, where the surface area dropped from 397 to 17 ha. The results disagreement among scenarios for this year ranged between 14 and 28 ha.

Regularly flooded marsh surface increased more than double in 2050 projections for all scenarios, maintaining similar values for this year (maximum variation between scenarios was 2 ha). The projections in 2075 and 2100 presented more disagreements when all the scenarios were compared. In 2075, this category increased between 1 and 135 ha for all the scenarios except for A1F1 that decreased in 30 ha. The variation among scenarios for this year was 167 ha. In 2100, the projection for this category decreased for all scenarios, reaching variations up to 330 ha.

Tidal flat surface projected for 2050 decreased between 40 and 41% for all scenarios, presenting surface area variations between 1 and 19 ha. The projections for 2075 revealed increments in the surface area of this category for all scenarios except for A1B that decreased its surface respect 2050. Total variation among scenarios projection was 349 ha. For 2100, there was an increment of this category under all scenarios. However, the absolute values of the surface area varied considerably, showing differences up to 360 ha between scenarios.

Irregularly flooded marsh decreased its surface area in 89% approximately for all scenarios in 2050. Absolute values went down from nearly 1,900 ha in 2013 to 200 ha in 2050. Projections for 2075 presented disagreements among scenarios. While the surface area increased about 8 ha for A1B scenario, decreased between 7 and 47 ha for the other scenarios. Differences among scenarios went up to 70 ha for this year. Projections for

2100 showed that this category decreased under all scenarios. However, the results among scenarios for 2100 varied more than for 2075, reaching differences of 115 ha.

Vegetated tidal flat surface area projected for 2050 decreased greatly (94%) for all the scenarios, reducing its surface area from nearly 6 ha to less than half hectare. Here, the results for all scenarios were very similar and the maximum variation between them was 0.03 ha. For 2075, the decreasing tendency carried on with a lower rate. However, differences between scenarios were greater for this year (~0.22 ha). For 2100, this category also decreased under all scenarios, varying between 0.14 and 0.03 ha. It should be noted that SLAMM does not consider new creation of this category.

Estuarine open water surface area projected for 2050 was very similar for all the scenarios, reaching values of roughly 2,345 ha (68% increment in the surface area respect 2013). In 2075, the surface area of this category also increased but the results varied between 2 and 135 ha depending on the scenario. Projections for this category in 2100 also predicted increments in the surface area for all scenarios. The disagreements among them varied between 12 and 101 ha.

Projections for *estuary beach* revealed an increasing tendency for all scenarios and years, except for A1B scenario in 2075. Between 2013 and 2050, these habitats are predicted to increased in about 41 ha for all scenarios (maximum variation= 0.7 ha). In 2075 and 2100, the projections showed increasing of less than haft hectare respect 2050 and 2075 respectively. The variation between scenarios was similar for both years, reaching a maximum of 0.8 ha.

Backshore habitats were predicted to be reduced in about 37% in 2050 respect the surface area in 2013. The total surface area was projected to be reduced from 32 ha in 2013 to 20 ha approximately in 2050. Variations between scenarios for this year were smaller than 0.5 ha. In 2075, the surface area for the scenario A1B increased slightly from the results obtained for 2050 (0.2 ha). However, for the rest of the scenarios the surface area was reduced in 2075 between 2 and 5 ha depending on the scenario. The surface area of this category was also predicted to be reduced in 2100 for all scenarios. For this year, results projected for different scenarios varied between 11 and 16 ha.

Ocean flat projected for 2050 reduced their habitats in about 28%. The total surface area was predicted to decrease from about 40 ha in 2013 to 28 ha in 2050. The maximum variation between scenarios was 0.5 ha. In 2075, these habitats are also projected to be reduced. However, there are significant disagreements in the quantity. For example, while the surface area under A1B scenario was predicted to be roughly 28 ha, under A2 scenario was 3.6 ha. In 2100, projections under different scenarios are more consistent than for 2075, ranging between 3.2 and 4.5 ha.

Finally, open ocean is projected to increase in the next decades. Projections for 2050 showed that these habitats increased 21% over the 2013 area and there is consistency between different scenarios (259 ha approximately). Projections for 2075 were less consistent and showed disagreements between scenarios. For example, for the scenario A1B this category decreased slightly (0.23 ha) respect 2050. For the rest of scenarios this category increased between 44 and 55 ha. For 2100, the projected results were more consistent, increasing for all scenarios. This category increased 68 ha for A1B scenario, and between 14 and 24 ha for the rest.

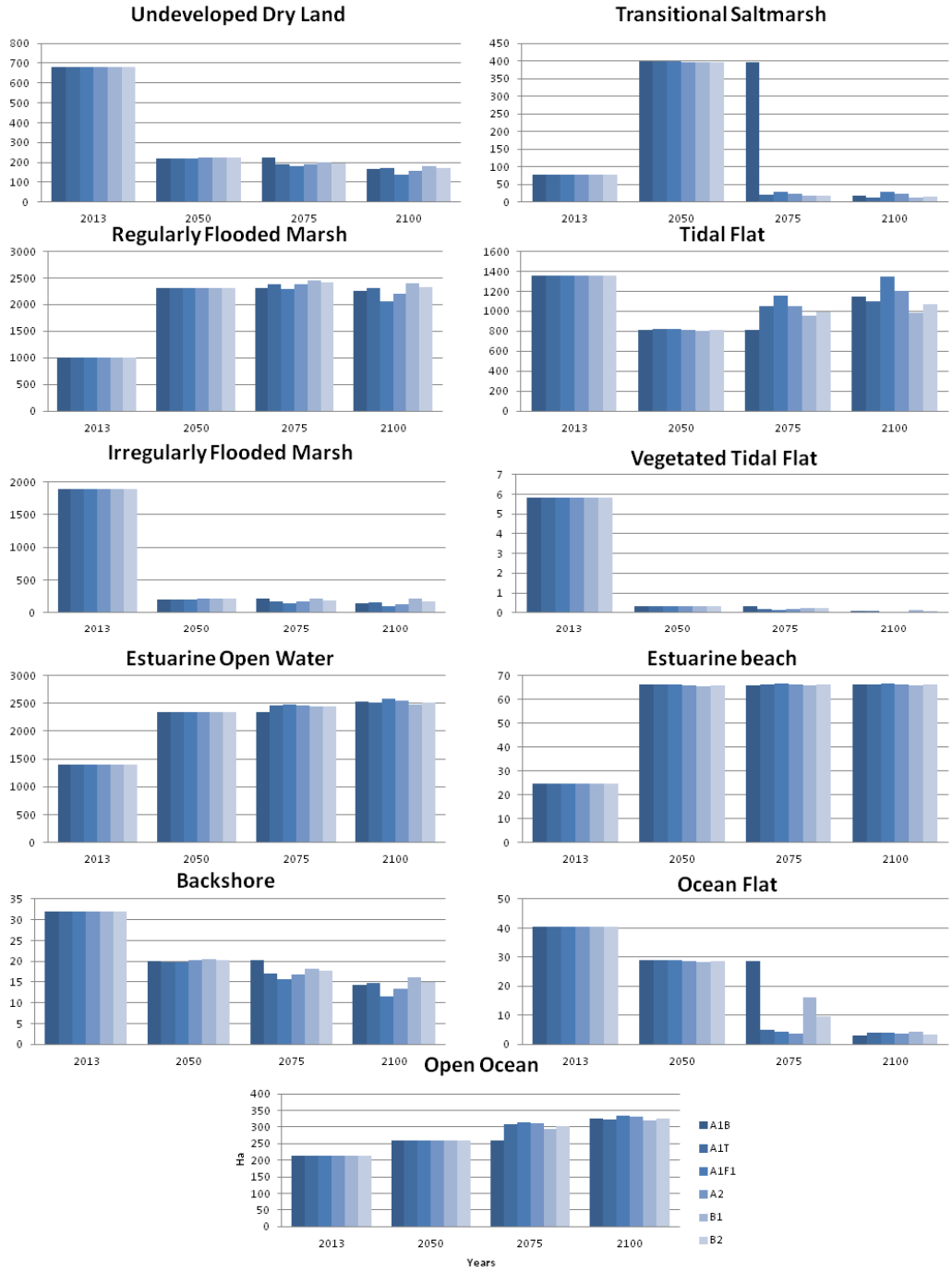

Figure 7.15 Potential Odiel saltmarshes habitat conversion (in ha) due to sea-level rise (A1B, A1T, A1F1, A2, B1 and B2 IPCC scenarios) projected for 2050, 2075 and 2100.

7.4.3. SLAMM uncertainty analysis

In order to assess whether the outputs follow a linear relationship, previous results from the sensitivity analysis based on inputs factors were assessed (Table 7.12). Change in the outputs (surface area of each habitat type) respect the base case was computed for every simulation run in SLAMM varying input factors by plus or minus 5, 10 and 15 %. Overall, although changes in model outputs (surface area) respect the base case varying inputs factors seemed to be quite linear for all habitat types, 'extreme' input values showed non-linear behaviours (highlighted cells in Table 7.12). These previous results also revealed that some habitats are more sensitive than others to variations in input factors and some habitats are not sensitive to certain input factors at all. For example, *undeveloped dry land* and *transitional marsh* are only sensitive to variations in sea-level rise and local historical trend, and *regularly flooded marsh* was sensitive to all parameters except great diurnal tidal range. The great diurnal tidal range variations only affected a few habitats such as *estuary beach*, *ocean flat*, *estuary open water* and *open ocean*.

In saltmarsh habitats particularly, model outputs were most sensitive to changes in sea-level rise projected to 2100 and saltmarsh accretion (Table 7.12). For example, by decreasing saltmarsh accretion by 15 %, the *regularly flooded marsh* area decreased by 3.2 % (~ 66 ha) and *tidal flat* area increased by 6.5 % (~ 66 ha); increasing sea level-rise by 15 % resulted in a 2.9 % (~ 61 ha) decrease in *regularly flooded marsh* area and a 1.5 % (~ 15 ha) increase in *tidal flat*. Saltmarsh model outputs were less sensitive to site historical sea-level rise, and were not sensitive to other parameters. *Irregularly flooded marsh* was less sensitive to sea-level rise (projected by 2100) and accretion rates than *regularly flooded marsh*, decreasing less than 4 ha when sea-level rise increased by 15 % and less than 1 ha for the same variation in saltmarsh accretion rates.

Table 7.12 Changes in the surface area (model outputs in hectares) of the each habitat type in comparison to the base case (parameters of the study site), varying ± 5, 10 and 15 % of inputs parameters directly related to saltmarsh habitats for a 1 m sea-level rise scenario in 2100; where SLR_{2100} is the projected sea-level rise by 2100, *HisTrend* site historical trend of sea-level rise, *GT* (great diurnal tidal range), *Reg-Accr* regularly flooded marsh accretion and *Irreg-accr* irregularly flooded marsh accretion. Numbers in bold indicate the maximum magnitudes of change for each input parameter, and highlighted cells state 'non-linear' behaviours for each input parameter in each category.

Habitat type	%	SLR_{100} (+)	SLR_{100} (-)	His Trend (+)	Hist Trend (-)	GT(+)	GT(-)	Reg-Accr +	Reg-Accr -	Irreg-Accr +	Irreg-Accr -
Dry Land	5	-3.74	4.33	-1.45	1.35	0.00	0.00	0.00	0.00	0.00	0.00
TransM	5	3.09	-3.68	1.21	-1.14	0.00	0.00	0.00	0.00	0.01	-0.01
RegFM	5	**-26.0**	**34.13**	**-9.28**	**10.17**	0.00	0.00	**37.21**	**-28.1**	**-0.36**	**0.35**
EstuBeach	5	-0.19	-0.01	-0.06	0.06	**0.57**	**-0.63**	0.00	0.00	0.00	0.00
Tidal Flat	5	8.26	-13.4	3.51	-4.19	0.00	0.00	**-37.2**	**28.1**	0.00	0.00
OceBeach	5	-1.35	1.38	-0.42	0.42	0.03	0.00	0.00	0.00	0.00	0.00
Ocean Flat	5	-0.06	0.03	-0.01	0.01	0.04	-0.18	0.00	0.00	0.00	0.00
EstuWater	5	**19.4**	**-22.5**	**6.30**	**-6.53**	**-0.59**	**0.63**	0.00	0.00	0.00	0.00
Open Ocean	5	2.31	-2.13	0.75	-0.72	-0.04	0.18	0.00	0.00	0.00	0.00
IrreFM	5	-1.30	1.49	-0.43	0.46	0.00	0.00	0.00	0.00	**0.35**	**-0.34**
Backshore	5	-0.36	0.38	-0.12	0.13	0.00	0.00	0.00	0.00	0.00	0.00
Dry Land	10	-7.09	9.92	-2.61	2.78	0.00	0.00	0.00	0.00	0.00	0.00
TransM	10	5.84	-8.19	2.17	-2.34	0.00	0.00	0.00	0.00	0.01	-0.01
RegFM	10	**-45.9**	**79.30**	**-17.8**	**21.20**	0.00	0.00	**86.5**	**-49.6**	**-0.74**	**0.69**
EstuBeach	10	-0.40	-0.21	-0.17	0.05	**1.11**	**-1.23**	0.0	0.00	0.00	0.00
Tidal Flat	10	10.9	-33.6	6.40	-8.52	0.00	0.00	**-86.5**	**49.6**	0.00	0.00
OceBeach	10	-2.72	2.65	-0.83	0.86	0.03	-0.03	0.00	0.00	0.00	0.00
Ocean Flat	10	-0.15	0.04	-0.03	0.02	0.05	-0.55	0.00	0.00	0.00	0.00
Estu Water	10	**38.1**	**-49.5**	**12.47**	**-13.8**	**-1.14**	**1.26**	0.00	0.00	0.00	0.00
Open Ocean	10	4.58	-4.32	1.50	-1.41	-0.05	0.55	0.00	0.00	0.00	0.00
IrreFM	10	-2.44	3.20	-0.87	0.94	0.00	0.00	0.00	0.00	**0.73**	**-0.68**
Backshore	10	-0.66	0.77	-0.23	0.25	0.00	0.00	0.00	0.00	0.00	0.00
Dry Land	15	-10.6	15.54	-3.69	4.25	0.00	0.00	0.00	0.00	0.00	0.00
TransM	15	8.97	-12.5	3.05	-3.60	0.00	0.00	0.00	0.00	0.0	-0.02
RegFM	15	**-61.4**	**127.4**	**-25.6**	**33.35**	0.00	0.00	**137.9**	**-66.1**	**-1.15**	**1.03**
EstuBeach	15	-0.62	-0.49	-0.18	-0.01	**1.62**	**-1.79**	0.00	0.00	0.00	0.00
Tidal Flat	15	14.8	-61.7	8.20	-13.1	0.00	0.00	**-137.9**	**66.1**	0.00	0.00
OceBeach	15	-4.10	3.76	-1.33	1.34	0.03	-0.09	0.00	0.00	0.00	0.00
Ocean Flat	15	-0.28	0.04	-0.05	0.03	0.05	-1.16	0.00	0.00	0.00	0.00
Estu Water	15	**50.9**	**-71.8**	**18.94**	**-22.0**	**-1.65**	**1.88**	0.00	0.00	0.00	0.00
Open Ocean	15	6.69	-6.57	2.26	-2.09	-0.05	1.16	0.00	0.00	0.00	0.00
IrreFM	15	-3.48	5.16	-1.28	1.46	0.00	0.00	0.00	0.00	**1.13**	**-1.01**
Backshore	15	-1.00	1.18	-0.35	0.38	0.00	0.00	0.00	0.00	0.00	0.00

Input factors in saltmarsh habitats were then qualitatively evaluated using the Morris method (Morris, 1991). The results from this analysis are shown in (Figure 7.16), indicating the 'important input factors' that influence uncertainty in the outputs based on

1 m sea-level rise scenario by 2100 (e.g. *Reg-accre, Irre-accre, HisTrend* and *GT*) and based on different scenarios of sea-level rise (SLR_{2100}) input factor, where were used. The interpretation of these results was facilitated by plotting the mean elementary effect (μ) on the vertical axis versus the standard deviation of the elementary effects (σ) as shown in Figure 7.16. The horizontal distance from the origin (μ - coordinate) reflects the qualitative importance of an input factor for a given output, while the vertical distance from the origin (σ- coordinate) indicates the presence of interactions. Results revealed that only four input factors were deemed to have a significant impact on model outputs in saltmarsh habitats at year 2100: the accretion rate of both *regularly flooded marsh* (*Reg-accre*) and *irregularly flooded marsh* (*irregFM*), site historical sea-level rise (*HisTrend*), and the projected sea-level rise (SLR_{2100}) by 2100. For example, SLR_{2100} input factor played an important role in all saltmarsh habitats, and *HisTrend* was found to be less sensitive for all the habitats as it was expected. *RegFM* accretion rates on the other hand were only significant for *regularly flooded marsh* and *tidal flat*. Interestingly, *RegFM* accretion rates were more important in the *regularly flooded marsh* and *tidal flat* than SLR_{2100}. None of the saltmarsh habitats were sensitive to the great diurnal tidal range (*GT*) inputs, showing that this input factor does not control uncertainty in these habitats.

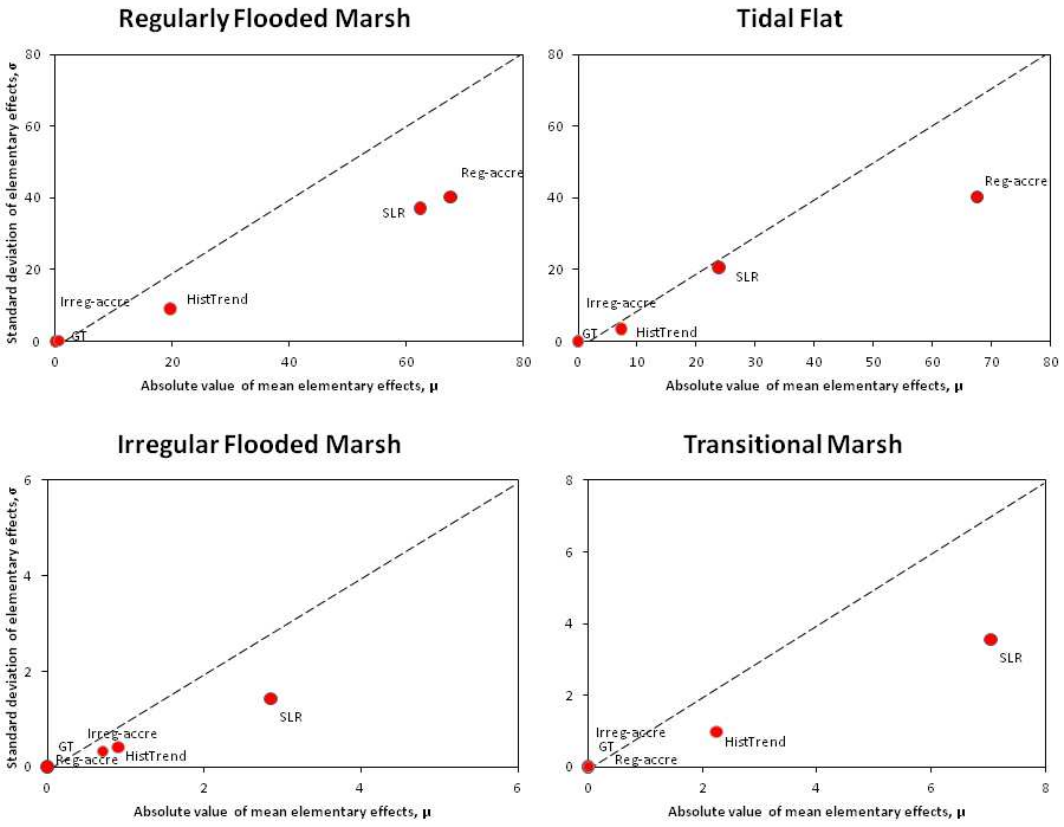

Figure 7.16 Results from Morris method showing the important input factors that influence uncertainty in the output based on 1 m sea-level rise scenario by 2100, where SLR_{2100} is the projected sea-level rise by 2100, *HisTrend* site historical trend of sea-level rise, *GT* (great diurnal tidal range), *Reg-accre* regularly flooded marsh accretion and *Irre-accr* irregularly flooded marsh accretion

The results from the input-output relationship have been focused on the saltmarsh outputs: *regularly flooded marsh*, *irregularly flooded marsh*, *tidal flat*, *transitional saltmarsh* and *estuarine open water*. The output variations obtained for these categories when the input factors were changed (varying one input factor at a time in SLAMM) is shown in Figure 7.17. Model output results showed that *estuary water* and *regularly flooded marsh* followed an inversely proportional relationship for all the input factors as was expected: for example, when the *regularly flooded marsh* surface area increases, the *estuarine water* decreases and vice versa. This is due to the *regularly flooded marsh* converting to *tidal flat* when inundation occurs, and conversion of *tidal flat* continues to *estuarine water*. The *tidal flat* behaviour showed a non-linear relationship when inputs factor were changed. Results showed negative changes in *tidal flat* area with respect to the baseline case when the input values were either increased or decreased for all the input factors, except for the *irreg-accre*. In SLAMM, the *tidal flat* category is integrated in the *regularly flooded marsh* accretion model, explaining the particular behaviour of this category in Figure 7.17. One would expect to see positive change in this area in relation to negative changes in the input values with respect to the baseline in all input factors, but this behaviour is only observed in the *irreg-accre* input factor. In the case of the *transitional* and *irregularly flooded marsh* surface area is projected to be lost under all the sea-level rise scenarios by 2100, and in general the remaining area showed small changes to the variation of all input factors. *Irregularly flooded marsh* showed slightly bigger changes in area when the *irreg-accre* rates were varied, following a proportional relationship between outputs and inputs. The predicted input-output relationship for sea-level rise results revealed that an 80% (0.2 m by 2100) decrease in sea-level rise of 1 m would mean an increase of 1,617 ha in *regularly flooded marsh*, a 280 ha decrease in *tidal flat* and a 1,536 ha decrease in estuarine open water when compared to the output base case for year 2100. If the sea-level rise is +80% (1.2 m; it should be note that the base case is 1 m and the change is 0%), then the change in output will be -444, -955 and +1,455 ha change respectively. Two interesting output behaviours that are closely related to each other are observed in the *regularly flooded marsh* and *tidal flat* categories:

A. With regard to the *regularly flooded marsh* output variation, results showed that negative variations from the baseline case closer to -1 (meaning a SLR_{2100} input closer to 0 m by 2100) created little impact in the *regularly flooded marsh* outputs. This is due to the accretion rates being higher than the potential sea-level rise by 2100. When the sea level rises more than 0.5 m by 2100 (which is roughly the accretion expected by that time in the baseline case), the surface area of the *regularly flooded marsh* dramatically drops with increase in SLR_{2100} until it reaches the value of 1.3 m. A SLR_{2100}

input value ≥1.3 m or higher (positive change with respect to the baseline case; Figure 7.18), *regularly flooded marsh* continues to lose area with increasing SLR. Changes in this category are much less dramatic, showing less variation in surface area with respect to the baseline case (ha). This behaviour is explained by the fact that lower SLR_{2100} values (in combination with the base case accretion rates) will prevent the loss of the initial (2013) *regularly flooded marsh* surface area by 2100, but it will not prevent the loss of *irregularly flooded marsh* and conversion to *regularly flooded marsh* will occur. Additionally, conversion from tidal flat to *regularly flooded marsh* will also occur due to increase in elevation on this habitat. These particular situations (with SLR_{2100} values ≤0.5 m) will considerably increase the surface area of the *regularly flooded marsh* as well as the differences with the base case. For SLR_{2100} values greater than the base case the *regularly flooded marsh* and SLR input change seems to follow a linear behaviour.

B. With regard to the *tidal flat* outputs, negative variations in the 'SLR_{2100}' input factor closer to -1 m change with respect to the base case (Figure 7.17) (-1 m SLR_{2100} change over the base case means 0 m sea-level rise by 2100) follow a decrease tendency. This behaviour is explained by the fact that lower values of SLR_{2100} (in combination with the base case accretion rate; ~ 0.5 m by 2100) will increase the initial (2013) tidal flat vertical elevation by 2100. The new higher elevation condition prevents permanent inundation in some of the lower elevation ranges in this category, and conversion from *tidal flat* to *regularly flooded marsh occurs* in the higher part of its elevation range. Due to the conversion into *regularly flooded marsh*, part of the *tidal flat* total surface area is lost. As the sea-level rises and gets closer to the 0.5 m inflexion point, *tidal flat* loss increases due to inundation of this category at the lower end of its elevation range reducing even more the total surface area of this category. This situation thus explains the unexpected initial drop in area change with respect to the baseline case. SLR_{2100} input values greater than 0.5 m and smaller than 1 m lead to a switch in the tidal flat behaviour, decreasing the hectare differences respect the base case as the input value gets closer to 1 m (base case). This behaviour is explained by the fact that sea-level rise is higher than the total accretion by 2100, and part of *regularly flooded marsh* is converted into tidal flat. This situation carries on until 1 m SLR_{2100}, where the tendency changed again establishing another important threshold. For SLR input values greater than 1 m, *tidal flat* follows the expected behaviour showing negative changes with respect to the baseline case as SLR_{2100} input values increase. In these cases, the sea level is much higher (more than double) than total accretion resulting in permanent inundation of *tidal flat* and *regularly flooded marsh*. Thus, greater surface area of *tidal flat* is lost with respect to the baseline case.

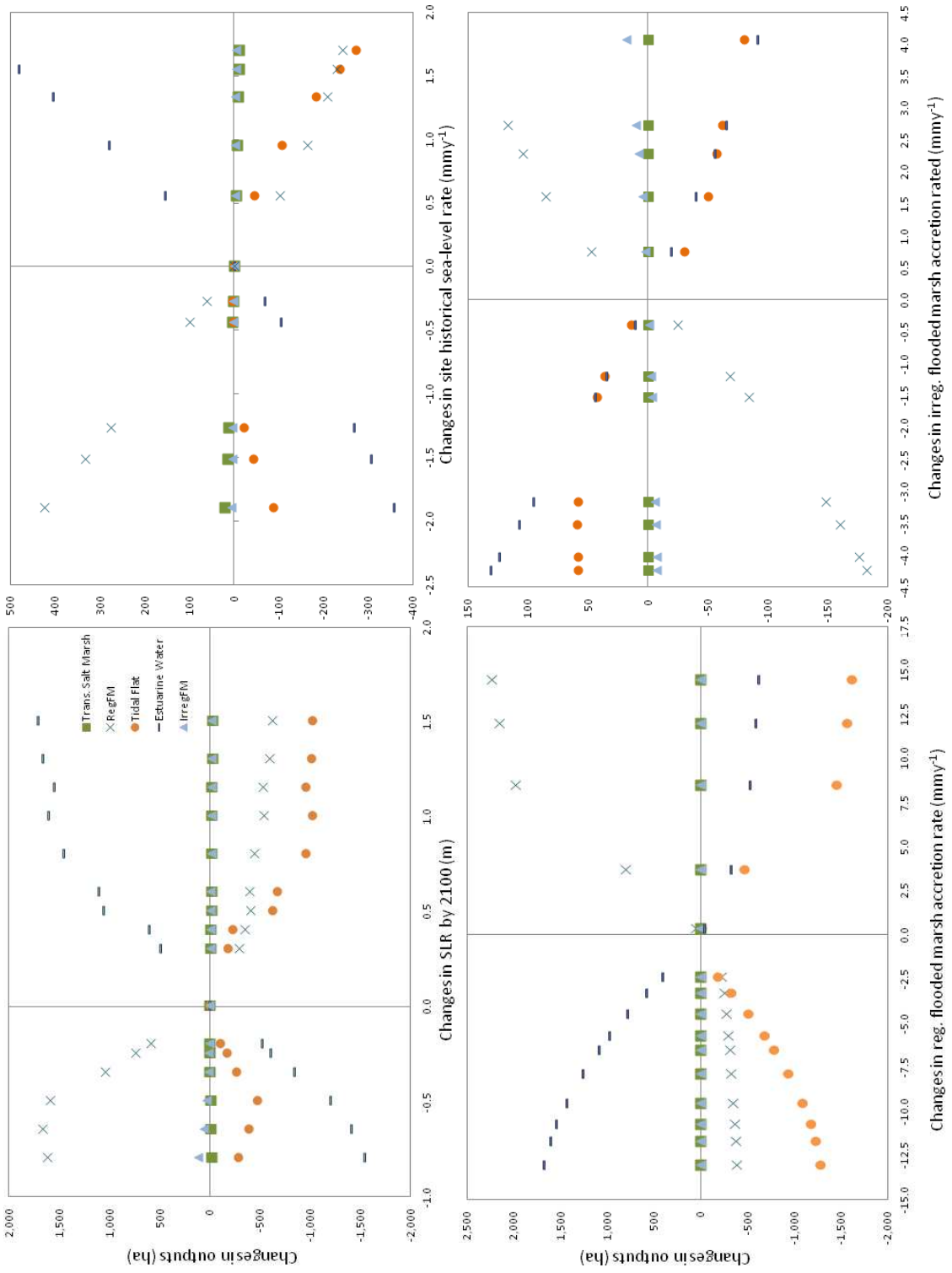

Figure 7.17 Input-output relationship for saltmarsh categories in SLAMM (v. 6.2), where one input factor was change at a time while the rest were held constant and equal to base case. The vertical axis states the changes in hectares of each saltmarsh category in comparison with the base case, and the horizontal axis the changes in the input factor values respect the base the case.

The uncertainty analysis based on the 'full calculation' approach (with linear interpolation) provided an appreciation of the range of variability of each output (habitat surface area). This work is primarily interested in how the 'total saltmarsh' fares in the

simulations, thus, for simplicity, the saltmarsh categories have been added together. The 'total saltmarsh' is defined as the combination of *regularly flooded marsh*, *irregularly flooded marsh*, and *transitional marsh* categories. For the total saltmarsh, the uncertainty is assessed in two ways. The first assessment is based on the uncertainty of the future sea-level rise by 2100 (keeping the other input factors constant). The second assessment is based on the uncertainty of the *Htrend*, *reg-accre* and *irreg-accre* input factors for a 1 m sea-level rise by 2100. For a given set of ten thousand simulations, the total saltmarsh changes were ordered from the largest negative to largest positive, and frequency distribution were calculated as shown in Figure 7.18 and Figure 7.19.

The effect of the 1 m scenario sea-level rise using the full range variability of input factors (*Histrend*, *reg-accre* and *irreg-accre*) was evaluated by analysing the variability of the outputs. Interestingly, total saltmarsh showed a bimodal distribution, one peak of which suggested a decrease in surface area while the other peak showed an increase (Figure 7.18). Overall, results revealed that there are 4,401 simulations that showed a decline of the total saltmarsh, which can be interpreted as a 44 % chance of this happening, where 214 simulations showed a complete elimination of marsh (~ 1 % chance of occurring). On other the hand, there are 5,599 simulations, where total saltmarsh increasing is observed (~ 56 % chance of happening).). This is encouraging as it demonstrates that saltmarsh creation is possible under a rising sea-level given a suite of favourable factors (related to sedimentation rates).

The bimodality observed in the output distribution states that there are combinations of input can result in either gain or loss of the saltmarsh surface area respect the base case. It should be noted that the variability in the saltmarsh categories (Figure 7.16) was mainly attributed to the individual effects of accretion rates (*reg-accre*) and SLR_{2100}. In the case of *regularly flooded marsh* (the category that contributes the most to the total saltmarsh hectares by 2100), *reg-accre* was the most important input factor controlling output variability. The gain in saltmarsh surface area can be due to *tidal flat* being converted to saltmarsh (as a result of increasing vertical elevation as observed in Figure 7.17) or due to higher-elevation coastal habitats being converted to saltmarsh (saltmarsh transgression). However, the loss of saltmarsh is because the saltmarsh is converted to *tidal flat*, where sedimentation rates are usually greater and could lead to new saltmarsh generation.

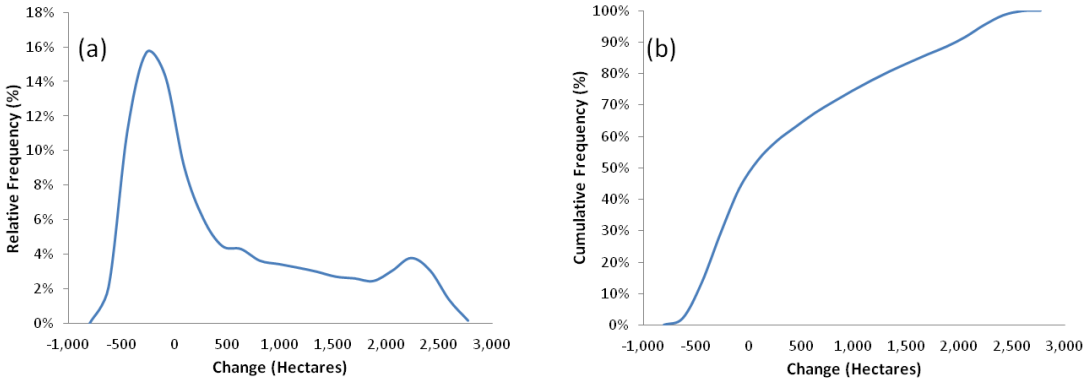

Figure 7.18 Uncertainty analysis for the total saltmarsh considering 1 m sea-level rise scenario and the full variability of the input factors (*Htrend*, *reg-accre* and *irreg-accre*), where (a) shows the relative frequency of the range of outputs variability (%), and (b) the cumulative frequency (%).

The effect of different sea-level rise scenarios (using the SLR_{2100} *uncertainty* distribution) on model uncertainty was also evaluated by analysing the variability of the total saltmarsh outputs (Figure 7.20). The overall saltmarsh here showed a unimodal distribution. Results revealed that there are 7,270 simulations that showed a decline of the total saltmarsh respect the base case, which can be interpreted as a 73 % chance of happening. However, the highest relative frequency shows (Figure 7.19, A) that there is a 22 % chance of losing between 52 and 66 % of the overall saltmarsh when uncertainty is only based on sea-level rise scenarios. There are 2,730 simulations where overall saltmarsh increasing is observed (27 % chance of happening). The probability of losing saltmarsh is higher when only sea-level rise scenarios are considered, suggesting the importance of the accretion in the survival of these environments.

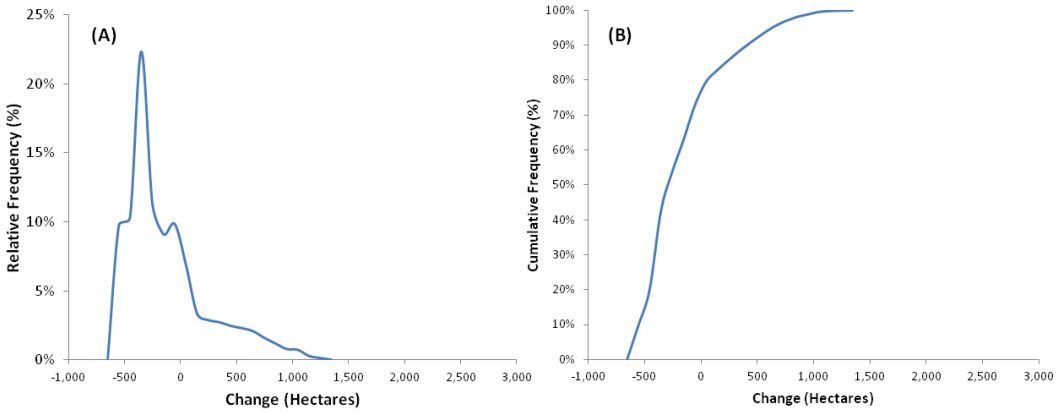

Figure 7.19 Uncertainty analysis for the total saltmarsh considering the full variability of the sea-rise scenarios defined in the uncertainty distributions, where (A) shows relative frequency of the range of outputs variability (%), and (B) the cumulative frequency (%).

When results are compared with the initial case (2013), the worst guess keeping the site parameter constant was a loss of 98 % of the vegetated saltmarshes (over 2013 saltmarsh surface area) in a sea-level rise scenario of 2.3 m, and the best guess was a loss of 91% in a sea-level scenario of 0.6 m. However, in simulations where saltmarsh accretion increased over time, the total saltmarsh loss over 2013 was reduced. For example, the best guess was a saltmarsh loss of 7% (over 2013 saltmarsh surface area) in a 1 m sea-level rise scenario by 2100, assuming 3.5 $mmyr^{-1}$ historical sea level trend, 18.5 $mm\ yr^{-1}$ accretion rates in regularly flooded marsh and 2.6 $mmyr^{-1}$ in irregularly flooded marsh. These findings showed once again the importance of the future accretion rates (and hence sediment availability and supply) in the fate of the Odiel saltmarshes.

7.4.4. Odiel saltmarsh vulnerability due to sea-level rise

The resulting map when ProjM was extracted from InitM is shown in Figure 7.20. This map showed those saltmarsh zones that did not experience any change, RegFM loss, TF loss and RegFM projected by 2050. It should be noted that more that 80% of the irregFM was converted into regFM, and that the remaining irregFM did not experience any change. New irregFM was not created in 2050 according to the model results, and it explains why this class did not appear in the method diagram (Figure 7.8).Based on this initial result, a summary classification of the Odiel saltmarsh sensitivity due to sea-level rise is shown in Figure 7.21 based on integration of the analyses of shoreline tendency, sea-level impacts on saltmarsh behaviour and estuary margin context. Results revealed that saltmarshes classified with high and very high sensitivity are mainly located in the mid- and low estuary. These zones comprise *irregularly flooded marsh*, *regularly flooded marsh* and *tidal flat* habitats that exhibit a high risk of being lost by 2050. The majority of the saltmarsh habitats that showed low and very low sensitivity were located in the upper estuary. These zones mainly included *irregularly flooded marsh* in 2013 that were converted in *regularly flooded marsh* by 2050.

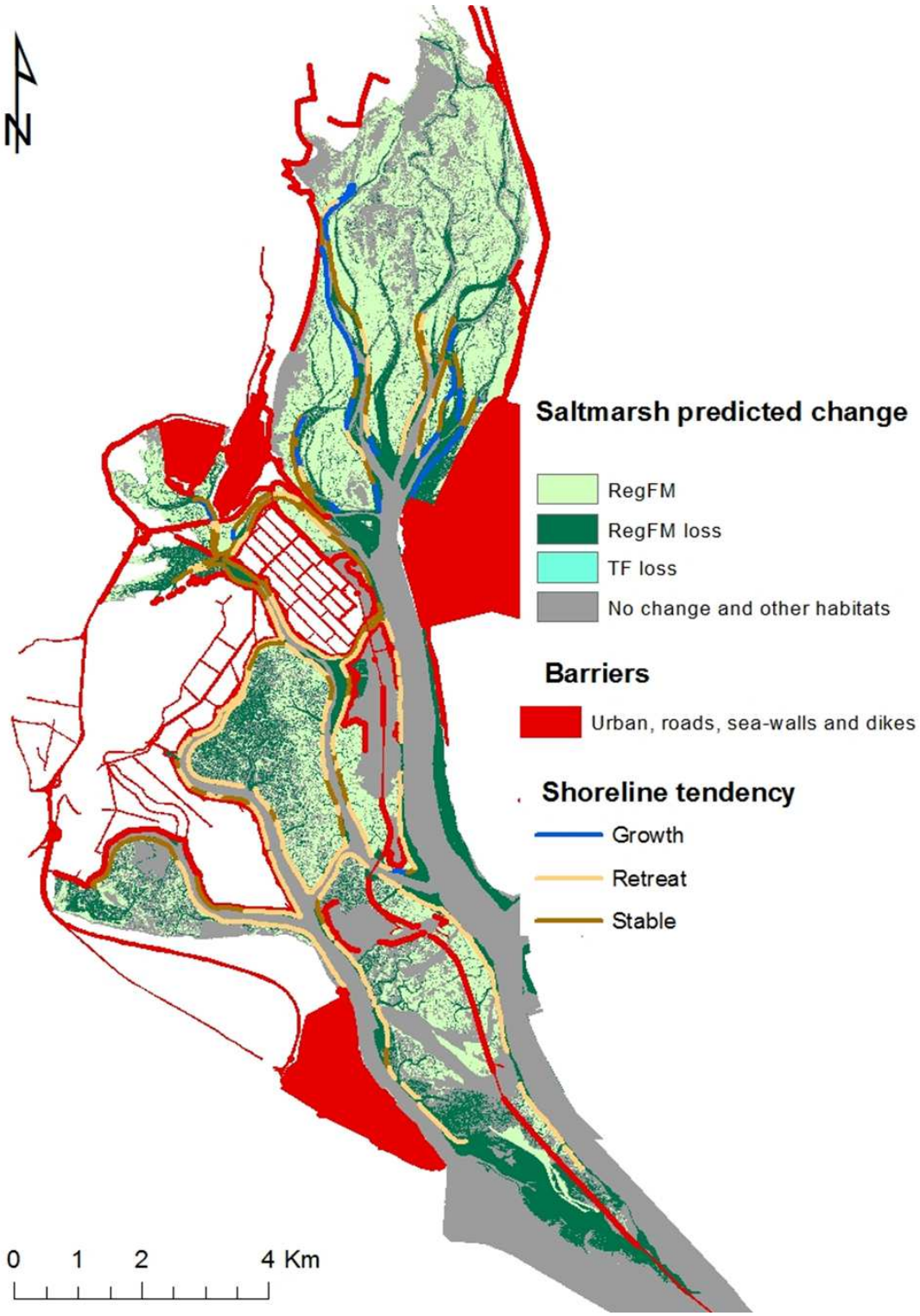

Figure 7.20 Odiel saltmarsh predicted change for 2050 under the IPCC scenario AB1, barriers presence in 2013, and shoreline tendency over the last 50 years.

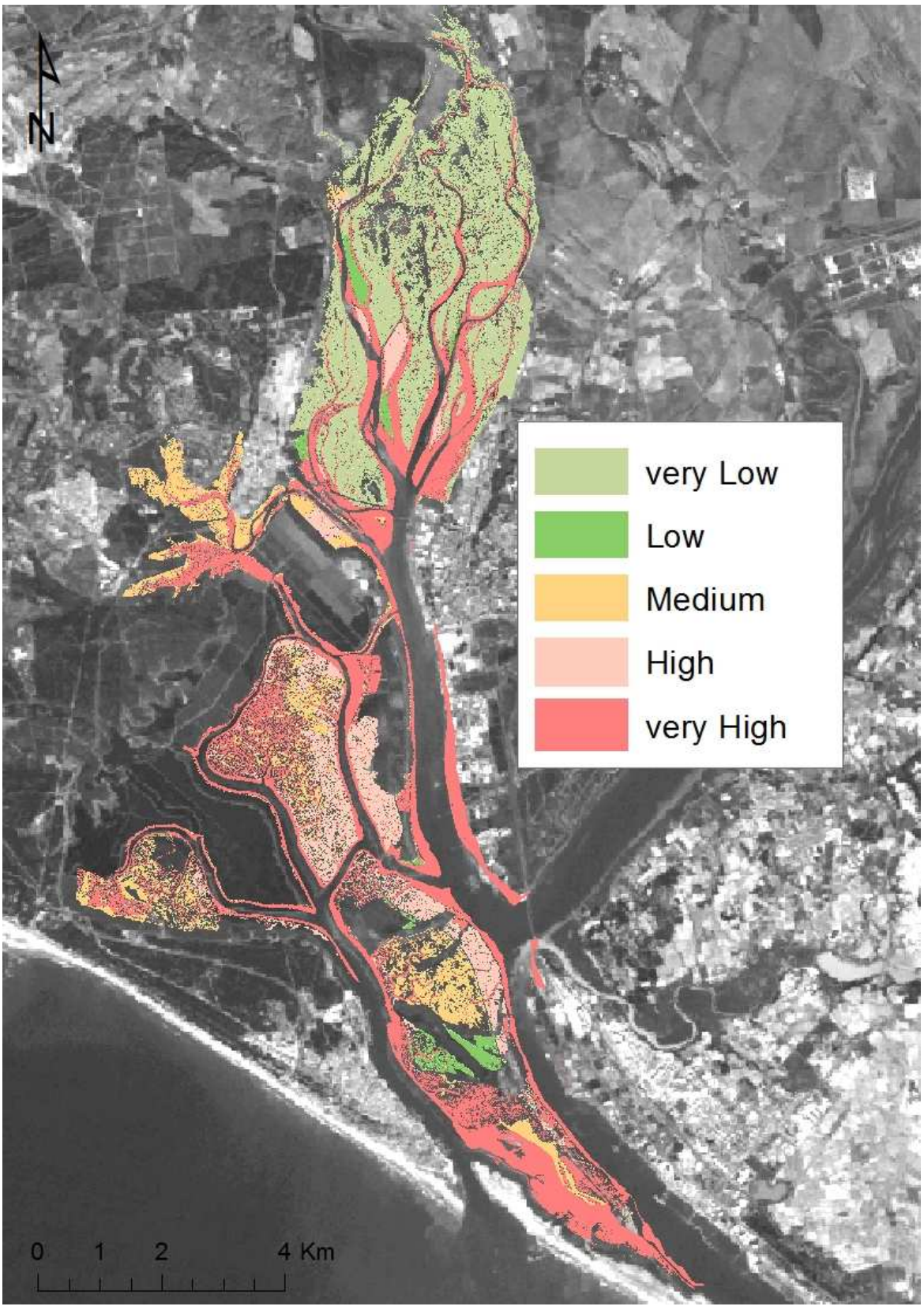

Figure 7.21 Classification of the Odiel saltmarsh vulnerability due to sea-level rise based on 2050 predicted change

7.4.5. Comparison of original and modified SLAMM

The results of habitat change for saltmarsh environments in the Odiel saltmarsh using the original and modified SLAMM are shown in Table 7.13 respectively. The results showed that the main habitat surface change was driven by the modified rules for defining habitat types. In the original version, SLAMM uses the ground elevation range defined by the user, while in the modified version this is overruled by the tidal frame elevations defined in the parameters (e.g. HAT, MHHW) for saltmarsh habitats. Thus when the model was run for the initial year (2013), the surface area of *low marsh* and *tidal flat* were significantly different to the results observed in the original version. It should be noted that in this first run, the site parameters (sea level rise, erosion and sedimentation for instance) are the same due the habitat map and elevation map have the same date (2013). This means that the model is adjusting their habitat types to the defined rules and elevation ranges. Due to these differences between original and modified version, these two versions are not directly comparable, and the results using the erosion module cannot be compared.

However, in order to investigate the importance of the erosion parameter in the model results at the Odiel saltmarshes, the modified version was run two times: 1) using the erosion rates (modified_E_1) for the study site (Table 7.6), and 2) assuming that the erosion rates were zero (modified_E_0) (as it is assumed in the original version when the fetch is smaller than 9 Km). The results are shown in Table 7.13 for those saltmarsh habitats that are affected by erosion: *tidal flat* and *low marsh*. The results revealed that erosion rates decrease the surface area in tidal flat by roughly 3.5 ha every 25 years. In the case of low marsh, the surface area was reduced 1.2 ha in 2050, 4.8 ha in 2075 and 3.3 ha in 2100. Although this number seems to be quite small (<1 %) compared with the total surface area of these habitats, it should be taken in account that erosion processes mainly occurs in the mid- estuary. Thus, ~20 ha of these habitats at the mid estuary would be lost by 2100, which is more significant than if whole saltmarshes are considered.

In terms of surface area, the erosion process do not seem to have a big impact in output results. However, the volume of sediment that potentially will be eroded and deposited on channel beds will be significant depending on the height of the marsh cliff. For example, if the marsh cliff is 0.5 m height, the potential sediment loss would be roughly 15.000 m^3 every 25 years for tidal flat. In the case of low marsh the sediment loss would be 6000 m^3 in 2050, 24000 m^3 in 2075and 16500 m^3 in 2100. But SLAMM results are based on surface areas and thus the contribution of including erosion rates do not change significantly the model outputs.

Table 7.13 Model results in hectares for Tidal flat and Low marsh habitats using the original SLAMM (v6.01), the modified SLAMM with zero erosion rates (Modified_E_0) and the modified SLAMM with erosion rates estimated for the Odiel saltmarshes (Modified_E_1).

Habitat type	Original	Modified_E_0	Modified_E_1	(E_1-E_0)
Tidal flat (ha)				
Initial condition	1358.07	1358.07	1358.07	0.00
2013	1043.48	519.32	519.32	0.00
2050	1243.45	461.86	458.78	-3.08
2075	1381.30	639.76	636.20	-3.56
2100	1420.27	719.88	716.03	-3.85
Low marsh (ha)				
Initial condition	996.45	996.45	996.45	0.00
2013	2515.71	2875.24	2875.24	0.00
2050	3081.07	3206.31	3207.54	-1.23
2075	3057.50	3059.59	3064.36	-4.77
2100	3065.48	3000.69	3004.01	-3.32

7.5. Summary and discussion

Broadly, results from all models are subject to uncertainty related to limitations in input data, incomplete knowledge about input factors that control the system behaviour, and simplifications to the system to accommodate the model (Clough *et al*., 2012). One of the main strengths of SLAMM is the ability to explore system responses to different sea-level rise scenarios, but uncertainties in the predicted response will also reflect uncertainties associated with the primary inputs and hence the quality of the original elevation data and habitat classification. Thus, it was crucial to undertake sensitivity analysis to explore the relative importance of data quality and resolution (spatial and vertical) in the key spatial inputs of elevation and saltmarsh habitat classification. Table 7.14**¡Error! No se encuentra el origen de la referencia.** summarises the sensitivity of each coastal habitat to different inputs. As expected, the DEM was the most important spatial input controlling output variability, which is in agreement with the work presented by other authors (Chu-Agor et al. 2011; Chu-Agor et al. 2010; Linhoss et al. 2013; Akumu et al. 2010; Pylarinou 2015) and bare-earth LiDAR-derived DEMs should be used to run the SLAMM as this reduces model uncertainty considerably (Gesch 2009). In the case of saltmarshes with high-density tall vegetation (>2 m height) such as those found in Mediterranean-Atlantic saltmarshes, it is also important to correct bare-earth LiDAR-derived DEMs to reduce model uncertainty (as it was indicated in Chapter 6).

Results from the sensitivity analysis showed that predicted habitat changes in all the analysed categories (except *backshore*) were sensitive to resolution in habitat and elevation maps. Elevation range (pre-defined for each habitat) and un-modified LiDAR-derived DEM only showed sensitivity to saltmarsh habitats (*transitional marsh*, *regularly flooded marsh*, *irregularly flooded marsh*, *tidal flat* and *vegetated tidal flat*). In the case of the un-modified DEM, it was expected that only saltmarsh habitats were sensitive to this input since these were the habitats to be corrected using habitat-specific correction factors (see Chapter 6 for more details). The elevation range that defines the boundaries of each saltmarsh category was also crucial to predict the fate of these habitats.

However, the key finding of the sensitivity analysis based on spatial data was the sensitivity of the model outputs to habitat distribution. It was previously assumed not to have great impact over the model inputs. Almost all categories were sensitive to the habitat maps when the rest of inputs (spatial layers and parameters) were held constant. In particular, saltmarsh habitats were especially sensitive to the creek network spatial resolution, showing variations in the model outputs when the creek network was simplified. In contrast with the findings presented by Pylarinou (2015), these results suggest that map modifications (or errors) influence model outputs for all saltmarsh categories. Pylarinou (2015) reported that only lower elevation saltmarsh habitats were

sensitive to map errors due to the initial 'adjustment' of the habitat map (considering the elevation of each cell and the defined elevation ranges for each category) based on the process of inundation, and ignoring the process of aggradation. However, she states that when a saltmarsh habitat is misclassified with a higher elevation category, conversion to the 'correct' category will take place when inundation occurs.

A different behaviour was observed in the results presented here, possibly because the sensitivity analysis was based on testing the model sensitivity to the spatial pattern resolution of a high resolution habitat map (mapping complex saltmarsh spatial patterns with an overall accuracy of 83 %) rather than testing the model sensitivity to misclassification of two categories. Model outputs showed variations in the saltmarsh habitat spatial distribution (Figure 7.12) for both lower and higher elevation categories. This behaviour could be explained by the fact that the elevation range of some saltmarsh categories (based on real data) defined in this work overlap one another as shown in Table 7.4. This means that two cells classified as *regularly flooded marsh* (from 1 to 1.6 m) and *tidal flat* (from 0.32 to 1.2 m) for instance can have the same elevation (ranging from 1 to 1.2 m) in the 'initial condition' based on the habitat map elevation. In this case, the *regularly flooded marsh* will convert into *tidal flat* when the elevation of that cell declines below 1 m (due to combined accretion and inundation processes). Thus, misclassified cells within a common elevation range are not 'adjusted' by the model when the 'initial condition' is run, making the model sensitive to the habitat map. In this sense, accurate habitat maps are essential in order to keep these possible errors to minimum. Values between 80 and 85 % are considered the minimum level of interpretation accuracy in the identification of land cover categories using remote sensed data (Anderson, 1971).

Table 7.14 Sensitivity of each habitat map category to spatial layer input data. Those cells that were ticked showed sensitivity to the input data described in each column.

	Habitat map	Elevation range	Poor resolution DEM3 (10m)	Un-modified DEM1(1m)
Developed Dry Land	✓		✓	
Undeveloped Dry Land	✓		✓	
Transitional Marsh	✓	✓	✓	✓
Regularly Flooded Marsh	✓	✓	✓	✓
Irregularly Flooded Marsh	✓	✓	✓	✓
Tidal Flat	✓	✓	✓	✓
Vegetated Tidal Flat	✓	✓	✓	✓
Estuarine Beach	✓		✓	
Estuarine Open Water	✓		✓	
Open Ocean	✓		✓	
Ocean Beach	✓		✓	
Backshore			✓	

In general, uncertainty analysis propagates the uncertainties in model inputs to the outputs, while sensitivity analysis determines the contribution of each input factor to the uncertainty of the outputs (Chu-Agor *et al*., 2011). Uncertainty analysis in this work was carried out using a Monte Carlo approach to provide confidence statistics for model results. However, to run 'full calculations' of a great number of simulations (e.g. 10,000) in SLAMM to develop this approach was not feasible for this work due to time constraints and lack of computational resources. Alternatively, linear interpolation based on a smaller set of SLAMM simulations (roughly 15 for each input factor) was used in order to get the 10,000 output variations needed for analysing uncertainty. The weakness in this approach is that inter-relationships between input factors are ignored as only one input was changed at a time, resulting in an overestimation of the results approximation. Thus, the output approximation of the 'linear interpolation' must be treated with caution especially with extreme input values.

In order to capture how inputs work together on the output would require more SLAMM runs. For example, in observing how two inputs behave together on four outputs would require 121 X 4 calculations (~ 40 hours). Given there are four inputs, this would lead to 6 combinations leading to potentially 240 hours of work which is roughly 25% of doing the full calculation method (~ 833 hours). Due to time constraints, the model inter-relationship was not calculated here. However, the development of these calculations could provide interesting results to fully understand the output behaviours and how much of the output variation is explained by interactions between the input factors. For example, Chu-Agor *et al*. (2011) used full calculations and concluded that 90% of the variance in saltmarsh outputs was explained exclusively by accretion and only 1% by historic trend, of which 7 % was explained by interactions with other input factors.

Previous sensitivity analysis based on model parameters (input factors) undertaken by other authors (Craft *et al.* 2009; Chu-Agor *et al.* 2011) has shown that saltmarsh model outputs are sensitive to historic trend of sea-level rise and accretion using earlier versions of SLAMM (v5 and v6). The sensitivity analysis carried out here for v6.2 of SLAMM showed results comparable to those presented by Chu-Agor *et al.* (2011) for a site at Santa Rosa Barrier Island, Florida. Interestingly, the results presented here have revealed that for regularly flooded marsh, the most important input factor driving output variation is accretion rate, which may outpace a 1 m sea-level rise by 2100. This finding is important for the management of the Odiel saltmarshes because it shows the importance of the accretion processes over other input factors, and the need to understand sediment sources, availability and budgets within the system.

Results from the uncertainty analysis showed the probabilty of ocurrence of different combinations of input factors in a context of sea-level rise and how it potentially

affects the fate of the Odiel saltmarshes. The key finding of this part of the analysis is the bimodality observed in the results, showing that the system can respond positively (gaining elevation above mean sea level) or negatively (losing elevation) to sea-level rise driven by change in the other main processes (e.g accretion rates). In this context, understanding the conditions driving saltmarsh increase or decrease is essential for assessing the vulnerability of the Odiel saltmarshes and developing management measurements For example, there is a 40 % chance that part of the Odiel saltmarshes will respond positively to increases in accretion rates in the context of a 1m sea-level rise by 2100 without introducing any specific management measures, reducing the total saltmarsh loss. This suggests that increasing saltmarsh accretion through specific measurements (e.g. planting *Sp. maritima* in bare tidal flats (for example see Castillo & Figueroa (2009), or controlling the vertical erosion processes) possibly help the system to cope as sea level rises and thus prevent 60% chance of losing saltmarsh.

The response of Odiel saltmarshes to sea-level rise using different IPCC scenarios showed similarities in 2050 model outputs for all scenarios, and significant discrepancies between scenarios in 2100 outputs. This suggests that as sea-level rise accelerates, more variability is introduced into the output highlighting the importance of sea-level rise scenarios in the prediction of potential impacts over saltmarsh habitats. Additionally, the differences found in the probability of losing saltmarsh when different sea-level scenarios and when 1 m sea-level scenario (plus variations in the input factors) were used reiterates the importance of accretion processes in the fate of the Odiel saltmarshes.

The short term accretion rates estimated in this thesis (Chapter 4) and the long term accretion rates estimated by other authors (Table 2.1) show that there is sediment available to enable saltmarsh vertical growth. However, what remains unknown is the time that these saltmarshes will need to cope in the case of a quick acceleration in sea-level rise. The short term sedimentation rates estimated in flat mud and vegetated flat mud close to main creeks are much greater than in other habitats and locations, meaning that longer flooding periods near to main creeks (source of sediments) increase sedimentation rates. This process ensures that lower surfaces raise at a faster rate, and catch up with the height of the marsh platform enabling marsh growth in a quasi-horizontal platform (Haslett, 2009). As the habitat conversion occurs and the geomorphology of the saltmarsh changes (e.g. creek network and lagoons), sedimentation rates within the saltmarsh will change, and those sites converted into tidal flat or low marsh will increase their rates. Additionally, based on the information reviewed about the Tinto and Odiel evolution, the sedimentation rates in this estuary increased as the sea-level rise (Figure 2.5), and it is very possible that it will occur again.

The spatial classification of saltmarsh vulnerability due to sea-level rise proposed here (Figure 7.21) is an important integration of the analyses undertaken and is a potentially powerful tool for those responsible for addressing management of the system in the medium term, and in particular in the context of sea-level rise. This map incorporates saltmarsh erosion tendency (it should be noted that original SLAMM does not take into account horizontal erosion rates when the fetch is < 9 km) facilitating the identification of the most vulnerable parts of the saltmarsh shoreline by 2050. Horizontal erosion (saltmarsh shoreline retreat) has been identified in Chapter 3 as an important factor driving saltmarsh loss in the last few decades and it is likely to increase predicted saltmarsh loss. As this factor can be controlled by soft engineering tecniques for instance (e.g. wooden revetments; (Castillo *et al*., 2000)), management schemes can be implemented by limiting erosion processes at those sites classified as sensitive. In the case of the Emedio Island, wooden revetments were inserted in order to reduce the horizontal erosion. This measurement has reduced the horizontal erosion rates in this island and it could be an effective measure to apply in other sectors of the Odiel saltmarsh.

A modified-version of SLAMM (Pylarinou, 2015) was compared with the original (v6.01) in order to explore the influence of horizontal erosion parameter in a context of sea-level rise. However, the results showed that these two models (original and modified) are not directly comparable due to the modifications of habitat type definition and conversion rules. The importance of the erosion parameter was then tested using the modified SLAMM only, and comparing model results when SLAMM was run with 'erosion' and 'not erosion'. The results revealed that the surface area of tidal flat and low marsh habitats in 2100 is reduced by ~10 ha (over 2013 surface area) when lineal erosion is taken in account. In terms of surface area, these numbers are not significantly important considering the total surface area of these habitats. However, these numbers become more important when the volume of the sediments that potentially will be eroded was estimated. Considering a marsh cliff of 0.5 m, the total sediment eroded would be 45,000 m^3 for tidal flat habitats and 46,500 m^3 for low marsh habitats.

Overall, SLAMM has resulted to be a useful landscape model in simulation of the Odiel saltmarshes for obtaining previous results and for detecting vulnerable areas within the whole saltmarshes. The utility of this model has also been recognised by other authors at other saltmarsh sites (Linhoss *et al*., 2013; Geselbracht *et al*., 2011; Mcleod *et al*., 2010). Some of the advantages of this model include (Table 7.15): its flexibility in scales; its ability to represent potential wetland impacts due sea-level rises; its ease and speed to run; and it contains the major processes involved in wetland. However, further investigations are needed in those areas considered very vulnerable due to the disadvantages found in this model (Table 7.15). One of the main disadvantages is that

SLAMM accretion relationships are empirical (defined between accretion rates and cell elevations among other factors) rather than mechanistic, and thus they do not integrate variables such as vegetation sediment trapping efficiency, inundation frequency, and sediment concentrations for instance (Clough *et al*., 2012). Other disadvantages are that SLAMM does not consider future changes in hydrodynamics and future tides are held constant. Due to these SLAMM limitations, it is recommended to use SLAMM in combination with other models such as physical models of sedimentation and/or hydrodynamic (e.g. Rinaldo *et al.*, 1999; Temmerman *et al.*, 2003b; D'Alpaos *et al.*, 2007) over those sites considered very vulnerable. Then, monitoring and data collection can be focussed on those vulnerable areas, providing detailed information for managers and decision makers.

Table 7.15 Disadvantages and advantages of sea level affecting marsh model (SLAMM)

Disadvantages	*Advantages*
• Future changes in hydrodynamics are not represented • Tide held constant over time • Spatially simple erosion model • Accretion rates are affected by bank sloughing • Do not consider erosion rates when the fetch is > 9 Km (Original version)	• Open source • Relatively quick to run • Flexibility in scales • Contains major processes pertinent to wetland fate • Provide spatial information to identify very sensitive sites due to sea-level rise

8. Final discussion and conclusions

8.1 The SLAMM model for saltmarsh management in the context of sea-level rise: uncertainties and limitations

SLAMM is an open source model that is easy to run and it has been used for investigating potential impacts due to sea-level rise over coastal wetland habitats due to sea-level rise in a range of different locations, though primarily the USA (e.g. Linhoss *et al.* 2013; Hauer *et al.* 2015; Ehman 2008; Craft *et al.* 2009; Akumu *et al.* 2010). Here, SLAMM was run to forecast the effect of sea-level rise on Mediterranean-Atlantic saltmarshes using the Odiel saltmarshes (Huelva, SW Spain) as study site. This study has shown that SLAMM was suitable for modelling large expanses of Mediterranean-Atlantic saltmarsh and that it could be a helpful tool for detecting sensitive areas within saltmarshes in the context of a rising sea level, and it could help managers to decide where to do further investigations and monitoring. For example, results from the model can help managers and decision makers to plan adaptation strategies for saltmarshes at local scales, and also to detect sensitive sites to run more complicate physical models. However, there are many uncertainties related to potential sea-level rise impacts over saltmarshes and it is important to be aware of them when projections are used in managing saltmarshes. The main uncertainties detected here were due to model limitations and data quality, and those surrounding forecast of sea-level rise.

The first uncertainty detected in saltmarsh modelling was related to the simplification of the saltmarsh processes assumed by SLAMM. Models and empirical relationships used to predict the effects of sea-level rise may simplify relationships (assuming a constant state) (Linhoss *et al*., 2013), and assume that coastal geomorphology does not change as sea level rises, which it is very unlikely. For example, as coastal barrier-lagoon systems breach, inundation dynamics will change (Murdukhayeva *et al.*, 2013). Particularly, SLAMM lacks feedback mechanisms that may play an important role in the system as sea-level accelerates. For example, increasing inundation of saltmarshes may increase macrophyte production and lead to increased vertical accretion (Morris *et al*., 2002). Additionally, processes such as tidal range are assumed to be constant and therefore with increasing progression from the initial condition into a simulation, uncertainties in model prediction will increase. In this sense, the historical evolution of the studied system plays an important role in identifying the main drivers acting within the system and how the system has evolved. By looking further into the past, the system response due to past sea-level rise for instance can provide useful information for contextualising the future response of the system. Furthermore, due to all these limitations of predictive models like SLAMM, uncertainty analysis considering probability distributions becomes essential to assess the probability of different system responses.

The accurate definition of these probability distributions is crucial to reduce uncertainty, and historical data should be analysed.

The second uncertainty surrounding modelling saltmarsh response to sea-level rise is data source quality and resolution. The resolution of input data is an important factor in spatial models like SLAMM, and is usually constrained by data source (Murdukhayeva *et al.*, 2013). Elevation data and habitat map accuracy have been identified here as key components contributing to uncertainty in SLAMM habitat predictions in the context of sea-level rise. In this work, a methodology for improving the accuracy of the LiDAR-derived DEM and saltmarsh habitat maps has been proposed, and this can be applied to other saltmarsh environments. In this sense, it is highly recommended to do a rigorous validation of the LiDAR-derived data (e.g. DEM), especially in saltmarshes where perennial tall vegetation and high vegetation density are found, such as those in the Mediterranean-Atlantic saltmarshes. For example, in the case of the Odiel saltmarshes, the LiDAR-derived DEM showed vertical errors of up to 0.5 m in areas colonised by tall vegetation (*Sp. densiflora*).

Apart from uncertainties related to the model and input data, there are also uncertainties directly linked to the effects of sea-level rise on saltmarshes to consider. The sea-level rise predictions themselves are uncertain, and different projections for global sea-level rise by 2100 range between 0.18 and 0.59 m (IPCC AR4 WG1, 2007), 1.4 m (Vermeer & Rahmstorf, 2009), and up to 2 m (Pfeffer *et al.,* 2008). These projections are based on historical and empirical methodologies. Additionally, local projections for the Odiel saltmarshes estimated from historical trends and future projections using a correlation factor (Fraile-Jurado & Fernandez-Diaz, in press.) include 0.64 – 0.86 m (IPCC scenarios: RCP2.0, RCP4.5, and RCP8.0), 1.07 – 2.27 m (Pfeffer *et al*., 2008) and 1.17 m (Rahmstorf, 2007).

Finally, management strategies themselves may have uncertain consequences. Thus, to make robust management decisions, it is essential to assess diverse information and their associated uncertainty (Linhoss *et al.*, 2013). For this purpose, a multi-criteria decision analysis (MCDA) can provide a suitable tool to integrate information of different nature (Kiker *et al.*, 2008; Linkov *et al,.* 2006), including results from several predictive models. The use of predictive models such as SLAMM can also be used as a tool for assessing the effectiveness of different management measures for instance. For this purpose, SLAMM can be run multiple times using different input data (for example, to include artificial measures to favour accretion rates and how the system will respond to those changes).

8.2. Conclusions

This thesis set out to show how a multifaceted methodology for investigating the response of saltmarshes due to sea-level rise at local scales in the Odiel saltmarshes (SW Spain) can inform managerial schemes in the context of sea-level change. The approach described here used elevation data derived from light detection and ranging (LiDAR), high spatial resolution multispectral imagery (1 m) and spatial modelling in combination with historical estuary evolution and field observations. The potential of reduced complexity models such as the Sea Level Affecting Marsh Model (SLAMM), widely used in the USA, has been assessed here as a tool to provide information for coastal managers regarding the impact of sea-level rise on saltmarsh habitats and their associated uncertainties.

In the Tinto-Odiel estuary, the system response to anthropogenic and natural drivers has been observed in changes to geomorphology and habitats, as well as movement in saltmarsh shorelines. A key finding here is that the effect of the sea-level rise is manifested in different ways in different parts of the estuarine system, depending particularly on their anthropogenic history. In the upper estuary, saltmarshes showed growth over recent decades. Sedimentation rates here (4.36 mmy^{-1}) are greater than the historical relative sea level rise (3.3 mmy^{-1}) recorded for the Tinto-Odiel estuary, but there have also been important restoration projects carried out here (e.g. plantation of pioneers over mud flats) that have benefitted the growth of the saltmarshes. In the mid estuary, saltmarsh habitats showed a recessional tendency driven by several factors such as reclamation, waves generated by the increase of passing boats, and possibly by sea-level rise. Sedimentation rates in this part of the estuary are lower than relative sea level rise, thus it is quite possible that sea level rise is outpacing sedimentation at this site. Additionally, it is possible that greater river discharge between 1984 and 2001 (reaching the maximum value recorded for the period 1969-2006: 1800 hm^3 in 1989) exacerbated the recessional tendency as the shoreline analysis shows enhanced rates of erosion during this period. In the lower estuary, the configuration of the estuary mouth has completely changed during the last 50 years with the construction of the Juan Carlos I dike, creating two lagoons, and a complex of new back-barrier and saltmarsh environments. Sea-level rise may have influenced some of the sediment transport processes here, but its impact is difficult to assess due to the far more imposing changes in the configuration of the lower estuary resulting from dike construction.

Plant communities found throughout the Odiel saltmarshes followed a habitat zonation that can be best described as comprising low marsh, salt pan, mid- marsh, high marsh and *Spartina* marsh. This zonation did not follow parallel rings from the shore, but a more complex distribution, showing the complexity of the saltmarsh micro-topography. Vegetation surveys showed that most species were always found within the same habitat

type, indicating a close relationship with soil elevation (that implies, more or less, tolerance to flooding and salinity conditions for instance). However, *A. portulacoides* and *Sp. densiflora* were found across a diverse range of elevations and situations, showing their great environmental adaptability. It is possible that these species will be more resilient to sea-level rise, and as such, they may have an advantage over other species, which could lead to a plant diversity loss. These species could be considered as key species to monitor medium term changes within the Odiel saltmarshes, and the increase in their spatial distribution within the estuary could be an indicator of environmental changes such as sea-level rise. The shift from *S. perennis subsp. alpini* (due to its intolerance of increasingly hypoxic soil conditions) to *S. perennis subsp. perenni* could also be an indicator of the effects of sea-level rise at the Odiel saltmarshes, and that sedimentation rates are not keeping pace with (or outpacing) sea level rates.

A relationship between habitat type and sedimentation rates was observed, where lower elevation habitats showed higher deposition rates. Furthermore, deposition rates within the same habitat type showed a spatial pattern depending on site location and geomorphology. As sea-level rises, the geomorphology and distance to main creeks are likely to change and thus the accretion rates. Based on short and long term accretion rates, sediment is clearly available for accretion across the Odiel saltmarshes. However, although vertical growth occurs across the saltmarshes, the horizontal erosion estimated at the central part of the Odiel estuary has caused retreat of the saltmarsh shoreline and loss of some habitat over recent decades. Erosion and sedimentation rates are very important variables to monitor within saltmarshes, and potential changes in these variables have important impacts on saltmarsh environments. Thus, the monitoring of these two variables should be prioritised in management strategies. In addition, the integrated management of sediment budgets within the river basin must be considered to ascertain future sediment availability.

Accurate spatial data, such as saltmarsh habitat map and digital elevation models (DEMs) are essential to deliver an effective representation of the system, and also reduce uncertainties in modelling procedures. Part of this thesis focused on improving accuracy in saltmarsh habitat (Chapter 5) and elevation (Chapter 6) data. In this sense, object based (OBIA) and pixel based (PBIA) image classification were explored for high resolution saltmarsh mapping (using spectral and elevation data) and the generation of habitat-specific correction factors for improving accuracy in LiDAR-derived DEMs. Image classification results showed that overall accuracy in object-based classification (combining spectral and elevation data) reached greater values (83.1%) than pixel based classification (0.65 %), suggesting that an OBIA approach using LiDAR-derived data was more suitable for mapping small spatial patterns within saltmarsh habitats. This method

would complement habitat monitoring to understand changes over the time and assess response of the plant communities to sea-level rise at the landscape scale. However, it should be noted that these results are highly dependent on data available and the site characteristics (e.g. vegetation patterns and plant species).

With regard to DEMs, the work undertaken here highlighted that LiDAR-derived data do not provide accurate DEMs in saltmarsh environments where high-density and tall vegetation is present. This is a significant limitation in the use of LiDAR-derived DEMs for applications and investigations that require high accuracy, such as tidal flooding, sedimentation, and management and conservation activities in a context of sea-level rise. The study undertaken here (Chapter 6) demonstrates that application of a habitat-specific correction factor is a suitable approach for improving DEM accuracy in Atlantic-Mediterranean saltmarshes. After applying the correction factors, the error of the corrected DEM was lower than the reported LiDAR-derived DEM accuracy (0.1 m) for all habitat types, except for the *Spartina* marsh that was slightly higher (0.13 m). High resolution habitat maps based on canopy heights are appropriate tools for applying correction factors to large study areas as has been shown in this work. Finally, this research also showed the importance of elevation accuracy in low-lying areas like saltmarshes and highlights the need for DEM corrections when certain applications such sea-level rise projections are used. In this sense, this work offers saltmarsh managers a robust approach that can be adopted by others where improvements in the accuracy of LiDAR-derived DEMs is required; this is particularly important for evaluating saltmarsh change in a context of sea-level rise.

A sensitivity and uncertainty analysis was undertaken to explore the relative importance of data quality and resolution (spatial and vertical) in elevation data and saltmarsh habitat classification layers, and also the global uncertainty of the model outputs using a Monte Carlo approach. Monitoring and measurement of saltmarsh habitats is time consuming and costly, and the acquisition of the SLAMM input layers (with high spatial resolution) can require significant resourcing. Thus the results presented here provide a better understanding of where surveying efforts should be focused, if necessary. The findings show that the SLAMM model is sensitive to DEM and habitat map resolution, and that historical sea-level trend and saltmarsh accretion rates are the predominant input factors that influence uncertainty in predictions of change in saltmarsh habitats. The understanding of the past evolution of the system as well as the contemporary situation is crucial to provide accurate uncertainty distributions and thus to set a robust baseline for future predictions.

9. The predicted response of the Odiel saltmarshes due to sea-level rise, based on the uncertainty analysis, suggested possible gain or loss of saltmarsh habitats (over the

base case which used the current site parameters) depending on the combination of input factors within their proposed uncertainty ranges for a 1 m sea-level by 2100, and considered the full range of variability of the most sensitive input factors (accretion rates and site historical sea-level rise). Based on local projections of sea-level rise through to 2100, and assuming that the accretion rates and historical sea level trend do not change over the time, the worst-case estimate was a loss of 98 % of the vegetated saltmarshes over the initial case (2013) with a sea-level rise scenario of 2.3 m, and the best case was a loss of 91% with a sea-level scenario of 0.6 m. However, in simulations where saltmarsh accretion increased over time, the total saltmarsh loss was reduced. For example, the best case was a saltmarsh loss of 7% (over the initial case , saltmarsh surface area in 2013) with a 1 m sea-level rise scenario (by 2100) assuming 3.5 $mmyr^{-1}$ historical sea level trend, 18.5 $mm\ yr^{-1}$ accretion rates in regularly flooded marsh and 2.6 $mmyr^{-1}$ in irregularly flooded marsh. These findings show the importance of the future accretion rates (and hence sediment availability and supply) in the fate of the Odiel saltmarshes.

The potential of reduced complexity models such as the Sea Level Affecting Marshes Model (SLAMM), widely used in the USA, has been assessed here as a tool to provide appropriate information for coastal wetland managers regarding the likely impact of sea-level rise on Mediterranean-Atlantic saltmarshes. The original version of SLAMM (v 6) does not take into account shoreline erosion rates where the fetch is less than 9 km (as is the case in the Tinto-Odiel saltmarshes). This should be considered when this model is run over tidal flat and low marsh habitats. Overall, SLAMM is able to provide general information about potential impacts due to sea-level rise at the landscape scale, but fails to provide detailed information at smaller scales due to the model limitations (e.g. simplified erosion model, and it hydrodynamic changes are not considered). Thus, in order to implement management strategies in a context of sea-level rise, it is highly recommended the use of this model at landscape scale in combination with other predictive models at the process scale at smaller sites that have been identified as very vulnerable to sea-level rise. Finally, SLAMM results should be treated with caution and they should be used in combination with uncertainty analysis to provide probability of occurrence.

9. References

Adam, E., Mutanga, O. & Rugege, D., 2009. Multispectral and hyperspectral remote sensing for identification and mapping of wetland vegetation: a review. *Wetlands Ecology and Management*, 18(3), pp.281–296. Available at: http://www.springerlink.com/index/10.1007/s11273-009-9169-z [Accessed March 7, 2013].

Adam, P., 1990. *Saltmarsh Ecology*, Cambridge: Cambridge University Press.

Adam, P., 2002. Saltmarshes in a time of change. *Environmental conservation*, 29(1), pp.39–61.

Adger, W.N. et al., 2005. Social-Ecological Resilience to Coastal Disasters. *Science*, 309(5737), pp.1036–1039. Available at: http://www.sciencemag.org/content/309/5737/1036.abstract.

Akumu, C.E. et al., 2010. Examining the potential impacts of sea level rise on coastal wetlands in north-eastern NSW, Australia. *Journal of Coastal Conservation*, 15(1), pp.15–22. Available at: http://www.springerlink.com/index/10.1007/s11852-010-0114-3 [Accessed November 15, 2011].

Allen, J.R.L., 1994. A continuity-based sedimentological model for temperate-zone tidal salt marshes. *Journal of the Geological Society*, 151, pp.41–49.

Allen, J.R.L., 2000. Morphodynamics of Holocene salt marshes: a review sketch from the Atlantic and Southern North Sea coasts of Europe. *Quaternary Science Reviews*, 19(12), pp.1155–1231. Available at: http://linkinghub.elsevier.com/retrieve/pii/S0277379199000347.

Allen, J.R.L., 1991. Saltmarsh accretion and sea-level movement in the inner Severn Estuary: the archaeological and historical contribution. *Journal of the Geological Society*, 148, pp.485–494.

Allen, J.R.L., 1990. Salt-marsh growth and stratification: A numerical model with special reference to the Severn Estuary, southwest Britain. *Marine Geology*, 95(2), pp.77–96. Available at: http://linkinghub.elsevier.com/retrieve/pii/002532279090042I.

Allen, J.R.L., 1997. Simulation models of salt-marsh morphodynamics: some implications for high-intertidal sediment couplets related to sea-level change. *Sedimentary Geology*, 113(3-4), pp.211–223. Available at: http://linkinghub.elsevier.com/retrieve/pii/S0037073897001012.

Allen, J.R.L., 2009. Tidal Salt marshes: Geomorphology and sedimentology. In G. M. E. Perillo et al., eds. *Coastal Wetlands: An Intergrated Ecosystem Approach*. Amsterdam: Elsevier, pp. 403–424.

Allen, J.R.L. & Pye, K., 1992. Coastal saltmarshes: their nature and importance. In J. R. L. Allen & K. Pye, eds. *Saltmarshes: morphodynamics, consercation and engeneering significance*. Cambridge, UK: Cambridge University Press, pp. 1–18.

Anderson, J.R., 1971. Land Use Classification Schemes Used in Selected Geographic Applications in Remote Sensing. *Photogrammetric Engineering and Remote Sensing*, 37(4), pp.379–387.

Armstrong, A.W. et al., 1985. Plant Zonation and the Effects of the Spring-Neap tidal cycle on Aeration in a Humber Salt Marsh. *Journal of Ecology*, 73, pp.323–339.

Armstrong, W. & Beckett, P.M., 1985. Root aeration in unsaturated soil: a multi-shelled mathematical model of oxygen diffusion and distribution with and without sectoral wet-soil blocking of the diffusion path. *New phytologist*, 100, pp.293–311.

Arnaud-Fassetta, G. et al., 2006. The western lagoon marshes of the Ria Formosa (Southern Portugal): Sediment-vegetation dynamics, long-term to short-term changes and perspective. *Continental Shelf Research*, 26(3), pp.363–384. Available at:

http://linkinghub.elsevier.com/retrieve/pii/S0278434305002633 [Accessed March 6, 2013].

Arroyo, L.A. et al., 2010. Integration of LiDAR and QuickBird imagery for mapping riparian biophysical parameters and land cover types in Australian tropical savannas. *Forest Ecology and Management*, 259(3), pp.598–606. Available at: http://linkinghub.elsevier.com/retrieve/pii/S0378112709008457 [Accessed March 6, 2013].

Artigas, F.J. & Yang, J., 2006. Spectral Discrimination of Marsh-Vegetation Types in the New Jersey Meadowlands, USA. *Wetlands*, 26(1), pp.271–277.

Ashley, G.M. & Zeff, M.L., 1988. TIDAL CHANNEL CLASSIFICATION FOR A LOW-MESOTIDAL SALT MARSH. *Marine Geology*, 82, pp.17–32.

Ayyad, M.A. & El-Ghareeb, R.E.M., 1982. Salt marsh vegetation of the western Mediterranean desert of Egypt. *Vegetatio*, 49(1), pp.3–19.

Baatz, M. & Schäpe, A., 2000. Multiresolution Segmentation: An Optimization Approach for High Quality Multi-Scale Image Segmentation (eCognition). Available at: http://www.ecognition.cc/download/baatz_schaepe.pdf.

De Baets, S. et al., 2005. *Effects of grass roots on the erodibility of topsoils during concentrated flow.*, Elsevier B.V.

Barros, A.P., 1996. An evaluation of model parameterizations of sediment pathways: a case study for the Tejo estuary. *Continental Shelf Research*, 16(13), pp.1725–1749.

Barthолody, J., 2012. Salt Marsh Sedimentation. In R. A. Davis & R. W. Dalrymple, eds. *Principles of Tidal Sedimentology*. Springer Netherlands, pp. 151–185.

Beeftink, W.G., 1977. The coastal saltmarshes of western and northern Europe: an ecological and phytosociological approach. In V. J. Chapman, ed. *Wet coastal ecosystems*. Amsterdam: Elsevier, pp. 107–150.

Beeftink, W.G., 1966. Vegetation and habitat of the salt marshes and beach plains in the south-western part of Netherlands. *Wentia*, 15, pp.83–108.

Belluco, E. et al., 2006. Mapping salt-marsh vegetation by multispectral and hyperspectral remote sensing. *Remote Sensing of Environment*, 105(1), pp.54–67. Available at: http://linkinghub.elsevier.com/retrieve/pii/S0034425706002227 [Accessed March 12, 2013].

Benoit, L.K. & Askins, R.A., 2002. Relationship between habitat area and the distribution of tidal marsh birds. *The Wilson Bulletin*, 114(3), pp.314–323.

Benz, U.C. et al., 2004. Multi-Resolution, Objectoriented Fuzzy Analysis of Remote Sensing Data for GIS-Ready Information. *Journal of Photogrammetry & Remote Sensing*, 58, pp.239–258.

Bertness, M.D. & Callaway, R., 1994. Positive interactions in communities. *Trends Ecology Evolution*, 9, pp.191–193.

Bertness, M.D. & Hacker, S.D., 2013. Physical stress and positive Associationss among marsh plants. *The American Naturalist*, 144(3), pp.363–372.

Bertness, M.D. & Yeh, S.M., 1994. Co-operative and competitive interactions in the recruitment of marsh elders. *Ecology*, 75, pp.2416–2429.

Blumberg, D.G. & Zhu, G., 2007. Using a hierarchical multi-resolution mechanism for the classification and semantic extraction of land use maps for Beer-Sheva, Israel. *International Journal of Remote Sensing*, 28(45), pp.3273–3289.

Boesch, D.F. & Turner, R.E., 1984. Dependence of fishery species on salt marshes: The role of food and refuge. *Estuaries and Coasts*, 7(4), pp.460–468.

Boon, P.I. et al., 2011. *Mangroves and coastal saltmarsh of Victoria: distribution, condition, threats and management*, Melbourne.

Boorman, L.A., 2003. *Saltmarsh Review. An overview of coastal saltmarshes, their dynamic and sensitivity characteristics for conservation and management*, Peterborough: JNCC Report, No. 334.

Boorman, L.A., Garbutt, A. & Barratt, D., 1998. The role of vegetation in determining patterns of the accretion of saltmarsh sediment. *In Sedimentary Process in the Intertidal Zone, Geological Society of London Special Publication*, 139, pp.389– 399.

Borja, C. et al., 2009. Hydrogeographical dynamic and man induced processes in "el Partido" river (NW Doñana National Park, Huelva, Spain). Analysis of currents processes. *Evaluacion de Procesos Actuales Cuaternario y Geomorfologia.*, 23(3-4), pp.64–65.

Borrego, J., 1992. *Sedimentología del estuario del río Odiel (Huelva, S.O. España)*. Thesis, University of Sevilla.

Borrego, J. et al., 1999. The Holocene transgression into the estuarine central basin of the Odiel River mouth (Cadiz gulf , SW , Spain): lithology and faunal assemblages. *Quaternary Science Reviews*, 18, pp.769–788.

Borrego, J., Morales, J.A. & Gil, N., 2000. Evolucion sedimentaria reciente de la desembocadura de la Ria de Huelva (suroeste de España). *Revista de la Sociedad Geológica de España*, 13(3-4), pp.405–416.

Boudreaux, J.P., 2009. *Shear strength evaluation of an erosional soil system at Fourchon Beach*. Louisiana State University.

Boyle, J.F., 2004. A comparison of two methods for estimating the organic matter content of sediments. *Journal of Paleolimnology*, 31, pp.125– 127.

BRANCH Partnership, 2007. *Planning for Biodiversity in a Changing Climate – BRANCH. Project Final Report*, England, UK.

Brennan, R. & Webster, T.L., 2006. Object-oriented land cover classification of LIDAR-derived surfaces. *Canadian Journal of Remote Sensing*, 32, pp.162–172.

Bricker-Urso, S. et al., 1989. Accretion Rates and Sediment Accumulation in Rhode Island Salt Marshes. *Estuaries*, 12(4), pp.300–317.

Britton, R.H. & Crivelli, A.J., 1992. Wetlands of Southern Europe and North Africa: Mediterranean wetlands. In D. F. Whigham, D. Dykyjová, & S. Hejný, eds. *Wetlands of the World I: Inventory, Ecology and Management*. Springer, pp. 144–150.

Broome, S.W., Seneca, E.D. & Woodhouse, W.W., 1988. Tidal salt marsh restoration. *Aquatic Botany*, 32, pp.1–22.

Brovelli, M.A., Cannata, M. & Longoni, U.M., 2004. Research Article LIDAR Data Filtering and DTM Interpolation Within GRASS. *Transactions in GIS*, 8(2), pp.155–174.

Brown, K., 2004. Increasing classification accuracy of coastal habitats using integrated airborne remote sensing. In *EARSeL eProceedings*. pp. 34–42.

Brown, S.L. et al., 1998. Sediment Fluxes in Intertidal Biotopes : BIOTA II. *Marine pollution bulletin*, 37(3-7), pp.173–181.

Bryant, J.C. & Chabreck, R.H., 1998. Effects of impoundment on vertical accretion of coastal marsh. *Estuaries*, 21, pp.416–422.

Cahoon, D.R. et al., 2000. Vertical accretion versus elevational adjustment in UK saltmarshes: an evaluation of alternative methodologies. *Geological Society, London, Special Publications*, 175(1), pp.223–238. Available at: http://sp.lyellcollection.org/content/175/1/223.short [Accessed April 15, 2013].

Cahoon, D.R., Lynch, J.C. & Powell, A.N., 1996. Marsh vertical accreation in a Southern California Estuary, U.S.A. *Estuarine, Coastal and Shelf Science*, 43, pp.19–32.

Cahoon, D.R., Reed, D.J. & Day, J.W., 1995. Estimating shallow subsidence in microtidal salt marshes of the southeastern United States: Kaye and Barghoorn revisited. *Marine*

Geology, 128(1-2), pp.1–9. Available at: http://linkinghub.elsevier.com/retrieve/pii/002532279500087F.

Cai, W., Wang, Z.A. & Wang, Y., 2003. The role of marsh-dominated heterotrophic continental margins in transport of CO2 between the atmosphere, the land-sea interface and the ocean. *Geophysical Research Letters*, 30(16), pp.1–4. Available at: http://www.agu.org/pubs/crossref/2003/2003GL017633.shtml [Accessed October 25, 2012].

Cánovas, C.R. et al., 2007. Hydrogeochemical characteristics of the Tinto and Odiel Rivers (SW Spain). Factors controlling metal contents. *The Science of the total environment*, 373(1), pp.363–82. Available at: http://www.ncbi.nlm.nih.gov/pubmed/17207846 [Accessed March 2, 2013].

Canovas, F., 2012. *Análisis de imágenes basado en objetos (OBIA) y aprendizaje automático para la obtención de mapas de coberturas del suelo a partir de imágenes de muy alta reso- lución espacial.*

Cao, M., Liu, G. & Zhang, X., 2007. An object-oriented approach to map wetland vegetation:a case study of yellow river delta. In *IEEE International Geoscience and Remote Sensing Symposium*. Barcelona, Spain, pp. 4585–4587.

Carro, B., Borrego, N., Lopez-Gonzalez, N., Grande, J.A., Gomez, T., de la Torre, M.L., Valente, T., 2011. Impact of Acid Mine Drainage on the hydrogeochemical characteristics of the Tinto-Odiel Estuary (SW Spain). *Journal of Iberian Geology*, 37(1), pp.87–96.

Cary, T., 2009. New research reveals current and future trends in LIDAR applications. *Earth Imaging Journal*, 1, pp.8–9.

Castellanos, E.M., Nieva, F.J., et al., 1998. Modelo anual de la dinamica sedimentaria en una marisma mareal mediterranea. *Cuaternario y Geomorfologia*, 12(3-4), pp.69–76.

Castellanos, E.M., Heredia, C., et al., 1998. Tiller dynamics of Spartina maritima in successional and non-successional mediterranean salt marsh. *Plant Ecology*, 137, pp.213–225.

Castellanos, E.M., Figueroa, M.E. & Davy, A.J., 1994. Nucleation and facilitation in saltmarsh succession: interactions between Spartina maritima and Arthrocnemum perenne. *British Ecological Society*, 82(2), pp.239–248. Available at: http://www.jstor.org/stable/2261292 .

Castillo, J.M., Luque, C.J., et al., 2000. Causes and consequences of salt-marsh erosion in an Atlantic estuary in SW Spain. *Journal of Coastal Conservation*, 6(1), pp.89–96. Available at: http://link.springer.com/10.1007/BF02730472.

Castillo, J.M., Fernandez-Baco, E.M., et al., 2000. Lower limits of Spartina densiflora in a and S . maritima Mediterranean salt marsh determined by different ecophysiological tolerances. *Journal of Ecology*, 88(5), pp.801–812.

Castillo, J.M. et al., 2010. The production of hybrids with high ecological amplitude between exotic Spartina densiflora and native S. maritima in the Iberian Peninsula. *Diversity and Distributions*, 164, pp.547–558.

Castillo, J.M. & Figueroa, M.E., 2009. Restoring saltmarshes using small-cord grass, Spartina maritima. *Restoration Ecology*, 17, pp.324–326.

Castillo, J.M., Luque, C.J. & Figueroa, M.E., 1999. Cuantificacion de la erosion en los canales mareales de las marismas del Odiel (Huelva , SW Spain). *Cuaternario y Geomorfologia*, 13(3-4), pp.7–16.

Cazenave, A. et al., 2009. Sea level budget over 2003–2008: A reevaluation from GRACE space gravimetry, satellite altimetry and Argo. *Global and Planetary Change*, 65(1-2), pp.83–88. Available at: http://linkinghub.elsevier.com/retrieve/pii/S0921818108001343 [Accessed March 19, 2012].

Cazenave, A. & Nerem, R.S., 2004. Present-Day Sea Level Change: Observations and Causes. *Reviews of Geophysics*, 42(3), pp.1–20.

Cendrero, A. et al., 2005. Impactos sobre las zonas costeras. In J. M. C. Moreno, ed. *Evaluación Preliminar Impacto sobre el Cambio Climático en España*. Ministerio de Medio Ambiente.

Chang, E.R., Veeneklaas, R.M. & Bakker, J.P., 2007. Seed dynamics linked to variability in movement of tidal water. *Journal of Vegetation Science*, 18, pp.253–262.

Chapman, V.J., 1974. *Saltmarshes and salt deserts of the World* Second., J. Cramer.

Chapman, V.J., 1941. Studies in ecology VIII. *Journal of Ecology*, 29, pp.69–82.

Chapman, V.J., 1939. Studies in saltmarsh ecology V, the vegetation. *Journal of Ecology*, 27, pp.181–201.

Chen, Z. et al., 2006. A new process for the segmentation of high resolution remote sensing imagery. *International Journal of Remote Sensing*, 27(22), pp.4991–5001. Available at: http://www.tandfonline.com/doi/abs/10.1080/01431160600658131 [Accessed March 23, 2013].

Chmura, G.L. et al., 2003. Global carbon sequestration in tidal, saline wetland soils. *Global Biogeochemical Cycles*, 17, pp.1111–1133.

Chu-Agor, M. et al., 2010. Global sensitivity and uncertainty analysis of SLAMM for the purpose of habitat vulnerability assessment and decision making. *World Environmental and Water Resources Congress 2010*, pp.4702–4709.

Chu-Agor, M.L. et al., 2011. Exploring vulnerability of coastal habitats to sea level rise through global sensitivity and uncertainty analyses. *Environmental Modelling & Software*, 26(5), pp.593–604. Available at: http://linkinghub.elsevier.com/retrieve/pii/S136481521000321X [Accessed January 26, 2014].

Church, J.A. et al., 2004. Estimates of the Regional Distribution of Sea Level Rise over the 1950 – 2000 Period. *Jouirnal of Clime*, 17(13), pp.2609–2625.

Church, J.A. et al., 2011. Revisiting the Earth's sea-level and energy budgets from 1961 to 2008. *Geophysical Research Letters*, 38(18), pp.1–8. Available at: http://www.agu.org/pubs/crossref/2011/2011GL048794.shtml [Accessed March 15, 2012].

Church, J.A. & White, N.J., 2006. A 20th century acceleration in global sea-level rise. *Geophysical Research Letters*, 33(1), pp.94–97. Available at: http://www.agu.org/pubs/crossref/2006/2005GL024826.shtml [Accessed June 12, 2011].

Chust, G. et al., 2008. Coastal and estuarine habitat mapping, using LIDAR height and intensity and multi-spectral imagery. *Estuarine, Coastal and Shelf Science*, 78(4), pp.633–643. Available at: http://linkinghub.elsevier.com/retrieve/pii/S0272771408000541.

Civis, J. et al., 1987. El Neogeno marino de la provincia de Huelva: antecedentes y definicion de las unidades litoestragraficas. In U. de Salamanca, ed. *Paleontologıa del Neogeno de Huelva (W. Cuenca del Guadalquivir)*. pp. 9–23.

Clough, J. et al., 2012. *SLAMM 6.2 Technical Documentation*,

Clough, J.S., Park, R.A. & Fuller, R., 2010. SLAMM 6 beta Technical Documentation SLAMM 6 Technical Documentation. *Wetlands*, (May), p.51.

Cohen, J., 1960. A Coefficient of Agreement for Nominal Scales. *Educational and Psychological Measurement*, 20(1), pp.37–46. Available at: http://epm.sagepub.com/cgi/doi/10.1177/001316446002000104 [Accessed March 4, 2013].

Conesa, H.M. et al., 2011. Influence of soil properties on trace element availability and plant accumulation in a Mediterranean salt marsh polluted by mining wastes: implications for phytomanagement. *The Science of the total environment*, 409(20), pp.4470–4479.

Corre, J., 1978. Étude phyto-ecologique des milieux littoraux salés en Languedoc et Camargue. IV Dinamique de la vegetation conclusion générales. *Vie Milieu*, 28/29(2c), pp.291–314.

Costa, J.C. et al., 2009. Finding the Boundary between Eurosiberian and Mediterranean Salt Marshes. *Journal of Coastal Research*, (56), pp.1340–1344.

Costanza, R. et al., 1997. The value of the world's ecosystem: services and natural capital. *Nature*, 387, pp.253–260.

Costanza, R., Sklar, F.H. & White, M.L., 1990. Modeling Coastal Landscape Dynamics. *BioScience*, 40(2), pp.91–107.

Cott, G.M. et al., 2013. Waterlogging affects the distribution of the saltmarsh plant Atriplex portulacoides. *Flora- Morphology, Distribution, Functional Ecology of Plants*, 208(5), pp.336–342.

Craft, C. et al., 2009. Forecasting the effects of accelerated sea-level rise on tidal marsh ecosystem services. *Frontiers in Ecology and the Environment*, 7(2), pp.73–78. Available at: http://www.esajournals.org/doi/abs/10.1890/070219 [Accessed January 27, 2014].

Crain, C.M. et al., 2004. Physical and biotic drivers of plant distribution across estuarine salinity gradients. *Ecology*, 85(9), pp.2539–2549.

Curco, A. et al., 2002. Net Primary Production and Decomposition of Salt Marshes of the Ebre Delta (Catalonia , Spain). *Estuaries*, 25(3), pp.309–324.

D'Alpaos, A. et al., 2007. Landscape evolution in tidal embayments: Modeling the interplay of erosion, sedimentation, and vegetation dynamics. *Journal of Geophysical Research*, 112(F01008). Available at: http://doi.wiley.com/10.1029/2006JF000537 [Accessed February 13, 2015].

Dabrio, C. et al., 2000. Depositional history of estuarine infill during the last postglacial transgression (Gulf of Cadiz, Southern Spain). *Marine Geology*, 162, pp.381–404.

Dabrio, C.J. et al., 2000. Depositional history of estuarine infill during the last postglacial transgression (Gulf of Cadiz , Southern Spain). *Marine Geology*, 162, pp.381–404.

Dale, P.E.., Chandica, A.. L. & Evans, M., 1996. Using image subtraction and classification to evaluate change in subtropical intertidal wetlands. *International Journal of Remote Sensing*, 17, pp.703–719.

Darke, A.K. & Megonigal, J.P., 2003. Control of sediment deposition rates in two mid-Atlantic Coast tidal freshwater wetlands. *Estuarine, Coastal and Shelf Science*, 57, pp.255–268. Available at: http://www.serc.si.edu/labs/biogeochem/publications/Darke_Megonigal_2003.pdf.

Davidson-Arnott, R.G.D., van Proosdij, D., et al., 2002. Hydrodynamics and sedimentation in salt marshes: examples from a macrotidal marsh, Bay of Fundy. *Geomorphology*, 48(1-3), pp.209–231. Available at: http://linkinghub.elsevier.com/retrieve/pii/S0169555X02001824.

Davidson-Arnott, R.G.D., Van Proosdij, D. & Schostak, L., 2002. Hydrodinamics and sedimentation in salt marshes: examples of macrotidal marsh, Bay of Fundy. *Geomorphology*, 48, pp.209–231.

Davis, R.A. et al., 2000. RíoTinto estuary (Spain): 5000 years of pollution. *Environmental geology*, 39(10), pp.1107–1126.

Day, J.H., 1981. The estuary flora. In J. H. Day, ed. *Estuarine ecology with particular*

reference to Southern Africa. Rotterdam, Balkema, pp. 77–79.

Dean, R.G. et al., 1987. *Responding to Changes in Sea Level: Engineering Implications*, Washington, DC, USA: National Academy Press.

Dijkema, K.S., 1984. Development and classification of main salt-marsh biotopes in Europe. In K. S. Dijkema, ed. *Salt marsh in Europe*. Strasbourg: Council of Europe, pp. 8–14.

DINAS-COAST Consortium, 2006. *DIVA 1.0 Postdam Institute for Climate Impact Research, Postdam, Germany, CR-ROM*,

Dodson, J.R. & Ramrath, A., 2001. An Upper Pliocene lacus- trine environmental record from south-Western Australia – preliminary results. *palaeogeography, Palaeoclim, Palaeoecology*, 167, pp.309–320.

Domingues, C.M. et al., 2008. Improved estimates of upper-ocean warming and multi-decadal sea-level rise. *Nature*, 453, pp.1090–3. Available at: http://www.ncbi.nlm.nih.gov/pubmed/18563162 [Accessed July 12, 2011].

Van Dongeren, A.R. & De Vriend, H.J., 1994. A model of morphological behaviour of tidal basins. *Coastal Engineering*, 22, pp.287–310.

Doody, J.P., 2004. "Coastal squeeze" - an historical perspective. *Journal of Coastal ConservationCoastal*, 10, pp.129–138.

Doody, J.P., 2012. Coastal squeeze and managed realignment in southeast England, does it tell us anything about the future? *Ocean & Coastal Management*, xxx, pp.1–8. Available at: http://linkinghub.elsevier.com/retrieve/pii/S0964569112001172 [Accessed October 18, 2012].

Doody, J.P., 2008. *Saltmarsh Conservation, Management and Restoration*, USA: Springer.

Douglas, B.., 1991. Global Sea Level Rise. *Journal of Geophysical Research*, 96(C4), pp.6981–6992. Available at: http://www.springerlink.com/content/p364381652174757/export-citation/.

Douglas, B.C., 2001. Change in the Era of the recording. In B. C. Douglas, M. S. Kearney, & S. P. Leatherman, eds. *Sea Level Rise: History and Consequences*. International Geophysics. San Diego: Academy Press, pp. 37–64. Available at: http://dx.doi.org/10.1016/S0074-6142(01)80006-1 [Accessed March 12, 2013].

Duarte, C. & Cebrian, J., 1996. The fate of marine autotrophic production. *Limnology and Oceanography*, 41, pp.1759–1766.

EEA, 2008. *Impacts of Europe's changing climate - 2008 indicator-based assessment*, Available at: http://www.eea.europa.eu/data-and-maps/indicators/sea-level-rise/sea-level-rise-assessment-published.

Ehman, J., 2008. *Data Report on SLAMM Model Results for Ten National Wildlife Refuges in South Carolina and Georgia : Wassaw NWR, Georgia*, Wassaw, Georgia. Available at: http://www.fws.gov/southeast/climate/action/Wassaw SLAMM Report.pdf.

Elzinga, C.L., Salzer, D.W. & Willoughby, J.W., 1998. *Measuring & monitoring plant populations*, Denver, CO, US: U.S. Dept. of the Interior Bureau of Land Management National Applied Resource Sciences Center.

Emery, N.C., Ewanchuk, P.J. & Bertness, M.D., 2001. Competition and salt-marsh plant zonation: stress tolerators may be dominant competitors. *Ecology*, 82(9), pp.2471–2485.

Erfanzadeh, R., 2010. Environmental determinism versus biotic stochasticity in the appearance of plant species in salt-marsh succession. *Plant Ecology and Evolution*, 143(1), pp.43–50. Available at: http://www.ingentaconnect.com/content/botbel/plecevo/2010/00000143/00000001/art00005 [Accessed February 13, 2013].

Fagherazzi, S. et al., 2012. NUMERICAL MODELS OF SALT MARSH EVOLUTION :

ECOLOGICAL , GEOMORPHIC , AND CLIMATIC FACTORS. *Reviews of Geophysics*, 50(RG1002), pp.1–28.

Fairbanks, R.G., 1989. A 17,000-year glacio-eustatic sea level record: influence of glacial melting rates on the Younger Dryas event and deep-ocean circulation. *Nature*, 342, pp.637–642.

Fairbridge, R.W., 1960. The changing level of the sea. *Scientific American*, 202, pp.70–79.

Figueroa, E. et al., 1987. Distribucion y Nutricion Mineral de Salicornia ramosissima J. Woods, Salicornia europaea L. y Salicornia dolichostachya Moss. en el estuario de los rios Odiel y Tinto (Huelva, SO España). *Limnetica*, 3(2), pp.307–310.

Fitzgerald, D.M., 1984. Interactions between the Ebb-Tidal Delta and Landward Shoreline: Price Inlet, South Carolina. *Journal of Sedimentary Research*, 54(4), pp.1303–1318.

Fraile, P., 2011. *Análisis de las problemáticas asociadas a la espacialización, evolución y representación de niveles del Mar presentes y Futuros en Andalucía*. University of Seville.

Fraile, P., 2005. *Niveles medios y máximos del mar en los mareógrafos del litoral andaluz*. University of Seville.

Fraile-Jurado, P. & Fernandez-Diaz, M., Escenarios de subida del nivel medio del mar en los mareógrafos de las costas peninsulares de España en el año 2100 (in press.). *Estudios Geograficos*, 77(280).

French, J.R., 2003. Airborne LiDAR in support of geomorphological and hydraulic modelling. *Earth Surface Processes and Landforms*, 28(3), pp.321–335. Available at: http://doi.wiley.com/10.1002/esp.484 [Accessed October 7, 2014].

French, J.R., 1991. Eustatic and neotectonic controls on salt marsh sedimentation. In D. L. Kraus, N. C., Gingerich, K. J. and Kriebel, ed. *Coastal Sediments '91*. American Society of Civil Engineers, New York, pp. 1223–1236.

French, J.R., 1993. Numerical Simulation of Vertical Marsh Growth and Adjustment to Accelerated Sea-Level Rise, Norfolk, U.K. *Earth Surface Processes and Landforms*, 18, pp.63–81.

French, J.R., 2006. Tidal marsh sedimentation and resilience to environmental change: Exploratory modelling of tidal, sea-level and sediment supply forcing in predominantly allochthonous systems. *Marine Geology*, 235(1-4), pp.119–136. Available at: http://linkinghub.elsevier.com/retrieve/pii/S0025322706002623 [Accessed August 8, 2011].

French, J.R. & Spencer, T., 1993. Dynamics of sedimentation in a tide-dominated backbarrier salt marsh, Norfolk, UK. *Marine Geology*, 110, pp.315–331.

French, J.R., Spencer, T. & Reed, D.J., 1995. Editorial—geomorphic response to sea-level rise: Existing evidence and future impacts. *Earth Surface Processes and Landforms*, 20(1), pp.1–6. Available at: http://doi.wiley.com/10.1002/esp.3290200102.

French, J.R. & Stoddart, D.R., 1992. Hydrodynamics of salt marsh creek systems: Implications for marsh morphological development and material exchange. *Earth Surface Processes and Landforms*, 17(3), pp.235–252. Available at: http://doi.wiley.com/10.1002/esp.3290170304.

Frey, W.F. & Basan, B.B., 1978. Coastal Salt Marshes. In R. A. Davis, ed. *Coastal Sedimentary Environments*. New York: Springer-Verlag, pp. 101–170.

Galván, L. et al., 2016. Hydrological modeling of a watershed affected by acid mine drainage (Odiel River, SW Spain). Assessment of the pollutant contributing areas. *Journal of Hydrology*, 540, pp.196–206.

Gedan, K.B., Silliman, B.R. & Bertness, M.D., 2009. Centuries of Human-Driven Change in Salt Marsh Ecosystems. *Annual Review of Marine Science*, 1, pp.117–141.

Gehu, J.M., 1972. Cartographie en reseaux et phytosociologie. In E. Van der Maarvel & R. Tuxen, eds. *Grundfragen und Methoden in der Pflanzesoziologie*. Vaduz, pp. 263–277.

Gehu, J.M., 1984. Mediterranean salt marshes and salt steppes. In K. S. Dijkema, ed. *Salt marsh in Europe*. Strasbourg: Council of Europe, pp. 129–142.

Gehu, J.M. & Rivas-Martinez, S., 1984. Classification of European salt plant communities. In K. S. Dijkema, ed. *Salt marsh in Europe*. Strasbourg: Council of Europe, pp. 34–40.

Genc, L., Dewitt, B. & Smith, S., 2004. Determination of wetland vegetation height with LIDAR. *Turkish Journal of Agriculture and Forestry*, 28, pp.63–71.

Gesch, D.B., 2009. Analysis of Lidar Elevation Data for Improved Identification and Delineation of Lands Vulnerable to Sea-Level Rise. *Journal of Coastal Research*, 10053, pp.49–58. Available at: http://www.bioone.org/doi/abs/10.2112/SI53-006.1 [Accessed November 14, 2012].

Geselbracht, L. et al., 2011. Retrospective and prospective model simulations of sea level rise impacts on Gulf of Mexico coastal marshes and forests in Waccasassa Bay, Florida. *Cilmate Change*, 107(1-2), pp.35–57.

Gilmore, M. et al., 2008. Integrating multi-temporal spectral and structural information to map wetland vegetation in a lower Connecticut River tidal marsh. *Remote Sensing of Environment*, 112, pp.4048–4060.

Gilvear, D., Tyler, A. & Davids, C., 2004. Detection of estuarine and tidal river hydromorphology using hyper-spectral and LiDAR data: Forth estuary, Scotland. *Estuarine, Coastal and Shelf Science*, 61, pp.379–392.

van Goor, M.A. et al., 2003. Impact of sea-level rise on the morphological equilibrium state of tidal inlets. *Marine Geology*, 202, pp.211–227.

Göpfert, J. & Heipke, C., 2006. ASSESSMENT OF LIDAR DTM ACCURACY IN COASTAL VEGETATED AREAS. *The InternationalArchivesof the Photogrammetry,Remote Sensing and Spatial Information Sciences*, 36, pp.79–85.

Gordon, D.C., Cranford, P.J. & Desplanque, C., 1985. Observations on the ecological importance of salt marshes in the Cumberland Basin, a macrotidal estuary in the Bay of Fundy. *Estuarine, Coastal and Shelf Science*, 20, pp.205–227.

Gornitz, V., 1995. Sea-Level Rise: A Review of Recent Past and Near-Future Trends. *Earth Surface Processes and Landforms*, 20, pp.7–20.

Gornitz, V. & Lebedeff, S., 1987. Global sea level changes during the past century. In D. Nummedal, 0. H. Pilkey, & J. D. Howard, eds. *Sea Level Fluctuation and Coastal Evolution*. Oklahoma: SEPM Special Publications, pp. 3–16.

Goy, J.L. et al., 1996. Global and regional factors controlling changes of coastlines in southern Iberia (Spain) during the Holocene. *Quaternary Science Reviews*, 15(96), pp.773–780.

Van der Graaf, A.J. et al., 2002. Short-term and long-term facilitation of goose grazing by livestock in the Dutch Wadden Sea area. *Journal of Coastal Conservation*, 8, pp.179–188.

Gracia, F.J. et al., 1990. Evolucion eustatica postflandriense en las marismas del Sur de la Bahia de Cadiz. *Geograceta*, 27, pp.71–77.

Gray, A.J., 1985. Adaptation in perennial coastal plants - with particular referenceto heritable variation in Punicciella maritima and Ammophila arenaria. *Vegetatio*, 61, pp.179–188.

Gray, A.J., 1992. Saltmarsh plant ecology: zonation and succession revisited. In J. R. L. Allen & K. Pye, eds. *Saltmarshes: Morphodynamics, Conservation and Engineering Significance*. Cambridge, UK: Cambridge University Press, pp. 63–79.

Gray, A.J., 1980. Saltmarshes and reclaimed land. In G. Halliday & A. W. Malloch, eds. *Wild*

Flowers: Their Habitats in Britain and North Europe. London: Peter Lowe, pp. 123–133.

Gray, A.J. & Brunce, R.G.M., 1972. The ecology of Morecambe bay VI. Soils and vegetation of salt marshes: a multivariate approach. *Journal of Applied Ecology*, 9, pp.221–234.

Green, D. & King, S., 2003. Progress in Geographical Information Systems and Coastal Modeling: An Overview. In V. (ed) Lakhan, ed. *Advances in Coastal Modeling*. Elsevier Science, pp. 553–580.

Gribsholt, B. & Kristensen, E., 2003. Benthic metabolism and sulfur cycling along an inundation gradient in a tidal Spartina anglica salt marsh. *Limnology and Oceanography*, 48, pp.2151–2162.

Groenendijk, A.M., 1987. Primary production and biomass on a Dutch salt marsh: emphasis on the below-ground component. *Vegetatio*, 70, pp.21–27.

Gutenberg, B., 1941. Changes in sea level, post-glacial uplift and mobility of the earth's interior. *Bulletin of the geological society of America*, 52, pp.721–722.

Hacker, S.D. & Bertness, M.D., 1995. Morphological and physiological consequences of a positive plant interaction. *Ecology*, 76, pp.2165–2175.

Hartig, E.K. et al., 2002. Anthropogenic and climate-change impacts on salt marshes of Jamaica Bay, New York City. *Wetlands*, 22(1), pp.71–89. Available at: http://link.springer.com/10.1672/0277-5212(2002)022[0071:AACCIO]2.0.CO;2.

Harvey, K.R. & Hill, G.J.E., 2001. Vegetation mapping of a tropical freshwater swamp in the Northern Territory, Australia: A comparison of aerial photography, Landsat TM and SPOT satellite imagery. *International Journal of Remote Sensing*, 22(15), pp.2911–2925. Available at: http://www.tandfonline.com/doi/abs/10.1080/01431160119174.

Haslett, S.K., 2009. *Coastal systems*, New York: Routledge.

Hauer, M.E., Evans, J.M. & Alexander, C.R., 2015. Sea-level rise and sub-county population projections in coastal Georgia. *Population and Environment*. Available at: http://link.springer.com/10.1007/s11111-015-0233-8 [Accessed April 2, 2015].

He, M., Zhao, B., Ouyang, Z., Yan, Y., Li, B., 2010. Linear spectral mixture analysis of Landsat TM data for monitoring invasive exotic plants in estuarine wetlands. *International Journal of Remote Sensing*, 31(16), pp.4319–4333. Available at: http://www.tandfonline.com/doi/abs/10.1080/01431160903252343 [Accessed April 10, 2013].

Heiri, O., Lotter, A.F. & Lemcke, G., 2001. Loss on ignition as a method for estimating organic and carbonate content in sediments: reproducibility and comparability of results. *Journal of Paleolimnology*, 25(1), pp.101–110.

Hill, M.O. & Šmilauer, P., 2005. TWINSPAN for Windows version 2.3. Centre for Ecology & Hydrology and University of South Bohemia, Huntingdon & České Budějovice.

Himmelstoss, E.A., 2009. Dsas 4.0. Instructions Installation Guide User. In E. R. Thieler et al., eds. *Digital Shoreline Analysis System (DSAS) version 4.0 — An ArcGIS extension for calculating shoreline change: U.S. Geological Survey Open-File Report 2008-1278*.

Hinde, H.P., 1954. The vertical distribution of salt marshes phanerogams in relation to tide levels. *Ecological Monographs*, 24, pp.209–225.

Hinkel, J., 2005. DIVA: An Iterative Method for Building Modular Integrated Models. *Advances in Geosciences*, 4, pp.45–50.

Hinkel, J. & Klein, R.J.T., 2007. Integrating Knowledge for Assessing Coastal Vulnerability to Climate Change. In E. C. (eds) McFadden, L., Nicholls, R.J., Penning- Rowsell, ed. *Managing Coastal Vulnerability: An Integrated Approach*. Amsterdam: Elsevier Science, pp. 61–78.

Hinkel, J. & Klein, R.J.T., 2009. "Integrating Knowledge to Assess Coastal Vulnerability to Sea-Level Rise: The Development of the DIVA Tool." *Global Environmental Change*, 19, pp.384–395.

Hladik, C. & Alber, M., 2012. Accuracy assessment and correction of a LIDAR-derived salt marsh digital elevation model. *Remote Sensing of Environment*, 121, pp.224–235. Available at: http://linkinghub.elsevier.com/retrieve/pii/S0034425712000557 [Accessed March 5, 2013].

Holgate, S.J. & Woodworth, P.L., 2004. Evidence for enhanced coastal sea level rise during the 1990s. *Geophysical Research Letters*, 31(7), p.L07305. Available at: http://www.agu.org/pubs/crossref/2004/2004GL019626.shtml [Accessed March 8, 2013].

Hopkinson, C., Lim, K., Chasmer, L.E., Treitz, P., Creed, I.F., Gynan, C., 2004. Wetland grass to plantation forest - estimating vegetation height from the standard deviation of lidar frequency distributions. *Remote Sensing and Spatial Information Science*, 36(Part 8/W2), pp.288–294.

Horning, N. et al., 2010. *Remote Sensing for Ecology and Conservation*, Oxford university press.

Houser, C., 2010. Relative Importance of Vessel-Generated and Wind Waves to Salt Marsh Erosion in a Restricted Fetch Environment. *Journal of Coastal Research*, 26(2), pp.230–240.

Howes, B.L., Howarth, R.W., Teal, J.M., Valiela, I., 1981. Oxidation-reduction potentials in a salt-marsh. Spatial patterns and interaction with primary production. *Limnology and Oceanography*, 26, pp.350–360.

Huckle, J.M., Potter, J.A. & Marrs, R.H., 2000. Influence of environmental factors on the growth and interactions between salt marsh plants : efects of salinity , sediment and waterlogging. *Journal of Ecology*, 88, pp.492–505.

Huiskes, A., Koutstaal, B.P., Herman, P.M.J., Beeftink, W.G., Markusse, M.M., De Munck, W., 1995. Seed dispersal of halo- phytes in tidal salt marshes. *Journal of Ecology*, 83, pp.559–567.

Hurd, J.D. Civco, D.L., Gilmore, M.S., Prisloe, S., Wilson, E.H., 2006. Tidal Wetland classification from LandSat Imagery using an Integrated Pixel-Based and Object Based Classification Approach. In *ASPRS Annual Conference*. Reno, Nevada.

Ihm, B.S., Lee, J.S., Kim, J.W., Kim, J.H., 2007. Coastal plant and soil relationships along the southwestern coast of south Korea. *Journal of Plant Biology*, 50(3), pp.331–335.

IPCC, 2007. *Climate Change 2007: Synthesis Report*, Valencia, Spain.

Kaswadji, R.F., Gosselink, J.G. & Turner, R.E., 1990. Estimation of primary production using five different methods in a Spartina alterniflora salt marsh. *Wetlands Ecology and Management*, 1(2), pp.57–64.

Katsman, C.A., Hazeleger, W., Drijfhout, S.S., Oldenborgh, G.J., Burgers, G., 2008. Climate scenarios of sea level rise for the northeast Atlantic Ocean: a study including the effects of ocean dynamics and gravity changes induced by ice melt. *Climatic Change*, 91(3-4), pp.351–374. Available at: http://www.springerlink.com/index/10.1007/s10584-008-9442-9 [Accessed March 12, 2013].

Kelly, M., Tuxen, K.A. & Stralberg, D., 2011. Mapping changes to vegetation pattern in a restoring wetland: Finding pattern metrics that are consistent across spatial scale and time. *Ecological Indicators*, 11(2), pp.263–273. Available at: http://linkinghub.elsevier.com/retrieve/pii/S1470160X1000083X [Accessed March 21, 2013].

Kennish, M.J., 2001. Coastal Salt Marsh Systems in the U.S.: A Review of Anthropogenic

Impacts. *Journal of Coastal Research*, 17(3), pp.731–748.

Kennish, M.J., 1986. *Ecology of estuaries, vol. I. Physical and Chemical aspect*, Boca Raton, Florida: CRC Press.

Kent, M. & Coker, P., 1992. *Vegetation Description and Analysis: A Practical Approach*, London: Belhaven Press.

Kiker, G.A., Bridges, T.S. & Kim, J., 2008. Integrating comparative risk assessment with multi-criteria decision analysis to manage contaminated sediments: an example from New York/New Jersey Harbor. *Human and Ecological Risk Assessment*, 14(3), pp.495–511.

Kim, D., Bartholdy, J., et al., 2011. Salt Marshes as Potential Indicators of Global Climate Change. *Geography Compass*, 5, pp.219–236.

Kim, D., Cairns, D.M. & Bartholdy, J., 2011. Multi-scale GEOBIA with very high spatial resolution digital aerial imagery: scale, texture and image objects. *International Journal of Remote Sensing*, 31(1), pp.58–78. Available at: http://bellwether.metapress.com/content/k6811v012504j153/.

King, S.E. & Lester, J., 1995. The value of salt marsh as a sea defence. *Marine Pollution Bulletin*, 30(3), pp.180–189.

Klige, R.K., 1982. Oceanic level fluctuations in the history of the earth. In P. A. Kaplin, R. K. Klige, & A. . Chepalyga, eds. *Sea and Oceanic Level Fluctuations for 15,00O years*. Moscow: Institute of Geography, pp. 11–22.

Korsman, T., Nilsson, M.B., Landgren, K., Renberg, I., 1999. Spatial variability in surface sediment composition characterisec by near-infrared (NIR) reflectance spectroscopy. *Journal of Paleolimnology*, 21, pp.61–71.

Kragtwijk, N.G., Zitman, T.J., Stive, M.J.F., Wang, Z.B.., 2004. Morphological response of tidal basins to human interventions. *Coastal Engineering*, 51, pp.207–221.

Krone, R.B., 1987. A method for Simulating Historic Marsh elevations. N Kraus, N.C. (ed). In N. C. Kraus, ed. *Coastal Sediments '87*. American Society of Civil Engineers, New York, pp. 316–323.

Lambeck, K. & Chappel, J., 2001. Sea level change during the last glacial cycle. *Science*, 292, pp.679–686.

Lambeck, K., Yokoyama, Y. & Purcell, T., 2002. Into and out of the Last Glacial Maximum: sea-level change during Oxygen Isotope Stages 3 and 2. *Quaternary Science Reviews*, 21(1), pp.343–360.

Landi, M. & Angiolini, C., 2015. Soil-Plant Relationships in Mediterranean Salt Marshes across Dune-Cultivated Land Gradient. *Journal of Coastal Research*, 313(3), pp.588–594. Available at: http://www.bioone.org/doi/10.2112/JCOASTRES-D-13-00009.1 [Accessed February 16, 2016].

Lario, J., Zazo, C., et al., 2002. Changes in sedimentation trends in SW Iberia Holocene estuaries (Spain). *Quaternary International*, 93-94, pp.171–176. Available at: http://linkinghub.elsevier.com/retrieve/pii/S1040618202000150.

Lario, J., Spencer, C., et al., 2002. Particle size characterisation of Holocene back-barrier sequences from North Atlantic coasts (SW Spain and SE England). *Geomorphology*, 42(1-2), pp.25–42. Available at: http://linkinghub.elsevier.com/retrieve/pii/S0169555X0100071X.

De Leeuw, J., De Munck, W., Olff, H., Bakker, J.P., 1993. Does zonation reflect the succession of salt-marsh vegetation? A comparison of an estuarine and a coastal bar island marsh in The Netherlands. *Acta botanica neerlandica*, 42(4), pp.435–445. Available at: http://cat.inist.fr/?aModele=afficheN&cpsidt=3962391 [Accessed February 15, 2013].

Lefeuvre, J.C. et al., 2003. Biodiversity in salt marshes: from patrimonial value to ecosystem functioning. The case study of the Mont-Saint-Michel bay. *Comptes Rendus Biologies*, 326, pp.125–131. Available at: http://linkinghub.elsevier.com/retrieve/pii/S1631069103000490 [Accessed October 18, 2012].

Lefeuvre, J.C. & Dame, R.F., 1994. Comparative studies of salt marsh processes in the New and Old Worlds: an introduction. In W. J. Mitsch, ed. *Global Wetlands: Old and New World*. Amsterdam: Elservier, pp. 169–179.

Leonard, L.A., 1997. Controls of sediment transport and deposition in an incised mainland marsh basin, southeastern North Carolina. *Wetlands*.

Leonard, L.A. & Reed, D.J., 2002. Hydrodynamics and Sediment Transport Through Tidal Marsh Canopies. *Journal of Coastal ConservationCoastal*, SI(36), pp.459–469.

Lepš, J. & Šmilauer, P., 1999. *Multivariate analysis of ecological data*, Ceske Budejovice, Czech Republic: University of South Bohemia.

Leuliette, E.W., Nerem, R.S. & Mitchum, G.T., 2004. Calibration of TOPEX/Poseidon and Jason Altimeter Data to Construct a Continuous Record of Mean Sea Level Change. *Marine Geodesy*, 27(1-2), pp.79–94. Available at: http://www.tandfonline.com/doi/abs/10.1080/01490410490465193 [Accessed March 12, 2013].

Levin, L.A. et al., 2001. The Function of Marine Critical Transition Zones and the Importance of Sediment Biodiversity. *Ecosystems*, 4(5), pp.430–451. Available at: http://link.springer.com/10.1007/s10021-001-0021-4 [Accessed April 15, 2013].

Levine, J.M., Brewer, J.S. & Bertness, M.D., 1998. Nutrients, competition and plant zonation in a New England salt marsh. *Journal of Ecology*, 86(2), pp.285–292.

Lillebø, A.I. et al., 1999. The effect of macrofauna, meiofauna and microfauna on the degradation of Spartina maritima detritus from a salt marsh area. *Acta Oecologica*, 20(4), pp.249–258. Available at: http://dx.doi.org/10.1016/S1146-609X(99)00141-1 [Accessed April 15, 2013].

Linhoss, A.C. et al., 2013. Decision analysis for species preservation under sea-level rise. *Ecological Modelling*, 263, pp.264–272. Available at: http://linkinghub.elsevier.com/retrieve/pii/S0304380013002767 [Accessed May 12, 2015].

Linkov, I. et al., 2006. From comparative risk assessment to multi-criteria decision analysis and adaptive management: recent developments and applications. *Environment International*, 32(8), pp.1072–1093.

Long, S.P. & Mason, F.C., 1983. *Saltmarsh ecology*, Glasgow: Blackie.

Lopez, E. et al., 2006. *Estudio de los drenajes acidos de minas y su tratamiento mediate sistemas pasivos en la cuenca del Rio Odiel (Faja Piritica, Huelva). Volumen I.*, Available at: http://info.igme.es/SidPDF%5C112000%5C148%5CTomo I%5C112148_0001.pdf.

Lopez, F. & Garcia, M., 1998. Open-channel flow through sim- ulated vegetation: Suspended sediment transport modeling. *Water Resources Research*, 34, pp.2341–2352.

Lopez-Gonzalez, N. et al., 2006. Variación estacional de las características texturales en los sedimentos intermareales del estuario de los ríos Tinto y Odiel (SO España). *Geogaceta*, 40, pp.291–294.

López-González, N. et al., 2006. Geochemical variations in estuarine sediments: Provenance and environmental changes (Southern Spain). *Estuarine, Coastal and Shelf Science*, 67(1-2), pp.313–320. Available at: http://linkinghub.elsevier.com/retrieve/pii/S0272771405004038 [Accessed March

2, 2013].

Lu, D. & Weng, Q., 2007. A survey of image classification methods and techniques for improving classification performance. *International Journal of Remote Sensing*, 28(5), pp.823–870. Available at: http://www.tandfonline.com/doi/abs/10.1080/01431160600746456 [Accessed February 28, 2013].

Luque, C.J. et al., 1998. Distribucion de metales pesados en sedimentos de las marismas del Odiel (Huelva, SW Spain). *Cuaternario y Geomorfologia*, 12(3-4), pp.77–85.

Lyon, J.G. & McCarthy, J., 1995. Introduction to Wetland and Environmental Applications of GIS. In J. (eds) Lyon, J.G and McCarthy, ed. *Wetland and Environmental Applications of GIS*. United States of America: Lewis Publishers, pp. 3–8.

Macdonald, K.B., 1977a. Coastal salt marsh. In M. G. Major & J. Barbour, eds. *Terrestrial vegetation of California*. New York, pp. 263–294.

Macdonald, K.B., 1977b. Plant and animal communities of Pacific North American salt marshes. In V. J. Chapman, ed. *Wet coastal ecosystems*. Amsterdam: Elservier, pp. 167–191.

Marani, M. et al., 2006. Analysis, synthesis and modelling of high-resolution observations of salt-marsh eco-geomorphological patterns in the Venice lagoon. *Estuarine, Coastal and Shelf Science*, 69(3-4), pp.414–426. Available at: http://linkinghub.elsevier.com/retrieve/pii/S0272771406001752 [Accessed February 28, 2013].

McCaffrey, R.J. & Thompson, J., 1980. A record of the accumulation of sediment and trace metals in a Connecticut salt marsh. *Advances in Geophysics*, 22, pp.165–236.

McClure, A. et al., 2015. Evaluation of Error Reduction Techniques on a LIDAR-Derived Salt Marsh Digital Elevation Model. *Just CERFing*, 6(11), pp.8–17.

Mcleod, E. et al., 2010. Sea-level rise impact models and environmental conservation: A review of models and their applications. *Ocean & Coastal Management*, 53(9), pp.507–517. Available at: http://linkinghub.elsevier.com/retrieve/pii/S0964569110000852 [Accessed September 18, 2013].

McLusky, D.S. & Elliot, M., 2004. *The Estuarine Ecosystem: Ecology, Threats, and Management* 3 rd ed., Oxford university press.

Meehl, G.A., Stocker, T.F., et al., 2007. Global Climate Projections. In S. Solomon et al., eds. *Contribution of Working Group I to the Fourth Assessment Report of IPCC on Climatic Change*. Cambridge, UK: Cambridge University Press, pp. 749–844.

Meehl, G.A., Covey, C., et al., 2007. The WCRP CMIP3 Multimodel Dataset: A New Era in Climate Change Research. *Bulletin of the American Meteorological Society*, 88(9), pp.1383–1394. Available at: http://journals.ametsoc.org/doi/abs/10.1175/BAMS-88-9-1383 [Accessed March 1, 2013].

Meng, X., Currit, N. & Zhao, K., 2010. Ground Filtering Algorithms for Airborne LiDAR Data: A Review of Critical Issues. *Remote Sensing*, 2(3), pp.833–860. Available at: http://www.mdpi.com/2072-4292/2/3/833/ [Accessed March 10, 2013].

Millennium Ecosystem Assessment, 2005. *Ecosystems and Human Well-Being: Wetlands and Water. Synthesis*, Washington, D.C.

Miller, L. & Douglas, B.C., 2006. On the rate and causes of twentieth century sea-level rise. *Philosophical transactions. Series A, Mathematical, physical, and engineering sciences*, 364(1841), pp.805–20. Available at: http://www.ncbi.nlm.nih.gov/pubmed/16537141 [Accessed March 20, 2012].

Mitsch, W.J. & Gosselink, J.G., 2000. The value of wetlands: importance of scale and landscape setting. *Ecological Economics*, 35(200), pp.25–33.

Moffett, K.B. & Gorelick, S.M., 2013. Distinguishing wetland vegetation and channel features with object-based image segmentation. *International Journal of Remote Sensing*, 34(4), pp.1332–1354.

Montané, J.M. & Torres, R., 2006. Accuracy Assessment of Lidar Saltmarsh Topographic Data Using RTK GPS. *Photogrammetric Engineering & Remote Sensing*, 72(8), pp.961–967.

Morales, J.A., 2016. *Un modelo 3D de arquitectura de facies de los sedimentos Holocenos del estuario del Odiel (Huelva , SO de España)*., Huelva.

Morales, J.A. & Borrego, J., 2000. Propagacion de la onda de marea en el Estuario del rio Tinto (Huelva, Espana). *Geogaceta*, 27, pp.115–118.

Morales, J.A. & Ojeda, J., 2010. Evolucion geomorfologica de la Ria de Huelva. In F. Sancho et al., eds. *Agua, Territorio y Ciudad: Huelva maritima y minera*. Sevilla: Agencia Andaluza del Agua, Consejeria de Medio Ambiente, pp. 36–40.

Morales, J.A., San Miguel, E.G. & Borrego, J., 2003. Tasas de sedimentation reciente en la Ria de Huelva . *Geogaceta*, 33, pp.15–18.

Morris, J.T., 2007. Ecological engineering in intertidal saltmarshes. *Hidrobiologia*, 577, pp.161–168.

Morris, J.T. et al., 2005. International Journal of Remote Integrating LIDAR elevation data, multi - spectral imagery and neural network modelling for marsh characterization. *International Journal of Remote Sensing*, 26(23), pp.5221–5234.

Morris, J.T. et al., 2002. Responses of coastal wetlands to rising sea level ¨. *Ecology*, 83(10), pp.2869–2877.

Morris, J.T. & Haskin, B., 1990. A 5-yr record of aerial primary production and stand characteristics of Spartina alterniflora. *Ecology*, 71, pp.2209–2217.

Morris, M.D., 1991. Factorial sampling plans for preliminary computational experiments. *Technometrics*, 33(2), pp.161–174.

Mudd, S.M., Howell, S.M. & Morris, J.T., 2009. Impact of dynamic feedbacks between sedimentation, sea-level rise, and biomass production on near-surface marsh stratigraphy and carbon accumulation. *Estuarine, Coastal and Shelf Science*, 82(3), pp.377–389. Available at: http://linkinghub.elsevier.com/retrieve/pii/S0272771409000560 [Accessed March 20, 2012].

Murdukhayeva, A. et al., 2013. Assessment of Inundation Risk from Sea Level Rise and Storm Surge in Northeastern Coastal National Parks. *Journal of Coastal Research*, 291, pp.1–16. Available at: http://www.bioone.org/doi/abs/10.2112/JCOASTRES-D-12-00196.1 [Accessed April 2, 2015].

Naidoo, G. & Naicker, K., 1992. Seed germination in the coastal halophytes Triglochin bulbosa and Triglochin striata. *Aquatic Botany*, 42(3), pp.217–229.

Nepf, H.M., 1999. Drag, turbulence, and diffusion in flow through emergent vegetation. *Water Resources Research*, 35, pp.479–489.

Nepf, H.M., Sullivan, J.A. & Zavistosk, R.A., 1997. A model for difussion within an emergent plant canopy. *Limnology and Oceanography*, 42(8), pp.85–95.

Neubauer, S.C. et al., 2002. Sediment Deposition and Accretion in a Mid-Atlantic (U.S.A.) Tidal Freshwater Marsh. *Estuarine, Coastal, and Shelf Science*, 54(4), pp.713–727. Available at: http://dx.doi.org/10.1006/ecss.2001.0854.

Neumeier, U. & Ciavola, P., 2004. Flow resistance and associ- ated sedimentary processes in a Spartina maritima salt-marsh. *Journal of Coastal Research*, 20, pp.435–447.

Nibbakeb, J.W. & Bertness, M.D., 2001. *Marine biology: an ecological approach*, San Francisco, California: Benjamin Cummings.

Nicholls, R.J., 2004. Coastal flooding and wetland loss in the 21st century: changes under the SRES climate and socio-economic scenarios. *Global Environmental Change*, 14(1), pp.69–86. Available at: http://linkinghub.elsevier.com/retrieve/pii/S0959378003000815 [Accessed June 12, 2011].

Nicholls, R.J., Hoozemans, F.M.J. & Marchand, M., 1999. Increasing flood risk and wetland losses due to global sea-level rise: regional and global analyses. *Global Environmental Change*, 9, pp.S69– S87.

Nieva, F.J.J. et al., 2001. Field Variability of Invading Populations of Spartina densiflora Brong. in Different Habitats of the Odiel Marshes (SW Spain). *Estuarine, Coastal and Shelf Science*, 52(4), pp.515–527. Available at: http://linkinghub.elsevier.com/retrieve/pii/S0272771400907509 [Accessed December 12, 2011].

Nixon, S.W., 1980. Between coastal marshes and coastal waters: a review of twenty years of speculation and research on the role of salt marsh in estuarine productivity and water chemistry. In P. Hamilton & K. . MacDonald, eds. *Estuarine and Wetland Processes with Emphasis on Modelling.* New York: Plenum Press, pp. 437–525.

Nixon, S.W., 1982. *The ecology of New England high salt marshes: a community profile*, Washington, D.C.

Nocete, F. et al., 2005. An archaelogical approach to regional environmental pollution in the south-western Iberian Peninsula related to Third Millenium B.C mining and metallurgy. *Journal of Archaeological Science*, 32, pp.1566–1576.

Nugent, R.A., 2011. *The effect of exopolymers on the compressibility and shear strength of kaolinite.*, Department of Civil & Environmental Engineering, LSU, Baton Rouge, LA.

Nunes, J.P. et al., 2003. A model for sustainable management of shell- fish polyculture in coastal bays. *Aquaculture*, 219, pp.257–277.

Odum, E.P., 1971. *Fundamentals of ecology, 3rd ed.*, Philadelphia: Sounders.

Ojeda, J. et al., 2011. *Análisis preliminar de la vulnerabilidad de la costa de Andalucía a la potencial subida del nivel del mar asociada al Cambio Climático*, Sevilla.

Ojeda, J., 2003. Las Costas Andaluzas. In *Geografia de Andalucia*. Sevilla: Ariel, pp. 118–135.

Ojeda, J., 1988. Peculiaridades morfodinamicas de la fachada Iberica del Golfo de Cadiz: geomorfologia litoral. *Revista de Estudios Andaluces*, 10, pp.53–68.

Olias Alvarez, M. et al., 2010. *La contaminacion minera de los Ríos Tinto Y Odiel*, Huelva.

Olías, M. & Nieto, J.M., 2015. Background conditions and mining pollution throughout History in the Río Tinto (SW Spain). *Environments*, 2, pp.295–316.

Ouyang, Z.-T. et al., 2011. A comparison of pixel-based and object-oriented approaches to VHR imagery for mapping saltmarsh plants. *Ecological Informatics*, 6(2), pp.136–146. Available at: http://linkinghub.elsevier.com/retrieve/pii/S1574954111000057 [Accessed March 8, 2013].

Pajak, M.J. & Leatherman, S., 2002. The High Water Line as Shoreline Indicator. *Journal of Coastal Research*, 18(2), pp.329–337.

Pasternack, G.B. & Brush, G.S., 1998. Sedimentation cycles in a river-mouth tidal freshwater marsh. *Estuaries*, 21(3), pp.407–415.

Pedrera, A. et al., 2011. Is there an active subduction beneath the Gibraltar orogenic arc? Constraints from Pliocene to present-day stress field. *Journal of Geodynamics*, 52, pp.83–97.

Peinado, M. et al., 1995. Similarity of zonation within California -Baja California and Mediterranean Salt Marshes. *The Southwestern Naturalist*, 40(4), pp.388–405.

Peltier, W.R., 2001. Chapter 4 Global glacial isostatic adjustment and modern instrumental

records of relative sea level history. In B. C. Douglas, M. S. Kearney, & S. P. Leatherman, eds. *Sea Level Rise: History and Consequences*. International Geophysics. San Diego: Academy Press, pp. 65–95. Available at: http://dx.doi.org/10.1016/S0074-6142(01)80007-3 [Accessed March 12, 2013].

Pendland, S.M., Suter, J.R. & McBride, R.A., 1987. Delta plain development and sea level history in the Terrebonne coastal region. In N. C. Kraus, ed. *Coastal Sediments '87*. New York: American Society of Civil Engineers, pp. 1689–1705.

Pendon, J.G. et al., 1998. Evolution of estuarine facies in a tidal channel environment , SW Spain: evidence for a change from tide- to wave-domination. *Marine Geology*, 147, pp.43–62.

Pethick, J.S., 1981. Long-term accretion rates on tidal marshes. *Journal of Sedimentary Petrology*, 61, pp.571–577.

Pethick, J.S., 1992. Saltmarsh geomorhology. In *Saltmarshes: morphodynamics, consercation and engeneering significance*. pp. 41–62.

Pezeshki, S.R., 2001. Wetland plant responses to soil flooding. *Environmental and Experimental Botany*, 46, pp.299–312.

Pfeffer, W.T., Harper, J.T. & O'Neel, S., 2008. Kinematic constraints on glacier contributions to 21st-century sea-level rise. *Science*, 321(5894), pp.1340–1343.

Pielou, E.C. & Routledge, R.D., 1976. Salt Marsh Vegetation: Latitudinal Gradients in the Zonation Patterns. *Oecologia*, 24(4), pp.311–321.

Platt, R.V. & Rapoza, L., 2008. An Evaluation of an Object- Oriented Paradigm for Land Use / Land Cover Classification An Evaluation of an Object-Oriented Paradigm for Land Use / Land Cover Classification *. *The Pofessional Geographer*, 60(1), pp.87–100.

Ponnamperuma, F.N., 1972. The chemistry of submerged soils. *Advances in Agronomy*, 24, pp.29–95.

Populus, J. et al., 2001. Assessment of the Lidar topographic technique over a coastal area. In *Proceedings of CoastGIS'01: 4th International Symposium on GIS and Computer Mapping for Coastal Zone Management (CoastGIS, Halifax, Nova Scotia)*. p. 11.

Pratolongo, P.D. et al., 2009. Temperate Coastal Wetlands: Morphology, Sediment Processes and Plant Communities. In *Wetland coastal ecosystem*. Amsterdam: Elservier B.V., pp. 89–112.

Provoost, S. et al., 2005. Remote sensing of coastal vegetation in The Netherlands and Belgium. In J. Herrier, ed. *Dunes and Estuaries -- International Conference on Nature Restoration Ptractices in European Coastal Habitats*. Kiksujde, Belgium, pp. 19–23.

Puertos del Estado, 2015. *Conjunto de datos SIMAR*, Madrid. Available at: http://calipso.puertos.es//BD/informes/INT_8.pdf.

Pugh, D.T., 1987. Tides, Surges and mean sea-level. *Marine and Petroleum Geology*, p.301. Available at: http://linkinghub.elsevier.com/retrieve/pii/026481728890013X.

Pylarinou, A., 2015. *Impacts of Climate Change on UK Coastal and Estuarine Habitats : A Critical Evaluation of the Sea Level Affecting Marshes Model (SLAMM)*. University College London.

Rahmstorf, S., 2007. A semi-empirical approach to projecting future sea-level rise. *Science*, 315(5810), pp.368–70. Available at: http://www.ncbi.nlm.nih.gov/pubmed/17170254 [Accessed March 5, 2012].

Ramsey, E.W. & Laine, S.C., 2013. Comparison of Landsat Thematic Mapper and High Resolution Photography to identify Change in Complex Coastal Wetlands. *Journal of Coastal Research*, 13(2), pp.281–292.

Redfield, A.C., 1972. Development of a New England salt marsh. *Ecological Monographs*, 42, pp.201–237.

Redondo, S. et al., 2004. Influences of salinity and light on germination of three Sarcocornia taxa with contrasted habitats. *Aquatic Botany*, 78(3), pp.255–264. Available at: http://linkinghub.elsevier.com/retrieve/pii/S030437700400004X [Accessed February 13, 2013].

Redondo-Gómez, S. et al., 2007. Fundamental niche differentiation in subspecies of Sarcocornia perennis on a salt marsh elevational gradient. *Marine Ecology Progress Series*, 347(Castroviejo 1990), pp.15–20. Available at: http://www.int-res.com/abstracts/meps/v347/p15-20/ [Accessed August 7, 2012].

Reed, D.J., 1990. The impact of sea-level rise on coastal salt marshes. *Progress in Physical Geography*, 14, pp.465–481.

Rees, G., 1999. *The remote sensing data book*, Cambridge: Cambridge University Press.

Reyes, E. et al., 2000. Landscape modeling of coastal habitat change in the Mississippi Delta. *Ecology*, 81(8), pp.2331–2349.

Reyes, E., 2009. Wetland Landscape Spatial Models. In G. M. E. Perillo et al., eds. *Coastal Wetlands: An Intergrated Ecosystem Approach*. Amsterdam: Elsevier B.V., pp. 885–902.

Rinaldo, A. et al., 1999. Tidal networks 3. Landscape-forming discharges and studies in empirical geomorphic relationships. *Water Resources Research*, 35(12), pp.3919–3929.

Robert, W.D., Yasuhiko, M. & Brian, A.Z., 1991. Temporal and Spatial Patterns of Rhythmite Deposition on Mud Flats in the Macrotidal Cobequid Bay-Salmon River Estuary, Bay of Fundy, Canada. *Clastic Tidal Sedimentology — Memoir*, 16, pp.137–160.

Rodriguez-ramirez, A. et al., 1996. Recent coastal evolution of the dorana national park (sw spain). *Quaternary Science Reviews*, 15(96), pp.803–809.

Roman, C.T., James-Pirri, M.J. & Heltshe, J.F., 2001. *Monitoring Salt Marsh Vegetation*, Wellfleet, Massachusetts.

Rossington, S.K. et al., 2011. Estuary schematisation in behaviour-oriented modelling. *Marine Geology*, 281(1-4), pp.27–34. Available at: http://linkinghub.elsevier.com/retrieve/pii/S0025322711000077 [Accessed April 1, 2015].

Rosso, P.H., Ustin, S.L. & Hastings, a., 2006. Use of lidar to study changes associated with Spartina invasion in San Francisco Bay marshes. *Remote Sensing of Environment*, 100(3), pp.295–306. Available at: http://linkinghub.elsevier.com/retrieve/pii/S0034425705003615 [Accessed March 6, 2013].

Rozema, J. et al., 1991. Effect of elevated atmospheric CO2 on growth, photosynthesis and water relations of salt marsh grass species. *Aquatic Botany*, 39, pp.45–55.

Rozema, J., 1993. Plant responses to atmospheric carbon dioxide enrichment: interactions with some soil and atmospheric consitions. *Vegetatio*, 104/105, pp.173–190.

Rozema, J. & Diggelen, J.. V., 1991. A comparative study of growth and photosynthesis of four halophytes in response to salinity. *Acta Oecologica*, 12, pp.673–681.

Rubio, J.C. & Figueroa, M.E., 1983. Medio Físico, Vegetación de las Marismas de los ríos Odiel y Tinto (Huelva). *Estudios Territoriales*, 9, pp.59–86.

Ruiz, F., Gonzalez-Regalado, M.L. & Borrego, J., 1994. Ostracods and pollution : the Odiel river estuary (Huelva , SO Spain). *Coloquios de Paleontologia*, 46, pp.175–189.

Rybczyk, J.M. & Callaway, J.C., 2009. Surface Elevation Models. In G. M. E. Perillo et al., eds. *Coastal Wetlands: An Intergrated Ecosystem Approach*. Amsterdam: Elsevier, pp. 835–853.

Saintilan, N., Rogers, K. & McKee, K.L., 2009. Salt marsh– mangrove Interactions in

Australasia and the Americas. In G. M. E. Perillo et al., eds. *Coastal Wetlands: An Intergrated Ecosystem Approachstal Wetalnd*. Amsterdam: Elsevier, pp. 855–883.

Sainz, A., Grande, J.A. & de la Torre, M.L., 2004. Characterisation of heavy metal discharge into the Ria of Huelva. *Environment international*, 30(4), pp.557–66. Available at: http://www.ncbi.nlm.nih.gov/pubmed/15031016 [Accessed March 11, 2013].

San Miguel, E.G. et al., 2001. 230Th/232Th activity ratios as a chronological marker complementing 210Pb dating in an estuarine system affected by industrial releases. *Environmental pollution*, 112(3), pp.361–8. Available at: http://www.ncbi.nlm.nih.gov/pubmed/11291442.

Sanchez, J.M., Otero, X.L. & Izco, J., 1998. Relationships between vegetation and environmental characteristics in a salt-marsh system on the coast of Northwest Spain. *Plant Ecology*, 136, pp.1–8.

Santisteban, J.I. et al., 2004. Loss on ignition: a qualitative or quantitative method for organic matter and carbonate mineral content in sediments? *Journal of Paleolimnology*, 32(3), pp.287–299. Available at: <Go to ISI>://000225691200006.

Schile, L.M. et al., 2014. Modeling tidal marsh distribution with sea-level rise: Evaluating the role of vegetation, sediment, and upland habitat in marsh resiliency. *PLoS ONE*, 9(2), p.e88760.

Schmid, K.A., Hadley, B.C. & Wijekoon, N., 2011a. Vertical Accuracy and Use of Topographic LIDAR Data in Coastal Marshes. *Journal of Coastal Research*, 275, pp.116–132. Available at: http://www.bioone.org/doi/abs/10.2112/JCOASTRES-D-10-00188.1 [Accessed December 20, 2012].

Schmid, K.A., Hadley, B.C. & Wijekoon, N., 2011b. Vertical Accuracy and Use of Topographic LIDAR Data in Coastal Marshes. *Journal of Coastal Research*, 275(1), pp.116–132. Available at: http://www.bioone.org/doi/abs/10.2112/JCOASTRES-D-10-00188.1 [Accessed April 25, 2012].

Schwimmer, R.A., 2001. Rates ad Processers of Marsh Shoreline Erosion in Rehoboth Bay, Delaware. *Journal of Coastal Research*, 17(3), pp.672–683.

Scott, T., Masselink, G. & Russell, P., 2011. Morphodynamic characteristics and classification of beaches in England and Wales. *Marine Geology*, 286(1-4), pp.1–20.

Sherwood, E.T. & Greening, H.S., 2014. Potential impacts and management implications of climate change on Tampa Bay estuary critical coastal habitats. *Environmental management*, 53(2), pp.401–15. Available at: http://www.ncbi.nlm.nih.gov/pubmed/24122098 [Accessed April 2, 2015].

Siddall, M. et al., 2003. Sea-level fluctuations during the last glacial cycle. *Nature*, 423, pp.853–858.

Silliman, B.R., Grosholz, E.D. & Bertness, M.D., 2009. *Human Impacts on Salt Marshes: A Global Perspective*, University of California Press. Available at: http://books.google.com/books?id=dZbvgaYT6JYC&pgis=1 [Accessed March 12, 2013].

Silva, T.S.F. et al., 2008. Remote sensing of aquatic vegetation: theory and applications. *Environmental monitoring and assessment*, 140(1-3), pp.131–45. Available at: http://www.ncbi.nlm.nih.gov/pubmed/17593532 [Accessed March 4, 2013].

Silvestri, S., Defina, A. & Marani, M., 2005. Tidal regime, salinity and salt marsh plant zonation. *Estuarine, Coastal and Shelf Science*, 62(1-2), pp.119–130. Available at: http://www.sciencedirect.com/science/article/pii/S0272771404002173.

Silvestri, S. & Marani, M., 2004. Salt-marsh vegetation and morphology: basic physiology, modelling and remote sensing observation. In *Ecomorpholgy of tidal marshes*. Washington, D.C.: American Geophysical Union, pp. 5–25.

Silvestri, S., Marani, M. & Marani, A., 2003. Hyperspectral remote sensing of salt marsh

vegetation, morphology and soil topography. *Physics and Chemistry of the Earth, Parts A/B/C*, 28(1-3), pp.15–25. Available at: http://linkinghub.elsevier.com/retrieve/pii/S1474706503000044 [Accessed July 26, 2011].

Di Silvio, G., 1989. Modelling the morphological evoluiton of tidal lagoons and their equilibrium configuration. In *Proc. XXIIIrd IAHR Congress, Ottawa*. pp. 169–175.

Simas, T., Nunes, J.. & Ferreira, J.., 2001. Effects of global climate change on coastal salt marshes. *Ecological Modelling*, 139(1), pp.1–15. Available at: http://linkinghub.elsevier.com/retrieve/pii/S0304380001002265.

Sklar, F.H., Costanza, R. & Day, J.W., 1985. Dynamic spatial simulation modeling of coastal wetland habitat succession. *Ecological Modelling*, 29, pp.261–281.

Smith, M.S., 2009. Multi-Decadal Changes in Salt Marshes of Cape Cod, MA: Photographic Analyses of Vegetation Loss, Species Shifts, and Geomorphic Change. - *Northeastern Naturalist*, 16(2), p.183. Available at: http://dx.doi.org/10.1656/045.016.0203.

Snow, A.. & Vince, S.., 1984. Plant zonation in an Alaskan salt marsh II: An experimental study of the role of edaphic conditions. *Journal of Ecology*, 72, pp.669–684.

Sobol, I.M., 1993. Sensitivity estimates for non-linear mathematical models. *Math. Modell. Comput. Exp.*, 4, pp.407–414.

Sousa, A.I. et al., 2010. The influence of Spartina maritima on carbon retention capacity in salt marshes from warm-temperate estuaries. *Marine pollution bulletin*, 61(4-6), pp.215–23. Available at: http://www.ncbi.nlm.nih.gov/pubmed/20304438 [Accessed October 19, 2012].

Stive, M.J.F. et al., 1995. Behaviour-oriented models of shoreface evolution. In *Coastal Dynamics '95*. pp. 998–1005.

Stive, M.J.F. et al., 1998. Morphodynamics of a tidal lagoon and the adjacent coast. In S. Dronkers, ed. *Physics of Estuaries and Coastal Seas*. Balkema, Rotterdam, pp. 397–407.

Suarez Bores, J., 1971. *Determinacion de la edad mediante medidas del contenido carbono-14, en muestras de conchas procedentes de los litorales de Huelva y Valencia.*,

Teal, J.M. & Kanwisher, J.W., 1961. Gas exchange in a Georgia salt marsh. *Limnology and Oceanography*, 6, pp.388–399.

Teisson, C. & Fritsch, D., 1988. Numerical modeling of suspended sediment transport in the Loire estuary. In *Proceedings of the 21st Conference of Coastal Engineering, Torremolinos, Spain*. Coastal Engineering, pp. 2707–2720.

Temmerman, S. et al., 2005. Flow paths of water and sediment in a tidal marsh: Relations with marsh developmental stage and tidal inundation height. *Estuaries*, 28(3), pp.338–352.

Temmerman, S. et al., 2004. Modelling estuarine variations in tidal marsh sedimentation: response to changing sea level and suspended sediment concentrations. *Marine Geology*, 212(1-4), pp.1–19. Available at: http://linkinghub.elsevier.com/retrieve/pii/S0025322704002853 [Accessed March 30, 2015].

Temmerman, S., Govers, G., Meire, P., et al., 2003. Modelling long-term tidal marsh growth under changing tidal conditions and suspended sediment concentrations, Scheldt estuary, Belgium. *Marine Geology*, 193(1-2), pp.151–169. Available at: http://linkinghub.elsevier.com/retrieve/pii/S0025322702006424.

Temmerman, S., Govers, G., Wartel, S., et al., 2003. Spatial and temporal factors controlling short-term sedimentation in a salt and freshwater tidal marsh, Scheldt estuary, Belgium, SW Netherlands. *Earth Surface Processes and Landforms*, 28(7), pp.739–755. Available at: http://doi.wiley.com/10.1002/esp.495 [Accessed March 31, 2015].

Thomas, E. & Varekamp, J.C., 1991. Paleo-environmental analysis of marsh sequences (Clinton, Connecticut): evidence for punctuated rise in relative sea level during the latest Holocene. *Journal of Coastal Research Special*, (11), pp.125–158.

Thomson, A.G. et al., 2004. Short-term vegetation succession and erosion identified by airborne remote sensing of Westerschelde salt marshes , The Netherlands. *International Journal of Remote Sensing*, 25(20), pp.4151–4176.

Thomson, A.G., 1998. Supervised versus unsupervised methods for classification of coasts and river corridors from airborne remote sensing. *International Journal of Remote Sensing*, 19(17), pp.3423–3431.

Tian, B. et al., 2008. Analyzing the habitat suitability for migratory birds at the Chongming Dongtan Nature Reserve in Shanghai, China. *Estuarine, Coastal and Shelf Science*, 80(2), pp.296–302. Available at: http://linkinghub.elsevier.com/retrieve/pii/S0272771408003156 [Accessed March 30, 2013].

Titus, J.G., 1988. *Greenhouse Effect, Sea Level Rise and Coastal Wetlands*, Washington, DC, USA.

Tooley, M.J., 1992. Recent sea-level change. In *Saltmarshes: morphodynamics, consercation and engeneering significance*. Cambridge, UK: Cambridge University Press.

Trupin, A. & Wahr, J., 1990. Spectroscopic analysis of global tide gauge sea level data. *Geophysical Journal International*, 100(3), pp.441–453. Available at: http://gji.oxfordjournals.org/cgi/doi/10.1111/j.1365-246X.1990.tb00697.x [Accessed March 12, 2013].

Tso, B. & Mather, P., 2009. *Classification methods for remotely sensed data*, Taylor & Francis Group, LLC.

Turner, R.E. & Rao, R.S., 1990. Relationships between wetland fragmentation and recent hydrologic changes in a deltaic coast. *Estuaries*, 13, pp.272–281.

Turner, R.K., Georgi, S. & Fisher, B., 2008. *Valuing ecosystem services : the case of multi-functional wetlands*, London: Earthscan.

Tyler, G., 1971. Distribution and turnover of organic matter and minerals in a shore meadow ecosystem. *Oikos*, 22, pp.265–291.

UNEP, 2006. *Marine and Coastal Ecosystems and HumanWell-being: A Synthesis Report Based on the Findings of the Millennium Ecosystem Assessment*, Nairobi, Kenya.

Ungar, I.A., 1998. Are biotic factors significant influencing the distribution of halophytes in saline habitats? *Botanical Review*, 64, pp.176–199.

Ungar, I.A., 1978. Halophyte seed germination. *The Botanical Review*, 44(2), pp.233–264.

Vermeer, M. & Rahmstorf, S., 2009. Global sea level linked to global temperature. *Proceedings of the National Academy of Sciences of United States of America*, 106(51), pp.21527–21532.

Vogt, P. et al., 2006. Mapping Spatial Patterns with Morphological Image Processing. *Landscape Ecology*, 22(2), pp.171–177. Available at: http://link.springer.com/10.1007/s10980-006-9013-2 [Accessed January 19, 2016].

Vranken, M., Oenema, O. & Mulder, J., 1990. Effects of tide range alterations on salt marsh sediments in the Eastern Scheldt, S. W. Netherlands. *Hydrobiologia*, 195, pp.13–20.

De Vriend, H.J. et al., 1993. Approaches to long-term modelling of coastal morphology : a review. *Coastal engineering*, 21, pp.225–269.

Van der Wal, D. & Pye, K., 2004. Patterns, rates and possible causes of saltmarsh erosion in the Greater Thames area (UK). *Geomorphology*, 61, pp.373–391.

Wang, X.-C. et al., 2007. Release of dissolved organic matter during oxic and anoxic decomposition of salt marsh cordgrass. *Marine Chemistry*, 105, pp.309–321.

Watts, C.W. et al., 2003. *In situ measurements of erosion shear stress and geotechnical shear strength of the intertidal sediments of the experimental managed realignment scheme at Tollesbury, Essex*, Elsevier Ltd.

Webster, T.L. et al., 2006. Flood-risk mapping for storm-surge events and sea-level rise using lidar for southeast New Brunswick. *Canadian Journal of Remote Sensing*, 32, pp.194–211.

Westhoff, V. & Schouten, M.G.C., 1979. The diversity of European coastal ecosystems. In R. L. Jefferies & A. J. Davi, eds. *Ecological processes in coastal environments: The 1st European Ecological Symposium and 19th Symposium of the British Ecological Society, Norwich, 12-16 September 1977.* Oxford: Blackwell Scientific Publications, pp. 3–21.

White, W. & Morton, R., 1997. Wetland losses related to fault movement and hydrocarbon production, southeastern Texas coast. *Journal of Coastal Research*, 13(4), pp.1305–1320. Available at: http://www.jstor.org/stable/10.2307/4298740.

Wolanski, E. et al., 2009. Coastal Wetlands: A Synthesis. In G. M. E. Perillo et al., eds. *Coastal Wetlands: An Intergrated Ecosystem Approach*. Amsterdam: Elsevier, pp. 1–62.

Woolnough, S.J., Allen, J.R.L. & Wood, W.L., 1995. An exploratory numerical model of sediment deposition over tidal salt marshes. *Estuarine, Coastal and Shelf Science*, 45(5), pp.515–543.

Wray, R.D., Leatherman, S.P. & Nicholls, R.J., 1995. Historic and future land loss for upland and marsh islands in the Chesa- peake Bay, Maryland, USA. *Journal of Coastal Research*, 11, pp.1195–1203.

Yang, X., 2005. Cover: Use of LIDAR elevation data to construct a high resolution digital terrain model for an estuarine marsh area. *International Journal of Remote Sensing*, 26(23), pp.5163–5166. Available at: http://www.tandfonline.com/doi/abs/10.1080/01431160500218630 [Accessed May 3, 2013].

Yang, X. & Liu, Z., 2005. Using satellite imagery and GIS for land-use and land-cover change mapping in an estuarine watershed. *International Journal of Remote Sensing*, 26(23), pp.5275–5296. Available at: http://www.tandfonline.com/doi/abs/10.1080/01431160500219224 [Accessed April 2, 2013].

Zazo, C., 1980. *El Cuaternario marino-continental y el limite pleistoceno en el litoral de Cadiz*. Complutense Madrid University.

Zazo, C. et al., 1994. Holocene Sequence of Sea-Level Fluctuations in Relation to Climatic Trends in the Atlantic-Mediterranean Linkage Coast. *Journal of Coastal Research*, 10(4), pp.933–945.

Zazo, C. et al., 2005. Landscape evolution and geodynamic controls in the Gulf of Cadiz (Huelva coast, SW Spain) during the Late Quaternary. *Geomorphology*, 68(3-4), pp.269–290. Available at: http://linkinghub.elsevier.com/retrieve/pii/S0169555X04003289 [Accessed April 20, 2013].

Zedler, J.B. & Callaway, J.C., 2001. Tidal wetland functioning. *Journal of Coastal Research Special*, (27), pp.38–64.

Zhang, C.B. et al., 2009. *Triaxial compression test of soil – root composites to evaluate influence of roots on soil shear strength*, Elsevier B.V.

Zhao, B. et al., 2009. Monitoring rapid vegetation succession in estuarine wetland using time series MODIS-based indicators: An application in the Yangtze River Delta area. *Ecological Indicators*, 9(2), pp.346–356. Available at: http://linkinghub.elsevier.com/retrieve/pii/S1470160X0800068X [Accessed March 6, 2013].